Simultaneous quantification of urinary oxidative stress markers in women using combined oral contraceptives

S Volschenk

orcid.org 0000-0001-8660-6086

Dissertation accepted in partial fulfilment of the requirements for the degree *Master of Science in Biochemistry* at the North-West University

Supervisor: Prof E Erasmus

Co-supervisor: Dr G Venter

Graduation December 2023

27230708

“Success is not final; failure is not fatal: it is the courage to continue that counts.” - Winston Churchill.

ACKNOWLEDGEMENTS:

Firstly, I would like to thank my heavenly Father for granting me the opportunity to complete my degree. Thank You for all the blessings, no matter how big or small over the past four years. You deserve all the honor and glory!

I would like to contribute this dissertation to my loving parents. Thank you, mom, and dad, for all the sacrifices you had to make, so that I can be here today. Thank you for all the financial provision throughout the past eight years. Thank you for never giving up on me, for believing in my abilities, for all your prayers, for always understanding and your everlasting love. I am forever grateful for you and love you very much.

I would like to acknowledge the financial assistance (bursary) that I received from Struwig-Germeshuysen Cancer Research (SGKN) Trust for the completion of my studies. The researcher's opinions alone, as always, and not necessarily those of the SGKN Trust, are expressed in the conclusions of this study.

To all in the BOSS laboratory, especially Prof E Erasmus, Dr G Venter, Peet, and Carien. I cannot express the amount of gratitude I have for all your support and guidance. Thank you for all your patience, troubleshooting, long hours of work, advice, and friendship throughout the past few years. You are a great team, and it was such a privilege to be part of the BOSS lab as a student and staff member.

To my co-students and friends at Biochemistry, thank you for all your emotional support. I would especially like to thank Tarien, thank you for our very special friendship, and all your prayers and care. It was such an honour to share an office with you. Thank you, Nadia, and Chantell, for always being keen on a coffee break when things got tough, it meant more than you would ever know. Thank you Seany for all the long hours, late nights, and holidays in the lab, the emotional support means the world to me.

To my loving family and friends, thank you for all your emotional support. Without your thoughts, prayers, and messages I would have given up already. Thank you for your words of encouragement during tough times, thank you for celebrating the small victories, and always giving advice when I needed it most.

Lastly, to my husband, Armand, thank you for all your love, support, late night proof reading, many pep talks, and coffee. Thank you for cooking, cleaning, and keeping the household together when I had to work long hours. Thank you for never complaining. This dissertation is the result of all your patience, prayers, and emotional support. I love you endlessly!

ABSTRACT

In physiological samples, it is difficult to measure the presence of free radicals. Therefore, secondary oxidative products excreted in urine after detoxification are quantified instead, as they are proportional to the oxidative species. Oxidative stress may initiate cancer or promote its progression, and some of these oxidative stress products are used as cancer markers. Combined oral contraceptives have been shown to induce oxidative stress and are also implicated in breast cancer development, whether these markers are involved in combined oral contraceptive induced oxidative stress is unknown. Most methods are developed for specific target groups such as lipid peroxidation or DNA damage, with only a few obtaining the broader oxidative stress status profile.

Therefore, this study aimed to develop a single analytical method that characterises the global oxidative stress status of an individual. The characterisation includes components of the lipid peroxidation pathways (hydroxynonenal, hydroxynonenal mercapturic acid, malondialdehyde, prostaglandin $F_{2\alpha}$, and prostaglandin E_2), the DNA oxidation pathway (8-hydroxydeoxyguanosine), and both protein nitration and oxidation pathways (nitro-tyrosine and dityrosine). The global characterisation of the oxidative stress status can be used for risk analysis testing that speeds up a clinical diagnosis, whilst shedding the light on cellular mechanisms involved in oxidative stress-induced pathologies, such as cancer.

This study was divided into three main parts, consisting of the partial development and optimisation of the method, the partial validation of the developed method, and the implementation of the method to a test group. The development and optimisation of the method included sample preparation (derivatisation with N-acetyl: chloride and dinitrophenylhydrazine, and solid phase extraction), as well as separation and detection using liquid chromatography-electrospray ionisation-tandem mass spectrometry (LC-ECI-MS/MS). During development and optimisation, the limitations of the method became clear, and it was decided to rather optimise two separate methods for the quantification of the urinary oxidative stress markers. The markers included in the first method were butyl esters (nitro tyrosine-butyl ester, and tyrosine butyl ester) and in the second method DNA oxidation and lipid peroxidation markers derivatised with dinitrophenylhydrazine was analysed.

After the successful development and optimisation, the methods were validated by evaluating parameters such as linearity, accuracy, precision, matrix effect, sensitivity, selectivity, and short-term stability. Lastly, the methods were applied to a study cohort (combined oral contraceptive users and non-users) to determine if the urinary oxidative stress profiles could be successfully characterised in biological samples.

The outcome was not as significant as expected. However, three oxidative stress markers (8-hydroxydeoxyguanosine, 3-nitrotyrosine and malondialdehyde) were of interest in women using combined oral contraceptives. However, 8-hydroxydeoxyguanosine, 3-nitrotyrosine and malondialdehyde were of statistical interest in the oxidative profiles of women using combined oral contraceptives.

Keywords: oxidative stress, derivatisation, solid phase extraction, liquid chromatography, mass spectrometry

TABLE OF CONTENTS

TABLE OF FIGURES

LIST OF TABLES

LIST OF EQUATIONS

ABBREVIATION AND SYMBOL LIST:

α:	alpha
*:	Asterisk
ºC:	degrees Celsius
<:	less than
>:	greater than
%:	percentage
µg:	microgram
µg/ml:	microgram per millilitre
µl:	microliter
σ:	standard deviation (sigma)
$^{13}C,^{15}N_2$-8-OHdG:	8-oxo-2'-deoxyguanosine-$^{13}C,^{15}N_2$
2-OHE_1(E_2):	2-hydroxyestrone-estradiol
3-NT:	3-nitrotyrosine
4-HNE:	4-hydroxynonenal
4-HNE-MA:	4-hydroxynonenal mercapturic acid
4-OHE_1(E_2):	4-hydroxyestrone-estradiol
8-OHdG:	8-hydroxydeoxyguanosine
8-oxoGua:	8-dihydroguanine
ACN:	acetonitrile
ANOVA:	Analysis of variance
BC:	breast cancer
BE:	butyl ester
CE:	catechol estrogens
-CH_2	methylene groups
CID:	collision cell
CO_3:	carbon trioxide
COC:	combined oral contraceptives
Cu^{2+}	copper ions

CV:	coefficient of variance
CYP450:	cytochrome P450
DIPEA:	diisopropylethylamine
Dityr:	dityrosine
DNA:	deoxyribonucleic acid
DNPH:	2,4-dinitrophenylhydrazine
E_1:	estrone
E_2:	estradiol
$E_1(E_2)$-3,4-Q:	4-hydroxyestrone-estradiol quinone
$E_1(E_2)$-3,4-SQ:	4-hydroxyestrone-estradiol semi-quinone
eBOSS:	estrogen Biotransformation and Oxidative Stress Status
EPR:	electron paramagnetic resonance
ER:	estrogen receptor
ESI:	electro spray ionisation
EtAc:	ethyl acetate
EtOH:	ethanol
Fe^{2+}:	iron ion
GSH:	glutathione
GST:	glutathione S-transferase
H_2O_2:	hydrogen peroxide
HCl:	hydrochloric acid
HClO:	hypochlorous acid
HMDB:	human metabolome database
HNO_3^-:	peroxynitrite anion
HPLC:	high performance liquid chromatography
HPLC-ESI-MS/MS:	high performance liquid chromatography- electrospray ionisation tandem mass spectrometry
LLOQ:	lower limit of quantification
LOD:	limit of detection

LOQ:	limit of quantification
m/z:	mass to charge ratio
MA:	mercapturic acid
MDA:	malondialdehyde
MDA -MA:	malondialdehyde mercapturic acid
MeOH:	methanol
mM:	millimolar
MS/MS:	triple quadrupole mass spectrometer
ng	nanogram
ng/ml	nanogram per
$NO^{\bullet}$:	nitric oxide
$^{\bullet}O_2^-$:	superoxide
$^{\bullet}OH$:	hydroxyl radical
$ONOO^-$:	peroxynitrite
PCA:	principal component analysis
PCs:	principal components
PGD_2:	prostaglandin D_2
PGE_2:	prostaglandin E_2
$PGF_{2\alpha}$:	8-isoprostaglandin-$F_{2\alpha}$
PLS-DA:	partial least squares-discriminant analysis
PR:	progesterone receptor
PUFA:	polyunsaturated fatty acid
P value	significance level
QC:	quality control
r^2:	coefficient of determination
R	Pearson’s correlation coefficient
RCF:	relative centrifugal force
RNS:	reactive nitrogen species
RPLC:	reverse phase liquid chromatography

$ROO^{\bullet}$:	peroxyl radical
ROS:	reactive oxygen species
RRF:	relative response factor
SOD:	superoxide dismutase
SPE:	solid phase extraction
SPSS:	statistical package for the social sciences
TBA:	thiobarbituric acid
TBARS:	thiobarbituric acid reactive substances
TCA:	trichloroacetic acid
Tyr:	tyrosine
ULOQ:	upper limit of quantification
UV:	ultraviolet

CHAPTER 1: INTRODUCTION:

1.1 Background, motivation, and problem statement

The short half-life of free radicals makes it difficult to measure their presence in physiological samples. These radicals can, however, be measured indirectly by analysing the more stable secondary products formed from free radicals (Bender, 2009). The levels of the secondary products are proportional to oxidative species (Sonowal & Ramana, 2019). After detoxification, the end-products of oxidation are excreted in measurable concentrations in urine (Martinez-Moral & Kannan, 2019).

The most studied biomarkers of oxidative stress include isoprostanes, malonaldehyde, hydroxynonenal, nitrotyrosine, 8-oxoguanine, 8-hydroxydeoxyguanosine, acrolein, and advanced glycation products (Il'yasova *et al.*, 2012; Shah *et al.*, 2014; Wu *et al.*, 2016). Ongoing research indicates that oxidative stress may initiate cancer or promote its progression (Lira *et al*., 2019; Saha et al., 2017). Deoxyribonucleic acid (DNA) oxidation and lipid peroxidation markers are considered reliable biomarkers for cancer studies (Saha *et al.,* 2017). Specifically, thiobarbituric acid reactive substances (TBARS) (Lira *et al*., 2019) and 8-hydroxydeoxyguanosine are used as confirmatory biomarkers for breast cancer (Nour Eldin *et al.,* 2019). Combined oral contraceptives have been associated with breast cancer development. However, it is not known whether these biomarkers are also involved in Combined oral contraceptive-induced oxidative stress.

Furthermore, although these biomarkers have been identified as important during disease diagnosis, only a few methods are available to quantify them simultaneously. Most methods are developed for specific target groups such as lipid peroxidation or DNA damage, with only a few obtaining the broader oxidative stress status. The development of a single analytical method to characterise the global oxidative stress status of an individual will speed up the clinical diagnostic and risk analysis testing, whilst it sheds light on cellular mechanisms involved in oxidative stress-induced pathologies, such as cancer.

1.2 Aims and objectives

The first aim of this study is to develop a single liquid chromatography-tandem mass spectrometry method (HPLC-ESI-MS/MS) that can analyse multiple urinary oxidative stress markers (dityrosine, tyrosine, nitrotyrosine, malondialdehyde, hydroxynonenal, hydroxynonenal mercapturic acid, prostaglandin $F_{2\alpha}$, and prostaglandin E_2) simultaneously. The secondary aim is to apply this method to determine and compare the oxidative stress profiles of women using combined oral contraceptives (COC) and non-users.

Some objectives were identified to successfully achieve these aims and can be summarised as:
1. The optimisation of both detection and ionisation conditions for the target metabolites from the method described by Martinez-Moral & Kannan (2019). This will include conditions such as source optimisation, optimisation of precursor and product ions, and ionisation parameters.

2. Optimisation of metabolite separation on the analytical column and liquid chromatography system. Including mobile phase gradient optimisation, column temperatures, flow rate, and injection volumes.

3. The optimisation of the sample preparation as described in literature (Martinez & Kannan, 2018; Martinez-Moral & Kannan, 2019; Martinez-Moral & Kannan, 2022; Vanova et al., 2018). The derivatisation and solid phase extraction techniques will be optimised.

4. Validating the developed and optimised method to establish if it is reproduceable and accurate. Linearity, sensitivity, accuracy, precision, short-term stability, the matrix effect, selectivity, and extraction recovery will be assessed during validation.

5. Implementing the validated method to a group of COC users and non-users to characterise and compare their oxidative stress profiles.

1.3 Dissertation layout

Chapter 2 contains the literature review and background on free radicals, oxidative stress, biotransformation, cancer, combined oral contraceptives, the oxidative stress markers of interest and method validation. Chapter 2 concludes with the aims of the study. In chapter 3, the experimental design, materials, and instrumentation are described. Chapter 4 entails the partial method development and optimisation for quantification of the oxidative stress markers. The method validation is described and discussed in chapter 5. In chapter 6 the method application and the oxidative stress profiles of the COC users and non-users are discussed. The conclusion and future recommendations are given in chapter 7. The Harvard reference style was used in this study, and the dissertation was written in British English. Annexure A contains information regarding the study cohort, whereas Annexure B contains supplementary information regarding the method development and optimisation. The supplementary results for the method validation and implementation can be found in Annexure C. The references for tables and figures in the annexures are shown as (Table A... or Figure B..; with the annexure as a prefix).

CHAPTER 2: LITERATURE & BACKGROUND

This chapter will detail all the literature that is relevant to this study. The definition, sources, and mechanisms of oxidative stress will be discussed, as well as the correlation between oxidative stress and cancer, and whether the use of combined oral contraceptives induces oxidative stress. This chapter also includes a discussion on oxidative stress markers and their role in cancer diagnosis.

2.1 Free radicals and oxidative stress

Free radicals are known to be reactive molecules with one or more unpaired electron(s) making them unstable (Preedy & Patel, 2015). These molecules only persist for around 10^{-9} –10^{-12} seconds in their free radical form and they achieve stability through interaction with other molecules (Bender, 2009). This stability is obtained by either donating or eliminating an electron, after which they form new radical species or a secondary product (Bender, 2009). When free radical concentrations become greater than normal physiological concentrations, it may induce oxidative damage inside cells and modify macromolecules such as proteins, lipids, and deoxyribonucleic acids (DNA) (Martinez-Moral & Kannan, 2019; Shah *et al.*, 2014). The damage caused by these molecules (radicals or secondary products) is known as oxidative or nitrative damage (Phaniendra *et al.*, 2015). Some free radical species, at physiological concentration, are important molecules for both physiological and biochemical processes within the body. Nitric oxide ($NO^{\cdot}$), for instance, plays a key role in blood pressure regulation, smooth muscle relaxation, enzyme regulation, neurotransmission, and immune regulation (Phaniendra *et al.*, 2015; Sonowal & Ramana, 2019). The ratio of antioxidants and pro-oxidants in a cell is termed the redox state, and oxidative stress is the occurrence of biological damage caused by an altered redox state (Chao *et al.*, 2015; Costantini, 2019; Milne *et al.*, 2011; Preedy & Patel, 2015).

2.2 Types of oxidative species

The most damaging radicals are the oxygen radicals, which include superoxide ($^{\bullet}O_2^-$), hydroxyl radicals ($^{\bullet}OH$), and peroxyl radicals ($ROO^{\bullet}$) (Milne et al., 2011; Ozcan & Ogun, 2015). Reactive oxygen species (ROS) can also consist of non-radical species such as hydrogen peroxide (H_2O_2), hypochlorous acid (HClO), and peroxynitrite anion (HNO_3^-) (Bender, 2009; Phaniendra et al., 2015; Sonowal & Ramana, 2019). Another group of oxidants, known as reactive nitrogen species (RNS) are nitrogen-containing radical- and non-radical species (Phaniendra et al., 2015).

The most abundant nitrogen radical is $NO^{\bullet}$, whereas peroxynitrite ($ONOO^-$) is the most abundant non-radical (Phaniendra et al., 2015). Nitric oxide is the primary substrate for $^{\bullet}O_2^-$, which can lead to the formation of $OONO^-$ (Cipak Gasparovic et al., 2017).

2.3 Sources of ROS and RNS

Free radicals, especially ROS and RNS can be formed from both endogenous and exogenous sources (Phaniendra *et al.*, 2015). The main source of endogenous ROS is the mitochondria, more specifically the electron transport chain, where both NADH dehydrogenase (complex 1) and ubiquinone-cytochrome reductase (complex 3) produce $^{\bullet}O_2^-$ (Milne *et al.*, 2011; Ozcan & Ogun, 2015; Phaniendra *et al.*, 2015). Other endogenous sources include mechanisms of an inflammatory response, enzymatic reactions, prostaglandin synthesis, infection/inflammation, ageing, and mental stress (Ligor *et al.*, 2015; Ozcan & Ogun, 2015; Phaniendra *et al.*, 2015; Preedy & Patel, 2015; Sonowal & Ramana, 2019). Another endogenous source of ROS is the biotransformation pathway, which is usually active in liver cells, but can also be active in the intestinal mucosal wall and other specific tissues (Liska *et al.*, 2006). During biotransformation, toxins and xenobiotics are detoxified through various reactions to be excreted in urine or bile (Islam *et al.*, 2019). Phase I reactions either result in intermediate metabolites that can be easily excreted by the body or reactive electrophilic compounds, which contribute to ROS formation (Fontana *et al.,* 2019, Liska *et al., 2006).* Exogenous sources of ROS and RNS include air and water pollution, environmental pollutants, ultraviolet (UV) light exposure, allergens, xenobiotics, exercise, heavy metals, and certain foods (Martinez-Moral & Kannan, 2019; Milne *et al.*, 2011; Phaniendra *et al.*, 2015; Shah *et al.*, 2014; Sonowal & Ramana, 2019).

2.4 Oxidative stress

An imbalance in the redox state is mostly caused by overexposure to pro-oxidants, but a lack of antioxidant defences, such as vitamins or enzymes, also play a key role (Milne *et al.*, 2011; Pisoschi & Pop, 2015; Preedy & Patel, 2015; Sonowal & Ramana, 2019). Oxidative stress can be initiated by either free radical-mediated oxidation (ROS/RNS), enzymatic oxidation, or free radical-independent non-enzymatic oxidation (spontaneously) (Bothma, 2012; Preedy & Patel, 2015). As mentioned in section 2.1, the free radicals interact with other compounds/molecules to obtain stability. These interactions mostly take place near the site of free radical production. However, the products formed can migrate to distant sites and cause damage elsewhere, even long after the initial ROS production (Sonowal & Ramana, 2019). In turn, the damage can also produce ROS which may lead to further damage. A summary of the most common free radicals and their sources are illustrated in Figure 2-1.

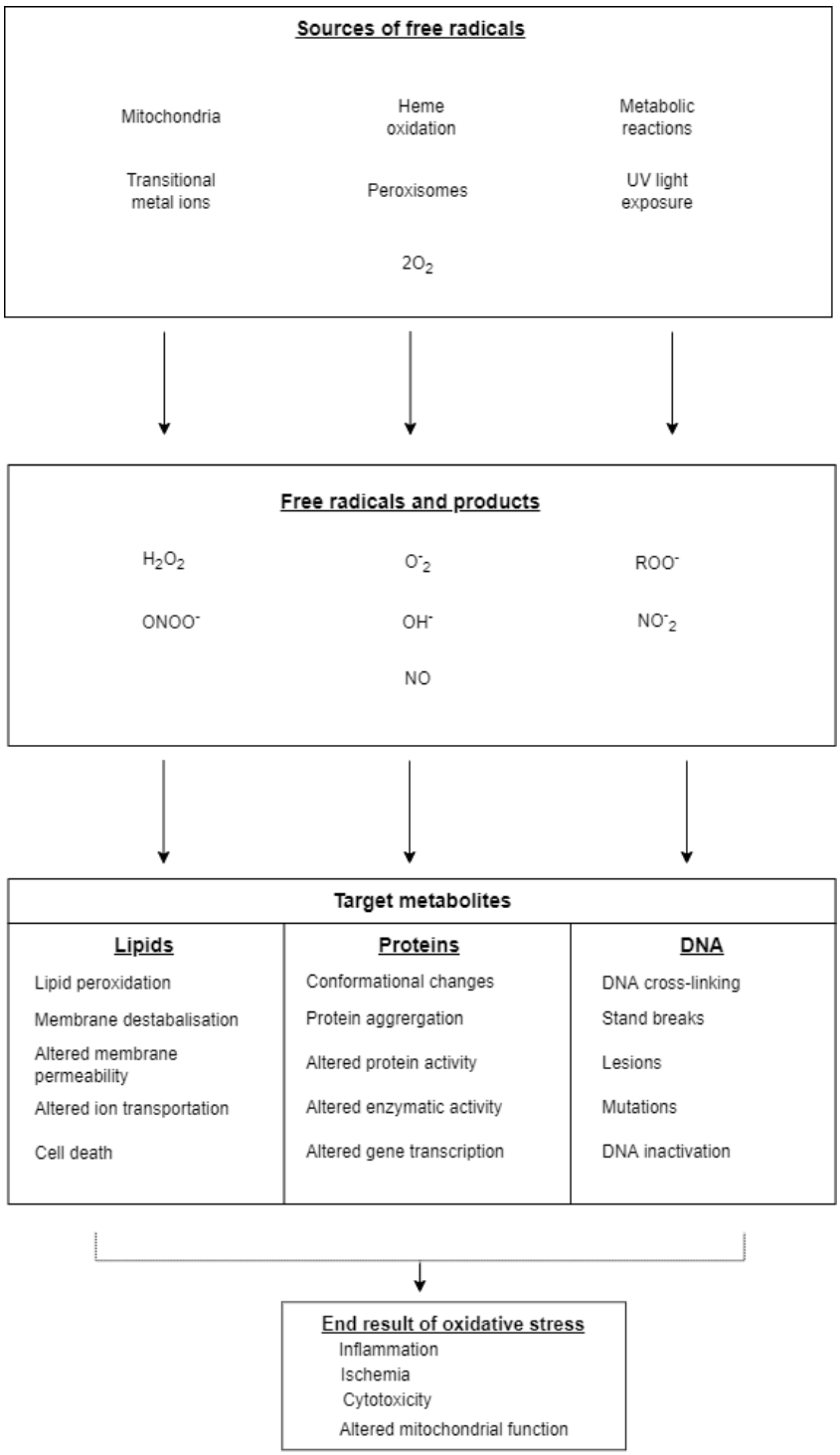

Figure 2-1. Free radical formation & effect on target metabolites. *H_2O_2: hydrogen peroxide, $^{\bullet}O_2$: superoxide anion, $NO^{\bullet}$: nitric oxide, $^{\bullet}OH$: hydroxyl radical, $ONOO^{-}$: peroxynitrite, $ROO^{\bullet}$: peroxyl radical, NO^{-}_2: nitrogen oxide radical*.

2.4.1 Lipid peroxidation

Oxidative stress can occur anywhere within the body, since ROS and RNS target almost any compound to achieve stability (Pisoschi & Pop, 2015). Lipids are essential components of cellular membranes and play a significant role in energy storage and normal metabolism, they also function as signalling molecules during membrane transport (Preedy & Patel, 2015). Lipids are the most susceptible macromolecule to undergo oxidation, due to the reactive double bonds within their structure (Ho *et al.*, 2013; Pisoschi & Pop, 2015).

Lipid peroxidation is the known process by which phospholipids and polyunsaturated fatty acids (PUFAs) are degraded into lipid radicals through a chain of reactions (initiation, propagation, and termination) (Ayala *et al.*, 2014; Preedy & Patel, 2015). During lipid peroxidation an alteration in membrane permeability occurs, leading to the inactivation of these membranes and cell death (Čolak, 2008; Milne *et al.*, 2011). During lipid peroxidation, phospholipids and unsaturated fatty acids are converted to lipid peroxides (LOOH), membrane lipid radicals ($L^{\bullet}$), and peroxyl radicals ($LOO^{\bullet}$) (Ayala *et al.*, 2014; Preedy & Patel, 2015). Lipid peroxidation is initiated by the extraction of an active hydrogen atom from the methylene group of unsaturated fatty acids; the formed ROS spreads by chain reactions until the peroxide levels are elevated to a level where they can result in non-radical molecules such as aldehydes, isoprostanes, alcohols, and lipid epoxides as secondary products (Lobo *et al.,* 2010; Montuschi *et al.*, 2004; Preedy & Patel, 2015).

2.4.2 Protein oxidation

Throughout the literature (Martinez-Moral & Kannan, 2019; Preedy & Patel, 2015; Shah *et al.*, 2014), it is evident that proteins are great targets for oxidative damage since they are abundantly present within the body and they can readily undergo nitration (Cipak Gasparovic *et al.*, 2017). ROS or RNS can oxidise the sidechains, fragment the backbone and/or unfold or misfold proteins. These alterations change the iso-electrical point and molecular weight of the proteins which results in loss of function (Čolak, 2008; Pisoschi & Pop, 2015; Preedy & Patel, 2015). Amino acids cysteine, histidine, tryptophan, and tyrosine are especially susceptible to the hydroxyl radical (Malencik & Anderson, 2003; Pisoschi & Pop, 2015), whereas lysine, arginine, threonine, or proline can form aldehydes or ketones (protein carbonyls) on their side chains during oxidation (Čolak, 2008; Dalle-Donne *et al.*, 2003; Preedy & Patel, 2015). Aromatic amino acids such as tyrosine can also undergo oxidation and nitration, because of their hydrophobic nature (Chao *et al.*, 2015; Cipak Gasparovic *et al.*, 2017; Čolak, 2008; Ho *et al.*, 2013; Pisoschi & Pop, 2015; Shah *et al.*, 2014). The metabolic fate of oxidised amino acids is unknown, but scientists suggest that they are filtered from blood into urine (Bhattacharjee *et al.*, 2001; DiMarco & Giulivi, 2007; Il'yasova *et al.*, 2012; Orhan *et al.*, 2005).

2.4.3 Nucleic acid oxidation

Oxidative damage to nucleic acids can lead to DNA-protein cross-linking, strand breaks, lesions, and mutations (Pisoschi & Pop, 2015; Preedy & Patel, 2015). Oxidative damage can also irreversibly inhibit transcription, translation, and DNA replication (Preedy & Patel, 2015). The DNA lesions occur at the C8 position of guanine (transversions of G-T and A-C), leading to the formation of 8-hydroxydeoxyguanosine (8-OHdG) (Preedy & Patel, 2015; Shah *et al.*, 2014). Single-strand breaks in DNA can lead to double-strand breaks that in turn, may lead to the alternation of the genome stability and causing cell death by stalling cell progression (Preedy & Patel, 2015). Mitochondrial DNA (mtDNA) undergoes more oxidation than nuclear DNA since it is located close to the site of ROS production (Lobo *et al.*, 2010; Phaniendra *et al.*, 2015).

Free radicals can, therefore, affect different macromolecules (Figure 2-1). Without regulation on a cellular level, these effects may have disastrous long-term consequences. Some of the direct damaging effects include inflammation, cell ischemia, altered mitochondrial function, DNA alterations, cell membrane alterations, and alterations in enzyme activity (Ozcan & Ogun, 2015), and can lead to disease onset. Oxidative stress has been implicated in various pathologies such as Parkinson's, cancer, Alzheimer's, Diabetes Mellitus, Lupus, cardiovascular diseases, stroke, and Atherosclerosis (Griendling et al., 2016; Ho et al., 2013; Mehta & Gowder, 2015; Phaniendra et al., 2015; Pisoschi & Pop, 2015; Shah et al., 2014). It is fundamental for a person's overall health to be able to maintain the redox balance by detoxifying these damaging substances they are exposed to (Liska et al., 2006).

2.5 Antioxidant defence mechanisms

There are various molecules and processes involved in antioxidant defence. Antioxidants stabilise free radicals by either donating hydrogen atoms/electrons, scavenging radicals, inhibiting enzymes, chelating metal ions, or regulating gene expression (Lobo *et al.*, 2010; Pisoschi & Pop, 2015), while processes like phase II biotransformation play a role in the detoxification of electrophilic or reactive intermediates that contribute to ROS formation (Liska *et al.,* 2006).

2.5.1 Antioxidants

Lobo and colleagues (2010) defined antioxidants as molecules that are stable enough to donate an electron to a free radical to neutralise it. Others define antioxidants as molecules that can scavenge free radicals to prevent oxidation (Bender, 2009; Gropper & Smith, 2013; Mehta & Gowder, 2015).

Antioxidants such as glutathione (GSH), ubiquinol, and uric acid are endogenous metabolic products and many enzymes are also known for their antioxidant properties such as superoxide dismutase (SOD), catalase, and glutathione reductase (Lobo *et al.*, 2010; Mehta & Gowder, 2015). Exogenous antioxidants can also be consumed in our daily diet. These antioxidants include Vitamin C, Vitamin E, Vitamin A, turmeric, garlic, zinc, and various flavonoids in fruits and vegetables (Gropper & Smith, 2013; Lobo *et al.*, 2010; Mehta & Gowder, 2015; Murray *et al.*, 2009; Tanvir *et al.*, 2017).

2.5.2 Biotransformation

During biotransformation, the first line of enzymatic defence is Phase I detoxification reactions, where functional groups are mostly exposed or added by enzymes such as cytochrome P450 (CYP450) (Fontana *et al.*, 2019; Liska *et al.*, 2006). Phase I reactions increase the polarity of the present xenobiotics, as well as the ability of compounds to undergo Phase II detoxification (Fontana *et al.*, 2019). Phase I reactions vary, and the type of reaction is determined by the structural properties of the xenobiotic (Liska *et al.*, 2006). Although Phase I reactions can result in inactive metabolites that can easily be excreted by the body, they can also yield reactive electrophilic compounds and ROS. The latter requires antioxidant support to be effectively neutralized, while the electrophilic compounds should undergo Phase II conjugation to prevent any further damage (Fontana *et al.,* 2019, Liska *et al., 2006)*. Phase II conjugation reactions include several reactions that take place such as glucuronidation, sulfation, glutathione conjugation, amino acid conjugation, acetylation, and methylation, again depending on the compound's properties, as indicated in Figure 2-2 (Liska *et al.*, 2006). Therefore, Phase II reactions require nutritional support. During Phase II conjugation, the biotransformed intermediate is conjugated with a polar group provided by co-factors and other donor molecules to make it more water-soluble (Liska *et al.*, 2006; Mathias & B'Hymer, 2016). The carcinogenic or damaging by-products of xenobiotics and other toxins are excreted in urine or bile (Islam *et al.*, 2019). As seen in Figure 2-2 biotransformation utilises antioxidants during the detoxification process, which entails the conversion of xenobiotics/toxic compounds that are lipid-soluble to water-soluble compounds for excretion (Fontana *et al.*, 2019; Liska *et al.*, 2006).

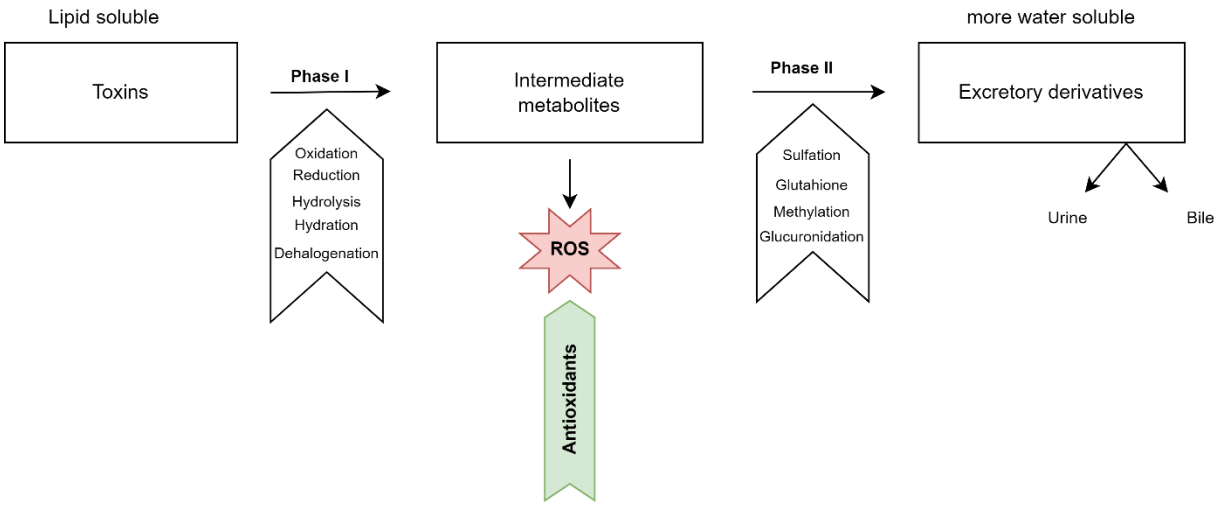

Figure 2-2. Schematic illustration of biotransformation (adapted from Liska et al., 1998).

Although this illustration indicates Phase I and Phase II as sequential processes, they happen simultaneously within the liver. *ROS: Reactive Oxygen Specie*s.

One detoxification process that is of specific interest is the mercapturic pathway, which facilitates the metabolic elimination of electrophilic compounds by yielding a product known as mercapturic acid (MA) (Deol & Josephy, 2017). This pathway forms part of Phase II detoxification, where GSH reacts with an electrophilic compound, via the catalysis of glutathione S-transferase (GST) (Deol & Josephy, 2017; Forman et al., 2009; Frigerio et al., 2019; Hanna & Anders, 2019; Völkel et al., 2005). When the GSH reacts with the electrophilic species, a GSH-S-conjugate is formed, which undergoes sequential hydrolysis to remove the glycine and glutamyl moieties enzymatically and eventually undergoes N-acetylation to yield the toxicant-MA (Deol & Josephy, 2017; Frigerio et al., 2019; Hanna & Anders, 2019; Mathias & B'Hymer, 2016). During acetylation, the metabolite is transformed to be water-soluble by increasing the polarity of the compound (Mathias & B'Hymer, 2016). The toxicant-MA can then be transported to the kidneys for excretion in urine (Hanna & Anders, 2019; Liska, 1998). Mercapturic acids are considered good biomarkers to determine a person's exposure to certain toxins and chemicals since they indicate the turnover of these toxins (Mathias & B'Hymer, 2016). However, the reliability of certain urinary MAs as biomarkers; is dependent on the activity of the biotransformation enzymes (Hanna & Anders, 2019). Therefore, not all MAs necessarily serve as good quality biomarkers.

2.6 Cancer and oxidative stress

Cancer is known to be one of the leading causes of death around the globe (Saha et al., 2017; Vorobiof *et al.*, 2001, World Health Organization, 2018). It is no secret that ROS have mutagenic properties and can promote cancer initiation by causing genomic instability (Gào & Schöttker, 2017; Gill et al., 2016; Islam et al., 2019; Lira et al., 2019; Saha et al., 2017).

Oxidative stress is implied in the first step of mutagenesis and carcinogenesis where it induces permanent modifications of genetic material (Shrivastava *et al.*, 2019). Both ROS and RNS play a physiological and pathological role in cancer biology and the transmission of cellular signals. This role is, however, concentration-dependent, where low concentrations lead to tumour promotion and higher concentrations have apoptotic effects leading to tumour suppression (Islam et al., 2019; Shrivastava et al., 2019).

2.6.1 Oxidative stress-induced cancer

Gào and colleagues (2017) identified redox pathways involved in cancer development by analysing literature published between 2005 and 2015. In this study, they found that the mitochondria, NADPH oxidase, mitogen-activated protein kinase, and transcription factors Nrf-2 & p53 were prominent (Gào & Schöttker, 2017). Endoplasmic reticulum stress, mitochondrial respiration, oncogenes, and hypoxia can all increase ROS in cancer cells (Gill *et al.*, 2016). ROS in cancer cells function as messengers in cellular signalling transduction pathways, they also promote cellular growth, proliferation, and development, as shown in Figure 2-3 (Shrivastava *et al.*, 2019).

During oncogene signalling, ROS levels increase, and it may contribute to ongoing mutagenesis which can stimulate cancer progression (Gill *et al.*, 2016; Lee *et al.*, 2017; Saha *et al.*, 2017). Cancer cells have metabolic plasticity that allows them to undergo dynamic mitochondrial changes in mass and function to manage oxidative stress (Gill *et al.*, 2016). Cancer cell survival, proliferation, chemo- and radiotherapy resistance, angiogenesis, and the inhibition of apoptotic mechanisms can be induced by oxidative stress (Gào & Schöttker, 2017). An increase in oxidative stress markers is usually associated with oxidative stress within the cancer cells due to uncontrolled ROS/RNS formation (Poprac *et al.,* 2017).

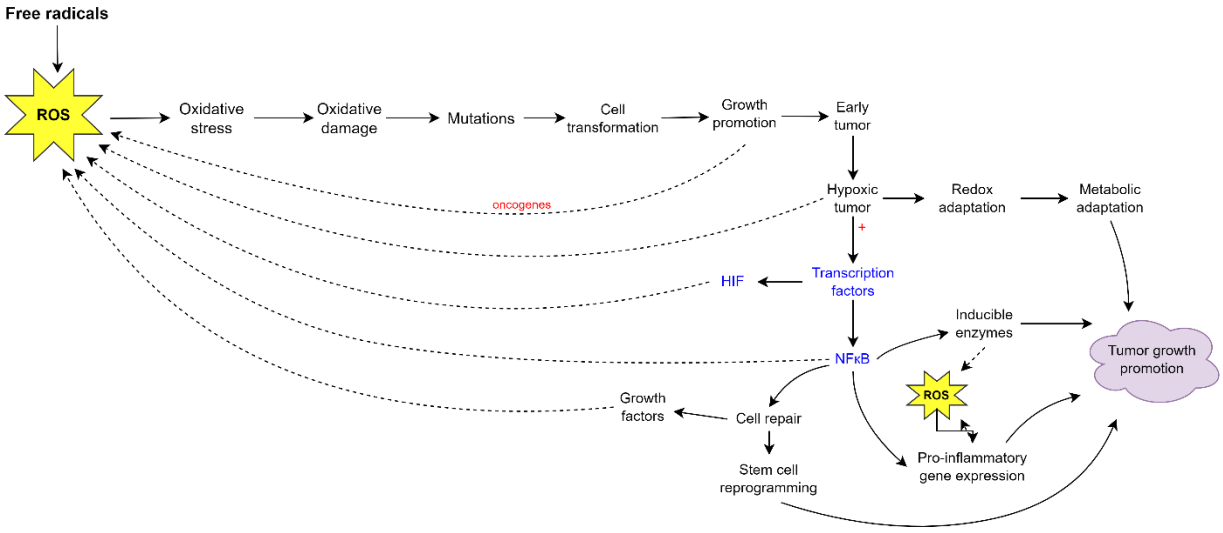

Figure 2-3. Effect of ROS on cancer initiation and progression (adapted from Tafani, 2016 & Saha et al., 2017). HIF triggers tumour progression, whereas NFκB regulates immune response. All the dotted lines indicate ROS production or ROS signalling. *ROS: Reactive oxygen species, HIF: Hypoxia-inducible factor, NF$_k$B: Nuclear factor-kappa B.*

At low concentrations, ROS can promote cancer progression by either signalling elements or by the stimulation of DNA alterations (Saha *et al.*, 2017). On the other hand, cancer cells are more susceptible to ROS than normal cells and rely on GSH and thioredoxin for protection against oxidative stress (Gill *et al.*, 2016). Induction of redox-sensitive pathways during cell proliferation is therefore necessary for survival (Shrivastava *et al.*, 2019). Evidence indicates that oxidative stress can kill cancer cells during any stage of metastases (Gill *et al.*, 2016).

2.6.2 Cancer diagnosis

There are numerous ways to diagnose cancer and, usually, a health practitioner will follow a range of screening procedures before diagnosis. According to the Mayo Clinic (2021), cancer screening starts with a physical exam, followed by laboratory and imaging tests and eventually a biopsy, which will confirm or reject the diagnosis. Laboratory tests are important during cancer screening because it reveals any abnormalities caused by cancer cells, such as the total blood count used to diagnose or detect Leukaemia (Mayo Clinic, 2021). 8-OHdG is a general biomarker of oxidative stress that is commonly used as a cancer biomarker (Wu *et al.*, 2016). Phosphatidylserine is also a general cancer cell biomarker (Sharma, 2018).

Other cancers such as prostate cancer can be identified by prostate-specific antigens and liver cancer by α-ferroprotein (Nour Eldin *et al.*, 2019). Another biomarker that is significantly increased in prostate, lung, cervical, and brain cancer is phosphocholine (Yang *et al.*, 2020).

In the context of breast cancer, Yang and colleagues (2020) identified a wide range of metabolomic biomarkers used in diagnosis, including elevated linoleic acids, increased choline, phosphocholine, leucine, valine, tyrosine, alanine, glutamine, and 5-methyluridine. Amino acids such as phenylalanine, tyrosine, serine, threonine, and methionine might be good diagnostic markers in gastric cancer (Xiao & Zhou, 2017), while Cancer antigen19-9 is a common biomarker for monitoring the progression and therapeutic response of pancreatic cancer (Zhang *et al.*, 2018).

2.6.3 Breast cancer

Breast cancer is the number one invasive cancer affecting women in South Africa (apart from non-melanoma skin cancer), one out of twenty-seven women of all races in South-Africa has a lifetime risk of breast cancer (CANSA, 2022). Breast cancer accounted for 0.7% of all deaths in South Africa in 2013 (CANSA, 2022). These statistics are concerning, and more research is required to better understand the aetiology thereof.

A study done on diagnostic strategies for breast cancer indicated that although 67% of the reported cases had warning signs of cancer, 70% of the positive mammogram cases were identified or found during routine screening, and not necessarily due to any symptoms or warning signs (Scheel & Holtedahl, 2015). This raises the question of whether it is possible to detect any breast lesions or tumours before it turns into breast cancer. Prognostic predictions always relied on morphological characteristics, but nowadays it also relies on molecular biomarkers such as aromatase expression, osteopontin, C-reactive protein, and methylation of paired-like homeodomain-2 (Kutomi et al., 2017).

As mentioned above, metabolic markers of breast cancer are also a novel approach in diagnosis, during a clinical study it was found that nitrogen, glutathione, cysteine-methionine, and other amino acid metabolic pathways tend to be significantly affected by breast cancer (Yang et al., 2020). Furthermore, a study done by Günter (2015) identified increased lactate, succinate, glycine, taurine, and carnitine derivatives in serum as well as altered phenylalanine, proline, lysine, and N-acetyl-cysteine levels in breast cancer patients.

2.7 Markers of oxidative stress

As seen in section 2.6.2, various biomarkers are used for different cancer types. Oxidative stress markers are commonly used in epidemiological studies and can be measured in various biological sample matrixes, and they are of specific interest in breast cancer studies (Lee *et al.*, 2017). Evidence showed that a high concentration of thiobarbituric acid reactive substances (TBARS) are present during breast cancer compared to normal physiological levels (Lira *et al.*, 2019).

Nour Eldin *et al.* (2019) highlighted the fact that serum diagnostic markers could not differentiate between breast cancer and benign breast lesions, making false positives a problem. They suggested that this could be overcome by measuring 8-OHdG as a confirmatory/surrogate marker of breast cancer (Nour Eldin, *et al.,* 2019). Several commonly used biomarkers of oxidative stress, including lipid products, protein biomarkers, and DNA damage markers have been identified as potential breast cancer biomarkers (Lee *et al.,* 2017).

2.7.1 Lipid peroxidation markers

During oxidative stress, the phospholipid bilayer becomes destabilised due to the formation of peroxyl radicals, which in turn can react with fatty acids to produce malondialdehyde (MDA) and ultimately isoprostanes (Preedy & Patel, 2015). MDA is the most studied lipid peroxidation marker and is formed during the oxidation of polyunsaturated fatty acids (PUFA) (Ho *et al.*, 2013; Il'yasova *et al.*, 2012; Shah *et al.*, 2014).

MDA is known to be remarkably reactive toward many proteins, lipoproteins, and some amino acids (Cui *et al.*, 2018; Tsikas, 2017a). It is also found that its concentration can be influenced by diet, making it an unreliable marker (Il'yasova *et al.*, 2012). In urine, MDA usually occurs in both free and conjugated forms, whereas only conjugated MDA is found in plasma (Tsikas, 2017a). Figure 2-4 illustrates the MDA formation from arachidonic acid. The number of MDA molecules formed depends on the number of methylene (-CH_2) groups in the molecule (Tsikas, 2017a).

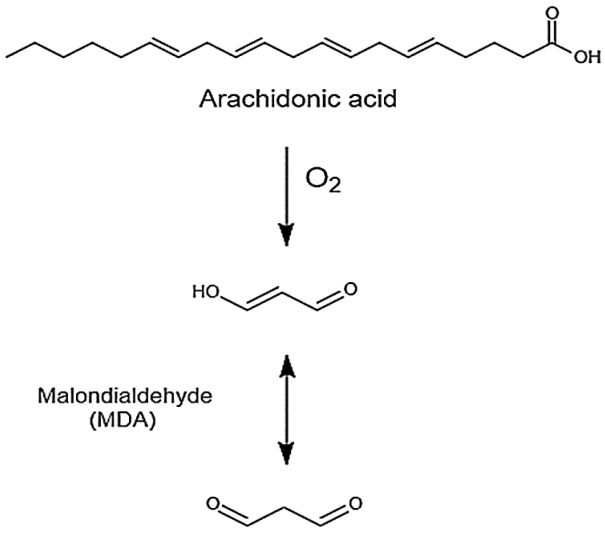

Figure 2-4. Formation of MDA from arachidonic acid (adapted from Martinez-Moral & Kannan, 2018).

Isoprostanes, on the other hand, are a group of prostaglandin-like compounds resulting from non-enzymatic lipid peroxidation (Čolak, 2008; Ho *et al.*, 2013; Milne *et al.*, 2011; Shah *et al.*, 2014). Isoprostanes are mostly formed from the peroxidation of arachidonic acid and may contribute to the impairment of cell membrane properties (Čolak, 2008; Il'yasova *et al.*, 2012). Isoprostanes are also stable compounds in all biofluids and can be found in both their esterified and unesterified forms (Langhorst *et al.*, 2010). Their concentrations are unaffected by diet, making them great oxidation-specific markers (Milne *et al.*, 2011; Montuschi *et al.*, 2004; Shah *et al.*, 2014). Preedy and Patel (2015) stated that even though isoprostanes are stable compounds, their concentrations in plasma or serum are affected by sample preparation or storage. Isoprostanoids are a class of prostaglandins, which includes multiple families of isoprostanes such as prostaglandin $F_{2\alpha}$, prostaglandin E_2 (PGE_2), prostaglandin D_2, prostaglandin I_2, and prostaglandin H_2 (Milatovic *et al.*, 2011). The formation of these isoprostanes is illustrated in Figure 2-5.

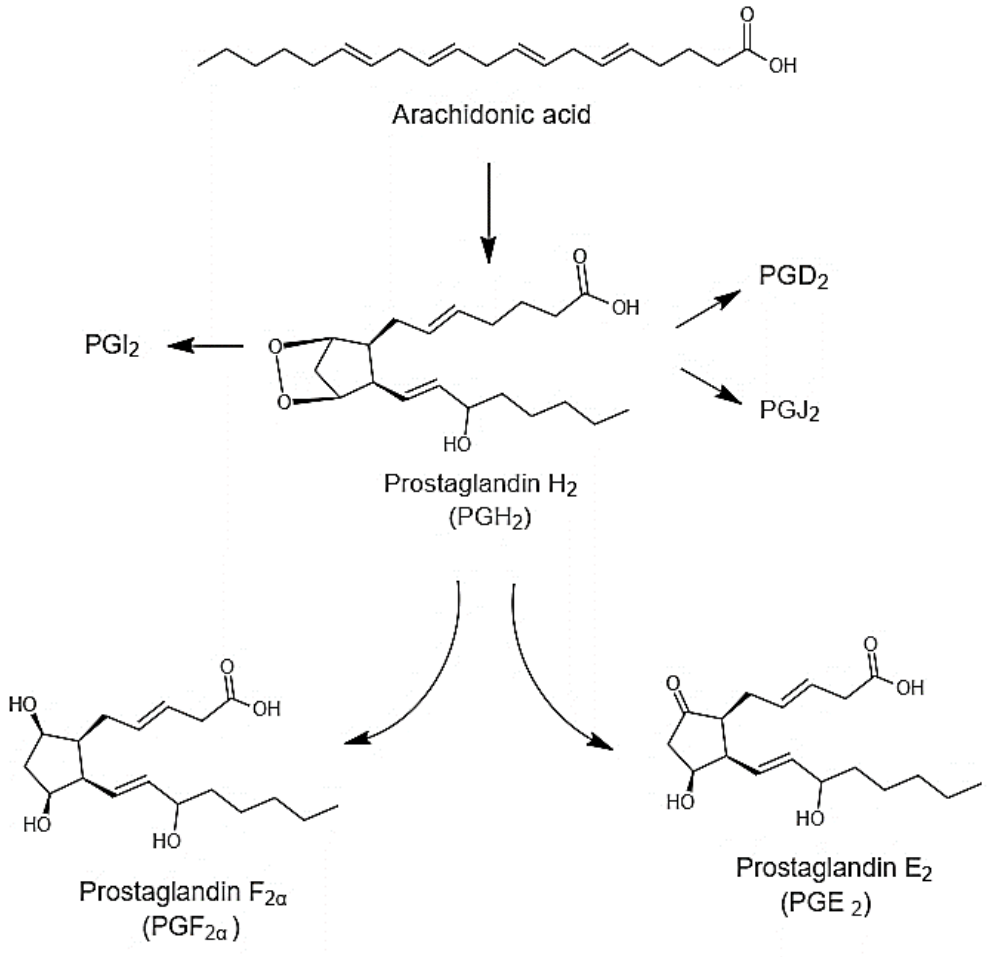

Figure 2-5. The formation of the isoprostanes from arachidonic acid (modified from Milne* et al.*, 2011).

The most common subfamily of isoprostanes is the $F_{2\alpha}$-family, of which 8-isoprostaglandin-$F_{2\alpha}$ ($PGF_{2\alpha}$) is the most studied isoprostane in oxidative stress studies (Montuschi *et al.*, 2004). The regio-isomeres are classified according to the position the radical link takes place on the molecule, as seen in Figure 2-6 (Preedy & Patel, 2015). Urinary $PGF_{2\alpha}$ is mostly produced from free radical catalysed peroxidation, making it the gold standard for *in vivo* oxidative stress studies, it is also more stable than PGE_2 or PGD_2 (Milne *et al.*, 2011; Montuschi *et al.*, 2004).

PGE_2 on the other hand is the most abundant prostanoid within the body (Wang *et al.*, 2019), which is formed competitively with $PGF_{2\alpha}$ (Milne *et al.*, 2011). PGE_2 is well correlated with oxidative stress (Udhesister, 2021), and is believed to play a role in cancer (Lone & Taskén, 2013). PGE_2 stimulates cancer growth by angiogenesis, inhibiting apoptosis, cell invasion, and metastasis (Filipenko *et al.*, 2016; Lone & Taskén, 2013). Therefore, PGE_2 is a biomarker to consider for this study.

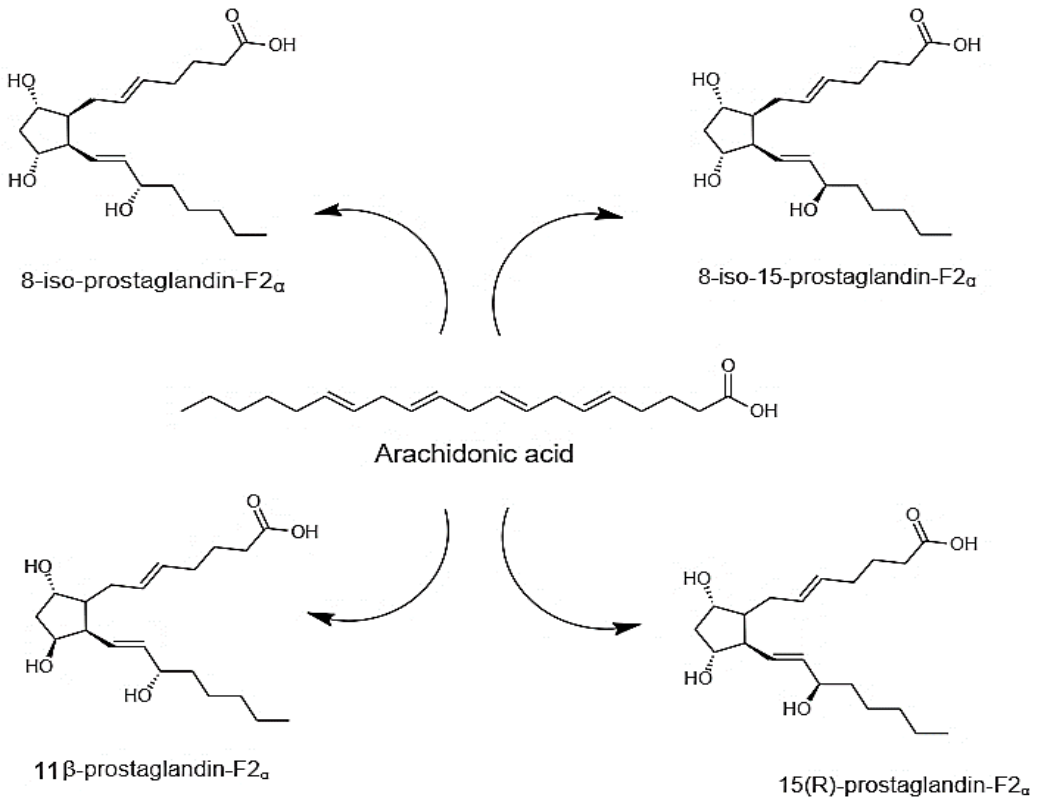

Figure 2-6. Illustration of the $F_{2\alpha}$-family (modified from from Martinez-Moral & Kannan, 2018).

4-hydroxynonenal (4-HNE) is another PUFA oxidation product (Kuiper & Stevens, 2011; Wu *et al.*, 2016), formed from arachidonic- and linoleic acids (Čolak, 2008; Il'yasova *et al.*, 2012; Shah *et al.*, 2014). Even though 4-HNE is highly reactive and can form adducts that may be cytotoxic or genotoxic, the compound itself is found to be weak mutagenic (Shrivastava *et al.*, 2019; Sonowal & Ramana, 2019; Wu *et al.*, 2016).

It is known that in low concentrations (<0.78 µg/ml), 4-HNE regulates the expression of GSH, an important antioxidant (Sonowal & Ramana, 2019). Sonowal & Ramana (2019) found that cysteine is the most susceptible amino acid to react with 4-HNE, but the HNE-histidine adducts tend to be more stable. Since 4-HNE can react with cysteine, it can undergo glutathione conjugation, where it is further metabolised to 4-hydroxy-2-nonenal-mercapturic acid (4-HNE-MA). (Kuiper & Stevens, 2011; Spickett, 2013; Wu *et al.*, 2016). Völkel and colleagues (2005) suggested that 4-HNE-MA is the main metabolic product of 4-HNE, and due to its stability in urine, it is a possible biomarker to consider when characterising oxidative stress profiles. The formation of 4-HNE and 4-HNE-MA can be seen in Figure 2-7.

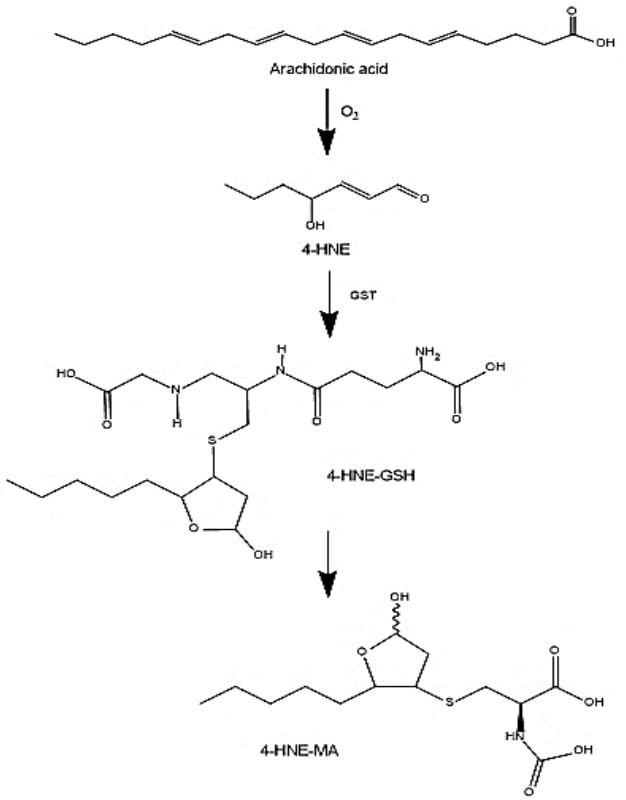

Figure 2-7. The formation of 4-HNE and 4-HNE-MA from arachidonic (adapted from Martinez-Moral & Kannan, 2018 and Alary* et al.*, 1995). *GST: Glutathione-S-transferase; 4-HNE-GSH: 4-hydroxynonenal-glutathione; 4-HNE-MA: 4-hydroxynonenal mercapturic acid.*

2.7.2 Protein damage markers

3-Nitrotyrosine (3-NT) is a chemically stable compound formed when nitrating agents ($ONOO^-$) react with the aromatic ring of tyrosine (Tsikas, 2012). When tyrosine reacts with hydroxyl radicals, carbon trioxide (CO_3), or oxo-metal complexes tyrosyl radicals are formed, which react with NO_2 to form 3-NT (Bothma, 2012). 3-NT is usually a product of dietary tyrosine molecules that underwent nitration in the gastrointestinal tract, making their presence unreliable to indicate nitrative stress (Cipak Gasparovic *et al.*, 2017; Tsikas, 2012). To overcome this challenge, Tsikas suggested cross-referencing the 3-NT concentrations with tyrosine levels, to compensate for the dietary effect (2012).

A popular protein-oxidation product is dityrosine (dityr), a modified, cross-linked amino acid formed from tyrosyl radicals (Bucknall, 2006; Il'yasova *et al.*, 2012). Dityr was discovered by Gross & Sizer as a product of a horseradish peroxidase catalysed reaction between tyrosine and hydrogen peroxide (Malencik & Anderson, 2003). Tyrosyl radicals undergo radical isomerisation and then a diradical reaction occurs. Finally, enolisation takes place and dityr is formed (Orhan *et al.*, 2005). Dityr formation normally occurs from UV irradiation, nitrative stress, peroxidase-catalysed reactions, and hydroxyl radicals, but their concentrations can be influenced by diet as well as pH (Bhattacharjee *et al.*, 2001; DiMarco & Giulivi, 2007; Malencik & Anderson, 2003; Pisoschi & Pop, 2015).

Compared to lipid peroxidation, protein oxidation markers are formed much faster and more linear, making them more sensitive oxidation markers (Čolak, 2008), even though their concentrations are influenced by diet (Chao *et al.*, 2015). It is also found that multiple protein oxidation products can be formed simultaneously under nitrative stress (Malencik & Anderson, 2003). Both 3-NT and dityr are representative of the turnover of nitrated proteins, as seen in Figure 2-8 (DiMarco & Giulivi, 2007; Ho *et al.*, 2013; Mongirdienė *et al.*, 2019; Vanova *et al.*, 2018). These compounds are, therefore, seen as good biomarkers of protein damage.

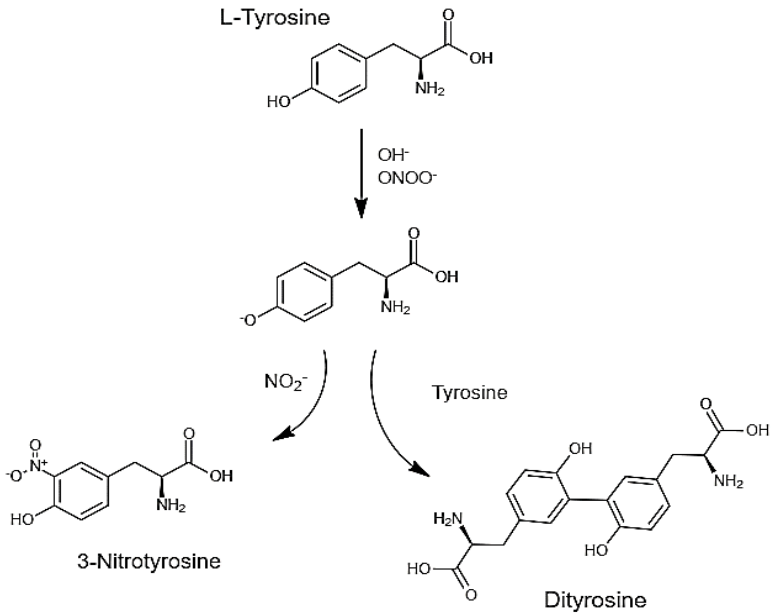

Figure 2-8. The formation of 3-Nitrotyrosine and dityrosine when tyrosine undergoes oxidative stress (modified from DiMarco & Giulivi, 2007).

2.7.3 DNA oxidation

As mentioned in section 2.4.3 oxidative stress on a cellular level can lead to various sorts of DNA damage. Some of the most studied DNA oxidation markers include 8-dihydroguanine (8-oxoGua) and 8-OHdG (Il'yasova *et al.*, 2012; Preedy & Patel, 2015). Since 8-OHdG has been identified as a marker of cancer risk (Dabrowska & Wiczkowski, 2017; Nour Eldin *et al.*, 2019), it will be discussed in more detail below.

When hydroxyl radicals attack the guanine base on the eighth carbon, the 8-OHdG adduct is formed, as seen in Figure 2-9 (Fan *et al.*, 2012). Repair mechanisms cleave off the formed adduct and it ends up in circulation, where it will be excreted in urine (De Martinis, 2002; Dokumacioglu *et al.*, 2018). During DNA replication 8-OHdG can transform GC pairs into TA pairs, which may contribute to mutagenesis and lead to cancer initiation (Saha *et al.*, 2017). The exact mechanism of 8-OHdG formation is still unknown, although several possible mechanisms were suggested by Dabrowska and Wiczkowski (2017). The formation of 8-OHdG is not influenced by factors such as cell death or diet, making it an oxidative stress-specific marker that is stable in urine (Il'yasova *et al.*, 2012). Genomic instability is mostly caused by oxidative damage to DNA molecules, therefore 8-OHdG is a sensitive marker of oxidative stress, mutagenesis, and cancer risk (De Martinis, 2002; Fan *et al.*, 2012; Maiti & Nazmeen, 2019).

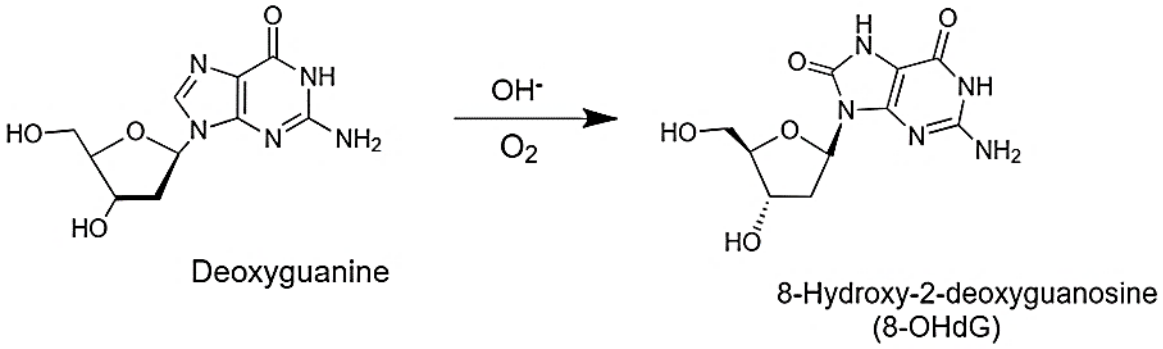

Figure 2-9. The formation of 8-OHdG (adapted from Martinez-Moral & Kannan, 2018).

2.8 Combined oral contraceptives and oxidative stress

Common risk factors for breast cancer include inactivity, obesity, excessive alcohol consumption, and oral contraceptive use (Ji *et al.*, 2019). Although all these risk factors can be associated with oxidative stress, combined oral contraceptive (COC) usage is of specific interest to this study.

Preliminary results from an ongoing study about estrogen metabolism, biotransformation, and oxidative stress status (eBOSS study) by our group, indicate that the use of COCs induces oxidative stress in women.

2.8.1 Combined oral contraceptives

COCs are hormonal products that contain a combination of estrogen and progestin (Sitruk-Ware & Nath, 2013). These pills are commonly prescribed for birth control, as well as various menstrual cycle disorders such as abnormal uterine bleeding, and endometriosis (Anjum *et al.*, 2019). These pills are classified as xenobiotics since they are foreign to the body (Patel & Sen, 2013) and, they can undergo Phase I and Phase II biotransformation in the liver (Figure 2-2). Elevated levels of natural and synthetic estrogens tend to increase carcinogenicity (NCI, 2015; NTP, 2011; Roy *et al.*, 2007).

2.8.2 COC induced oxidative stress and cancer

The International Agency for Research on Cancer confirmed the carcinogenic effects of COCs (Del Pup *et al.*, 2019; Graafland *et al.*, 2020). In 2002, COCs were listed as human carcinogens by the U.S. National Toxicology Program, and in 2003 a study based on COC use identified increased breast cancer risk among COC users (NCI, 2015; Roy *et al.*, 2007).

However, the extent to which it increases breast cancer risk is still unknown (Anjum *et al.*, 2019; Ji *et al.*, 2019; Sawicka *et al.*, 2017). The study by Del Pup *et al.* indicated that COCs increase the risk of estrogen receptor (ER) and progesterone receptors (PR) negative breast cancer, whereas progestogen-only contraceptives increase ER and PR positive breast cancer (2019). Controversy exists around this topic and other studies indicate that COCs have a neutral risk in breast cancer formation (Graafland *et al.*, 2020). However, it is important to realise that lifestyle factors as mentioned earlier may also alter the COC-induced risk (Del Pup *et al.*, 2019). Ji and colleagues (2019) highlighted that oral contraceptive use decreased the risk of colorectal, cervical, and endometrial cancer, but the risk of breast cancer is still unknown. Figure 2-10 summarises the possible role of COCs in cancer initiation, with the emphasis on the protein and DNA adducts formed from the free radical intermediates. Figure 2-10 depicts the non-hormonal pathway, in which estrogens serve as chemical carcinogens and result in cancer-causing mutations (Cavalieri & Rogan, 2014).

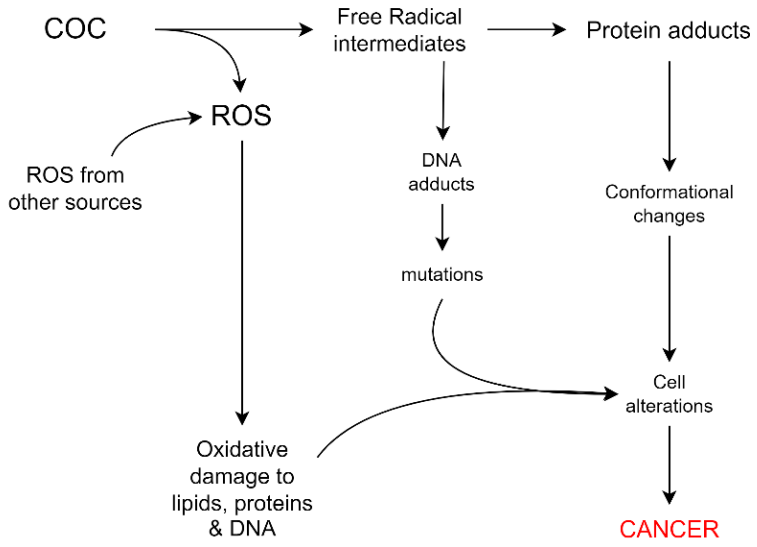

Figure 2-10. Role of combined oral contraceptives in cancer initiation (modified from Islam, 2018). *COC: Combined Oral Contraceptives; ROS: Reactive Oxygen Species.*

2.8.3 Natural estrogen contribution to oxidative stress

Two potential mechanisms — one hormonal and the other non-hormonal — are linked to estrogen-induced cancer (Cavalieri & Rogan, 2014). Estrogens bind to estrogen receptors, which set the hormonal mechanism in motion. Numerous signals that promote cell growth are produced, and when those signals are mediated, a genotoxic event occurs. The latter is required for the genetic material to be permanently altered and eventually for cancer to start (Cavalieri & Rogan, 2014).

Estrone (E_1) and estradiol (E_2) are found to be epigenetic carcinogens and their metabolic products are endogenous chemical carcinogens (Cavalieri & Rogan, 2014). A previous study identified that both androgens and estrogens contribute to breast cancer risk, based on a dose-response relationship (Cavalieri *et al.*, 2006).

During Phase I metabolism, E_1 and E_2 are converted to catechol estrogens (CE) (Maiti & Nazmeen, 2019), these CEs undergo further oxidation, which results in semi-quinone and quinone formation under the presence of transition metals (Cu^{2+}, Fe^{2+}) (Cavalieri *et al.*, 2006). Figure 2-11 illustrates the metabolic fate of estrogen, which can involve two different pathways. The major CEs formed are 2-hydroxy estrone-estradiol (2-$OHE_1(E_2)$) and 4-hydroxy estrone-estradiol (4-$OHE_1(E_2)$) (Cavelieri *et al.,* 2006). 4-$OHE_1(E_2)$ is oxidised in the presence of Fe^{2+} to form 4-hydroxy estrone-estradiol semi-quinone ($E_1(E_2)$-3,4-SQ), which undergoes further oxidation to form 4-hydroxy estrone-estradiol quinone ($E_1(E_2)$-3,4-Q). $E_1(E_2)$-3,4-Q can then react with DNA molecules and form DNA adducts. These adducts generate apurinic sites that can transform cells and possibly initiate cancer (Cavalieri *et al.,* 2006; Cavalieri & Rogan, 2014). 2-$OHE_1(E_2)$ also undergoes the same metabolic pathway as 4-$OHE_1(E_2)$, but the depurinating adducts are formed to a lesser extent (Cavalieri & Rogan, 2014). Therefore, a disruption of estrogen metabolism homeostasis, can lead to the excessive formation of catechol quinones and possibly cancer initiation (Cavalieri & Rogan, 2014).

Estrogen metabolism also contributes to additional ROS formation as indicated in Figure 2-11 (Jacobs, 2018). During the conversion of semi-quinones to quinones, $^{\bullet}O_2^-$ and $^{\bullet}OH$ are generated, and this ROS participates in a radical cascade reaction that results in damaging effects on lipids, proteins, and DNA (Cavalieri *et al.*, 2006; Maiti & Nazmeen, 2019). The CEs are inactivated by various conjugation reactions such as methylation, sulfation, and glucuronidation, GSH conjugation also occurs to prevent CE-quinones from interacting with DNA (Cavalieri *et al.*, 2006; Cavalieri & Rogan, 2014). Compared to synthetic estrogens, natural estradiol has a reduced effect on hepatic metabolism (Klipping *et al.*, 2021).

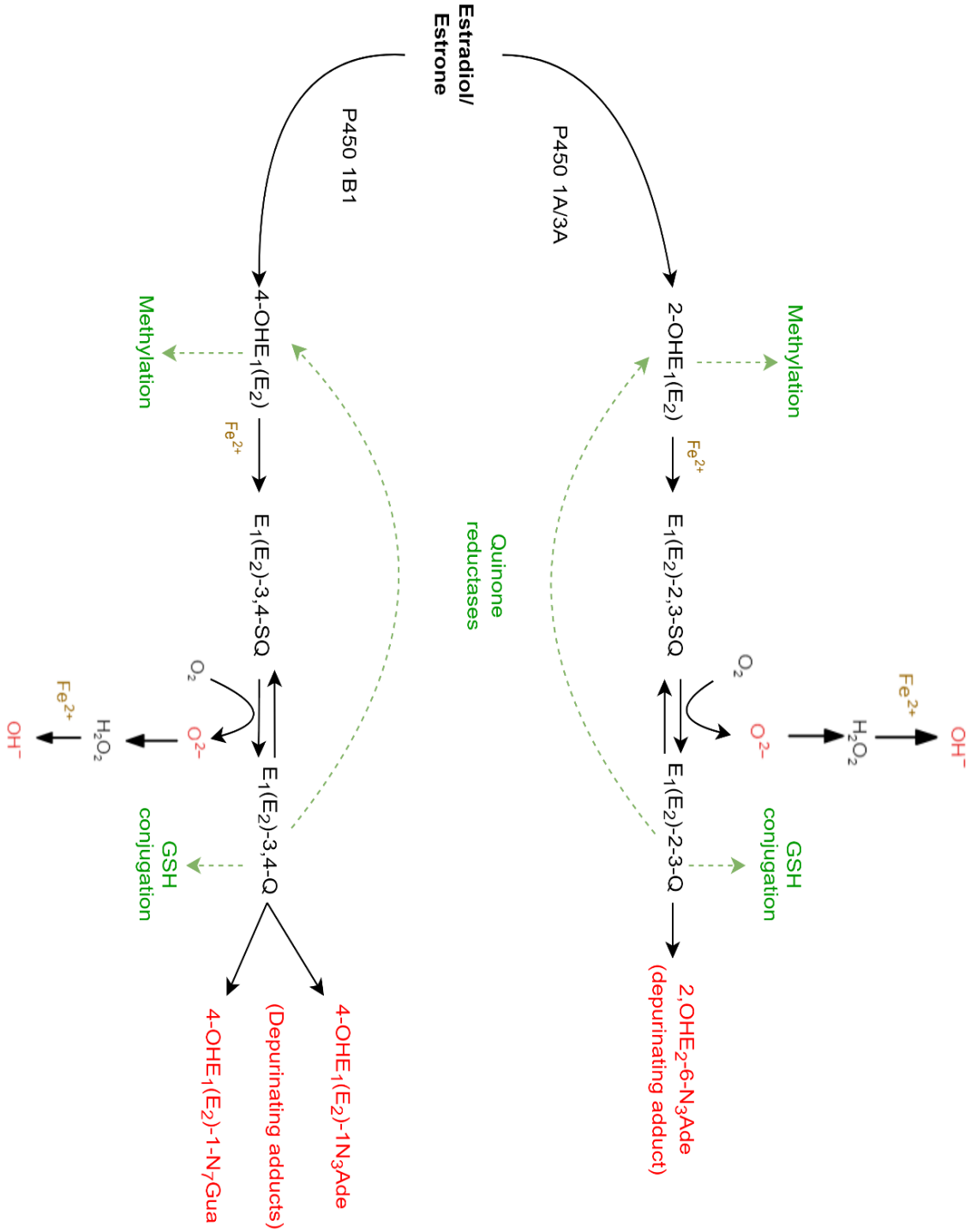

Figure 2-11. Estrogen metabolic pathway (modified from Cavalieri, 2006). The green indicates antioxidant and conjugation mechanisms to prevent DNA damage, whereas the red indicates the damaging adducts, as well as ROS formation. The brown indicates co-factors, and black the general reactions and products *P450: Cytochrome P450; 2-OHE$_1$(E$_2$)): 2-hydroxy estrone-estradiol; 4-OHE$_1$(E$_2$)): 4-hydroxy estrone-estradiol; E$_1$(E$_2$)-3,4-SQ: hydroxy estrone-estradiol semi-quinone; E$_1$(E$_2$)-3,4-Q: 4-hydroxy estrone-estradiol quinone; E$_1$(E$_2$)-2,3-SQ: hydroxy estrone-estradiol semi-quinone; E$_1$(E$_2$)-2,3-Q: 4-hydroxy estrone-estradiol quinone.*

2.8.3.1 Synthetic estrogen contribution to oxidative stress

Synthetic estrogens are chemically synthesised compounds that have estrogenic activity (Gupta, 2020). Synthetic estrogens (mestranol, ethinyl estradiol, estradiol valerate) differ from natural estrogens based on their chemical structures (Delgado & Lopez-Ojeda, 2021; Hilakivi-Clarke *et al.*, 2013). Ethinyl estradiol is of specific interest because it is commonly utilised in COCs as well as hormone replacement therapy (Telfer, 2019). Ethinyl estradiol (also known as 17α-ethinyl estradiol) has been found to be a powerful synthetic estrogen with a ten-fold higher binding potential to ERs than natural estrogens (Bhandari *et al.*, 2015). Telfer (2019) also indicated that less ethinyl estradiol is needed to produce the same effect as natural estrogen, establishing its effectiveness. Klipping and colleagues (2021) found that natural estradiol and progesterone were suppressed during COC use, leading to the hypothesis that the natural estrogen metabolism pathway is also suppressed.

The primary endpoints of the Women's Health Initiative launched by the National Institute of Health (NIH) where combined hormone therapy was applied, were invasive breast cancer and coronary heart disease (Hilakivi-Clarke *et al.*, 2013). In a study led by Yang (2015), higher breast cancer development was associated with COC use containing ethinyl estradiol, supporting the study of the NIH. However, other studies indicated that the increased breast cancer risk decreased over a time of 10 years after the women had stopped using COCs (Hilakivi-Clarke *et al.*, 2013). Over time the concentration of estrogens and progestins in COCs was decreased to reduce the risk of cardiovascular disease (Fruzzetti *et al.*, 2012), but the effect on breast cancer risk remains controversial.

2.9 Analysis of oxidative stress markers

Studies on oxidative stress began in the early 1950s but rapidly expanded in the late 1980s (Phaniendra et al., 2015). Analysis of several biomarkers is essential because there is no one recognised optimal biomarker for oxidative stress. These biomarkers have been measured using a variety of analytical techniques as described below (Griendling et al., 2016; Martinez & Kannan, 2018; Orhan et al., 2004; Vanova et al., 2018; Wu et al., 2016).

Usually, ROS and oxidative stress are measured using chemical assays, with electron paramagnetic resonance (EPR) being the most direct detection method (Griendling *et al.*, 2016; Rahman & Biswas, 2004). EPR spectroscopy is utilised to detect $^{\bullet}O_2^-$, $^{\bullet}OH$, and NO in biological samples (Griendling *et al.*, 2016). Free radicals can also be analysed using the cytochrome c reduction assay, the nitro blue tetrazolium assay, and other fluorometric techniques (Griendling et al., 2016). *In vivo* redox imaging and glutathione: glutathione disulphide ratio on the other hand are popular methods to measure the redox state (Griendling *et al.*, 2016).

RNS is detected with colorimetric assays, such as the Griess reaction, fluorescent assays, EPR-based techniques, or chemiluminescence (Griendling *et al.*, 2016). One problem faced with all these methods is the degradation/oxidation of biological molecules during sample preparation, contaminants present in laboratory reagents, and other reactions that may lead to a variety of end products (Griendling *et al.*, 2016).

Since secondary oxidation products reflect the turnover of oxidative damage, they serve as good biomarkers of oxidative stress (Il'yasova *et al.*, 2012). A biomarker is mostly defined as any molecule that acts as an objective indicator of certain biological states, such as pathogenic processes and pharmacologic responses (Ho *et al.*, 2013; Preedy & Patel, 2015). Good biomarkers should be sensitive and localised to the site of damage, analytically stable in a biological matrix, associated with a known mechanism, and detectable before histopathological damage (Gârban *et al.*, 2005; Robinson *et al.*, 2008).

Even though there are numerous, well-established analytical techniques for measuring various oxidative stress biomarkers, the simultaneous detection of multiple oxidative stress biomarkers is a novel and difficult analytical technique. Given that different biomarkers have varying chemical structures and properties, it is important to take several factors into account while developing these assays to get the best results for all relevant analytes. These factors include the best biological material to use, sample preparation and purification methods, and the chosen analytical techniques.

2.9.1 Biological material

For the measurement of oxidative stress biomarkers, biological matrices such as urine, tissue, and blood (plasma/serum) are frequently used (Barbosa et al., 2020; DiMarco & Giulivi, 2007; Milne et al., 2011; Schwedhelm et al., 2007; Tsikas, 2017a). Since urine has a low organic and inorganic metal content, and most oxidation products are excreted at measurable levels, making it a reliable matrix (Il'yasova *et al.*, 2012). The availability, quantity, and non-invasive collection of urine also make it the ideal matrix to use (Hecht, 2002; Martinez-Moral & Kannan, 2019). According to research by Čolak (2008) and Langhorst et al. (2010), some substances, such as isoprostanes, are less likely to undergo auto-oxidation in urine.

Tsikas et al. (2017a) also discovered that lipid peroxidation products are more stable in urine than in plasma. These lipid peroxidation products also tend to have up to 40 times higher concentrations in urine than other biofluids (Langhorst et al., 2010). The concentration of urine, however, varies from person to person, for this reason creatinine values are used as a corrective index for the fluctuation of urinary analytes (Preedy & Patel, 2015).

Urine is also a highly polar biofluid containing various salts, phosphates, proteins, metabolic products, and phosphates (Britannica, 2019; Folin, 1905; Siener & Hesse, 2002) and therefore, a preliminary purification step is required to eliminate the unwanted analytes.

2.9.2 Derivatisation

Besides a preliminary purification step, some analytes such as MDA or tyr require derivatisation to increase their detection properties, especially during ionisation (HTA, 2016; Jacobs, 2018). Derivatisation entails chemical reactions that alter the structure of a compound to facilitate its detection, separation, or isolation (Poole, 2013). Derivatisation improves the ionisation efficiency of compounds, as well as improving the selectivity and separation, which in turn improves the sensitivity and the general data quality of a method (Qi *et al.*, 2014).

MDA, which is unstable in its free form, can easily be derivatised with thiobarbituric acid (TBA) or 2,4-dinitrophenylhydrazine (DNPH) (Cui *et al.*, 2018; Martinez & Kannan, 2018; Tsikas, 2017a). DNPH is the most used derivatisation agent for ketones and aldehydes (Clark, 2013). DNPH reacts with the carbonyl group on compounds, leading to the formation of DNP-hydrazone derivatives (Uchiyama *et al.*, 2011). This derivatisation technique is extremely specific for carbonyl groups in ketones and aldehydes and does not interact with those containing amides or carboxylic esters (Uchiyama *et al.*, 2011). The general reaction of DNPH derivatisation is illustrated in Figure 2-12. A and the DNPH derivatisation of MDA is presented in Figure 2-12. B.

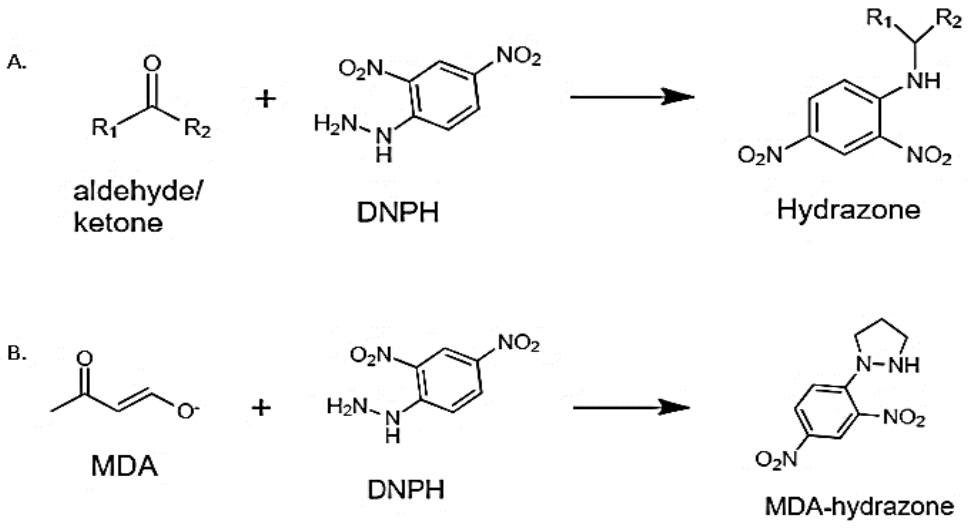

Figure 2-12. Derivatisation with DNPH. A. General schematic of DNPH reaction with aldehydes or ketones. B. Schematic of DNPH reaction with MDA (modified from Chen, 2011). *DNPH: 2,4-dinitrophenyl hydrazine; MDA: malondialdehyde.*

The TBARS assay, however, lacks sensitivity and specificity, and it also requires more extensive temperatures compared to DNPH (Tsikas, 2017a). To compensate for the lack of sensitivity and specificity, the TBARS assay can be applied as a derivatisation technique and analysed on a mass spectrometer. The TBA reacts with the carbonyl groups of the aldehydes. Figure 2-13 illustrates the reaction between TBA and aldehydes to form TBA-derivatives.

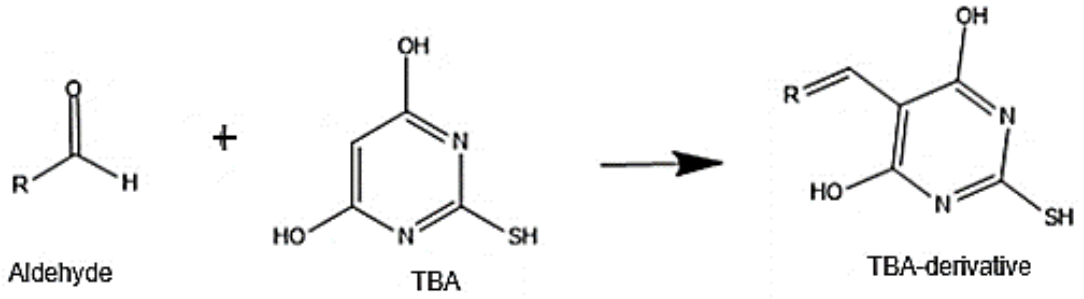

Figure 2-13. Reaction taking place during the TBARS assay (modified from Zhang* et al.*, 2010).

When considering reverse phase HPLC (RPLC) polar compounds, such as tyrosine, exhibit poor retention (Harder *et al.*, 2011; Qi *et al.*, 2014; Zhao & Li, 2020), and, therefore, chemical modification may be required.

The derivatisation reagents phenyl isothiocyanate, alkyl chloroformate, n-butanol, o-phtalaldehyde, and dansyl chloride all improve the sensitivity and selectivity of amino acid detection (Harder et al., 2011; Zhao & Li, 2020). The formation of butyl esters occurs when N-butanol:acetyl chloride and compounds containing carboxyl groups, such as amino acids, react under mild conditions (Figure 2-14.).

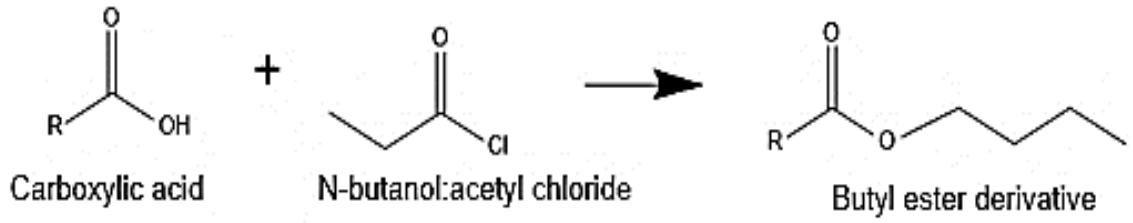

Figure 2-14. Derivatisation with N-butanol:acetyl chloride (adapted from Wright* et al.*, 1997).

2.9.3 Extraction

Solid-phase extraction (SPE) is a common purification technique used in oxidative stress studies, especially before high-performance liquid chromatography-mass spectrometry (HPLC-MS) (Chen & Chiu, 2008; Langhorst *et al.*, 2010; Martinez & Kannan, 2018; Schwedhelm *et al.*, 2007; Vanova *et al.*, 2018; Wu *et al.*, 2016). Except for extracting wanted analytes, SPE has the advantage of decreasing ion suppression, which is caused by the matrix effect with co-eluting components (Kushnir *et al.,* 2011). Lastly, SPE also increases analyte concentrations (Waters, 2018).

During SPE, the sample is passed through a small disposable cartridge packed with a stationary phase like the HPLC column (Figure 2-15). Adsorption reactions between the analytes of interest and the stationary phase take place as the sample passes through (Wilson & Walker, 2010). Compounds with weaker interactions are washed out, and the compounds with stronger interactions are retained. The retained analytes can be obtained by applying a wash solvent that can either change the pH leading to elution or by disrupting the binding mechanisms (Sigma Aldrich, 1998). The stationary phase in the SPE cartridges depends on the type of molecules of interest (Harvey, 2000). Normal phase SPE relies on hydrophilic interactions, whereas reversed phase relies on hydrophobic interactions to separate analytes, and ion exchange SPE utilises electrostatic attraction (Sigma Aldrich, 1998). Compared to other sample clean-up techniques such as liquid-liquid extraction, SPE has higher recoveries, fewer emulsion problems, and is suitable for smaller sample sizes (Jacobs, 2018).

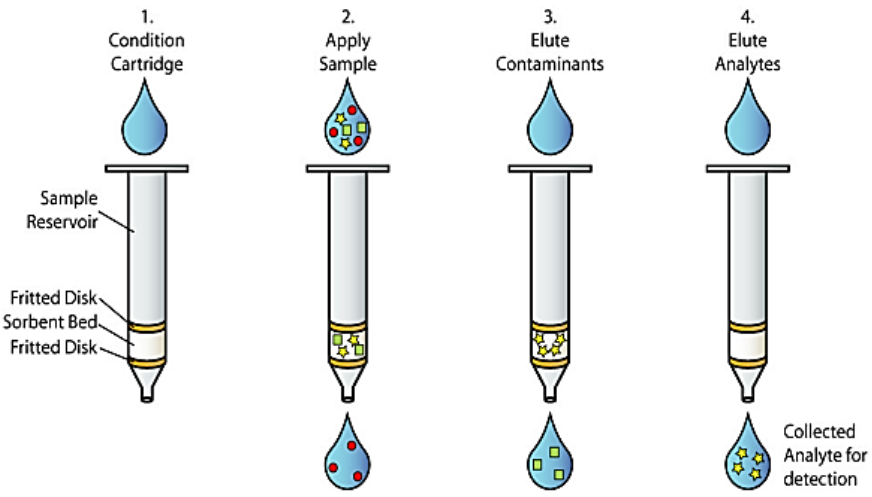

Figure 2-15. Illustration of SPE steps (Watkinson, 2008).

2.9.4 Separation and detection

HPLC-ESI-MS/MS is a sensitive, selective, and accurate technique that requires minimal sample preparation (Griendling *et al.*, 2016; Langhorst *et al.*, 2010; Ohashi & Yoshikawa, 2000; Schwedhelm *et al.*, 2007). Separation of analytes occurs according to their interactions with the mobile phase and stationary phase during HPLC (Wilson & Walker, 2010). Factors such as diffusion, adsorption, ion-pairing, molecule exclusion, etc. influence these interactions (Wilson & Walker, 2010). Therefore, one should carefully consider the chemical properties of the analyte(s) to be analysed. During normal phase HPLC, separation is based on polarity. The stationary phase is polar, and the mobile phase is non-polar, which will allow the polar compounds to be retained on the column (Thammana, 2016). Due to the polarity of our metabolites of interest, this study will be using RPLC, where the mobile phase is polar and the stationary phase is non-polar, leaving the non-polar compounds retained on the column (Chawla & Chaudhary, 2019). There are two methods of separation during RPLC, namely isocratic and gradient separation (Wilson & Walker, 2010). During gradient separation, the mobile phase composition gradually changes, whereas the composition stays the same during isocratic separation (Chawla & Chaudhary, 2019; Wilson & Walker, 2010).

To record the presence of analytes after separation on the column, a detector is required (Wilson & Walker, 2010). There is a variety of detectors that can be used. The most common detectors are known to be UV detectors, mass spectrometers, and fluorescence detectors (Kishikawa *et al.*, 2019; Wilson & Walker, 2010). One of the advantages of using mass spectrometers as detectors is that the compounds are detected whilst structural information is obtained at the same time (Wilson & Walker, 2010). Once the sample emerges from the column the sample is converted to gaseous ions that are further separated according to their mass-to-charge ratio (m/z) and detected (Wilson & Walker, 2010). The conversion of the sample to gaseous ions is called ionisation (Siuzdak, 2004), and can involve various techniques as discussed by Wilson and Walker (2010).

Electro spray ionisation (ESI) is known to be a soft ionisation technique used for the analysis of proteins, DNA, carbohydrates, lipids, and synthetic polymers (Siuzdak, 2004; Wilson & Walker, 2010). This soft ionisation is achieved through a spray of charged liquid droplets produced by nebulisation (Wilson & Walker, 2010). As the solvent elutes from the column, a high voltage (2-6 kV) is applied to the tip of a metal capillary relative to the surrounding heated capillary, as seen in Figure 2-16 (Banerjee & Mazumdar, 2012).

The strong electrical field causes dispersion of the sample solution into an aerosol of highly charged electrospray droplets (Banerjee & Mazumdar, 2012; Wilson & Walker, 2010). Nitrogen gas is applied as both sheath and drying gas.

The sheath gas increases nebulisation and helps to direct the spray emerging from the capillary tip towards the mass spectrometer (MS) (Banerjee & Mazumdar, 2012). The size of the droplets diminishes due to evaporation, facilitated by the drying gas. The ions are then eventually released from the droplets (Banerjee & Mazumdar, 2012; Wilson & Walker, 2010). ESI can be summarised as the effect of the strong electrical field that acts on the surface of the sample solution (Wilson & Walker, 2010).

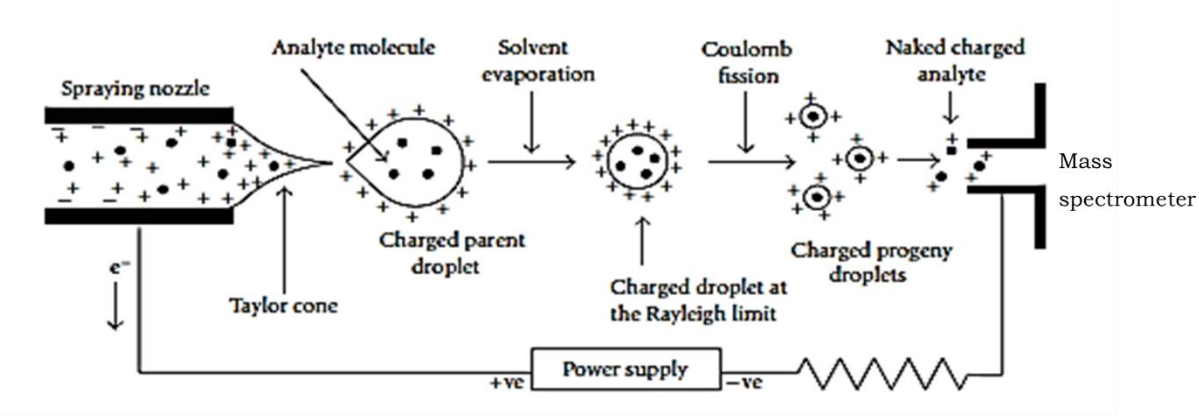

Figure 2-16. Illustration of electrospray ionisation (Banerjee and Mazumdar, 2012).

A continuous electrical field is formed between the rods in the mass analyser, which forces the ions to move toward the detector (Wilson & Walker, 2010). This electrical field can be precisely controlled such that ions with a specific m/z ratio can be detected (Wilson & Walker, 2010). The ions that do not have that specific m/z ratio collide with these rods and are eliminated (El-Aneed *et al.*, 2009). The triple quadrupole (MS/MS) is of specific interest since it is cost-effective, robust, and can analyse biomolecules easily (El-Aneed *et al.*, 2009). This MS consists of three quadrupole systems as seen in Figure 2-17 (Shi *et al.,* 2012).

The first system (Q1) selectively separates ions with a specific m/z (usually the precursor ions), but instead of detecting these ions, they are passed through to the second system (Q2), also known as the collision cell (CID) (El-Aneed *et al.*, 2009; Wilson & Walker, 2010). In the collision cell, the ions are subjected to fragmentation with the help of collision gas. From here, the fragmented ions are channelled to the third system (Q3) which acts as a second mass analyser, the fragmented ions are again separated based on a specific m/z ratio (El-Aneed *et al.*, 2009; Wilson & Walker, 2010). The ions are detected and displayed as a mass spectrum or chromatogram, which plots the relative abundance of each m/z ratio (Banerjee & Mazumdar, 2012; Wilson & Walker, 2010). It is assumed that the abundance of the peak is directly proportional to the number of ions detected (Banerjee & Mazumdar, 2012).

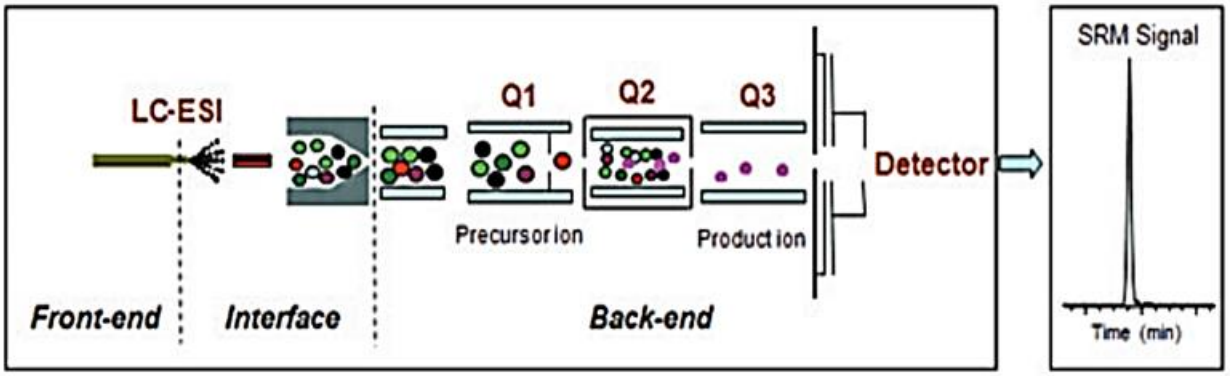

Figure 2-17. Illustration of mass spectrometer resulting in a chromatographic peak (Shi et al., 2012).

During HPLC-MS/MS an internal standard (IS) is generally used to quantify the target compounds with. A good IS mimics the response and separation of the target compounds (Meng & Bennett, 2012), as it should have similar characteristics of the target compound. Internal standards are known to increase the accuracy and precision of a method (Oliveira *et al.*, 2010), as it compensates for any loss during sample preparation (Prichard & Barwick, 2003).

2.10 Method validation

Even though LC-ESI-MS/MS methods result in great sensitivity and selectivity, validation is still required to ensure the method is suitable for its intendent purpose (United Nations Office on Drugs and Crime, 2009) before implementing the method. A standardised set of experimental tests are followed during method validation (United Nations Office on Drugs and Crime, 2009), including linearity, accuracy, precision, stability, recovery, etc.

2.10.1 Linearity

According to Wal and colleagues (2010), linearity is the ability of an analytical procedure to produce results which are proportional to the concentration of the analyte within the sample. Linearity is determined by analysing six quality control samples with a concentration range consisting of 80 - 120% of the expected concentration range (Lynch, 2016). The response of these samples is illustrated on a calibration curve, the least squares regression linear model can then be used to determine linearity. Calibration curves are constructed by plotting the response area of the metabolite/area response of the internal standard against the theoretical concentration of the metabolite/internal standard concentration, a procedure is considered linear when a coefficient of determination (r^2) is close to 1 ($r^2 > 0.995$) as displayed in Figure 2-18 (Lynch, 2016).

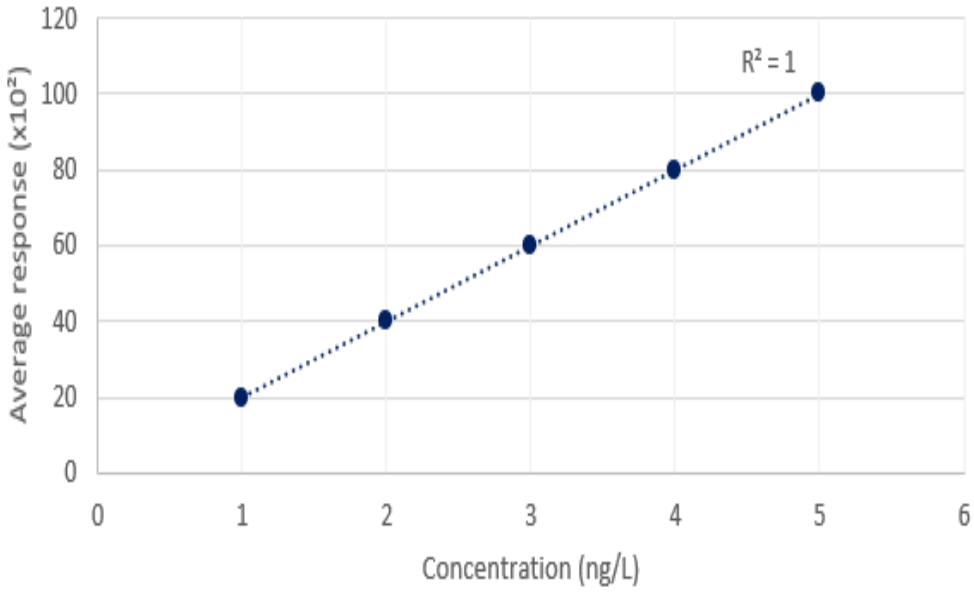

Figure 2-18. Calibration curve with perfect linearity.

2.10.2 Limits of detection & quantification

The limit of detection (LOD) is the smallest measurement that can be detected with acceptable confidence (Sanchez, 2018), but not quantitated to an exact value (APVMA, 2004), whereas the limit of quantification (LLOQ) is the smallest measurement that can be confidently detected whilst meeting predefined goals for imprecision and bias (Armbruster & Pry, 2008). The upper limit of quantification (ULOQ) is the highest concentration that can be confidently quantified whilst meeting the same predefined goals for imprecision and bias (Wal *et al.,* 2010). The detection and quantification limits can be calculated from the linear ranges based on standard deviation using the Equation 2-1 and Equation 2-2 (Ismail *et al.*, 2014). Where *m* is the slope of the calibration curve, and *σ* is the standard deviation (calculated from y-residuals and y-intercepts of the regression line of the linear range).

Equation 2-1. The formula for calculating limit of detection.

$$LOD = \frac{3.3(\sigma)}{m}$$

Equation 2-2. The formula for calculating the limit of quantification.

$$LOQ = \frac{10(\sigma)}{m}$$

2.10.2.1 Sensitivity

Sensitivity represents how sensitive the instrument is for detecting the desired metabolite. Instrument sensitivity can be determined by measuring the detection limits of the instrument, especially the LLOQ (Wal *et al.,* 2010). The LLOQ can be determined by analysing a concentration series of each metabolite, from which the standard deviation and mean are calculated. The standard deviation of the chosen concentration should be < 20% to qualify as a limit of detection (Lynch, 2016). This deviation can be calculated by dividing the standard deviation by the mean of the measured calibration curves and multiplying the value by 100 to get a percentage (Rao, 2018).

2.10.3 Accuracy

Accuracy of a method is known to be the degree to which the evaluated value corresponds to the true value within the sample (Lynch, 2016). Accuracy is normally assessed by a recovery analysis which includes analysing five determinations for three concentration levels, spiking each sample with a known concentration and re-analysing them (Lynch, 2016).

The three concentrations levels should differ from the calibration concentrations. The accuracy can be calculated by using Equation 2-3. Accuracy can also be expressed as an estimation of error (relative error), where the deviation from the target concentration is calculated (Equation 2-4) (Onyango & Plews, 1987).

Equation 2-3. Formula used to calculate the accuracy of a method as described by Wal et al. (2010) .

$$accuracy\ (\%) = 100\ \times \frac{average\ concentration}{nominal\ concentration}$$

Equation 2-4. Formula used to calculate the deviation of the measurements from the theoretical concentration (Onyango & Plews, 1987).

$$relative\ error\ (\%) = 100\ \times \frac{(nominal\ concentration - measured\ concentration)}{nominal\ concentration}$$

Accepted accuracy lies between 85-115%, and the average concentration should not deviate more than 15% from the nominal concentration (Lynch, 2016). Accuracy can be an estimation of stability, although it doesn't identify under which conditions stability may be altered (Rao, 2018).

2.10.4 Precision

Precision represents the degree of scatter of analytical results between a series of replicate measurements, and it is a represents the repeatability of a method (Lynch, 2016). A standard addition recovery analysis is used to determine the precision. The percentage precision is calculated with Equation 2-5. A method is accepted as precise/repeatable if the precision percentage is lower than 20% for the LLOQ, and 15% for the other concentrations (Lynch, 2016).

Equation 2-5. Formula to calculate precision described by Wal et al. (2010).

$$Precision\ (\%) = \frac{Std\ dev}{average} \times 100$$

Figure 2-19 summarises accuracy and precision as main quality control characteristics (Meng & Bennett, 2012). The ideal outcome of any quality control is both accuracy and precision, where the results are all repeatedly measured near the true value of the analyte.

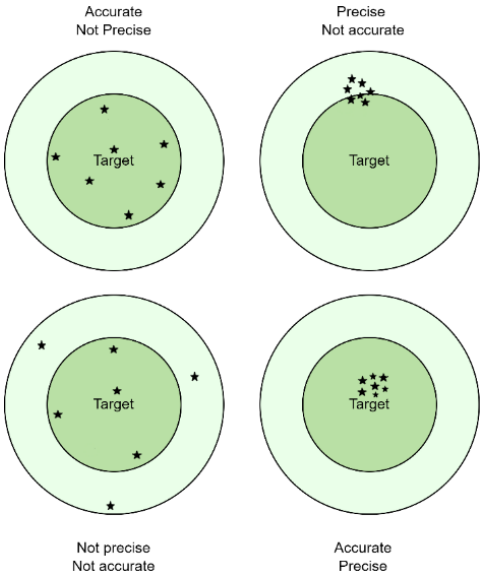

Figure 2-19. Illustration of accuracy and precision of a method (modified from Ferrante & Cameriere, 2009).

2.10.5 Stability

According to Wal and colleagues (2010) stability can be defined as the analyte's chemical stability over a period and under specific conditions. There are many circumstances under which compounds can degenerate, such as extraction/sample clean-up, temperature, pH, light sensitivity, etc. (Rao, 2018). Stability is an important parameter to consider during method validation, as it has a direct effect on the chromatographic behaviour (Wal *et al., 2010)*.

Short-term storage stability is determined by comparing freshly prepared samples, with samples stored at different temperatures, the deviation of the stored samples should be <15% (van de Merbel *et al.*, 2014).

2.10.6 Matrix effect

The matrix effect is defined as the interfering effect caused by other components present in a sample, resulting in the alteration of the sensitivity of the analysis (Panuwet *et al.*, 2016; Wal *et al.*, 2010). The effect of these interferences can lead to ion suppression or enhancement (Panuwet *et al.,* 2016), it is important to know to what extent the matrix influences the response of the analyte.

The matrix effect is expressed as a percentage and can be calculated by Equation 2-6. The matrix effect is accepted when the imprecision is <15% (Lynch, 2016). If the matrix effect is greater than 100%, ion enhancement occurs, where ion suppression occurs when the matrix effect is lower than 100% (Panuwet *et al.,* 2016).

Equation 2-6. The formula used to calculate the matrix effect on the target metabolites.

$$matrix\ effect\ (\%) = \frac{Average\ analyte\ area\ in\ matrix}{Average\ analyte\ area\ in\ standard} \times 100$$

2.10.7 Carry over and selectivity

Carry over occurs when an analyte (or part thereof) from a previous run is present in the following sample in the analytical process (Zeng *et al.*, 2006). Carry over can be determined by injecting a blank sample after analysing a sample with a high concentration, the response obtained from the blank sample should be <20% from the response of the analyte in the high concentration sample analysed (Lynch, 2016). Whereas the selectivity is the extent to which a method can detect a specific analyte in a specimen (Wal *et al.,* 2010).

A method is known to be selective when it can quantify and differentiate an analyte in the presence of other compounds (Wal *et al.,* 2010). A comparison between a blank or QC sample and a pooled urine sample, which is spiked post extraction, will give a good indication on how selective the method is for the specific analyte (Lynch, 2016). If there's no peak within 10% of the retention time of the analyte, the method is considered selective (Wal *et al.,* 2010).

2.10.8 Extraction recovery

Recovery can be defined as the percentage analyte originally in the specimen/sample that reaches the end of the analytical procedure (Lynch, 2016). Recovery should be measured when an extraction step is present in the sample preparation step.

Recovery is measured by comparing the results of spiked samples that underwent extraction with spiked samples that did not undergo extraction (Wal *et al*., 2010). Recovery is expressed as a percentage and can be calculated by means of accuracy (Equation 2-3).

2.11 Summary

To summarise, the direct analysis of free radicals to determine one's oxidative stress status remains a challenging task. Although secondary products of oxidative stress are mainly studied for this purpose, a single method as developed by Martinez-Moral and Kannan (2018) can improve the characterisation of the oxidative stress status. This will be indicative of any risk or diagnosing oxidative stress-induced diseases such as Alzheimer's or cancer. The oxidative stress markers included in this study are representative of the oxidation of lipids (MDA, 4-HNE-MA, $PGF_{2\alpha}$, and PGE_2), proteins (tyr, 3-NT, and dityr), and DNA (8-OHdG). The method developed by Martinez-Moral and Kannan (2018) will be partially optimised, partially validated and implemented on a LC-ESI-MS/MS system and applied on a cohort consisting of COC users and non-users.

CHAPTER 3: MATERIALS AND INSTRUMENTATION

This chapter describes the experimental design (sample collection, sample size, ethics), chemicals, reagents, and apparatus utilised. The sample preparation, data analysis and statistical analysis are also described in detail.

3.1 Experimental design

The first aim of this study was to partially develop, optimise, and validate the method described by Martinez-Moral & Kannan method (2018, 2022). The second aim was to apply the method on urine samples collected in a previous study from a cohort of COC users and non-users to characterise the oxidative stress status profiles. Strict inclusion and exclusion criteria were used to recruit and select the participants (see Annexure A). Figure 3-1 illustrates the experimental design for the study.

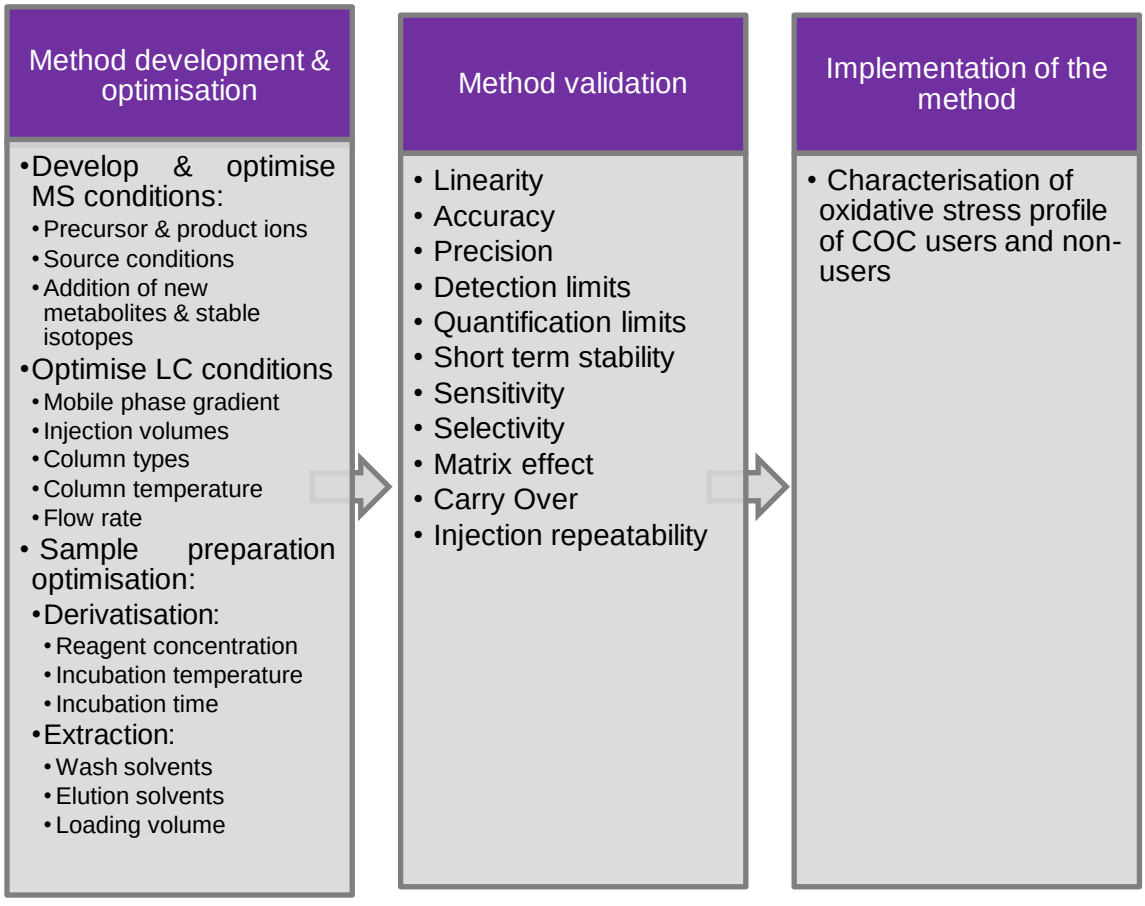

Figure 3-1. Experimental design for this study.

3.1.1 Sample collection and sample size

A pooled urine sample and standard stock solutions were used to develop and optimise the method. The baseline urine samples already collected for the estrogen, biotransformation, and oxidative stress (eBOSS) study were utilised for this study (Annexure A). The participants collected their urine samples at home in specimen bottles provided by the laboratory. The laboratory also provided a manual, indicating how and when the samples should have been collected. Based on the applied criteria, a total of 74 participants were included in this study cohort.

3.1.2 Ethics

The Declaration of Helsinki's guidelines were followed in this investigation. The North-West University's Health Research Ethics Committee granted this study ethical approval (NWU-00169-21-A1). This current study is also an affiliated study of the continuing North-West University eBOSS study (NWU-00344-16-A1) (Jacobs, 2018). All subjects who took part provided their written informed consent. Only baseline urine samples were made available for this study. Privacy of the participants was ensured by only providing the participants unique laboratory number assigned in the eBOSS study (NWU-00344-16-A1).

3.2 Analytical standards, chemicals, and reagents

The following reagents and standards were purchased from Sigma Aldrich Co., now ©Merck KGaA, Darmstadt, Germany: 8-hydroxy-2-deoxyguanosine (H5653), Prostaglandin-$F2_{\alpha}$ (P0424), Prostaglandin-E_2 (P5640), malondialdehyde tetrabutylammonium salt (63287), L-tyrosine (≤98%) (T3754), trichloroacetic acid (T6399), 2-thiobarbituric acid (T5500), 2,4-dinitrophenylhydrazine (04732), 3-nitrotyrosine (N7389), as well as the following chemicals: Ammonium acetate (101116), hydrochloric acid (100319), n-Hexane (100795), ethyl acetate (100789), acetic acid (160305), ethanol (100983), and formic acid (111670) . 4-hydroxy-2-nonenal (32100), 4-hydroxy-2-nonenal-mercapturic acid (32110), L,L-dityrosine (>99%) (27657), and prostaglandin E_2-d_4 (34210-10-1) were purchased from Caymen Chemicals, supplied by the South African distributor Biocom Africa (Pty) Ltd, Centurion. 8-Ox-2-deoxyguanosine-^{13}C, $^{15}N_2$ (TRCO850252) was purchased from Toronto Research Chemicals, supplied by the South African distributor Industrial Analytical (Pty) Ltd, Johannesburg. D_5-Phenylalanine (56253-90-8) was purchased from Cambridge Isotope Laboratories (Inc), also supplied by Industrial Analytical (Pty) Ltd, Johannesburg. Malondialdehyde-1,3-d_2 (D-6469/0.01) were purchased from EQ Laboratories GmbH, Augsburg, Germany supplied by the South African distributor Promolab Pty Ltd T/A Separations, Johannesburg.

Solvents used for standard preparation and on the LC-ESI-MS/MS instrument included high purity water (BJ365CS), methanol (BJ230CS), acetonitrile (BJ017CS), and acetone (34885), and were obtained from Honeywell, Burdick & Jackson, supplied by Anatech, South Africa.

3.3 Standard stock preparation

For method development and optimisation, standard solutions as well as a pooled urine sample were prepared. Urinary physiological concentrations obtained from the Human Metabolome Database (HMDB), and as measured by Martinez & Kannan (2018) and others (Orhan *et al.,* 2004) were used as reference for the calibration curve.

Standard stock solutions were prepared to a final concentration of 0.1 mg/ml in various organic solvents, from which working-solutions were prepared by diluting the stock solution with 45:55 H_2O:MeOH (v/v) to the desired concentration of 1 µg/ml.

8-Oxo-2'-deoxyguanosine-^{13}C,$^{15}N_2$ (^{13}C,$^{15}N_2$-8-OHdG) stock solution of 0.5 mg/ml was prepared and the intermediate solution was diluted to a final concentration of 5 µg/ml. Prostaglandin E_2-d_4 (PGE-d_4) were diluted to a stock solution of 5 µg/ml. Malondialdehyde-1,3-d_2 (MDA-d_2) were diluted to a stock solution of 100 µg/ml after which it was hydrolysed with 0.02 M HCl to a final concentration of 1 µg/ml as described by Chen *et al* (2011).

A master mix with a final concentration of 20 ng/ml of each standard were also prepared for analysis and matrix spiking during method development and optimisation. A working mixture of internal standards was prepared in 45:55 H_2O:MeOH (v/v) with a final concentration of 950 ng/ml ^{13}C,$^{15}N_2$-8-OHdG, 780 ng/ml PGE-d_4, and 510 ng/ml MDA-d_2. MDA, $PGE_{2\alpha}$, d_5-Phenylalanine (d_5-phe), ^{13}C,$^{15}N_2$-8-OHdG and dityr stock solutions were prepared in methanol (MeOH), $PGF_{2\alpha}$ was prepared in ethanol (EtOH), and 8-OHdG was prepared in milli-Q water. Tyrosine and 3-NT were prepared in 1 M hydrochloric acid (HCl). Both 4-HNE and HNE were provided as an ethanol solution, which was dried under a gentle N_2 stream and redissolved in MeOH.

A standard working solution was prepared by diluting the stock solution to the desired concentration of 1 µg/ml. A working mixture of internal standards was prepared with a final concentration of 0.1 µg/ml for each internal standard. All the working and stock standards were stored at – 20 °C, except for 4-HNE and 4-HNE-MA which were stored at 80°C. Internal standards (8-ox-2-deoxyguanosine-^{13}C, $^{15}N_2$, and phenylalanine-d_5, MDA-d_2, and PGE-d_4) were also stored at -20°C.

The DNPH was prepared at a concentration of 5 mM in pre-mixed water, acetonitrile (ACN), and 1 M acetic acid (8:1:1 v/v), and sonicated three times at 40-45 °C. The DNPH did not dissolve completely, the solution was then filtrated with gravity through a filter paper to get rid of the undissolved reagent. Thiobarbituric acid (TBA) derivatisation reagent mix was prepared as described by Konieczka (2014). The TBA reagent (10 mM) and a trichloroacetic acid (TCA) reagent (1 mM) were prepared in milli-Q water. These solutions were prepared freshly before analyses.

A pooled urine sample was prepared by combining 200 ml of each urine sample (5 samples), and the metabolite concentrations measured were 4.72 ng/mg creatinine (8-OHdG), 492.21 ng/mg creatinine (MDA), 156.74 ng/mg creatinine (PGE_2), 17.23 µg/mg creatinine (tyr), and 5.25 ng/mg creatinine (3-NT). These concentrations were determined by analysing the pooled urine sample with the COC cohort as described in chapter 6. The pooled urine sample was spiked with a standard master mix, this was done by drying the working standard of specified concentrations (1 µg/ml, 5 ng/ml, 10 ng/ml, and 20 ng/ml), and resuspending with 1 ml urine. The samples were vortexed to ensure all the compounds dissolved in the urine.

The samples used for calibration curves were prepared from the stock standard solutions; a working mixture of 1 µg/ml of each standard were prepared. For the spiked urine calibration curves, a working mixture of 1 µg/ml of each standard were prepared and dried under a gentle stream of nitrogen. The samples were reconstituted with 1 ml urine, and vortexed to ensure the target compounds dissolved in the urine. A serial dilution series (1:2) were made from both the spiked urine and the standard mixture, covering a broad range of concentrations including the physiological concentration ranges of the metabolites as expected in urine. After serial dilution, the IS were added, and the samples were treated as any other samples.

The quality control (QC) samples were prepared from the same standard working solution (1 µg/ml) as the calibration curve samples. The QC concentrations were chosen based on the physiological concentrations, as well as the LOD, LOQ, and linear range from the calibration curve for each metabolite. A total of six QC concentrations were chosen for each metabolite. Each QC level is described in Table 3-1.

Table 3-1. Summary of quality control samples used for validation.

QC level	Description
LOD	Limit of detection
LOQ	Limit of quantification
LQC	Low QC – Concentration representing the lower range of the physiological concentrations
MQC	Medium QC – Concentration representing the mean of the expected concentration range
HQC	High QC – Concentration representing the higher range of physiological concentrations
eQC	Extreme QC – Concentration representing abnormal concentrations (110 – 150% of HQC).

3.4 Sample preparation

The collected samples from the eBOSS study were stored at -80 °C until analysis. The samples were thawed at room temperature, then the samples were vortexed to ensure sufficient mixing of urinary contents. Only 1 ml aliquots of the samples were collected for this study, the remaining volumes were kept for 7 days at -80 °C, should re-analysis be necessary. After 7 days the samples were discarded.

3.5 Instrumentation

For the sample preparation, a Phenomenex SPE column vacuum manifold (AHO-6024) with ABS ElutNexus (60mg/3ml) SPE cartridges (12103101) from Agilent were used. The LC system used was an Agilent 1290 Infinity, with a binary pump (G4220A), vacuum degasser (G1330B), thermostat autosampler (G4226A), and a temperature-controlled column compartment (G1216C). The Agilent instruments were supplied by Agilent Technologies, Santa Clara CA, USA, through the local supplier Chemetrix.

For chromatographic separation an Agilent Zorbax SB-Aq Rapid Resolution Column (2.1 x 150mm, 3.5µm) (830990-914) and guard columns (821125-933), as well as an Agilent Zorbax Eclipse plus (2.1 x 50mm, 1.8 µm) were purchased from Chemetrix.

Additional supportive instrumentation included an Eppendorf microcentrifuge (5414R; Merck), an Heraeus multifuge X3R centrifuge (Thermo Scientific), and a Mermle centrifuge (2206A, Lasec/SA, Angela technologies).

In addition, a BFC nitrogen evaporator (Stargate scientific), a WX vortex, a RC series heating plate (Velp Scientific, Amanzi Tech), a Modop Digital sonicator, a WTW series inolab pH meter 720, a Virtis freeze dryer, and a Mettler Toledo classic plus balance (AB265-s/fact) was used for sample preparation. The creatinine values of the eBOSS samples were determined using the Thermo ScientificTM KonelabTM 20 Clinical Chemistry Analyzer.

3.6 Data analysis

Data acquisition and quantification of the analytes were done using Agilent MassHunter workstation software. These included LC/MS Data Acquisition software (B.07.00) for 6460 series triple quadrupole (G6460A) with a Jetstream ion source, Quantitative Analysis software (B.06.00) and Qualitative Analysis for QQQ software (B.06.00). Additional software programs used for ionisation optimisation and source conditions included Agilent technologies MassHunter workstation software Optimiser for 6400 series triple quadrupole (B.07.01) and the iFunnel Source Optimiser for 6400 series (B.07.01). Further data processing was done on Microsoft Excel 365. For presentation purposes, most optimisation graphs were presented on a log 10 scale.

3.7 Statistical analysis

For statistical analysis of the data obtained during validation and application, IBM SPSS (Statistical package for the social sciences) V29.01.0 (171) software and Metaboanalyst 5.0 were used.

CHAPTER 4: PARTIAL METHOD DEVELOPMENT AND OPTIMISATION

This chapter describes the partial optimisation of the method described by Martinez and Kannan (2018), as well as the expansion of the method to include the other target metabolites, 3-NT, 4-HNE, 4-HNE-MA, PGE_2 and tyr guided by the work of others (Bothma, 2012; Douny *et al.*, 2016; Fan *et al.*, 2012; Konieczka, 2014; Martinez-Moral & Kannan, 2022; Vanova *et al.*, 2018; Wu *et al.*, 2016). The method development process included optimisation of the derivatisation, extraction, separation, and detection of all our target metabolites (8-OHdG, 3-NT, dityr, tyr, 4-HNE, 4-HNE-MA, PGE_2, $PGF_{2\alpha}$, and MDA) in a single method.

4.1 Optimisation of LC-MS/MS analysis of underivatised metabolites

For parameter optimisation, individual standards were analysed by infusing them directly into the MS. The standards were then analysed on the LC column to obtain their retention times, after which further optimisation was done. Uracil (U0750-5G) is known to be a good detector of dead volume in RPLC (Trebel *et al.*, 2021). An uracil sample (2 µg/ml) was analysed to determine the dead volume (volume of mobile phase that passes through the column without interacting with the stationary phase) of the column with the given conditions. The retention time for uracil was 2.26 minutes.

LC and MS conditions were optimised for each metabolite individually. The optimal conditions and parameters were similar for the target analytes. The optimal liquid chromatography parameters for the underivatised metabolites of interest are listed in Table 4-1. The gas temperature was 250 ºC, the gas flow was 6 l/min, the capillary voltage was ± 2500 V (for both optimisation modes), and the nebulizer was set to 30 psi. The sheath gas flow was 10 l/min, the sheath temperature was 350 ºC, and the nozzle voltage was 500 V (for both ionisation modes).

Table 4-1. Optimised parameters for oxidative stress marker detection. These parameters include the precursor and product ions used for detection, the polarity of the ions detected, the energy used to break the compounds (collision energy), energy used to carry the ions (CAV) and energy needed in the capillary (fragmentor).

Compound	Precursor (m/z)	Product (m/z)	Polarity	CAV (V)	Collision Energy (V)	Fragmentor (V)
Tyr	182.1	141	+	7	0	76
3-NT	227.0	132.9	+	7	20	99
Dityr	361.1	201.8	+	7	44	93
8-OHdG	284.1	110.9	+	7	12	86
4-HNE	157.1	43.2	+	7	20	91
4-HNE-MA	318.1	162	-	7	4	94
MDA	71.1	53.1	-	7	20	59
$PGF_{2\alpha}$	353.2	309.2	-	7	16	147
PGE_2	351.0	315	-	7	4	98

Firstly, a working standard mix (1 ng/ml) was analysed untreated to determine whether the target metabolites are detectable without any sample preparation. The samples (5 µl) were analysed using a gradient previously reported by Martinez and Kannan (2018). The column temperature was kept constant at 25 °C. The overall response of our target metabolites was very low. Most metabolites (dityr, tyr, 3-NT, and 8-OHdG) had poor retention, as they eluted within the first four minutes of the analysis. In the working mix, PGE_2, $PGF_{2\alpha}$, 4HNE, and MDA were not detected.

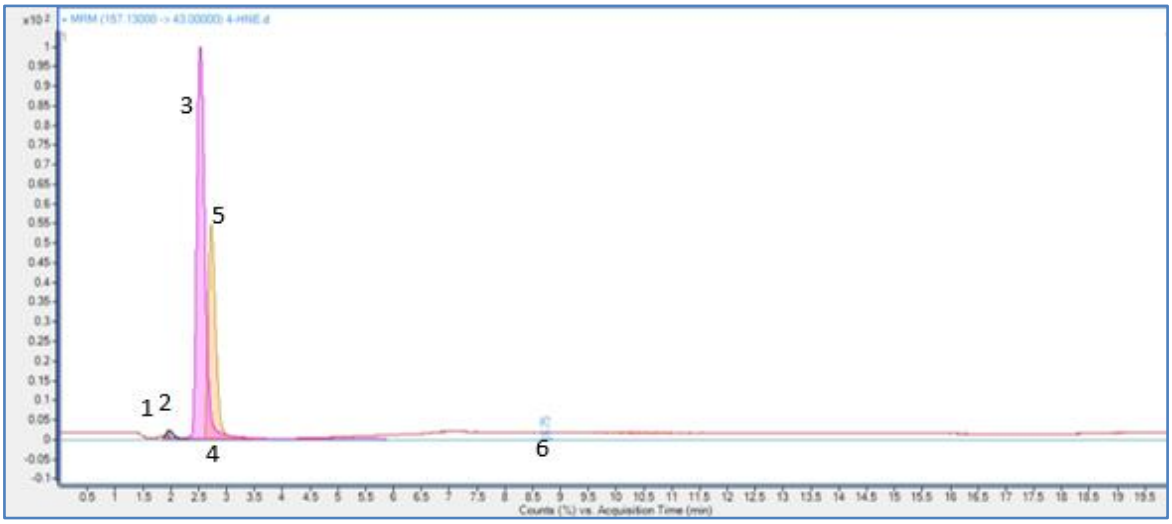

***Figure 4-1. Chromatogram of standard mix without any sample preparation**. 1. dityrosine, 2. 3-nitrotyrosine, 3. d_5-phenylalanine, 4. tyrosine, 5. 8-hydroxy-2-deoxyguanosine & 8-oxo-2-deoxyguanosine-^{13}C, $^{15}N_2$ 6. 4-hydroxynonenal. Malondialdehyde, prostaglandin $F_{2\alpha}$, prostaglandin E_2 were not detected.*

To improve the separation and detection of the metabolites, the method was separated into two methods for further development. MDA, 4-HNE-MA, PGE_2, and PGF were analysed in negative ionisation mode, whereas tyr, 3-NT, dityr, 4-HNE, 8-OHdG, d_5-phe, and ^{13}C-N^{15}_2-8-OHdG were analysed in positive ionisation mode. The gradient was also adjusted (Table B-1). Figure 4-2 and Figure 4-3 illustrate the detection of a master mix sample containing 1 ng/ml of each analyte using this gradient.

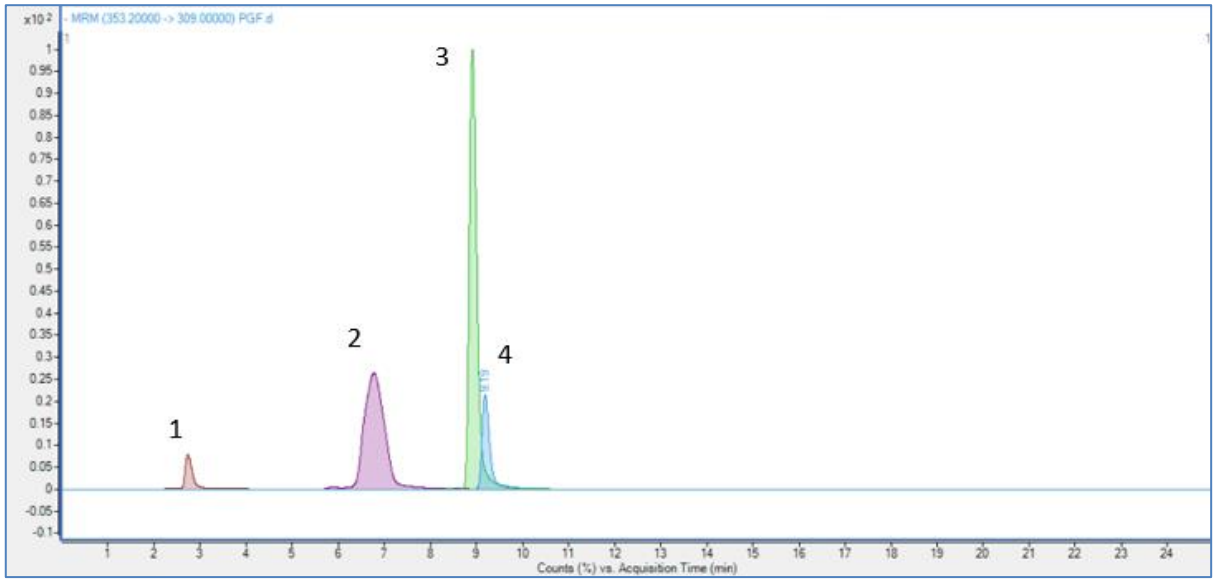

Figure 4-2. Chromatogram of negatively ionised analytes. 1. malondialdehyde 2. 4-hydroxynonenal-mercapturic acid 3. prostaglandin E_2 4. prostaglandin $F_{2\alpha}$.

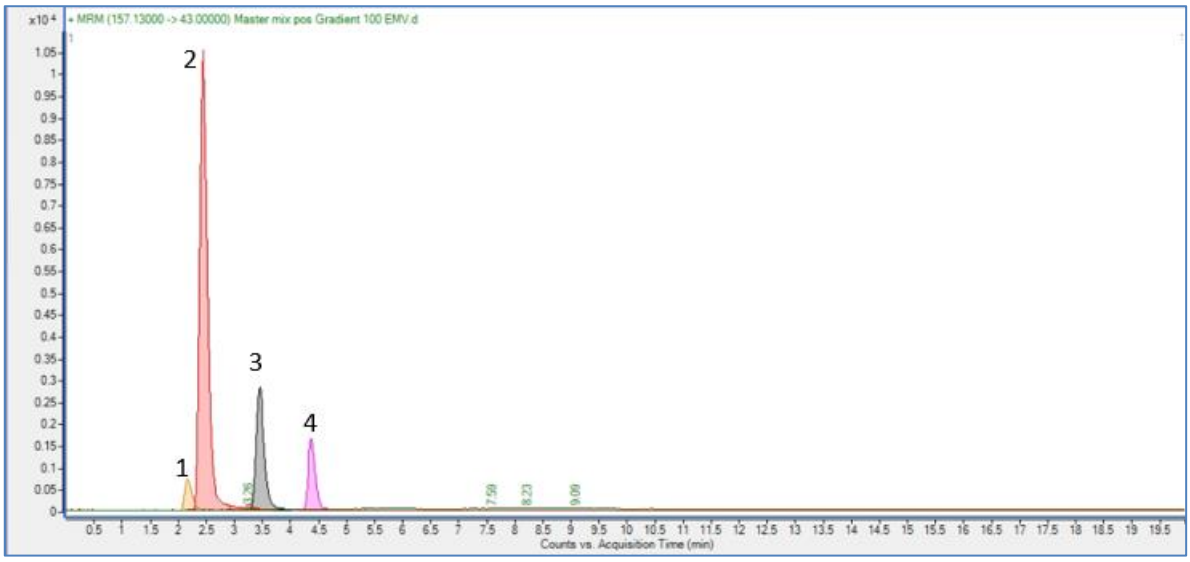

Figure 4-3. Chromatogram of positive ionised analytes. 1*. dityrosine 2. tyrosine & d_5-phe 3. 3-nitrotyrosine 4. 8-hydroxy-2-deoxyguanosine & 8-oxo-2-deoxyguanosine-^{13}C, $^{15}N_2$.*

To further enhance the separation of compounds such as dityr, tyrosine, and d_5-phe the gradient was adjusted (Table B-2). With this gradient, some polar compounds could be better retained, as seen in Figure 4-4.

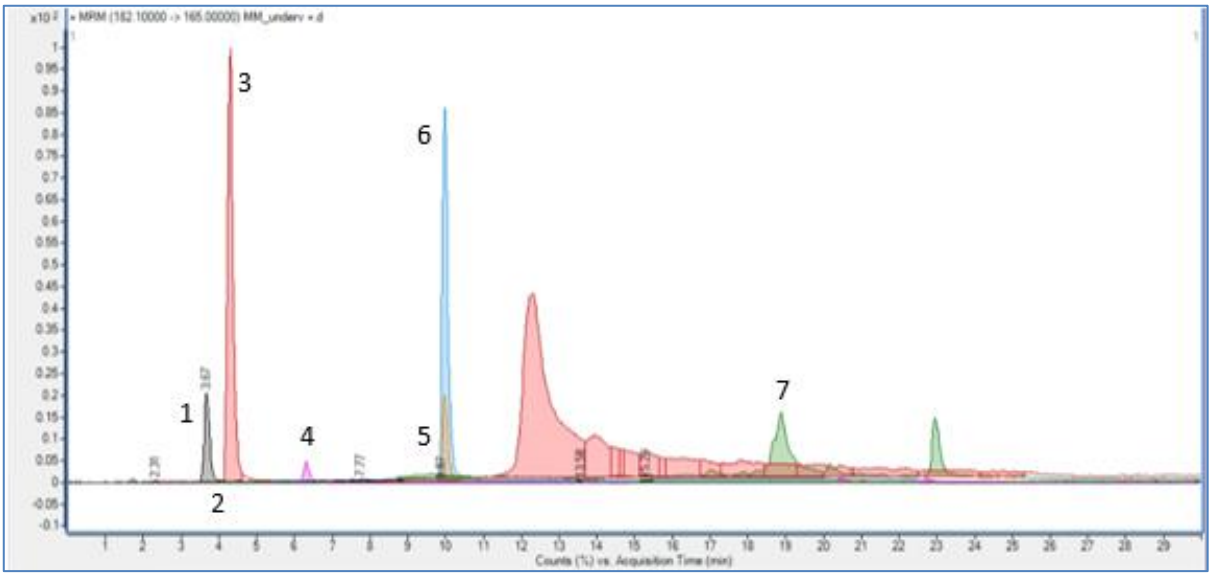

Figure 4-4. Chromatogram of positive ionisation after gradient adjustment. 1. tyrosine 2. dityrosine 3. d_5-phe 4. 3-nitrotyrosine 5. 8-hydroxy-2-deoxyguanosine 6. 8-oxo-2-deoxyguanosine-^{13}C, $^{15}N_2$ 7. 4-hydroxynonenal.

The adjusted gradient also increased the retention of the negatively ionised analytes; their detection, however, was poor compared to positively ionised analytes (Figure B-1). To improve the detection of these compounds, derivatisation was considered next.

4.2 Comparison of derivatisation techniques

Derivatisation can be an effective way to enhance the detection of metabolites such as aldehydes and amino acids. Martinez-Moral and Kannan, used DNPH as derivatisation reagent in their method (2018). Unfortunately, due to a global shortage of raw material, DNPH could not be obtained as derivatisation reagent. Whilst waiting for the delivery of DNPH, alternative derivatisation reagents were considered. Thiobarbituric acid (TBA) and N-butanol:acetyl chloride was tested to determine which is most effective for our target metabolites. The derivatisation optimisation and development were done on individual standards as well as a working standard (1 µg/ml). All derivatives had to be optimised for both LC and MS conditions, and the results can be seen in Table B-3.

The chosen derivatisation technique had to be optimised, including different incubation temperatures and reagent concentrations. This was achieved by first optimising the derivatisation reagent concentration, followed by the incubation temperature, and then lastly, the incubation time.

4.2.1 TBA derivatisation

As mentioned in section 2.9.2 it is known that the TBARS assay is non-specific for MDA, but the specificity can be drastically improved by implementing this assay as a derivatisation method (Tsikas, 2017). Four different variations of the TBARS assay were compared to determine the best option for our target metabolites. Most of the methods found in the literature feature UV or spectrophotometry analysis. To use the TBARS assay as derivatisation reagent, these methods needed to be optimised.

All four methods were applied on MDA, 4-HNE, and the working standard mix.

The method described by Zeb & Ulah (2016) was first implemented, where 1 ml of sample was added to 1 ml TBA in acetic acid (4 mM). The samples were incubated at 95 °C for 60 min. Once the samples were cooled to room temperature, the samples were ready for further analysis.

The second method described by Konieczka *et al.* (2014) was adjusted, where 500 µl sample, 250 µl of TBA (46.5 mM) and 100 µl TCA (1mM) were added together in a Pyrex culture tube (Z653578), and the samples were incubated at 95 °C for 60 min. The samples were cooled down to room temperature, before analysis.

The third TBARS assay protocol was reported by one of our colleagues (Bothma, 2012), where 800 µl sample was added to 800 µl TBA reagent mix (15 % TCA (m/v), 0.375 % TBA (m/v), 0.25 N HCl) in a Pyrex culture tube.

The samples were incubated at 90 °C for 60 minutes, cooled to room temperature and centrifuged at 1753 RCF (relative centrifugal force) for 4 min at 25 °C before further analysis.

Ferrante *et al.* (2017) described the fourth method which was adjusted and applied twice to accommodate the optimal incubation conditions for both 4-HNE and MDA. An aqueous TBA solution of 34.68 mM was prepared. In two different culture tubes, 100 µl sample, 125 µl TBA reagent, 150 µl milli-Q water, and 325 µl 2M HCl were added together. One tube was incubated at 45 °C for 60 min (described incubation temperature for 4-HNE), and the other tube was incubated at 95 °C for 60 min (described temperature for MDA). The samples were cooled to room temperature before further analyses.

4.2.2 N-butanol:acetyl chloride derivatisation

It is well known that butylating amino acids improve detection limits, whilst minimising ion suppression effects (Sandlers, 2019). The methods described by Esterhuizen *et al.*, (2019), Huang *et al.* (2016), and Dietzen *et al.*, (2008) were optimised. A mixture of 400 µl sample and 50 µl internal standard was prepared and dried under a gentle nitrogen gas stream at 45 °C. The samples were resuspended with 200 µl N-butanol:acetyl chloride, and incubated for 20 min at 65 °C. The samples were dried again under a gentle nitrogen gas stream and reconstituted with 150 µl premixed acidified (0.1% acetic acid) H_2O: MeOH (45:55 v/v). The samples were centrifuged at 1753 RCF for 5 minutes before further analysis.

4.2.3 DNPH derivatisation

During N-butanol:acetyl chloride derivatisation analyses, the delayed DNPH order arrived. DNPH derivatisation was considered as described by Martinez-Moral & Kannan (2018), where 500 µl of the sample was added to 200 µl DNPH (0.05 M). The samples were incubated for 30 minutes at room temperature (25 °C). After derivatisation, the samples were diluted with 1 ml H_2O before further analysis.

4.2.4 Results

The first derivatisation reagent (TBA) is the most popular when analysing the lipid peroxidation product MDA (Dator *et al.,* 2019). The TBARS assay is a colorimetric assay used to determine the presence of lipid peroxidation products in the form of yellow or pink adducts (Jardine *et al.*, 2002). All four method variations were tested, due to the variation in TBA concentrations, solvents for preparing TBA, as well as in the added acid. After derivatisation, only the MDA-containing samples yielded a pink product of which the intensity of the colour differed between the different protocols.

The intensity of the colour was only observed by visually inspecting the samples post-derivatisation. A colour change indicated that the reaction occurred successfully, but the variation in intensity indicated that the reaction did not occur to the same extent for the different methods (Figure B-2). The latter was confirmed by the variation of the derivatives' response by analysing The samples on the LC-ESI-MS/MS. The analytical results also indicated that the visual observation was not efficient, as derivatives were detected in samples that did not indicate any colour change. Based on the analytical results, it was concluded that the second protocol (Konieczka, 2014) was the best for MDA. Derivatisation with TBA increased the detection of MDA significantly (Figure 4-5).

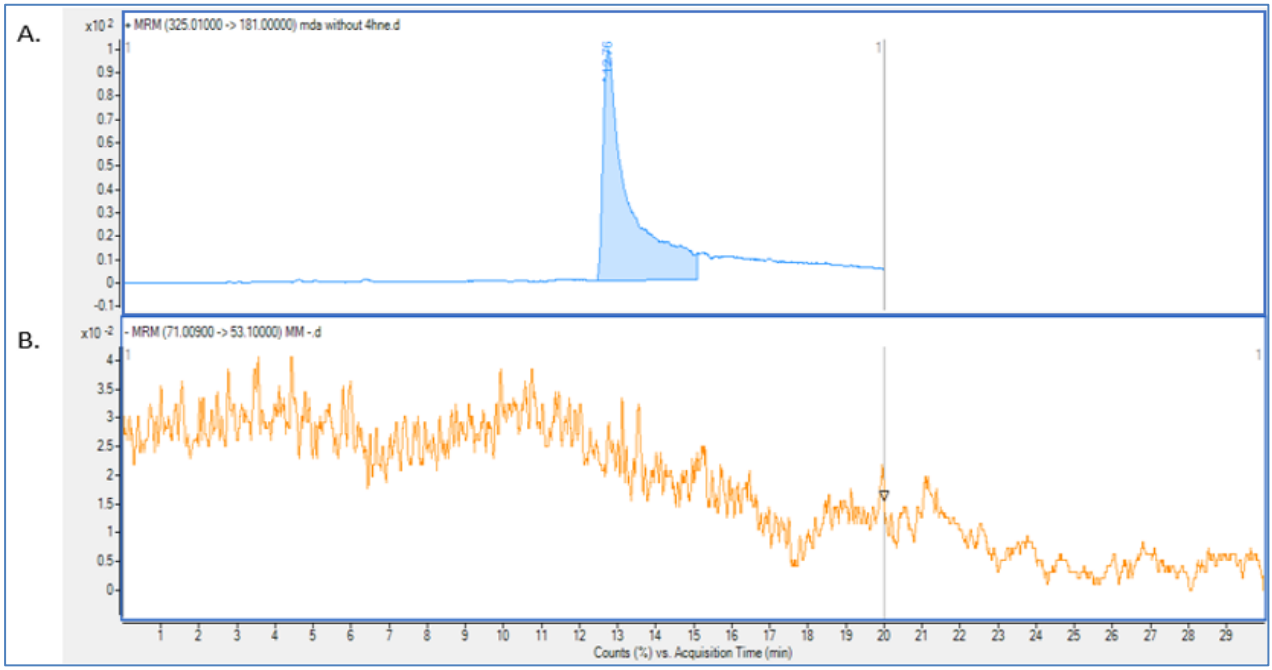

Figure 4-5. The effect of TBA derivatisation on MDA detection. A: Chromatogram of MDA-TBA derivative after derivatisation described by Konieczka (2014). B: Chromatogram of MDA without derivatisation.

Although Ferrante and colleagues (2017) optimised TBA derivatisation at a much lower incubation temperature, 4-HNE derivative was also detected when implementing the method described by Konieczka (2014). In Figure 4-6, the 4-HNE derivative was observed after 4.65 min, this indicates that although no colour change was observed, 4-HNE did react with TBA as some precursor analytes were observed.

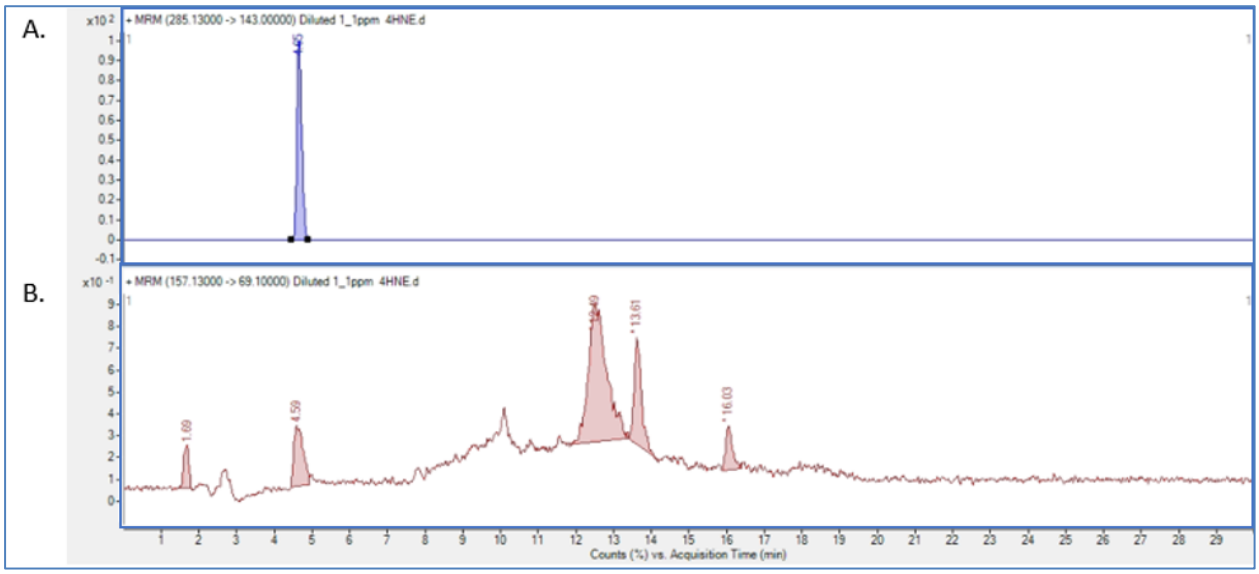

Figure 4-6. Detection of 4-HNE A. 4-HNE-TBA derivative (Rt 4.65 min) B. Underivatised 4-HNE (Rt 16.02 min).

After derivatisation with TBA, some of the compounds (MDA-TBA, PGE_2, 4HNE-MA) delivered a much lower response compared to the other metabolites (Figure 4-7). Even though 4HNE-TBA indicated a good response, the MDA-TBA response was insignificant. For this reason, another derivatisation reagent was tested.

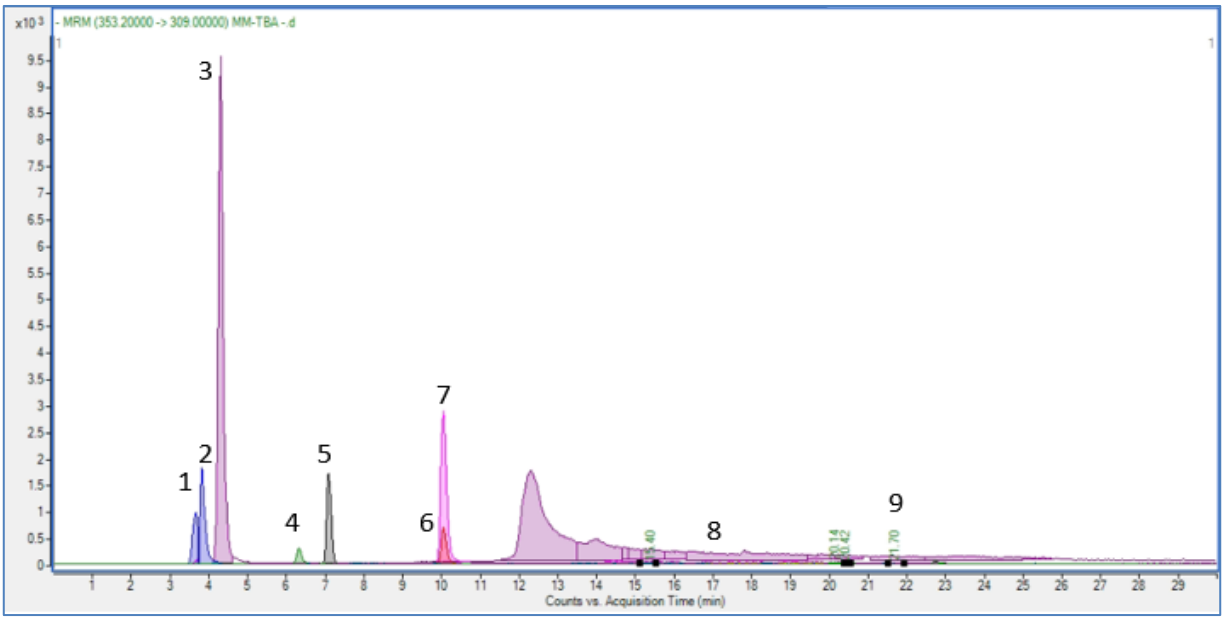

***Figure 4-7. Detection of all metabolites after TBA derivatisation**. 1. tyrosine 2. dityrosine 3. d_5-phenylalanine 4. 3-nitrotyrosine 5. 4-hydroxynonenal derivative 6. 8-hydroxy-2-deoxyguanosine 7. 8-oxo-2-deoxyguanosine-^{13}C, $^{15}N_2$ 8. malondialdehyde derivative 9. prostaglandin $F_{2\alpha}$.*

The amino acids tyr, 3-NT, dityr, and d_5-phe are known to form butyl esters (BE) during butylation with N-butanol:acetyl chloride (Bothma, 2012; Dietzen *et al.*, 2008; Esterhuizen *et al.*, 2019; Marvin *et al.*, 2003). To detect the formed derivatives, the LC-ESI-MS/MS method had to be modified; this included some MS parameters, as well as mobile phase gradient as indicated in Table B-3 and Table B-4.

Figure 4-8 illustrates the chromatogram of a working standard mix after derivatisation with N-butanol:acetyl chloride. From Figure 4-8, one can easily see that the retention and response increased with butylation. However, N-butanol:acetyl chloride might be too harsh on other metabolites (8-OHdG, $^{13}C^{15}N_2$-8OHdG, 4HNE, and MDA), as their response decreased significantly compared to underivatised analysis.

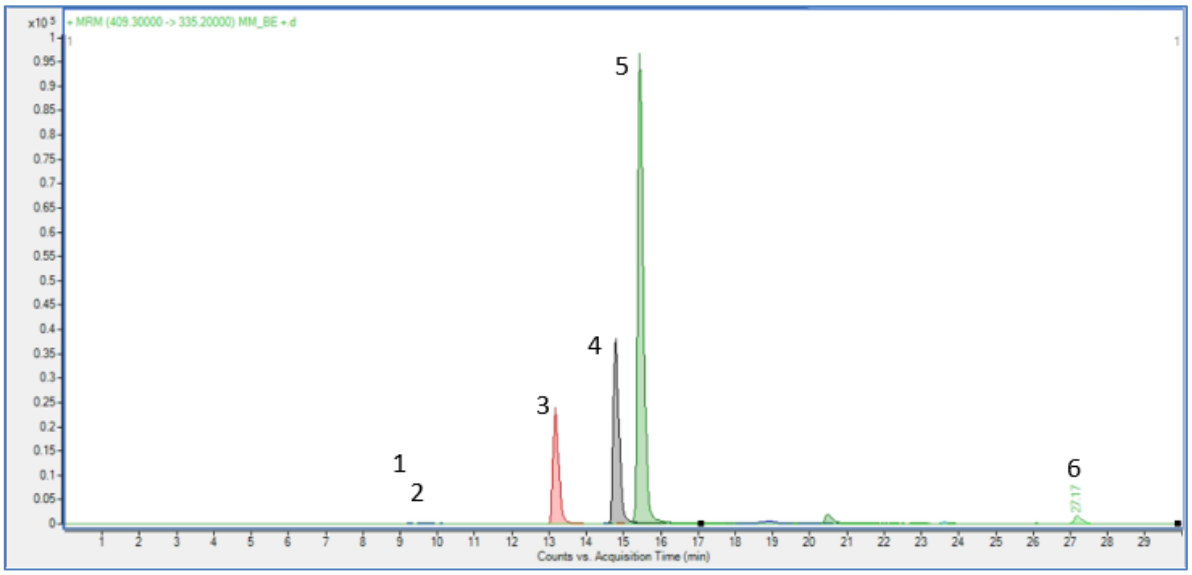

Figure 4-8. Derivatisation with N-butanol:acetyl chloride. 1: 8-hydroxy-2-deoxyguanosine 2: 8-oxo-2-deoxyguanosine-^{13}C, $^{15}N_2$ 3: tyrosine 4: 3-nitrotyrosine 5: d_5-phenylalanine 6: prostaglandin $F_{2\alpha}$.

Finally, DNPH derivatisation was applied to improve the detection of MDA specifically. MDA-DNPH was analysed in positive ionization mode, whereas MDA was analysed in negative ionisation mode. The retention of the MDA-DNPH derivative was 19 minutes (Figure 4-9).

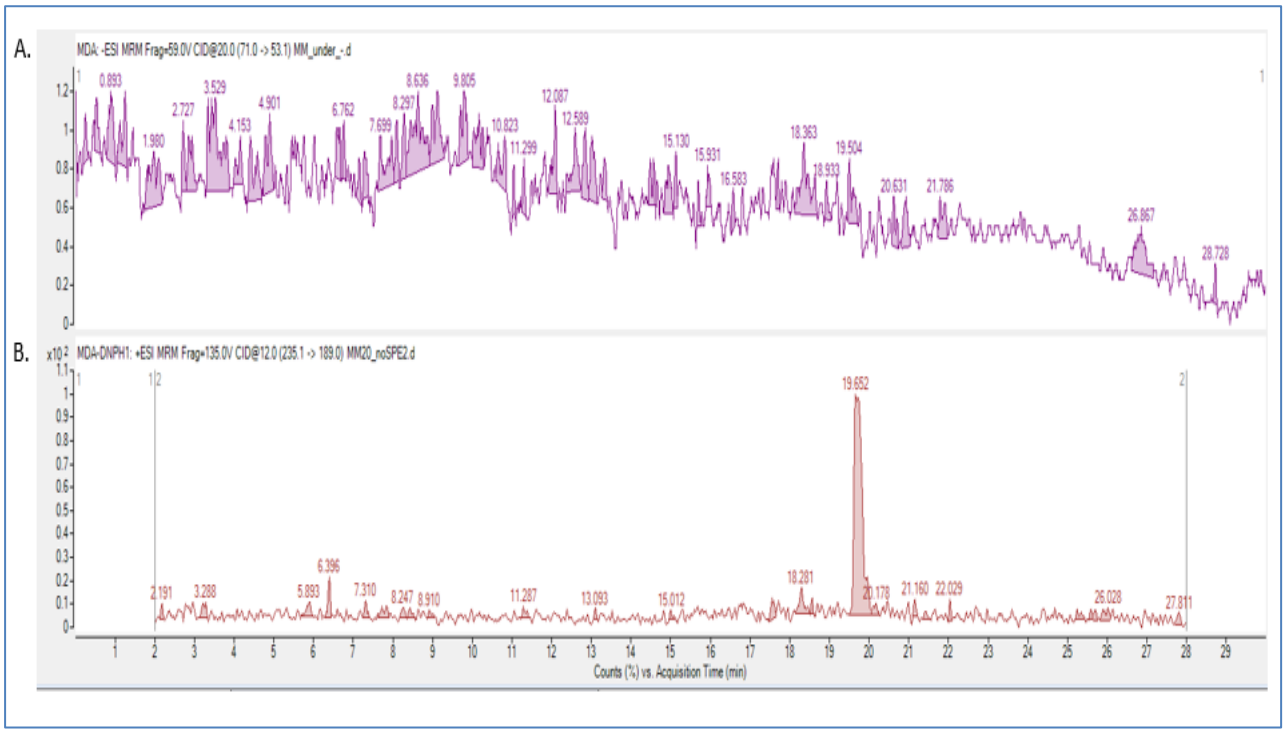

Figure 4-9. The effect of DNPH derivatisation on MDA detection. A: MDA detection before derivatisation. B: MDA-DNPH detection after derivatisation.

Even though the derivatisation of 4-HNE was successful during the TBARS assay, the incubation conditions, were harsh on some of the target metabolites (4-HNE, 8-OHdG, 4-HNE-MA, PGE_2 and $^{13}C^{15}N_2$-8OHdG), and the results for MDA-TBA were not as significantly improved as expected. On the other hand, these metabolites yielded a higher response with DNPH derivatisation (Figure 4-5 A). The BEs, in turn, were easily detected and indicated much greater sensitivity compared to underivatised analysis, but some metabolites, such as 8-OHdG, were suppressed during this derivatisation reaction (Figure 4-5. B).

The purpose of derivatising amino acids was to decrease their polarity, resulting in more non-polar butyl esters, which has much better retention on the analytical column. This was successfully achieved (Figure 4-8). However, since some of the other metabolites were negatively affected during derivatisation with N-butanol:acetyl chloride, this technique was discarded. Overall, derivatisation with DNPH was the best technique considering the sample preparation, derivatisation conditions, simultaneous metabolite detection, and effect on other metabolites.

The authors of the reference article published another paper in early 2022, where they analysed 19 oxidative stress-related markers. This method included the target metabolites MDA, 4-HNE-MA, dityr, 8-OHdG, 3-NT and $PGF_{2\alpha}$ (Martinez-Moral and Kannan, 2022). Therefore, the alterations of their method were also considered to improve the current method.

First, a comparison between the partially optimised method and the method described by Martinez-Moral and Kannan was done (2022). Some of the main differences observed were the number of analytes, the analytical column, the mobile phase composition, the gradient, and DNPH concentration was adjusted. These adjustments could have been made to compensate for the added analytes. Thereafter, comparison analyses were performed, this included analysing both methods on both analytical columns, as well as optimising the DNPH concentration.

4.2.5 Comparison of current and Martinez-Moral and Kannan methods

Firstly, the method described by Martinez-Moral and Kannan (2022) was applied on both analytical columns (Agilent Zorbax SB-Aq and Zorbax Eclipse plus), for all comparison purposes the columns will be referred to as *Zorbax* and *Eclipse*. The source conditions were kept the same as for the current method, as Martinez-Moral and Kannan used a different detection system. Only 4-HNEMA, dityr, 8-OHdG, $^{13}C^{15}N_2$-8OHdG, and $PGF_{2\alpha}$ was detected, as these were the analytes of interest. The results obtained were compared to the current method, to determine whether the adjustments from Martinez-Moral and Kannan (2022), improved the detection of the oxidative stress markers.

It was seen that the peak shapes improved with the adjusted mobile phases, the gradient also increased retention significantly (Figure B-3). For this reason, the mobile phase B composition (8:2 MeOH:ACN, v/v) was adjusted on the current method as described by Martinez-Moral and Kannan (2022). The addition of acetonitrile to the mobile phase B mix helped with the elution of the non-polar compounds such as the prostaglandins (PGE_2, PGF, and PGE-d_4); the selectivity of the method was also increased when combined with MeOH (Hopkins, 2019). The gradient was also adjusted as described by Martinez-Moral and Kannan (Table B-5) (2022).

The second comparison was to determine which column was optimal. This was done by applying the adjusted method onto both columns. For this comparison analysis, all the analytes of interest were included (Table B-6). Besides slight better retention on the Zorbax column, the columns delivered similar results for all analytes. It was decided to use the Zorbax column for further development and optimisation. The chromatographic separation of the target metabolites and their responses can be seen in Figure 4-10.

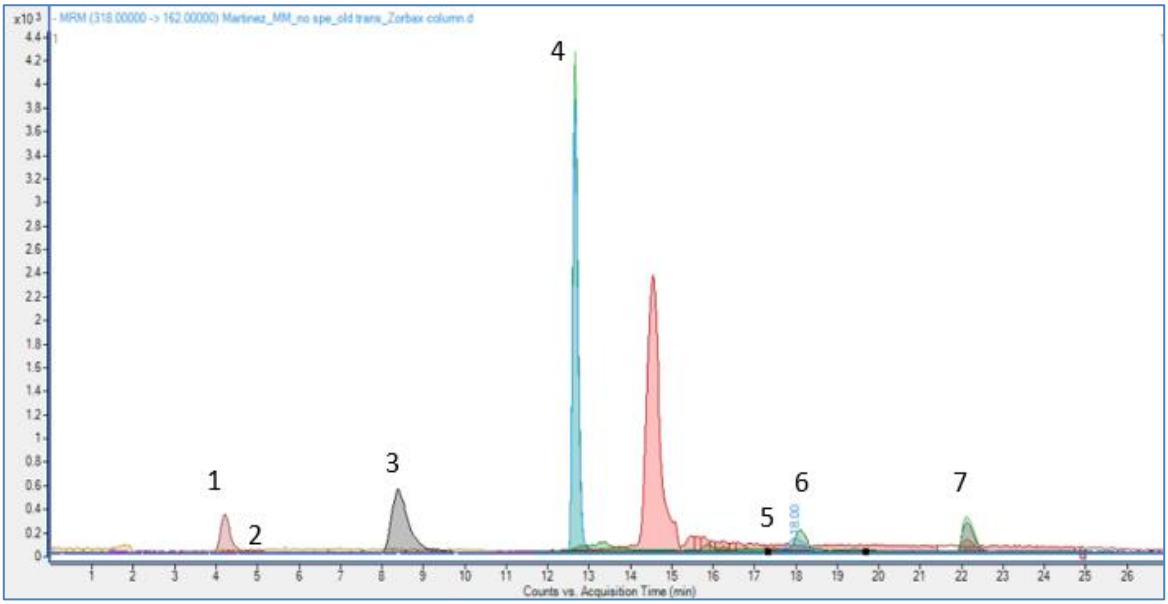

Figure 4-10. Chromatographic separation of target metabolites after derivatisation with DNPH. *1: dityrosine & tyrosine. 2: d_5-phenylalanine. 3: 3-nitrotyrosine. 4: 8-hydroxy-2-deoxyguanosine & 8-oxo-2-deoxyguanosine-^{13}C, $^{15}N_2$. 5: malondialdehyde-hydrazone & malondialdehyde-d_2-hydrazone. 6: 4-hydroxynonenal-mercapturic acid. 7: prostaglandin $F_{2\alpha}$, prostaglandin E_2 & d_4- prostaglandin E_2.*

4.3 Optimisation of DNPH derivatisation

After determining that DNPH was the most effective derivatisation technique and optimising the method as described in section 4.2.5, optimisation of the derivatisation technique was done on individual standards only.The DNPH concentration used by Martinez-Moral & Kannan (2018) was 50 mM, and 5 mM (2022). Because the authors used a 10x dilution in their latest method, DNPH reagent concentration was investigated. The lowest optimal concentration for DNPH was determined by derivatising with DNPH prepared at different concentrations (50 mM, 25 mM, and 6.25 mM); these concentrations would have an in-vial concentration of 8.2 mM, 4.1 mM, and 1.03 mM, respectively. An MDA standard (1 µg/ml) was derivatised with each concentration, to determine whether a lower DNPH concentration delivered better results. The derivatised sample with 50 mM DNPH was the most optimal; however, the presence of excess DNPH suppressed the ionisation of the other target metabolites. To ensure optimal detection in the presence of 50 mM DNPH, a 1 ml sample was used instead of 500 µl.

For the optimisation of the incubation temperature, four samples containing MDA were derivatised with 50 mM DNPH and incubated for 60 minutes at 25 ºC, 37 ºC, 45 ºC, and 65 ºC, respectively. The MDA-DNPH response increased with temperature, although the difference between 45 ºC and 65 ºC was not as significant as the difference between 25 ºC and 37 ºC, or 37 ºC and 45 ºC. It was, therefore, decided that 45 ºC was the optimal incubation temperature, as it is closer to physiological temperature (Figure 4-11).

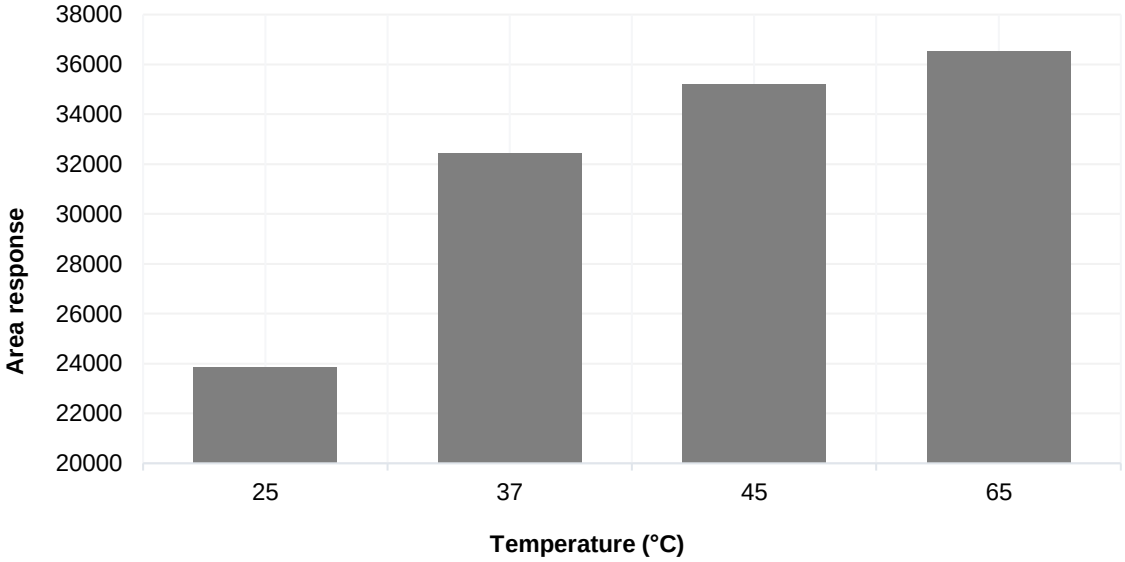

Figure 4-11. Response of MDA-DNPH after incubating at different temperatures.

The incubation time was optimised by incubating the samples at 45 ºC for 15 minutes, 30 minutes, 45 minutes, and 60 minutes, respectively. The MDA-DNPH response increased with incubation time. However, no significant change in the response was observed after 45 minutes. For this reason, an incubation time of 45 minutes was chosen as optimal (Figure 4-12).

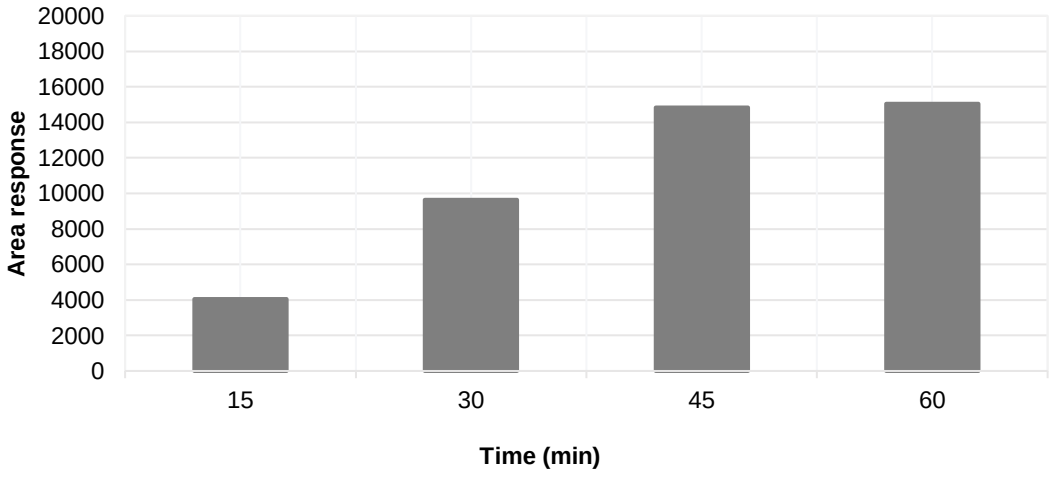

Figure 4-12. Response of MDA-DNPH during incubation time optimisation.

During the optimisation of DNPH derivatisation, the column temperature was also optimised using 8-OHdG as response indicator. Four different temperatures were compared (Figure B-4). From these results, the column temperature was adjusted to 35 °C for further analyses, while the flow rate was kept at 0.2 ml/min.

4.4 Solid Phase Extraction

Urine is a general biofluid for metabolic analyses, due to its availability, non-invasive collection, and abundance (Hecht, 2002; Martinez-Moral & Kannan, 2019), however, it is also known to be a complex biofluid (Bouatra *et al.*, 2013). For this reason, an extraction step is usually included in the sample preparation to discard all unwanted salts, sugars, and proteins that may be present in the urine sample, and excess derivatisation reagent (such as DNPH). Extraction of target analytes is known to decrease the matrix effect (ion suppression) caused by these excess compounds (Gerssen *et al.*, 2009; Isaguirre *et al.*, 2016; Xiao & Zhou, 2017).

The SPE method applied was described by Martinez-Moral & Kannan (2018; 2022). The cartridges were pre-conditioned and equilibrated with 2 ml of MeOH, followed by 2 ml of deionised water. The derivatised samples were diluted to 2 ml and loaded onto the cartridges. The cartridges were washed with 1 ml 5 % MeOH. The cartridges were dried under full vacuum for 5 minutes, after which the analytes were eluted by adding 1 ml of MeOH, followed by 1 ml Ethyl acetate (EtAc). The eluate fractions were evaporated under a nitrogen stream and reconstituted with 150 µl of 8:2 H_2O: MeOH (v/v).

4.4.1 Results

The LC-MS/MS results indicate that some compounds had poor recovery using the protocol described by Martinez-Moral & Kannan (2018). A fraction analysis was done, where the flow-through of all the steps (loading, washing, and elution) were collected separately, dried, resuspended, and analysed. It was apparent from the results that the polar compounds (tyr, dityr, and 3-NT) had poor retention, resulting in elution during the wash step (Table 4-2). For this reason, the method described by Martinez and Kannan had to be optimised to ensure optimal extraction of the target metabolites.

Table 4-2. LC-MS/MS results of the amino acids of interest after fraction analysis.

Name		Wash: 5% MeOH	Eluate 1: 100% MeOH	Eluate 2: EtAc
Tyr	Peak area	**44867.93**	715.19	183.02
Dityr	Peak area	**782.78**	1.12	1.32
d_5-phe	Peak area	**8887.74**	73.72	18.49
3-NT	Peak area	**16688.00**	1199.11	2.45

4.4.2 Optimisation of the extraction method

A working standard mix (20 ng/ml) was used for extraction optimisation. A second wash step was added to determine if the polar compounds also eluted when the cartridges were washed with water. The cartridges were pre-conditioned and equilibrated with 2 ml of MeOH, followed by 2 ml water, after which the derivatised samples were loaded onto the cartridges. The cartridges were first washed with 2 ml water, followed by 2 ml 5% MeOH and dried under full vacuum for 5 minutes; elution occurred by adding 1 ml of MeOH, followed by 1 ml EtAc. The samples were evaporated under a gentle nitrogen stream, reconstituted with 150 µl 55:45 MeOH: H_2O (v/v), and analysed. Even with the addition of the wash step with water, the polar compounds still had poor retention (Table 4-3). For further optimisation of the analytical method, it was required that both the wash and eluate fractions be collected and analysed.

Table 4-3. Fraction analysis results of the amino acids of interest.

Compound name		**Wash 1: H_2O**	**Wash 2: 5% MeOH**	**Eluate 1: 100% MeOH**	**Eluate 2: EtAc**
Tyr	Peak area	**3177.65**	352.27	325.23	416.72
d_5-phe	Peak area	**243812.91**	**83681.44**	3944.54	27.83
3-NT	Peak area	**5465.37**	**10501.03**	1777.27	16.12

The equilibrating and conditioning volumes were also altered to see whether it would improve the retention of the amino acids (Table 4-4). In addition, 2 ml of EtAc was used instead of 1 ml to ensure all target compounds were eluted from the cartridge. However, no MDA-DNPH was detected in the second elution step with EtAc. Furthermore, only 1 ml sample was loaded onto the cartridge instead of 2 ml. Finally, the water for the washing step was also acidified with 0.1 % acetic acid to enhance adsorption. The samples were dried under a gentle nitrogen stream at 45 °C and reconstituted with 150 µl 55:45 MeOH: acidified H_2O (v/v) before analysis. Unfortunately, these adjustments still resulted in the polar compounds eluting with the wash step (Figure 4-13).

Table 4-4. Adjusted SPE protocol after DNPH derivatisation.

Equilibrate	2 ml MeOH 2 ml H_2O + acetic acid
Load	Load 1 ml sample
Wash	1 ml H_2O + acetic acid
	Dry under vacuum
Elute	1 ml MeOH 1 ml EtAc

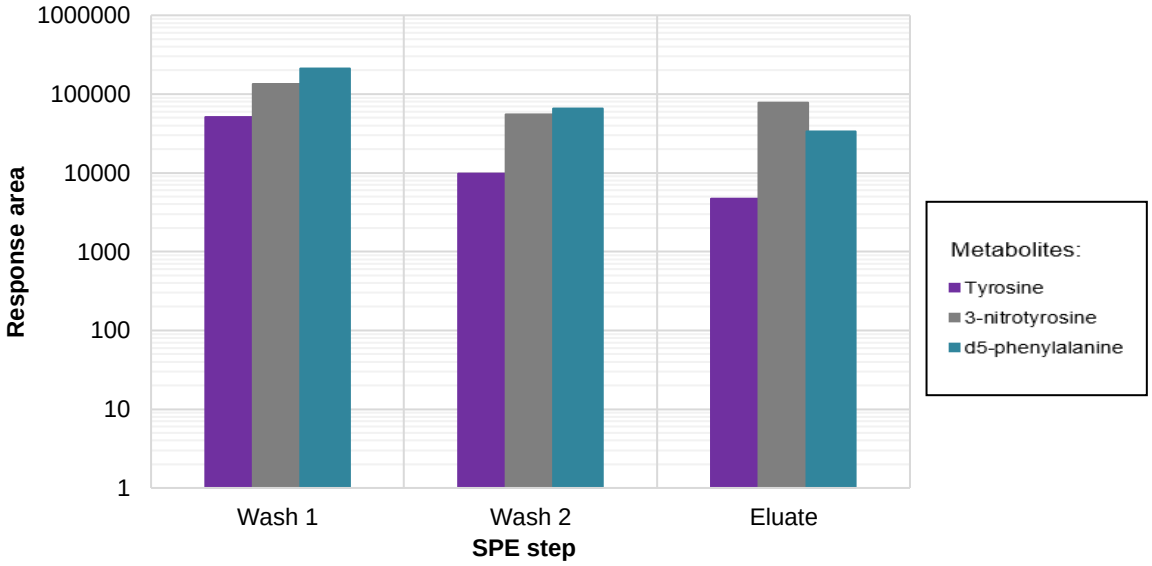

Figure 4-13. Amino acid response after SPE protocol adjustment.

Next, alternative SPE cartridges were considered to improve the retention problem. Phenomenex Strata CN cartridges (200 mg/3 ml) were tested as they can be used for both reversed and normal phase extraction. The cartridges were preconditioned and equilibrated with MeOH and milli-Q water as per recommendation (Phenomenex, 2017). The rest of the SPE was done as summarised in Table 4-4. Both wash steps and elution fractions were collected, dried, and analysed. Unfortunately, the polar compounds (tyr, 3-NT, and d_5-phe) still eluted during the water wash step (Figure 4-14).

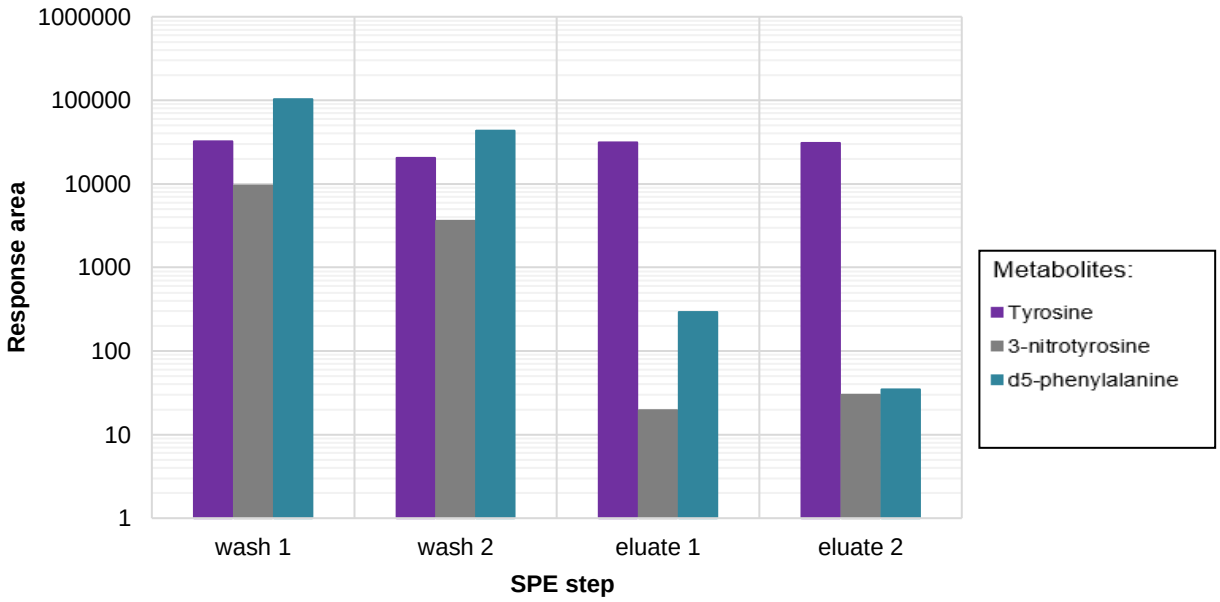

Figure 4-14. Response of polar compounds when using alternative SPE cartridges.

As a final resort, butylation was reconsidered as a derivatisation reagent for the polar compounds (amino acid markers), in combination with DNPH derivatisation. By combining DNPH and N-butanol:acetyl chloride derivatisation, MDA would be more stable as a hydrazone, and the polar metabolites would be more non-polar as butyl esters. However, the butylation derivatisation method had to be optimised first before continuing with the extraction optimisation.

4.5 Optimisation of N-butanol:acetyl chloride derivatisation

For the optimisation of the N-butanol:acetyl chloride derivatisation, the same approach as the optimisation of DNPH derivatisation was followed. The N-butanol:acetyl chloride volume, incubation temperature, and incubation time were optimised. A working standard mix (20 ng/ml) was used for butylation optimisation.

Firstly, the N-butanol:acetyl chloride volume was optimised, three samples containing 400 µl working standard and 50 µl internal standard was dried under a gentle nitrogen gas stream at 45 °C. The samples were resuspended in 100 µl, and 200 µl N-butanol:acetyl chloride respectively, incubated for 20 min at 65 °C, dried again under a gentle nitrogen gas stream and reconstituted with 150 µl premixed acidified H_2O: MeOH (45:55 v/v). The samples were centrifuged at 1753 RCF for 5 minutes before analysis. The responses obtained for the metabolites of interest are presented in Figure 4-15. The reduced responses of the samples resuspended in 200 µl and 300 µl reagent may be due to ion suppression caused by the excess reagent present, since there was no extraction after derivatisation.

The response of the 3-NT showed little difference between the 100 µl and 200 µl samples (Figure 4-15), whereas the response for d_5-phe decreased, and tyr-BE increased with 200 µl. Therefore a 200 µl resuspension volume was selected to ensure excess reagent in the sample.

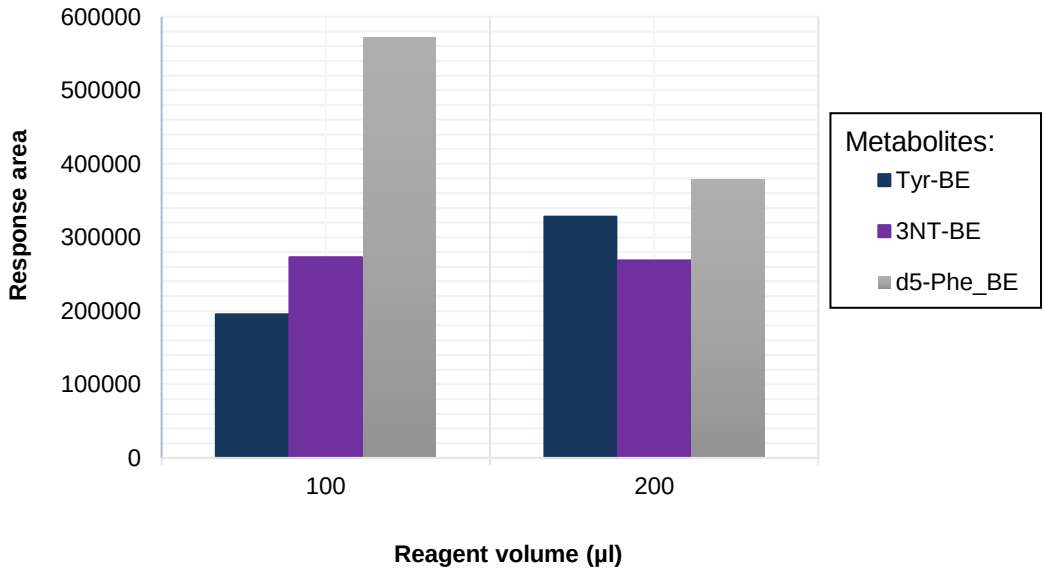

Figure 4-15. Optimisation of N-butanol:acetyl chloride derivatisation. An effect of reagent volume. *d_5-phe-BE: d_5-phenylalanine butyl ester, tyr-BE: tyrosine butyl ester, 3-NT-BE: 3-nitrotyrosine butyl ester.*

Secondly, the incubation temperature was optimised. Three samples (400 µl sample and 50 µl internal standard, each) were dried under a gentle nitrogen gas stream at 45 °C. The samples were resuspended with 200 µl N-butanol:acetyl chloride, and incubated for 60 minutes at 45 °C, 55 °C, and 65 °C, respectively. Again, the samples were dried under a gentle stream of nitrogen gas and reconstituted in 150 µl H_2O: MeOH (45:55 v/v). The samples were then centrifuged at 1753 RCF for 5 minutes before analysis.

From these results (Figure 4-16), the butyl esters all indicated similar results for incubation temperatures 45 °C and 65 °C. Due to the extensive sample preparation of the method thus far, it was decided to use the higher incubation temperature for a shorter time, typically described in literature (Esmati *et al.*, 2021; Esterhuizen *et al.*, 2019; Huang *et al.*, 2016).

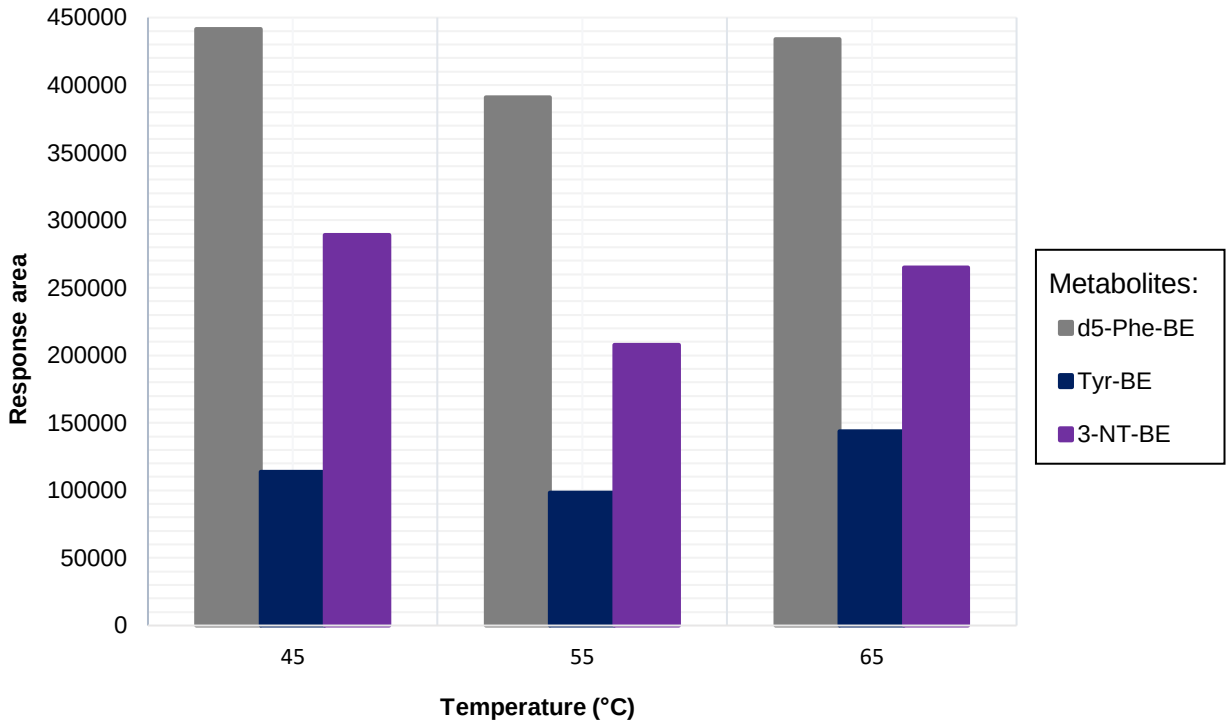

Figure 4-16. Optimisation of incubation temperature of N-butanol:acetyl chloride for 60 minutes. *d_5-phe-BE: d_5-phenylalanine butyl ester, tyr-BE: tyrosine butyl ester, 3-NT-BE: 3-nitrotyrosine butyl ester.*

As stated in section 4.2.4, N-butanol:acetyl chloride derivatisation suppressed 8-OHdG, $^{13}C^{15}N_2$-8OHdG, 4HNE, and MDA detection. For this reason, two separate aliquots of each sample were derivatised both N-butanol:acetyl chloride (fraction A) and DNPH (fraction B), and the derivatised samples were combined to be quantified simultaneously.

4.6 Optimisation of extraction when using two derivatisation methods

To see whether samples could be loaded onto the SPE cartridges immediately after performing the N-butanol-acetyl chloride derivatisation, the whole sample was loaded onto the pre-conditioned cartridge after incubation. The extraction procedure described by Martinez-Moral & Kannan (2018) was modified for the butyl ester derivatives. EtAc was included as an eluting solvent for the MDA-DNPH derivative (Martinez-Moral & Kannan, 2018), since this product was absent during butylation, the eluting solvent was 2 ml MeOH, instead of 1 ml MeOH and 1 ml EtAc. However, none of the target butyl esters were detected.

The assumption that N-acetyl: butanol chloride interfered with cartridge interaction was made. It was decided to first dry the sample under nitrogen after incubation to get rid of the N-acetyl: butanol chloride. The dried sample was then resuspended in 200 µl 20:80 MeOH/H_2O (v/v).

The sample was then diluted with 800 µl acidified H_2O before loading it onto the pre-conditioned SPE cartridge. The detection of butyl esters improved significantly after drying and resuspending the samples after derivatisation.

To further optimise the SPE protocol for butyl esters, a fraction analysis was done. The wash solvent composition was tested with a fraction analysis. A range of eluting solvents was prepared as seen in Table 4-5. A wash step with H_2O was also included in the fraction analysis. 3-NT-BE and d_5-phe-BE started to elute with 20:80 MeOH/acidified H_2O (v/v) and tyr-BE eluted with 10:90 MeOH/acidified H_2O (v/v) (Figure 4-17).

Table 4-5. Solvents used in the fraction analysis of BE.

Step	Solvent
Wash 1	1 ml H_2O
Wash 2	1 ml 5:95 MeOH/acidified H_2O
Elute 1	1 ml 10:90 MeOH/acidified H_2O
Elute 2	1 ml 20:80 MeOH/acidified H_2O
Elute 3	1 ml 30:70 MeOH/acidified H_2O
Elute 4	1 ml 40:60 MeOH/acidified H_2O
Elute 5	1 ml 50:50 MeOH/acidified H_2O
Elute 6	1 ml 60:40 MeOH/acidified H_2O
Elute 7	1 ml 70:30 MeOH/acidified H_2O
Elute 8	1 ml 80:20 MeOH/acidified H_2O
Elute 9	1 ml 90:10 MeOH/acidified H_2O
Elute 10	1 ml MeOH

The wash solvent was kept 5:95 MeOH/H_2O (v/v) as described by the article (Martinez & Kannan, 2018). The optimal extraction method for butyl esters is described in Table 4-6

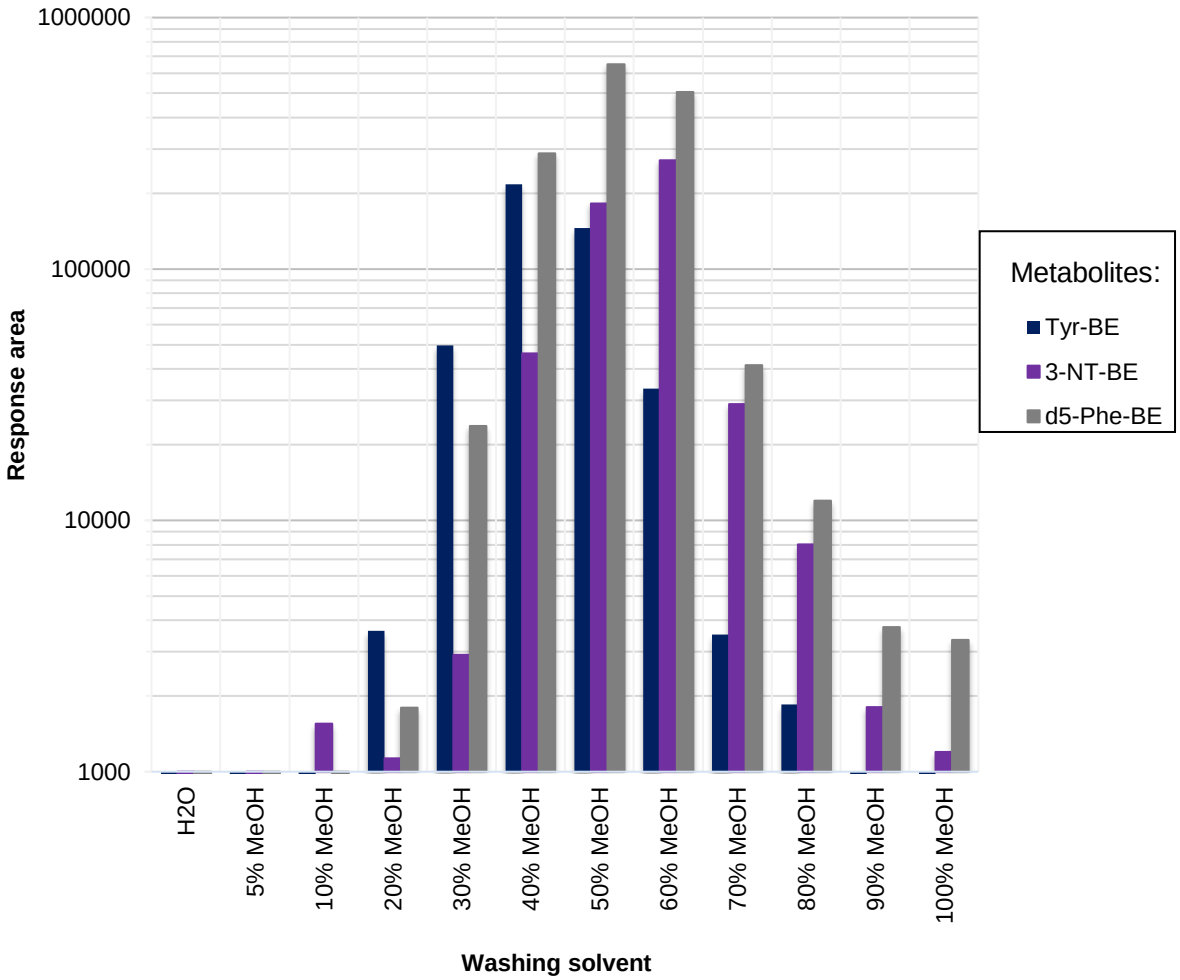

Figure 4-17. Response of butyl esters with different washing solvents. *d_5-phe-BE: d_5-phenylalanine butyl ester, tyr-BE: tyrosine butyl ester, 3-NT-BE: 3-nitrotyrosine butyl ester.*

Table 4-6. Optimal SPE method modified for butyl esters from Martinez & Kannan (2018; 2022).

Equilibrate	2 ml MeOH 2 ml H_2O
Load	Load 1 ml sample
Wash	2 ml 5 % MeOH Dry under vacuum
Elute	2 ml 100 % MeOH

Once the extraction for the butyl esters was optimised, two approaches were considered for the effective extraction of our target metabolites. The first approach entailed loading both butyl ester and DNPH samples onto the same SPE cartridge, whereas the second approach included parallel SPE extraction and combining the eluates before evaporating to dryness (Figure B-5). Both would result in a single sample to be analysed on the LC-ESI-MS/MS.

As seen in Figure 4-18, most metabolites indicated a better response with the SPE where both samples were extracted separately, and the eluates combined. For all further optimisation, this approach was used. Figure 4-19 summarises the optimal sample preparation.

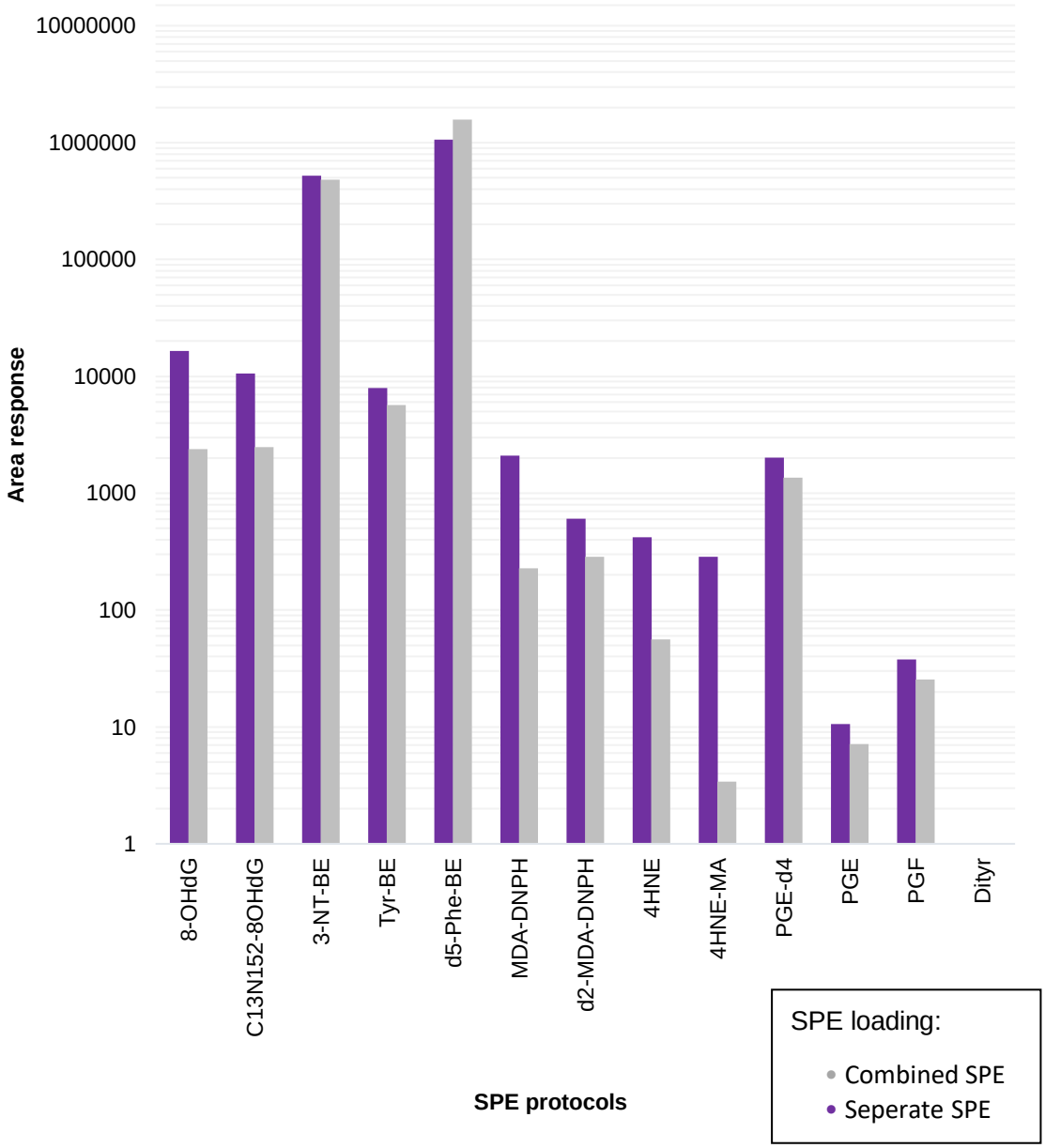

Figure 4-18. Comparison of metabolite responses after SPE optimisation.

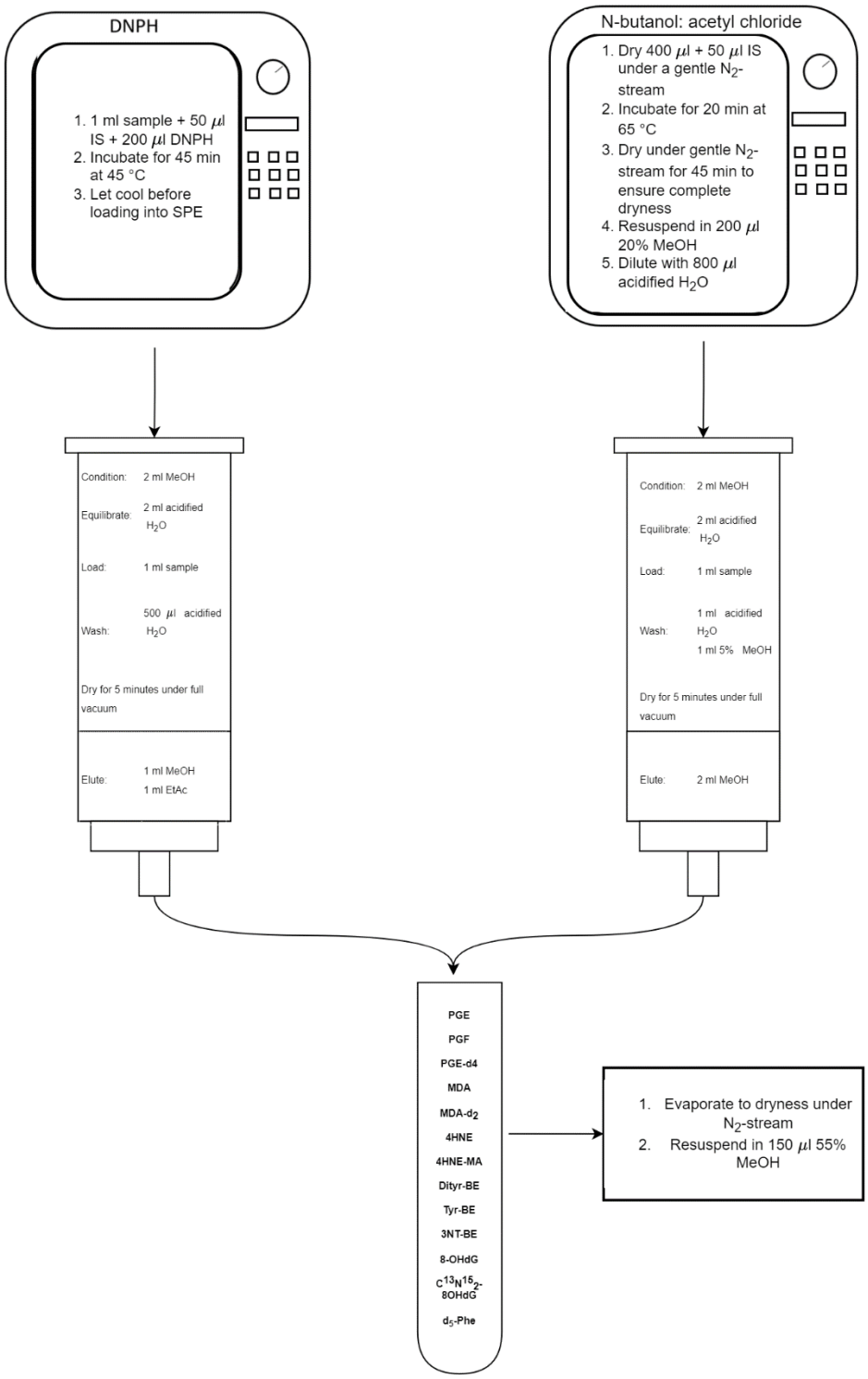

Figure 4-19. Parallel extraction (separate SPE) where eluates are combined before evaporation. *DNPH: 2,4-dinitrophenylhydrazine, SPE: solid phase extraction, IS: internal standard, MeOH: methanol, BE: butyl ester, PGE_2: prostaglandin-E_2, PGF: prostaglandin-Fα_2, PGE-d_4: d_4-prostaglandin-E_2, MDA: malondialdehyde, MDA-d_2: malondialdehyde-d_2, 4-HNE: 4-hydroxynonenal, 4-HNE-MA: 4-hydroxynonenal-mercapturic acid, Dityr-BE: dityrosine butyl ester, Tyr-BE: tyrosine butyl ester, 3NT-BE: 3-nitrotyrosine butyl ester, 8-OHdG: 8-hydroxy-2-deoxyguanosine, $^{13}C^{15}N_2$-8OHdG: 8-oxo-2-deoxyguanosine-^{13}C, $^{15}N_2$.*

4.7 Optimisation of LC-ESI-MS/MS method for analysis of derivatised metabolites

After the sample preparation was optimised, a standard working solution was injected onto the LC-MS/MS to determine whether the polar compounds (amino acids) exhibited better retention. For the first 10 minutes of the method, no elution occurred (Figure 4-20). The LC-ESI-MS/MS was once again optimised; this optimisation included a few gradients, flow rate and column temperature adjustments on a working standard mix (5 ng/ml).

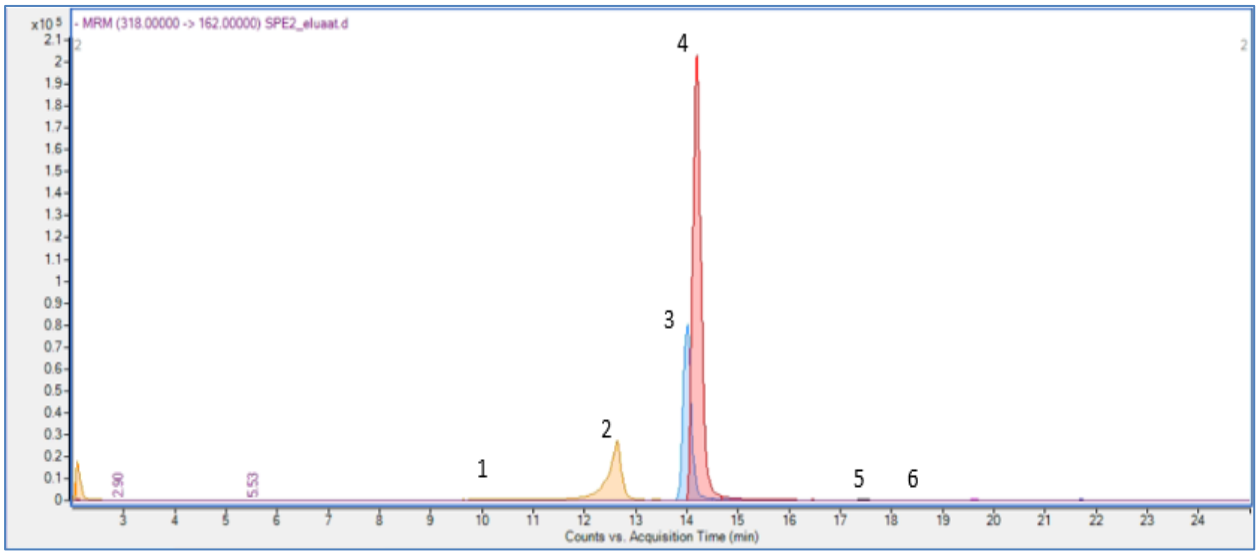

Figure 4-20. Chromatographic profile after optimising the sample preparation techniques. *1. 8-hydroxy-2-deoxyguanosine & 8-oxo-2-deoxyguanosine-^{13}C, $^{15}N_2$, 2. tyrosine-butyl ester, 3. 3-nitrotyrosine-butyl ester, 4. d_5-phenylalanine-butyl ester, 5. 4-hydroxynonenal mercapturic acid, d_2-malondialdehyde-hydrazone & malondialdehyde-hydrazone, 6. prostaglandin E-d_4, prostaglandin $F_{2\alpha}$, & prostaglandin E_2.*

From the results presented in Figure 4-20, dityr was not detected. Dityr, as described in section 2.7.2, is an oxidation product of tyrosine. A dityr sample was prepared and analysed as summarised in Figure 4-19 to investigate the absence of dityr. During this investigation, a great amount of tyrosine butyl ester was detected (Table 4-7). It was concluded that dityr is unstable during N-butanol:acetyl chloride derivatisation, and that dityr reduced to tyr during butylation, resulting in tyr-BE. This possible reduction of dityr could influence the results of tyr. For this reason, dityr was excluded as a target metabolite.

Table 4-7. Investigation of dityrosine detection problem.

Compound	Transition	Peak area	
		Working standard mixture containing dityr	**Dityr standard**
Dityr	361 → 315	ND	ND
Dityr-BE	473.3 → 269.2	48.81	451.76
Tyr-BE	238.0 → 136.1	**150 227.35**	33 246.25

It was also found that the detection of 4-HNE was poor compared to its downstream metabolite 4-HNE-MA. 4-HNE is known to be unstable and reactive towards nucleophiles (Völkel *et al.*, 2005). Therefore, 4-HNE was also excluded from our panel, as 4-HNE-MA, which is more stable, represents the parent metabolite. For further analysis, tyr-BE, 3-NT-BE, PGE_2, $PGF_{2\alpha}$, MDA-DNPH, 8-OHdG, and 4-HNE-MA were analysed.

The method was first optimised by making few gradient adjustments (results not shown), and the final gradient applied is summarised in Table 4-8. This gradient allowed a shorter run time (21 minutes instead of 30 minutes), whilst separating all the compounds effectively (Figure 4-21).

Table 4-8. Optimal conditions for simultaneous analysis.

Time (min)	Mobile phase B (%)
0	0
3	10
5	50
8	65
13	70
17	100
21	Stop

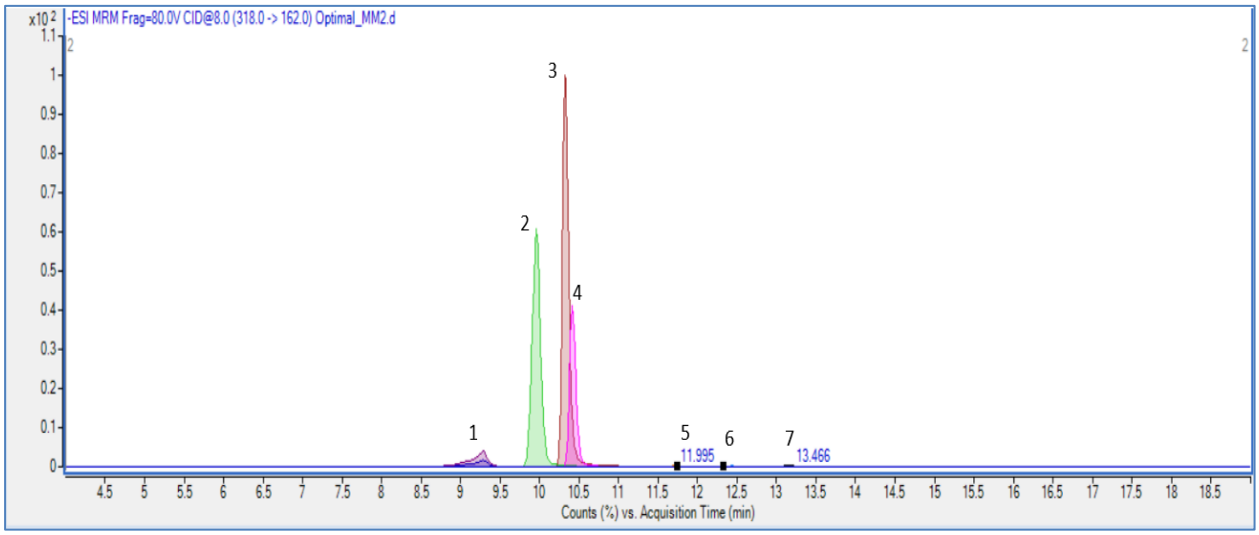

Figure 4-21. Metabolite responses after gradient optimisation. *1: 8-hydroxy-2-deoxyguanosine & 8-oxo-2-deoxyguanosine-^{13}C, $^{15}N_2$, 2: tyrosine-butyl ester, 3: 3-nitrotyrosine-butyl ester, 4: d_5-phenylalanine-butyl ester, 5: 4-hydroxynonenal mercapturic acid, 6: d_2-malondialdehyde-hydrazone & malondialdehyde-hydrazone, 7: prostaglandin E-d_4, prostaglandin $F_{2\alpha}$, & prostaglandin E_2.*

Once the gradient was optimised, the resuspension volume after extraction was optimised. Up until this point a resuspension volume of 150 µl was used. However, when a multiple injection analysis is required and the injection volume exceeds 10 µl, 150 µl might be too little. Therefore, resuspending in 200 µl was considered. Two samples were prepared, as summarised in Figure 4-19.

After evaporation under $N_{2(g)}$, one of the samples was resuspended in 150 µl, and the other was resuspended in 200 µl. For some metabolites (butyl esters & $PGF_{2\alpha}$), a resuspension volume of 150 µl was slightly better than 200 µl. On the other hand, the rest of the metabolites had a much greater response with 200 µl compared to 150 µl (Figure 4-22). From these results, 200 µl resuspension volume was optimal. To determine if it is better to inject a larger volume of a diluted sample, rather than a small volume of a concentrated sample, the injection volume was optimised next.

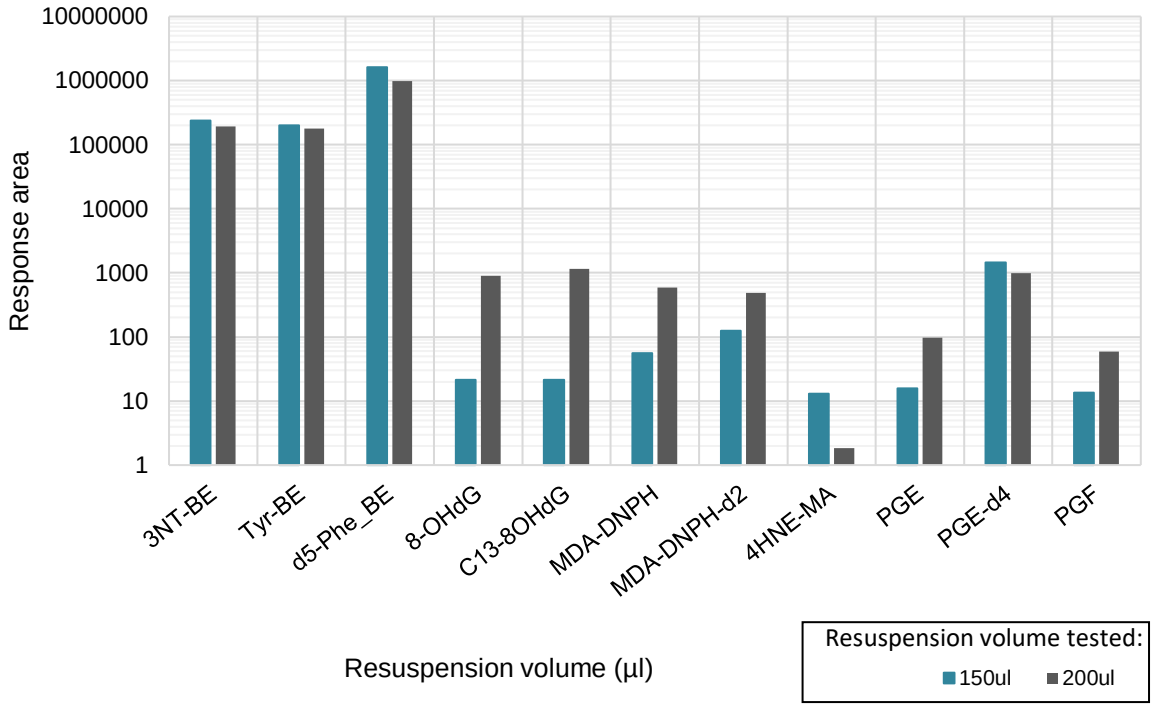

Figure 4-22. Differences in response with resuspension volume optimisation. *3NT-BE: 3-nitrotyrosine, Tyr-BE: tyrosine butyl ester, butyl ester, d5-Phe_BE: d_5-phenylalanine butyl ester, 8-OHdG: 8-hydroxy-2-deoxyguanosine, $^{13}C^{15}N_2$-8OHdG: 8-oxo-2-deoxyguanosine-^{13}C, $^{15}N_2$, MDA: malondialdehyde-hydrazone, MDA-d_2: malondialdehyde-d_2-hydrazone, 4-HNE-MA: 4-hydroxynonenal-mercapturic acid, PGE_2: prostaglandin-E_2, PGF: prostaglandin-Fα_2, PGE-d_4: d_4- prostaglandin-E_2.*

The same samples, both 150 µl and 200 µl were used for the optimisation of injection volume. The samples were analysed with an injection volume range (5 µl, 10 µl, 15 µl, and 20 µl). An increase in response was expected as the injection volume increased. However, this was not the case for all the metabolites. An injection volume of 10 µl was best for d_5-phe-BE and tyr-BE, whereas 15 µl and 20 µl yielded similar responses for the rest of the metabolites (150 µl sample). For the sample resuspended in 200 µl, an injection volume of 20 µl was the best for all metabolites (results not shown). Therefore, it was decided to resuspend in 200 µl H_2O: MeOH (45:55 v/v) and inject 20 µl thereof into the LC-ESI-MS/MS, which would allow six injections per sample. It was also concluded for this study, that injecting a greater volume of a diluted sample was better than injecting a small volume of concentrated sample.

After the injection volume was optimised, the column temperatures were optimised again. A sample was injected into the system and analysed with column temperatures at 20 °C, 25 °C, 30 °C, 35 °C, 40 °C, and 45 °C. Due to retention shifts, peak shape, and response of metabolites an optimal column temperature of 35 °C was selected (figure B-6).

Lastly, the flow rate was optimised. A single sample was injected into the system and analysed with flow rates of 0.1 ml/min, 0.15 ml/min, 0.2 ml/min, 0.25 ml/min, 0.3 ml/min, and 0.35 ml/min. As the gradient was optimised for retention purposes, a flow greater than 0.35 ml/min was not considered for the optimisation as the flow rate influences retention times. With a flow rate of 0.1 ml/min, there was a lot of interference at the start of the analysis. A flow of 0.3 ml/min on the other hand resulted in some metabolites detected far earlier than expected, for this reason, a flow rate of 0.25 ml/min was chosen as optimal.

As a final optimisation step, the gradient was slightly adjusted, and the method was split into segments to ensure optimal sensitivity. In the first part of the method (0-4 min), the diverter valve in the binary pump was set to waste, to ensure that any polar compounds still present were prevented from entering the MS and causing ion suppression. After 4 min, the valve was switched to the MS for detection, for this segment; the mass analysers were set to scan for the target compounds. The final LC-ESI-MS/MS method is summarised in Table 4-9. The initial sample volume for DNPH derivatisation was adjusted from 1 ml to 400 µl. This modification was done to make the concentration calculations comparable between the two analysed fractions (Butyl esters and DNA and lipid peroxidation markers). Because of the sample volume adjustment, the DNPH concentration was also adjusted by factor 10, to prevent excess DNPH as mentioned in section 4.3. The IS mix was also adjusted for both fractions. The butylated fraction only contained d_5-phe (0.01 µg/ml), whereas the DNA and lipid peroxidation marker fraction contained PGE–d_4, $^{13}C^{15}N_2$-8OHdG, and MDA-d_2 (0.1 µg/ml).

Table 4-9. Optimised LC-ESI-MS/MS method.

Segments	Time (min)	Diverter Valve	Mobile phase B (%)	Flow rate (ml/min)	Column temperature (°C)	Injection volume (µl)
1.	0	Waste	0	0.25	35	20
	3		10			
	4		21.1			
2.	6	MS	65	0.25	35	20
	13		70			
	17		100			
	19		Stop			

A standard working mixture (5 ng/ml) and a spiked urine (5 ng/ml) were analysed after optimisation. The standard working mixture sample was used to establish the retention times of the target analytes (Table 4-10). The spiked urine sample was used to assess the matrix effect. The spiked urine sample resulted in poor detection of our target metabolites, especially 8-OHdG, $PGF_{2\alpha}$, PGE_2, and 4-HNE-MA, this might be ascribed to the influence of the matrix.

Table 4-10. Retention times and optimal LC parameters of our target analytes. These parameters include the precursor and product ions used for detection, the polarity of the ions detected, the energy used to break the compounds (collision energy), energy used to carry the ions (CAV) and energy needed in the capillary (fragmentor).

Compound	**Transitions (m/z)**	**Retention time (minutes)**	**Polarity**	**Collision energy (V)**	**Fragmentor (V)**	**Cell accelerator voltage (V)**
Tyr–BE	238 → 136	10.68	+	12	97	7
3-NT–BE	283 → 181	11.33	+	12	107	
d_5-phe-BE	227 → 125	11.47	+	12	86	
8-OHdG	284 → 168	7.94	+	8	91	
$C^{13},N^{15}{}_2$- 8–OHdG	287 → 171	7.94	+	8	91	
MDA - DNPH	235 →189	13.07	+	12	135	
MDA-d_2-DNPH	237 → 191	13.05	+	12	135	
4-HNE-MA	318 → 162	13.38	-	8	80	
PGE_2	351 → 271	14.9	-	12	74	
PGF	353 → 309	14.97	-	12	74	
PGE–d_4	355 → 275	14.84	-	12	74	

One possible contributing factor to the poor detection of analytes in the spiked urine sample, is overloading the analytical column due to the complexity of this matrix. To assess this, the loading volume was adjusted. After derivatisation, either 500 µl or 1 ml was loaded onto the SPE cartridges, and the final eluates were analysed. The results for the working standards were comparable (Figure B-7) for the different loading volumes whereas, for the spiked urine samples a smaller loading volume resulted in better detection for most metabolites (Figure 4-23).

From the results obtained here, it was concluded that the SPE cartridges were possibly overloaded when 1 ml sample was used, resulting in poor recovery, especially for 8-OHdG and $^{13}C^{15}N_2$-8OHdG. Therefore, a loading volume of 500 µl was used. Furthermore, the butyl esters (fraction A) were resuspended in 800 µl instead of 1 ml, which made the dilution factor the same as for fraction B.

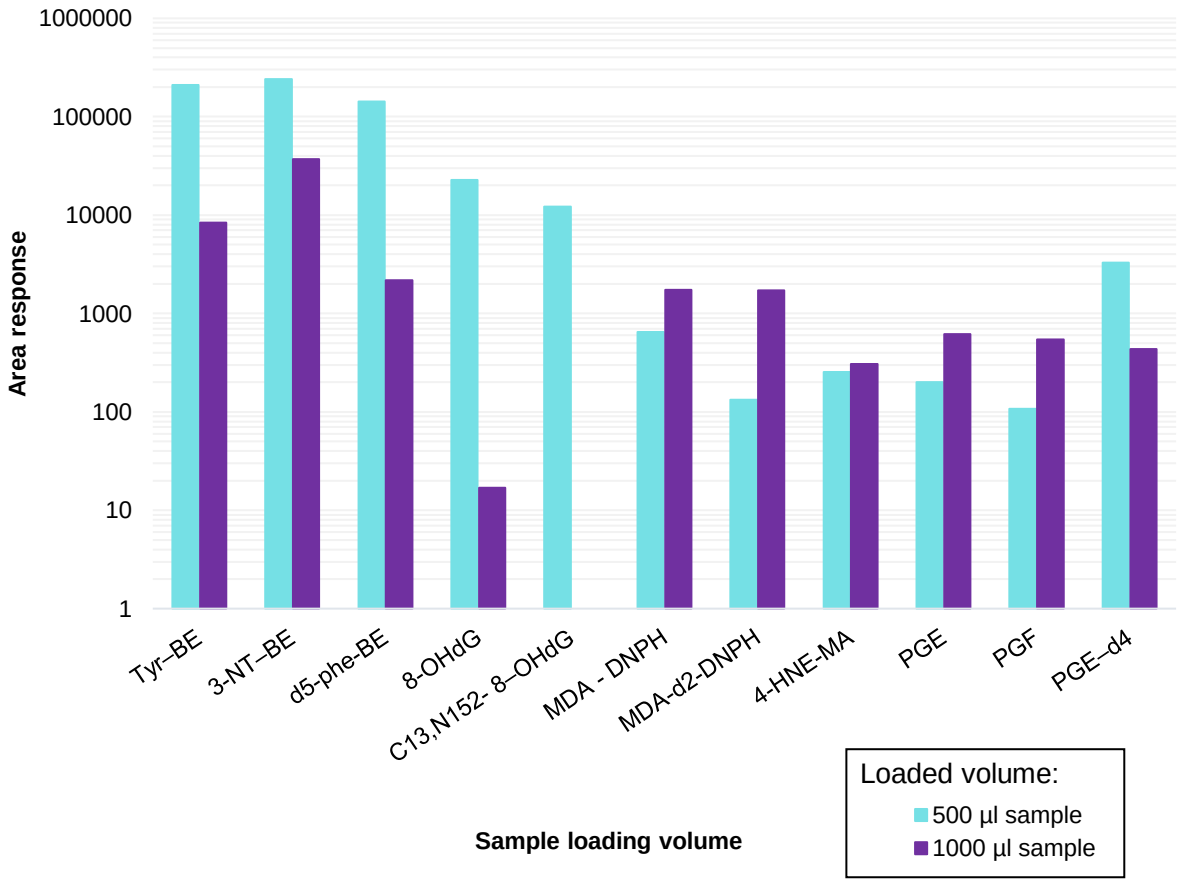

Figure 4-23. Response of metabolites with different SPE loading volumes (spiked urine 5 ng/ml). *3NT-BE: 3-nitrotyrosine, Tyr-BE: tyrosine butyl ester, butyl ester, d5-Phe_BE: d_5-phenylalanine butyl ester, 8-OHdG: 8-hydroxy-2-deoxyguanosine, $^{13}C^{15}N_2$-8OHdG: 8-oxo-2-deoxyguanosine-^{13}C, $^{15}N_2$, MDA: malondialdehyde-hydrazone, MDA-d_2: malondialdehyde-d_2-hydrazone, 4-HNE-MA: 4-hydroxynonenal-mercapturic acid,* PGE$_2$*: prostaglandin-E$_2$, PGF: prostaglandin-Fα_2, PGE-d_4: d_4- prostaglandin-E$_2$.*

It was also decided to analyse a serial dilution series (starting concentration: 1 µg/ml; lowest concentration: 0.06 ng/ml) to determine the detection limits. From these results (Table B-7), it was evident that the physiological concentrations (Annexure C) of the target metabolites were below the detection and quantification limits. To improve the detection of these low levels, the internal standard concentrations were adjusted (Table 4-11). Since stable isotopes and the natural compounds are nearly identical, only a trace amount of analyte present in a sample would be sufficient for quantification. This is possible because the instrument response for both compounds would be identical, if a larger amount of isotopes is added into the sample, the greater the response of the natural compound.

Table 4-11. Adjusted isotope concentrations for further analysis.

Isotope	**Starting concentration (ng/ml)**	**In-vial concentration (ng/ml)**
$^{13}C^{15}N_2$-8OHdG	950	641.25
d_5-phe	1000	250
MDA-d_2	780	344.25
PGE–d_4	510	526.5

Despite the increase in IS concentrations, some metabolites (8-OHdG, ^{13}C $^{15}N_2$-8-OHdG, 4-HNE-MA, both PGE_2 and $PGF_{2\alpha}$) resulted in a poor response in relation to others (butyl esters) (Figure 4-24). To determine whether the metabolites may be influencing each other when the eluates are combined before analysis, the butyl esters were analysed separately from the rest of the compounds.

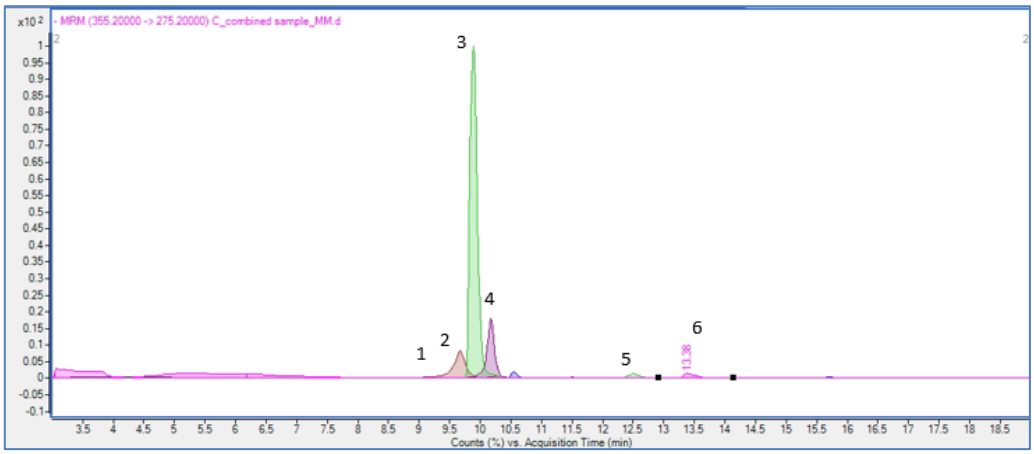

Figure 4-24. Chromatographic separation after new internal standard concentrations. *1. 8-hydroxy-2-deoxyguanosine & 8-oxo-2-deoxyguanosine-^{13}C, $^{15}N_2$, 2. tyrosine-butyl ester, 3. 3-nitrotyrosine-butyl ester, 4. d_5-phenylalanine-butyl ester, 5. d_2-malondialdehyde-hydrazone & malondialdehyde-hydrazone, 6. prostaglandin E-d_4, prostaglandin $F_{2\alpha}$, & prostaglandin E_2.*

For the butyl ester analysis (fraction A), the compounds in the working standard mix were detected somewhat better with the combined analysis compared to separate analysis (Figure 4-25). The difference in response was not as prominent in the urine matrix, although, the response of the combined analysis still appeared to be slightly higher. Almost all the remaining analytes indicated a better response when analysed separately for both spiked urine and working standard mix (Figure 4-26). The response of the metabolites in urine was much lower than the working standard mix. As the aim of this study is to analyse urine samples, it was decided that analysing the fractions separately would be the better choice.

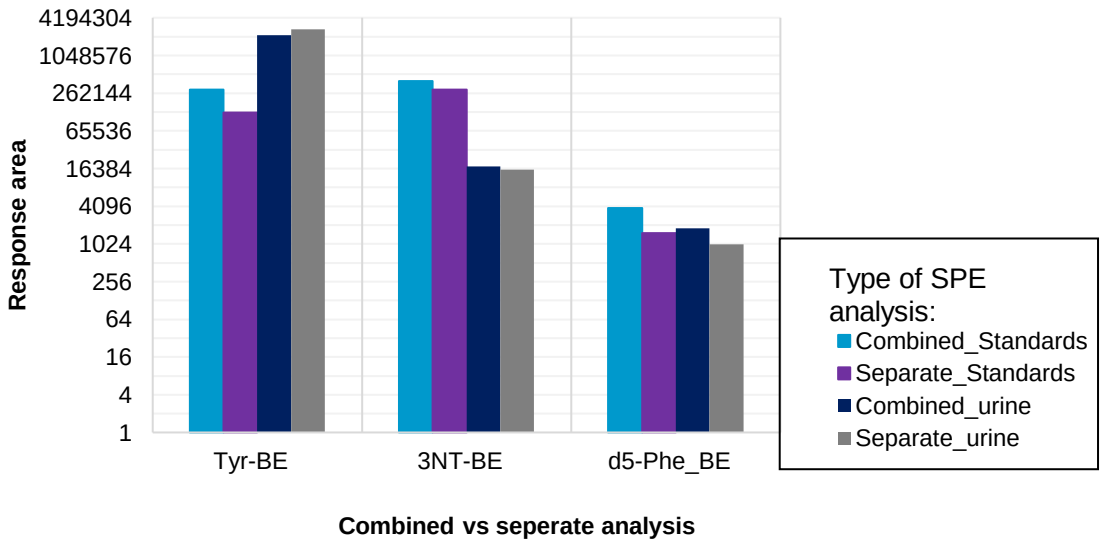

Figure 4-25. Comparison of butyl ester (fraction A) response when analysing the fractions combined or separate. *d_5-phe-BE: d_5-phenylalanine butyl ester, tyr-BE: tyrosine butyl ester, 3-NT-BE: 3-nitrotyrosine butyl ester.*

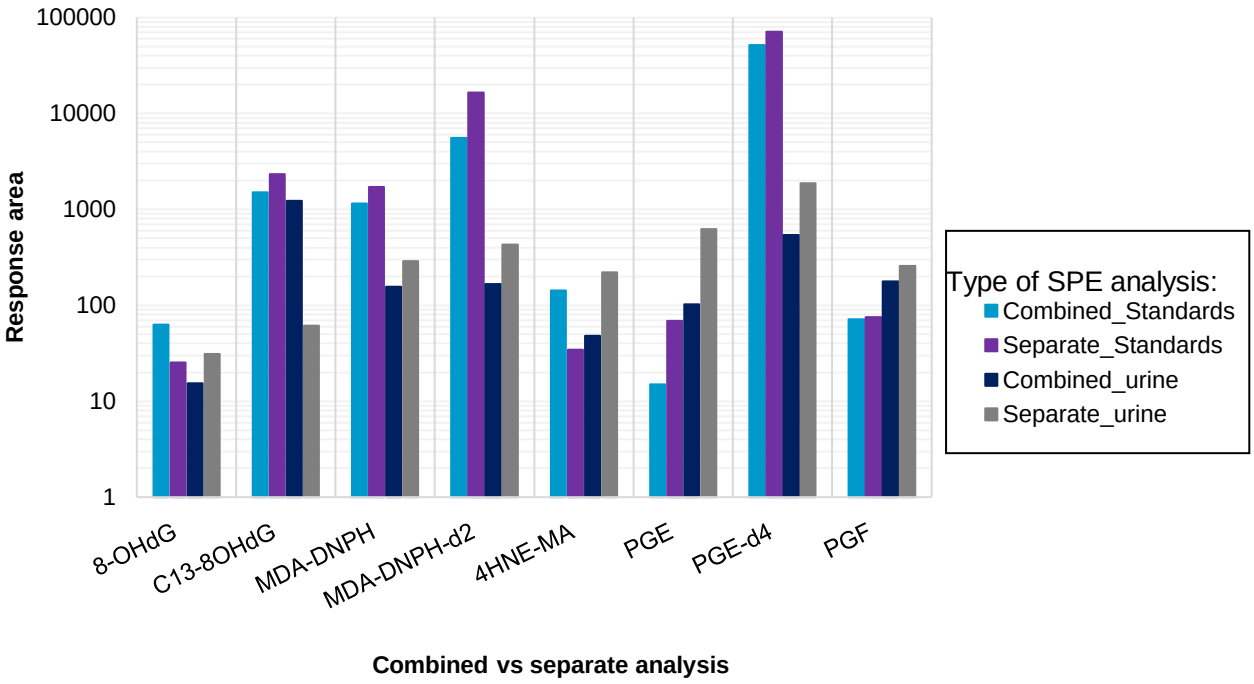

Figure 4-26. Comparison of fraction B metabolite response when analysing the fractions combined or separate. *8-OHdG: 8-hydroxy-2-deoxyguanosine, ^{13}C-8OHdG: 8-oxo-2-deoxyguanosine-^{13}C, $^{15}N_2$, MDA: malondialdehyde-hydrazone, MDA-d_2: malondialdehyde-d_2-hydrazone, 4-HNE-MA: 4-hydroxynonenal-mercapturic acid, PGE_2: prostaglandin-E_2, PGF: prostaglandin-Fα_2, PGE-d_4: d_4- prostaglandin-E_2.*

Taking the separate responses for both urine and working standards into account, it was decided to split the method into two separate methods. As the sample preparation was optimised at this point, the LC-ESI-MS/MS methods had to be re-optimised to ensure that the optimal instrument conditions were used for both analyses.

4.8 Optimisation of separate methods

From previous data (Figure 4-23 & Figure 4-24) it was evident that metabolite detection was suppressed in the urine matrix. Therefore, optimisation was done on working standard solutions (10 ng/ml) to ensure that the results were reliable. The injection volume, gradient, column temperature, and flow rate were re-optimised for both methods separately.

The fraction A and B samples were prepared according to the optimised sample preparation protocol (described below in section 4.9.1 and section 4.9.2 respectively). For the injection volume analysis, a single sample was analysed with the following injection volume range (5 µl, 10 µl, 15 µl, and 20 µl). After the optimisation of the injection volume, the respective gradients were optimised based on previous data obtained in this study (Annexure B).

After the gradient adjustments were made, the flow rate was optimised. A single sample was injected into the system and analysed with flow rates of 0.15 ml/min, 0.2 ml/min, 0.25 ml/min, 0.3 ml/min, and 0.35 ml/min. Finally, the column temperature was optimised by analysing a single sample at different column temperatures (20 °C, 25 °C, 30 °C, 35 °C, 40 °C, and 45 °C).

4.8.1 Optimisation of butyl ester fraction

For the injection volume analysis, the butyl ester responses increased slightly with the injection volume. From the working standard analyses, 20 µl injection gave the highest response, as seen in Figure 4-27, and was considered most optimal. These results correspond with the results obtained in section 4.7. Therefore, a 20 µl injection volume was used for further analysis.

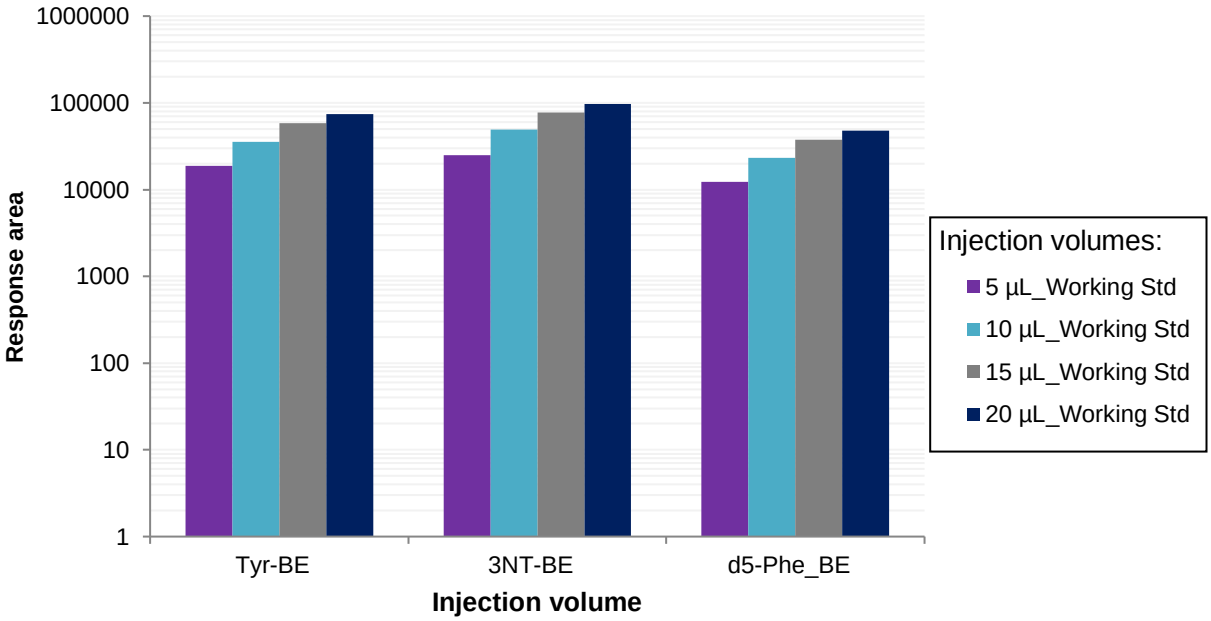

Figure 4-27. Injection volume optimisation of butyl esters. *d_5-phe-BE: d_5-phenylalanine butyl ester, tyr-BE: tyrosine butyl ester, 3-NT-BE: 3-nitrotyrosine butyl ester.*

Secondly, a gradient adjustment was made (Table 4-12). In the first part of the method (0-3 min), the diverter valve in the binary pump was set to waste, to ensure that any polar compounds still present were prevented from entering the MS and causing ion suppression. The starting mobile phase composition was 20% mobile phase B. After 3 min, the valve was switched to the MS for detection. For this segment, the mass analysers were set to scan for the target compounds (tyr-BE, 3-NT-BE and d_5-Phe). The mobile phase composition was increased to 60% 3.5 min after analysis started. Within the next 5 minutes the gradient increased to 70% mobile phase B and after another 0.5 minutes to 100% mobile phase B, where it was kept constant until the analysis stopped at 10 minutes.

With this gradient, the runtime could be shortened significantly, whilst retaining the compounds and separating them successfully. The post time was set for 5 minutes, resulting in a total runtime of 15 minutes.

Table 4-12. Gradient adjustment for butyl ester method.

Segments	Time (min)	Diverter Valve	Mobile phase B (%)
1.	0	Waste	20
2.	3	MS	57
	3.5		60
	8		70
	8.5		100

Next, the flow rate was optimised. Flow rates of 0.25, 0.3, and 0.35 ml/min yielded high responses results (Figure 4-28). When adjusting the flow rate, the retention times of the analytes shift, resulting in more/less compounds in the ion source at a certain time. Therefore, a great change in the flow rate would require source condition optimisation to be repeated. For this reason, 0.25 ml/min was chosen as the best flow rate for further analyses.

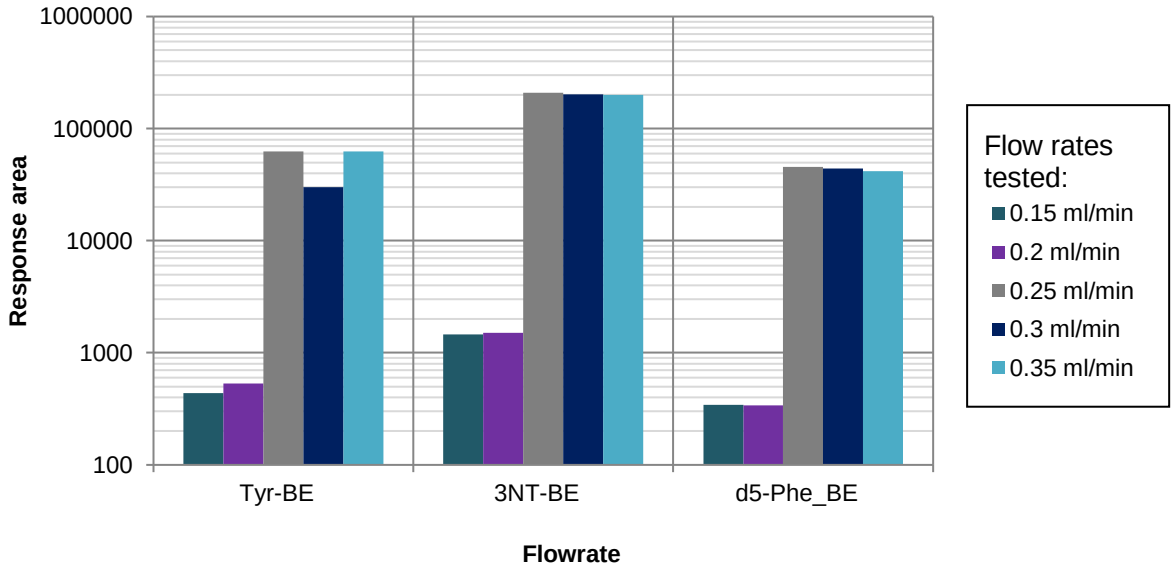

Figure 4-28. Optimisation of flow rate for butyl ester analysis. *d_5-phe-BE: d_5-phenylalanine butyl ester, tyr-BE: tyrosine butyl ester, 3-NT-BE: 3-nitrotyrosine butyl ester.*

From the column temperature analysis results (Figure 4-29), it was evident that 35 °C was least optimal for the butyl esters. The other temperatures gave similar results. tyr-BE and d_5-Phe-BE gave the best response with a column temperature of 30 °C, therefore, this was the chosen temperature.

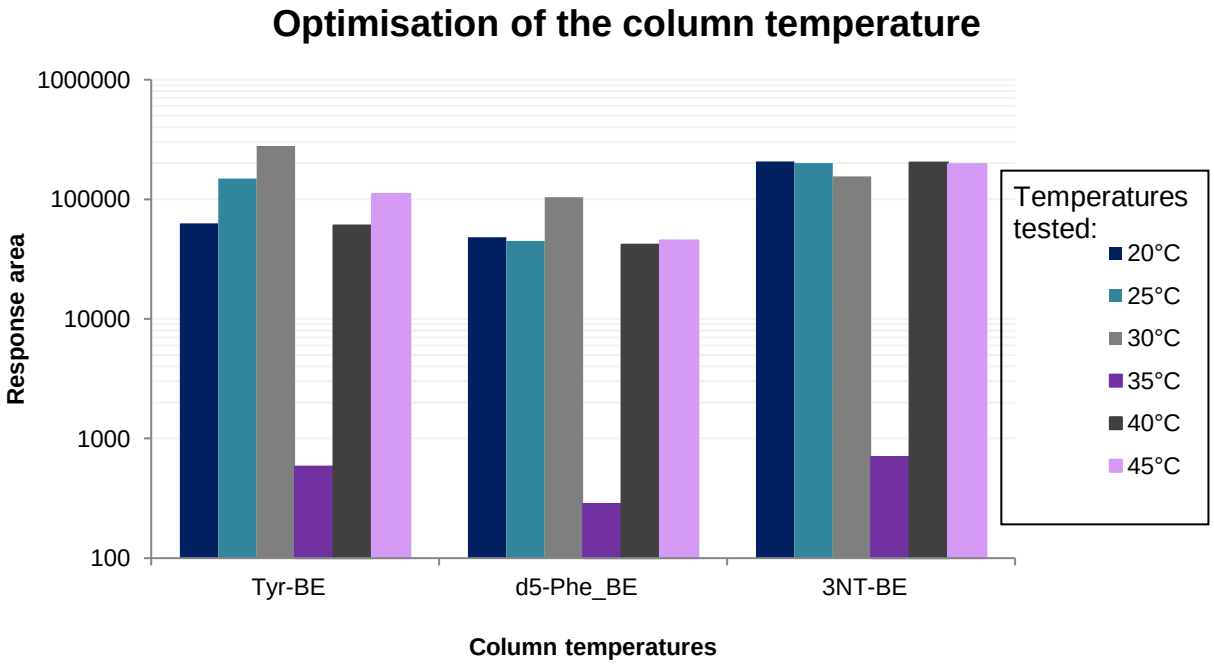

Figure 4-29. Column temperature optimisation. *d_5-phe-BE: d_5-phenylalanine butyl ester, tyr-BE: tyrosine butyl ester, 3-NT-BE: 3-nitrotyrosine butyl ester.*

Once all the conditions were optimised, a spiked urine sample was analysed to test the method on matrix. It was during this time that it was found that the response lowered significantly, this may be caused by ion suppression (matrix effect) (Table B-8). To determine whether a lower injection volume might resolve the problem, the injection volume range (as tested with the working standard mix) was tested on the spiked urine sample. From this data, a slight decrease in response occurred with increased injection volume (Figure 4-30). For this reason, the injection volume was adjusted again to 10 µl for both working standards and the matrix. The rest of the conditions seemed appropriate for the urine sample and were left unaltered.

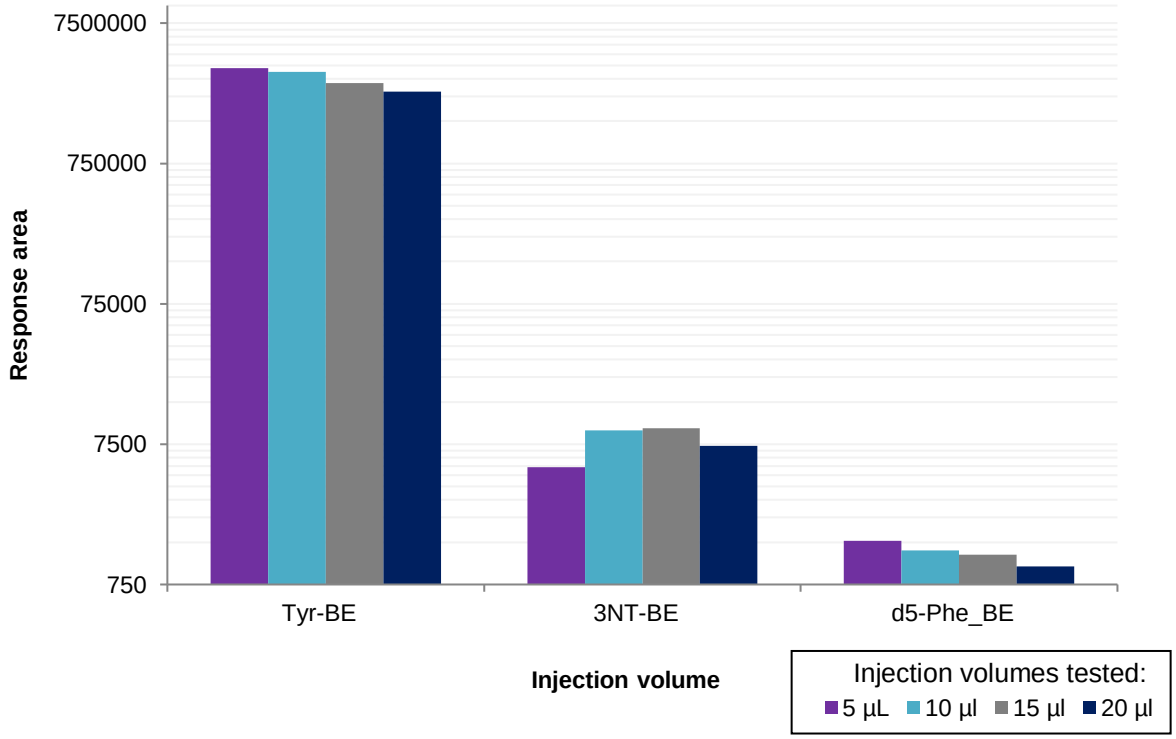

Figure 4-30. Injection volume optimisation on a spiked urine sample.

4.8.2 Optimisation of DNA and lipid peroxidation marker fraction

For the injection volume optimisation of the DNA and lipid peroxidation marker fraction, an injection volume of 15 µl gave the highest response for most of the analytes (Figure 4-31). The response of the target analytes did not increase as the injection volume increased. This might be due to ion suppression during ionisation, especially for highly concentrated analytes such as the internal standards.

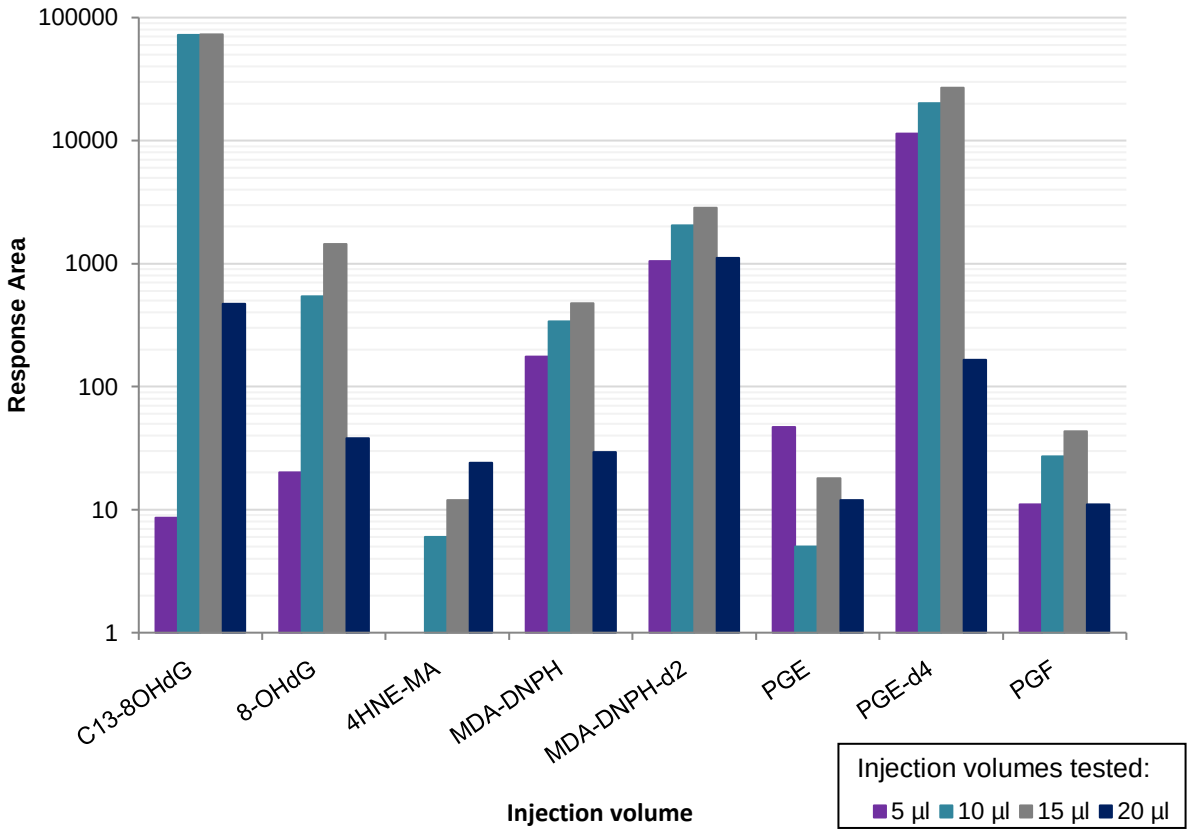

Figure 4-31. Injection volume optimisation of DNA and lipid peroxidation marker fraction (working standard). *8-OHdG: 8-hydroxy-2-deoxyguanosine, ^{13}C-8OHdG: 8-oxo-2-deoxyguanosine-^{13}C, $^{15}N_2$, MDA: malondialdehyde-hydrazone, MDA-d_2: malondialdehyde-d_2-hydrazone, 4-HNE-MA: 4-hydroxynonenal-mercapturic acid, PGE: prostaglandin-E_2, PGF: prostaglandin-Fα_2, PGE-d_4: d_4- prostaglandin-E_2.*

Once the injection volume to be used was established, the gradient was re-adjusted according to previous data. The gradient adjustment was made to shorten the total run-time, whilst retaining and separating the target analytes efficiently. During gradient adjustment, segments were also inserted into the method to increase sensitivity, as the retention times of the target analytes were still far apart (Table 4-13). The method was split into four segments. During the first segment (0-1.8 min) the diverter valve was set to waste, and during the following three segments the valve was diverted to the MS (1.8 – 12 min). The starting mobile phase composition was 20% mobile phase B. The gradient increased to 60% within 4.5 minutes from the start of the run. At 10 minutes, the composition was 70% mobile phase B. After 2 more minutes, the gradient was at 100% mobile phase B and kept constant until the end of the run (15 minutes). The method also included a 5-minute post-time to allow the pressure to stabilise before the next analysis, resulting in a total runtime of 20 minutes for the DNA and lipid peroxidation marker fraction.

Table 4-13. Gradient adjustment for DNA and lipid peroxidation marker fraction.

Segments	Time (min)	Diverter Valve	Mobile phase B (%)
1	0	Waste	20
2	1.8	MS	27
	4.5		60
3	7	MS	64
	10		70
4	11.5	MS	94
	12		100

Once the gradient was successfully altered, the flow rate was optimised. For most metabolites, the difference in response was very little between different flow rates (Figure 4-32). However, the response of 8-OHdG varied between the different flow rates, with 0.25 ml/min giving the best result. This might have been because the source conditions were originally optimised for a 0.25 ml/min flow rate and may not have been optimal for the other flow rates. For these reasons, the flow rate was kept to 0.25 ml/min.

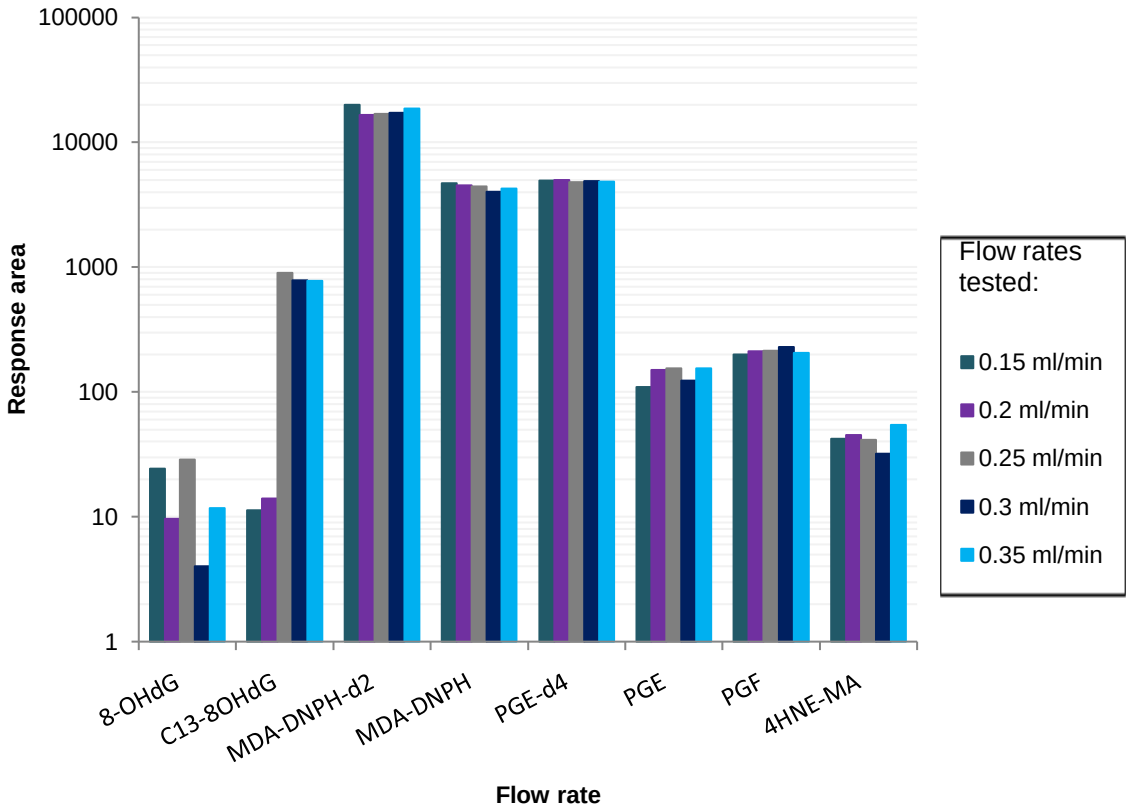

Figure 4-32. Optimisation of the flow rate for the DNA and lipid peroxidation marker fraction. *8-OHdG: 8-hydroxy-2-deoxyguanosine, ^{13}C-8OHdG: 8-oxo-2-deoxyguanosine-^{13}C, $^{15}N_2$, MDA: malondialdehyde-hydrazone, MDA-d_2: malondialdehyde-d_2-hydrazone, 4-HNE-MA: 4-hydroxynonenal-mercapturic acid, PGE: prostaglandin-E_2, PGF: prostaglandin-Fα_2, PGE-d_4: d_4-prostaglandin-E_2.*

Lastly, the column temperature was optimised. Both 20 ºC and 25 ºC yielded good responses compared to higher temperatures (Figure 4-33). In the end, a column temperature of 25 ºC was selected since it yielded slightly higher responses.

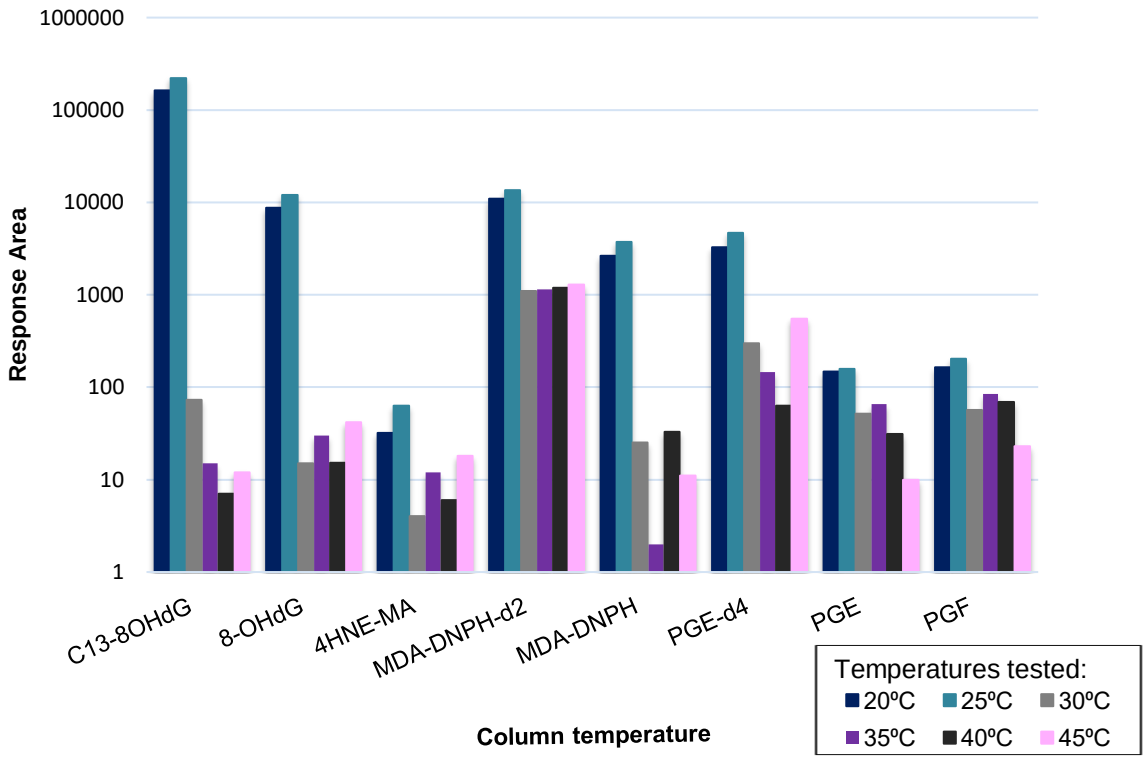

Figure 4-33. Column temperature optimisation for DNPH analysis. *8-OHdG: 8-hydroxy-2-deoxyguanosine, ^{13}C-8OHdG: 8-oxo-2-deoxyguanosine-^{13}C, $^{15}N_2$, MDA: malondialdehyde-hydrazone, MDA-d_2: malondialdehyde-d_2-hydrazone, 4-HNE-MA: 4-hydroxynonenal-mercapturic acid, PGE: prostaglandin-E_2, PGF: prostaglandin-Fα_2, PGE-d_4: d_4- prostaglandin-E_2.*

As with the BE analysis, all the conditions were optimised, and a spiked urine sample was analysed to test the method on matrix. Again, the analyte response in the spiked urine sample was much lower, compared to the working standard (Table B-9), possibly due to ion suppression (matrix effect). The decrease was, however, not as great as for the BE metabolites, therefore, no LC-ESI-MS/MS parameters were re-optimised.

4.9 Final methods until validation

Two aliquots (400 µl) of each sample were used for this analysis. The first aliquot (fraction A) was used for butylation, and the second aliquot (fraction B) was used for DNPH derivatisation. The fractions were analysed via two separate methods which are individually described below.

4.9.1 Butyl ester fraction

4.9.1.1 Sample preparation of butyl esters

For butylation, 50 µl d_5-phe (1 µg/ml) was added to the aliquots and dried under a gentle nitrogen gas stream at 45°C. Once the samples were dried, 200 µl N-butanol:acetyl chloride was added, and the samples were incubated for 20 minutes at 65 °C.

The samples were evaporated to dryness under a gentle nitrogen gas stream at 45 °C. Before loading onto the SPE cartridge, the samples were resuspended in 200 µl 20:80 MeOH:H_2O (v/v), and then diluted with 600 µl acidified H_2O.

While the samples were derivatising, the Bond Elut Nexus SPE (60mg/3ml) cartridges for each sample were equilibrated and conditioned with 2 ml MeOH and 2 ml acidified water. Firstly, fraction A samples were extracted by loading 500 µl of sample onto the cartridge. The cartridges were washed with 1 ml acidified H_2O followed by 1 ml 5% MeOH and vacuumed to dryness for 5 minutes. Elution occurred with 2 ml MeOH. The eluates were collected and dried under a gentle nitrogen gas stream at 45 °C. The samples were then resuspended in 200 µl 55:45 MeOH/H_2O (v/v), and vortexed for 30 seconds to ensure everything was dissolved. The samples were filtered by centrifugation for 2 minutes at 1753 RCF using 0.2 µm Nylon Spin-X filters. The supernatant was transferred to a clean vial for analysis on the LC-ESI-MS/MS.

4.9.1.2 Separation and detection of butyl esters

The samples were inserted into the autosampler, which was kept at a constant temperature (4 ˚C). The samples (10 µl) were injected onto the SB-Zorbax Aq column, which was kept at a constant temperature of 30 °C. Mobile phase A consisted of acidified H_2O (0.1% acetic acid) and mobile phase B consisted of 80:20 acidified MeOH:ACN (v/v). The starting mobile phase composition was 20% B and increased to 60% within 3.5 minutes. The mobile phase composition increased to 70% B after another 5 minutes. The diverter valve was switched to waste for the first 3 minutes of the analysis, after which it was diverted to the MS for analysis. After 8.5 minutes since the analysis started, the mobile phase composition was 100% B (Table 4-13). The runtime was 10 minutes, together with a 5-minute post time to equilibrate for the next analysis resulting in a total analysis time of 15 minutes. A gas flow of 4 l/min, a gas temperature of 200 °C, a sheath flow of 8 l/min, a sheath temperature of 350 °C, a nebulizer pressure of 30 psi, nozzle voltage of ± 500V, and capillary voltage of ± 3000V were used. The MRMs and final LC parameters and conditions are summarised in Table 4-14

Table 4-14. Retention times and optimal LC parameters for the butyl ester fraction method. These parameters include the precursor and product ions used for detection, the polarity of the ions detected, the energy used to break the compounds (collision energy), energy used to carry the ions (CAV) and energy needed in the capillary (fragmentor).

Compound	Transitions (m/z)	Retention time (minutes)	Polarity	Collision energy (V)	Fragmentor (V)	Cell accelerator voltage (V)
Tyr–BE	238 → 136	5.8	+	12	97	7
3-NT–BE	283 → 181	6.85	+	12	107	7
d_5-phe-BE	227 → 125	6.91	+	12	86	7

4.9.2 DNA and lipid peroxidation marker fraction

4.9.2.1 Sample preparation of DNA and lipid peroxidation marker fraction

For the DNPH derivatisation, 135 µl IS mixture and 200 µl DNPH (0.005 M) were added to the aliquots. The samples were incubated at 45 °C for 45 minutes and then cooled to room temperature before further analysis. For samples where extraction was used, 500 µl sample was loaded onto the pre-conditioned SPE cartridges. The columns were washed with 500 µl acidified water and vacuumed to dryness for 5 minutes. Elution occurred with 1 ml MeOH, followed by 1 ml EtAc. The eluates were dried under a gentle nitrogen gas stream at 45°C. The samples were resuspended in 200 µL 55:45 MeOH/H_2O, and vortexed for 30 seconds to ensure everything is dissolved. The samples were filtered and centrifuged for 2 minutes at 1753 RCF, using 0.2 µm Nylon Spin-X filters. The supernatant was transferred to a clean vial for analysis on the LC-ESI-MS/MS.

4.9.2.2 Separation and detection of DNA and lipid peroxidation marker fraction

The samples were inserted into the autosampler, which was kept at a constant temperature (4 ˚C). The samples (15 µl) were injected into the SB-Zorbax Aq column, which was kept at a constant temperature of 4 °C. Mobile phase A consisted of acidified H_2O (0.1% acetic acid) and mobile phase B consisted of 80:20 acidified MeOH:ACN (v/v). The starting mobile phase composition was 20% B and increased to 60% within 4.5 minutes. The diverter valve was switched to waste for the first 2.5 minutes of the analysis, after which it was diverted to the MS for analysis.

After 10 minutes from the start of the analysis, the mobile phase composition was 70% B, and the gradient was increased to 100% B within 2 minutes (Table 4-14). The runtime was 15 minutes. A 5-minute post time to equilibrate for the next analysis was included, resulting in a total analysis time of 20 minutes. A gas flow of 4 l/min, a gas temperature of 200 °C, sheath flow of 8 l/min, sheath temperature of 350 °C, nebulizer pressure of 30 psi, nozzle voltage of ± 500V, and a capillary voltage of ± 3000V were used. The MRMs and final LC parameters and conditions are summarised in Table 4-15.

Table 4-15. Retention times and optimal LC parameters of our target analytes. These parameters include the precursor and product ions used for detection, the polarity of the ions detected, the energy used to break the compounds (collision energy), energy used to carry the ions (CAV) and energy needed in the capillary (fragmentor).

Compound	Transitions	Retention time (minutes)	Polarity	Collision energy (V)	Fragmentor (V)	Cell accelerator voltage (V)
8-OHdG	284 → 168	3.13	+	8	91	7
$C^{13},N^{15}{}_2$- 8–OHdG	287 → 171	3.12	+	8	91	7
MDA - DNPH	235 →189	10.14	+	12	135	7
d_2-MDA-DNPH	237 → 191	10.12	+	12	135	7
4-HNE-MA	318 → 162	11.32	-	8	80	7
PGE_2	351 → 271	12.85	-	12	74	7
PGF	353 → 309	12.76	-	12	74	7
PGE–d_4	355 → 275	12.87	-	12	74	7

4.10 Conclusion

The original aim of this study was to develop an LC-ESI-MS/MS method for the simultaneous quantification of a collection of urinary oxidative stress markers. In the end, this proved to be much more complex than originally thought due to the broad spectrum of target compound characteristics.

However, two separate methods could successfully be developed and implemented to analyse seven of the nine target analytes, using four isotopes for quantification. During method development different sample preparation techniques were applied and compared to determine the optimal sample treatment. This included different derivatisation techniques and the optimisation thereof, the optimisation of the extraction methods, as well as the optimisation of the LC-ESI-MS/MS methods. Both methods were partially validated, as described in chapter 5.

CHAPTER 5: PARTIAL METHOD VALIDATION

This chapter presents the results of the method validation process as described in chapter two. Linearity, accuracy, precision, recovery, carryover, and the matrix effect were all addressed during validation, both butyl ester and DNA and lipid peroxidation marker methods were validated separately over three consecutive days. During sample preparation, the samples were concentrated (2x) during the drying and resuspension step that followed SPE. Therefore, all data processing and reporting were done based on in-vial concentrations, unless stated otherwise.

5.1 Partial validation of butyl esters

5.1.1 Calibration curve and linearity

For the evaluation of the linear range, the calibration standards for the calibration curves were prepared as described in section 3.3. These concentrations were chosen to cover all metabolites' preliminary physiological range (Table C-1). The calibration curves (standards and spiked urine) were used to determine the linear ranges of each metabolite, as well as the detection and quantification limits. Each concentration level (15 concentrations including a blank) was injected in triplicate, after which an average response could be determined of each concentration level.

5.1.1.1 Linearity of butyl esters

For this study, the concentration range of the calibration curve covered much more than the suggested 80-120%, the reason for this wide concentration range was to ensure that the linear range are fully characterised (from low to very high concentrations). The linear ranges of each metabolite in both working standards and spiked urine are summarised in Table 5-1. Calibration curves were generated by plotting analyte response/internal standard response versus theoretical analyte concentration/internal standard concentration (as described in section 2.10.1). The linear least squares regression model was used to determine the linearity of the curve. From the best-fit line equation, the concentration of the analyte can be calculated, and the r^2 closest to 1 gave the best fit, resulting in the linear range (Rawski et al., 2016).

Table 5-1. Summary of calibration curves of butyl esters. In this table the linearity of the working standards is compared to linearity of the spiked urine.

Metabolite	**Tyr-BE**	**3-NT-BE**
Expected physiological concentration (ng/ml)	5.44 – 1811.90	0.36 - 28
Expected in-vial physiological concentration (ng/ml)	10.88 – 3623.80	0.72 – 56
Evaluated in-vial concentration range (ng/ml)	0.24 - 2000	0.24 - 2000
Linear in-vial concentration range with working standards (ng/ml)	**0.24 – 1000**	**0.24 - 1000**
r^2 from curve of working standards	**0.999**	**0.998**
Linear in-vial concentration range with spiked urine (ng/ml)	**0.24 - 500**	**0.24 - 1000**
r^2 from curve of spiked urine	**0.999**	**0.995**

As seen in Table 5-1, the linear ranges for 3-NT in both the urine matrix and working standards were 0.24 – 1000 ng/ml. Whereas the linear range for tyr in urine was 0.24 – 500 ng/ml, and the linear range in the working standards was 0.24 – 1000 ng/ml. It is believed that the column is overloaded at these high concentrations (< 1000 ng/ml), resulting in a decrease in response as the concentration increases. Therefore, the working range for the butyl esters can be summarised as 0.24 – 1000 ng/ml for standards and 0.24 – 500 ng/ml for matrix. The calibration curves of each butyl ester in working standards and spiked urine can be seen in Figure C-1 and Figure C-2 respectively.

5.1.1.2 Limits of detection & quantification

The detection and quantification limits were determined from the same calibration curves mentioned in section 5.1.1.1., and the linear regression model was also used for the calculation of the detection and quantification limits.

These are calculated using Equation 2-1 and Equation 2-2 as described in section 2.10.2. The calculations were performed in Microsoft Excel using the *lineST function*. The response standard deviation was calculated by measuring the standard deviation of y-intercepts and y-residuals from the regression line. The least squares model is, unfortunately, strict on linearity, as the concentrations are calculated from standard errors based on the regression line and therefore the chosen range should have a regression close to 1 (r^2>0.990). Since this model is sensitive to possible errors (that may influence the linearity of the curve), the limits had to be calculated in the urine matrix as well. The calculated limits on both working standards and spiked urine are summarised in Table 5-2 and Table 5-3 respectively. The detection and quantification limits for both butyl esters were below the physiological concentrations in the working standards.

Table 5-2. Summary of butyl ester linear concentrations, calibration curve slopes, limit of detection and limit of quantification in working standards estimated from the lineST function.

Metabolite	Linear concentration range with working standards (ng/ml)	Slope (m) of the calibration curve	LOD (ng/ml)	LLOQ (ng/ml)	ULOQ (ng/ml)
Tyr-BE	0.24 – 1000	0.97	0.05	0.15	1000
3-NT-BE	0.24 – 1000	1.74	0.14	0.42	1000

Table 5-3. Summary of butyl ester linear concentrations, calibration curve slopes, limit of detection and limit of quantification in spiked urine.

Metabolite	Linear concentration range with spiked urine (ng/ml)	Calibration curve slope (m)	LOD (ng/ml)	LLOQ (ng/ml)	ULOQ (ng/ml)
Tyr-BE	0.24 – 500	8.42	0.04	0.12	500
3-NT-BE	0.24 – 2000	1.46	0.55	1.68	2000

The LOD and LLOQ of tyr in both the working standard and urine, were below the linear range, and the expected physiological concentration. Which means that physiological concentrations could be accurately quantified. On the other hand, the LOD and LLOQ of 3-NT in working standards were below the physiological concentration, with only the LLOQ being part of the linear range. In urine, both the LOD and LLOQ of 3-NT were within the linear range, with the LOD below the expected physiological concentration and the LLOQ above the lowest expected physiological concentration. Therefore, the lower concentrations of 3-NT in urine could not be accurately quantitated. The ULOQ is represented by the highest concentration of the linear ranges (Wal et al., 2010), the ULOQ of tyr in urine, unfortunately, lied within the expected physiological concentration range. This means that samples with concentrations greater than 500 ng/ml will have to be diluted for accurate quantification. The ULOQ for 3-NT in urine was far greater than the expected physiological range, therefore, high urinary 3-NT concentrations (up to 1000 ng/ml) can be accurately quantified without any required dilutions.

5.1.2 Sensitivity

The samples in the calibration curve closest to the calculated LOQs were used to determine the sensitivity. This was done by calculating the CV%, where the standard deviation is divided by the mean, and multiplied by 100 to express a percentage (Equation 2-4). The samples were prepared as described in section 4.9.1; the samples were injected in triplicate to determine the CV% for each butyl ester. The calculated sensitivity in the working standards is summarised in Table 5-4.

Table 5-4. Summary of LLOQ of the butyl esters in working standards used to determine the sensitivity for the method.

Metabolite	**Tyr-Be**	**3-NT BE**
LLOQ (ng/ml)	0.15	0.42
Spiked concentration (ng/ml)	0.24	0.49
Average measured concentration (ng/ml)	1.03	0.591
Standard deviation	0.02	0.02
CV (%)	**2.32**	**2.68**

Under ideal circumstances (working standards), the method was sensitive for both butyl esters, since the CV% was below the accepted 20% variation, as seen in Table 5-4. As there was a difference in detection and quantification limits between the urinary matrix and the working standards, the sensitivity of the method in the urine matrix was established (Table 5-5).

Table 5-5. Summary of LLOQ of the butyl esters in urine used to determine the sensitivity for the method.

Metabolite	Tyr-Be	3-NT BE
LLOQ (ng/ml)	0.12	1.68
Spiked concentration (ng/ml)	0.24	1.95
Average measured concentration (ng/ml)	0.4	3.4
Standard deviation	0.042	0.05
CV (%)	**9.82**	**1.47**

The method was still sensitive for both butyl esters in the matrix as the CV% were well under 20%, however, the concentrations measured in this sample were much lower for tyr than in the working standards, and the variance was much more (9.82% vs 2.32%).

This variation may be caused by other compounds present in the matrix affecting the accurate quantification of urinary analytes (matrix effect). Since the LOQ differs between the matrix and working standards for 3-NT, no comment can be made on the measured concentrations, however, the CV% was lower in the matrix compared to the working standards (2.68% vs 1.47%), this might be because of the higher concentrations measured in the matrix, where a larger deviation has less of an effect.

5.1.3 Accuracy

For this study, the QC samples were prepared as described in section 3.3. A spiked urine sample (spiked to the same concentration as the MQC sample) was also analysed with the QC samples to determine how the matrix affects the accuracy. The concentrations (ng/ml) for the QC levels are summarised in Table 5-6. Both intra- and inter-day instrument accuracy was determined by analysing the QC samples (6 samples) in triplicate over three consecutive days.

Table 5-6. Quality control concentrations for butyl esters to determine accuracy, precision, stability, recovery, and other validation parameters.

QC level	Concentrations (ng/ml) prior to sample preparation			In-vial concentrations (ng/ml)		
	Tyr-BE	**3-NT-BE**	**d_5-Phe-BE**	**Tyr-BE**	**3-NT-BE**	**d_5-Phe-BE**
LOD	0.025	0.070	111	0.05	0.14	250
LOQ	0.075	0.205	111	0.15	0.41	250
LQC	2.00	5.00	111	4.00	10.00	250
MQC	20.00	15.00	111	40.00	30.00	250
HQC	75.00	22.50	111	150.00	45.00	250
EQC	100.00	30.00	111	200.00	60.00	250

The average of the triplicate injections from day 3 was used in Equation 2-4. to calculate intraday accuracy (better known as within batch accuracy), whereas, for inter-day accuracy (or between batch accuracy), the averages for each day was used to calculate the average accuracy percentage over the 3 days. Table 5-7 summarises the average intra- and inter-day accuracy for the method at each QC level.

Table 5-7. Instrument intra- and inter-day inaccuracy for butyl esters.

QC level	Intraday inaccuracy (%)		Inter-day inaccuracy (%)	
	Tyr-BE	**3-NT-BE**	**Tyr-BE**	**3-NT-BE**
LOD	> 100	8.83	> 100	2.67
LOQ	> 100	> 100	> 100	> 100
LQC	74.22	97.29	82.02	77.86
MQC	84.29	47.39	85.11	55.95
HQC	87.98	69.85	88.96	67.91
EQC	87.88	46.24	87.91	49.18
Spiked urine (MQC)	> 100	76.21	> 100	72.87

As described in chapter 2, accuracy is presented as a percentage of deviation, indicating how close the mean measured concentrations are to the nominal concentration, and the acceptable deviation from the mean (inaccuracy) is 20% LLOQ and 15% for all the other concentrations. From Table 5-7, it is evident that the accuracy deviations are more than the acceptable percentages of 15-20% for both inter- and intra-day accuracy. This means that the method is not accurate within or between batches. The method tends to be very inaccurate at lower concentrations (LOD and LOQ), this might be ascribed to various factors such as preparation errors. To establish if the inaccuracy was random or systematic, analyst accuracy was examined by preparing and analysing the MQC working standard in triplicate. Both inter- and intra-day accuracy was determined.

Table 5-8. Analyst inter- and intra-day inaccuracy for butyl esters.

QC level	Intraday inaccuracy (%)		Inter-day inaccuracy (%)	
	Tyr-BE	**3-NT-BE**	**Tyr-BE**	**3-NT-BE**
MQC	15.79	23.88	85.00	56.00

The average of the triplicate injections from day 3 was used in Equation 2-4 to calculate intra-day accuracy and for inter-day accuracy, the averages for each day was used to calculate the average inaccuracy percentage over the 3 days. The percentage deviations for analyst accuracy (both inter-day and intra-day) were also above the accepted 15%, but the deviations are much lower compared to the instrument accuracy. The instrument and analyst inter-day precisions were similar, indicating that the inaccuracy is systematic rather than random.

5.1.4 Precision

The QC samples were prepared as described in section 3.3. A spiked urine sample (spiked to the same concentration as the MQC sample) was also analysed with the QC samples to determine how the matrix affects the precision. The concentrations (ng/ml) for the QC levels are summarised in Table 5-6. Intra- and inter-day instrument precision was determined by analysing the QC samples (6 samples) in triplicate over three consecutive days.

The precision of the method can be determined by Equation 2-5 where the relative standard deviation is divided by the mean and multiplied by 100. This equation is used to typically calculate the CV% as mentioned in section 5.1.2. The CV% should be less than 15% for all concentration levels except for LLOQ where a CV% of 20% is acceptable (Lynch, 2016). The average results (both within and between days) for the QC samples and spiked urine are shown in Table 5-9. The averages and standard deviations from the 3rd day were used to investigate intra-day precision, whereas the CVs of each day were used to calculate inter-day precision.

Table 5-9. Instrument intra- and inter-day precision for butyl esters.

QC level	Intraday precision (%)		Inter-day precision (%)	
	Tyr-BE	**3-NT-BE**	**Tyr-BE**	**3-NT-BE**
LOD	6.11	4.87	5.49	6.25
LOQ	0.60	3.15	0.76	1.84
LQC	0.35	4.69	1.50	4.08
MQC	2.16	3.27	> 20	2.66
HQC	8.63	3.28	3.42	2.31
EQC	1.21	0.40	1.49	0.80
Spiked urine (MQC)	> 20	12.41	> 20	9.82

Overall, both intra- and inter-day precision were acceptable for this method as the variance overall had an inaccuracy of less than 15%. Both MQC and spiked urine matrix inter-day variation for tyr was unacceptable, as well as the intraday variation of tyr in the matrix. This could have been due to a random error during sample preparation. To establish if the imprecision was random, the analyst precision was examined by preparing and analysing the MQC sample in triplicate. Both inter- and intra-day precision was determined.

Table 5-10. Intra- and inter-day analyst precision for butyl esters.

QC level	Intraday precision (%)		Inter-day precision (%)	
	Tyr-BE	**3-NT-BE**	**Tyr-BE**	**3-NT-BE**
MQC	> 20	13.17	6.12	13.48

The average of the triplicate injections from day three was used in Equation 2-5 to calculate intra-day precision, whereas the average deviations for each day were used to calculate the inter-day precision.

Both intra- and inter-day precision for 3-NT was acceptable, as the deviations are within the 15% imprecision range. The inter-day precision for tyr was also within this range, on the other hand, the intra-day precision was unacceptable (CV > 15%). The variation of tyr for both the instrument and the analyst indicated that tyr might be more sensitive compared to 3-NT.

Since both accuracy and precision are important quality control parameters, the overall accuracy and precision of the methods were also investigated. The average intra- and inter-day accuracy and precision results are shown in Table 5-11.

Table 5-11. Average intra- and inter-day inaccuracy and precision for the quality control concentrations of the method for butyl esters.

QC level	Average Intraday inaccuracy (%)	Average Intraday precision (%)	Average Inter-day inaccuracy (%)	Average Inter-day precision (%)
LOD	> 100	1.88	> 100	1.30
LOQ	> 100	2.52	> 100	2.79
LQC	85.75	2.71	79.94	15.17
MQC	65.84	5.95	70.53	2.86
HQC	78.92	0.80	78.44	1.15
EQC	67.06	1.28	68.55	2.09
Spiked urine (MQC)	> 100	> 20	> 100	> 20

From Table 5-11 it is evident that although the method is not accurate for the butyl esters, it is precise at all concentration levels. The average results from the spiked urine sample varied significantly from the working standards and could be ascribed to the matrix effect.

5.1.5 Stability

Short-term storage (24-hour) stability of the samples after sample preparation was investigated to determine whether the target metabolites deteriorate when stored at different temperatures in the autosampler/fridge (4 ºC) and freezer (-20 ºC).

Two sets of QC samples were prepared as described in chapter 4.1 and analysed freshly. After analysis, one set was stored in the freezer for 24 hours, and the other set was left in the autosampler for 24 hours, after which the samples were re-analysed. The response of the fresh samples was compared to the response after 24 hours, the stability was then determined as a percentage of fresh samples, as seen in Table 5-12. As with the other validation parameters, the acceptable deviation for all values is 15%, and the LOQ deviation of 20% is accepted. Therefore, the accepted range for LLOQ is 80-120% and 85 – 115% for all the other QC levels.

Table 5-12. Short-term stability of butyl esters during storage at different temperatures for 24 hours following sample preparation. The stability is expressed as a percentage of fresh samples.

Metabolite	**Tyr-BE**		**3-NT-BE**	
	Autosampler (%)	**Freezer (%)**	**Autosampler (%)**	**Freezer (%)**
LOD	< 85	> 115	< 85	< 85
LLOQ	> 120	> 120	< 120	< 120
LQC	> 115	> 115	> 115	> 115
MQC	< 85	< 85	< 85	< 85
HQC	> 115	> 115	> 115	> 115
EQC	> 115	> 115	> 115	> 115

From Table 5-12, the storage of butyl esters in the autosampler, as well as the fridge, was rejected as a short-term storage option. It was decided that the samples should be analysed freshly and discarded afterwards.

5.1.6 Matrix effect

As mentioned in chapter 2, the matrix effect can cause compounds to respond differently in a biological matrix compared to a standard solution. The enhancement or ion suppression caused by the matrix can be calculated and expressed as a percentage by using Equation 2-6.

The response of the spiked urine sample was divided by the response of the MQC sample, multiplied by 100 to determine the effect of the matrix. The urine and MQC samples were prepared as described in section 3.3 and section 4.1. The matrix effects are summarised in Table 5-13.

Table 5-13. The matrix effect of urine on butyl esters and whether ion suppression or enhancement occurs.

Metabolite	**Tyr-BE**	**3-NT-BE**	**d_5-Phe-BE**
Matrix effect (%)	> 150	24.67	32.58
Ion suppression/enhancement	Ion enhancement	Ion suppression	

As seen in Table 5-13, the butyl esters responded differently in the urine matrix. For tyrosine, the ions were enhanced, whereas the 3-NT and the d_5-phe were suppressed in the urine. From this data (not indicated), 3-NT was mostly affected.

5.1.7 Carry-over and selectivity.

Carry-over is an important parameter in method validation as it can directly affect the accuracy of the results. The carry-over can easily be seen after injecting a highly concentrated sample; therefore, a blank injection was added after the injections of urine, spiked urine, and HQC level (prepared as described in section 4.9.1). Carry-over is acceptable when the response of an analyte in the blank is less than 20% of the analyte response in the concentrated sample. The results indicated that there was little to no carry-over during the analysis (Table C-3).

Method selectivity was determined by visually examining the chromatograms of each analyte and comparing them between a standard, the pooled urine sample, and a spiked urine sample. The standard sample represents the blank sample where the retention times of the analytes can be confirmed without any explainable interference. The blank urine sample represented a normal sample containing matrix components that compensate for individual variability and the matrix effect.

The spiked urine sample was used to ensure the detection of the target analytes as their concentration was significantly elevated. Despite a slight shift in retention of the metabolites between the standard and the urine sample, the overall selectivity of the method for butyl ester was acceptable. In urine (both spiked and normal) it was seen that there was a second peak within a 10% retention time of 3-NT at low concentrations, but this peak did not co-elute with 3-NT (Figure C-4).

Preliminary results from a previous study performed at the BOSS laboratory (Bothma, 2012) showed an interfering peak eluting with 3-NT that was not present in the standard solution analyses. Bothma attempted to identify and characterise this contaminating peak, but unfortunately the peak could not be identified (2012). The separation of these co-eluting compounds was successfully achieved by applying stereospecific derivatisation (Bothma, 2012).

5.1.8 Extraction recovery

Since this method had a few sample preparation steps, an extraction recovery analysis was performed to determine the amount of analyte loss during the analysis. A set of QCs was prepared as described in section 4.9.1. The samples that were not loaded onto the SPE cartridges were analysed and compared to the samples post-extraction. By analysing the same samples, any errors occurring before SPE were compensated for.

Table 5-14. Recovery analysis of butyl esters post-extraction. The results are expressed as percentage of unextracted samples.

QC level	Tyr-BE (%)	3-NT-BE (%)	d_5-Phe-BE (%)
LOQ	66	> 120	96
LQC	85	51	67
MQC	101	69	59
HQC	40	61	42
EQC	99	97	83

The recovery analysis, unfortunately, did not deliver the expected results. As seen in Table 5-14, most analytes had a significant loss during SPE. Various factors could have contributed to the loss seen, such as poor retention on the SPE columns, poor extraction from the SPE columns, loss during evaporation, and poor redissolving of analytes during resuspension.

5.2 Partial validation of DNA and lipid peroxidation markers

5.2.1 Calibration curve and linearity

Calibration curves were constructed to evaluate the linear range as described in section 3.3. As with the butyl esters, the concentrations of the calibration curve were chosen so that they cover the physiological range of all metabolites (Table C-1). The detection limits (LLOD, LOQ and ULOQ) and the linearity were determined from the calibration curves. Each of the concentration levels was injected in triplicate, after which an average response of each level could be determined. PGE was not included in the calibration working solution due to an insufficient number of standards available. Each concentration level (15 levels including a blank) was injected in triplicate, after which an average response of each concentration could be determined.

5.2.1.1 Linearity of DNA and lipid peroxidation markers

As with the butyl esters, the linearity was determined with the least square linear regression model (section 5.1.1). The expected physiological concentrations, evaluated concentration range, linear ranges and r^2 values are presented in Table 5-15.

Table 5-15. Summary of calibration curves of DNA and lipid peroxidation markers. This table compared the linearity of working standards with spiked urine.

Metabolite	**8-OHdG**	**MDA-DNPH**	**4-HNE-MA**	**$PGF_{2\alpha}$**
Expected physiological concentration (ng/ml)	0.95 – 14.2	1.46 – 84.2	2.85 – 128	0.12 – 1.95
Expected in-vial physiological concentration (ng/ml)	1.9 – 28.4	2.92 - 168	5.7 – 256	0.24 – 3.9
Evaluated in-vial concentration range (ng/ml)	0.12 – 2000	0.12 – 2000	0.12 – 2000	0.12 – 2000
Linear in-vial concentration range with working standards (ng/ml)	***0.12 – 2000***	***0.12 – 2000***	***125 – 2000***	***3.84 – 2000***
r^2 from curve of working standards	***0.999***	***0.998***	***0.986***	***0.946***
Linear in-vial concentration range with spiked urine (ng/ml)	***0.12 - 1000***	***0.12 - 500***	***250 - 2000***	***No linear range***
r^2 from curve of spiked urine	***0.999***	***0.934***	***0.948***	***-***

For most metabolites in the working standard, the concentration range evaluated resulted in a linear response between 0.12 - 2000 ng/ml (Figure C-5). The results in a matrix sample were not so promising (Figure C-6), as the linear range for 4-HNE-MA was at the higher end of the curve, which unfortunately was above the expected physiological concentration. $PGF_{2\alpha}$ yielded no linear response ($r^2 < 0.90$), although PGE was not analysed, it was assumed that it would produce results like that of $PGF_{2\alpha}$ since they are isomers.

5.2.1.2 Detection & quantification limits of DNA and lipid peroxidation markers

As with the butyl esters, the limits of detection and quantification were calculated from the concentration in the vial. These were calculated using Equation 2-1 and Equation 2-2 as described in section 2.10.2., and the calculations were performed in excel using the *lineST* function. As mentioned in section 5.1.1.2 this model is sensitive to possible errors that influence the linearity, for this reason the limits had to be calculated in the urine matrix as well, to account for the matrix effect. The calculated limits on both working standards and spiked urine are summarised in Table 5-16 and Table 5-17 respectively.

Table 5-16. Summary of DNA & lipid peroxidation marker linear concentrations, calibration curve slopes, limit of detection and limit of quantification in working standards estimated from the lineST function.

Metabolite	Linear concentration range with working standards (ng/ml)	Slope (m) of the calibration curve	LOD (ng/ml)	LLOQ (ng/ml)	ULOQ (ng/ml)
8-OHdG	0.12 – 2000	1.335	0.09	0.28	2000
MDA-DNPH	0.12 – 2000	0.265	0.82	2.50	2000
4-HNE-MA	125 – 2000	0.059	0.66	2.00	2000
$PGF_{2\alpha}$	3.84 – 2000	0.141	1.09	3.29	2000

Table 5-17. Summary of DNA & lipid peroxidation marker linear concentrations, calibration curve slopes, limit of detection and limit of quantification in spiked urine.

Metabolite	Linear concentration range with working standards (ng/ml)	Slope (m) of the calibration curve	LOD (ng/ml)	LLOQ (ng/ml)	ULOQ (ng/ml)
8-OHdG	0.12 - 1000	1.14	0.05	0.14	1000
MDA-DNPH	0.12 - 500	0.22	0.15	0.46	500
4-HNE-MA	250 - 2000	0.05	1.66	5.03	2000
$PGF_{2\alpha}$	ND	ND	ND	ND	ND

For all metabolites, except 4-HNE-MA, in the working standard solution and urine sample, the LOD and LLOQ lied within the linear range. The LLOQ for 8-OHdG, MDA-DNPH, and 4-HNE-MA (working standard solution) were below the expected physiological concentrations, whereas the LOD and LLOQ for $PGF_{2\alpha}$ lied within the higher physiological concentration range (3.5 ng/ml). This means that physiological 8-OHdG, MDA-DNPH, and 4-HNE could be detected and quantified accurately. Unfortunately, for $PGF_{2\alpha}$ the greatest part of the physiological concentrations could not be quantified. The ULOQ for the analytes in the urine varied from 500 - 2000 ng/ml, abnormal concentrations of 8-OHdG, MDA-DNPH, and 4-HNE could be accurately quantified.

5.2.2 Sensitivity

As described in sections 2.10.2.1 and 5.1.2, the LLOQ is used to determine sensitivity. The samples in the calibration curve closest to the calculated LOQs were used to determine the sensitivity. A standard sample containing the LLOQ concentrations of DNA and lipid peroxidation markers was prepared as described in section 4.9.2, the sample was injected in triplicate to determine the CV% for each metabolite (Equation 2-4). The calculated sensitivity of the working standards is summarised in Table 5-18. The method is acceptable as sensitive when the CV% is lower than 20%.

Table 5-18. Summary of LLOQ of the DNA and lipid peroxidation markers in working standards used to determine the sensitivity for the method.

Metabolite	**8-OHdG**	**MDA-DNPH**	**4-HNE-MA**	**$PGF_{2\alpha}$**
LLOQ (ng/ml)	0.28	2.50	2.00	3.29
Spiked concentration (ng/ml)	0.48	3.84	3.84	3.84
Average measured concentration (ng/ml)	1.27	22.07	ND	ND
Standard deviation	0.27	1.71	ND	ND
CV (%)	> 20	7.73	ND	ND

For the concentrations closest to the calculated quantification limits, only MDA-DNPH had an acceptable CV%. The CV% for 8-OHdG is slightly above the accepted CV% of 20%. Neither 4-HNE-MA nor PGF was detected at these concentrations. This indicated that although the LLOQ was determined as described in section 5.2.1.2 the method was not sensitive for the analytes at these low concentrations. The method, however, was relatively sensitive for both 8-OHdG and sensitive for MDA-DNPH in the working standards. The sensitivity for these metabolites was also tested in the urine matrix to compensate for the matrix effect and the results were presented in Table 5-19.

Table 5-19. Summary of LLOQ of the DNA and lipid peroxidation markers used to determine the sensitivity for the method in urine.

Metabolite	**8-OHdG**	**MDA-DNPH**	**4-HNE-MA**	**$PGF_{2\alpha}$**
LLOQ (ng/ml)	0.14	0.46	5.03	ND
Spiked concentration (ng/ml)	0.48	0.48	7.68	ND
Average measured concentration (ng/ml)	0.99	5.7×10^6	ND	ND
Standard deviation	0.46	3.6×10^6	ND	ND
CV (%)	> 20	> 20	ND	ND

The measured concentrations of the metabolites in the urine sample were much higher compared to the standard working solution. As expected, the method was much less sensitive for the analytes in the urinary matrix compared to the working standards. This may be the result of derivatization, as mentioned in section 2.9.2. Derivatization improves the sensitivity of a method, as the chemical structure of the target compound is altered to be more detectable (Qi *et al.*, 2014). Another explanation for the great deviation is the matrix effect. Since MDA already underwent derivatization to increase sensitivity, the latter may be the reason for the observed decrease.

5.2.3 Accuracy

Again, the QC samples were prepared as described in section 3.3. A spiked urine sample (spiked with the same concentration as the MQC sample) was also analysed with the QC samples to establish to which extent the matrix influences the accuracy. The concentrations (ng/ml) for the QC levels are summarised in Table 5-20 and Table 5-21. Intra- and inter-day instrument accuracy validation were determined by analysing the QC samples (6 samples) in triplicate, over three consecutive days, whereas the analyst accuracy was investigated by preparing an MQC sample in triplicate and analysed.

Table 5-20. Concentrations of QC samples prior to sample preparation to determine accuracy, precision, stability, recovery, and other validation parameters for DNA and lipid peroxidation markers.

QC level	Concentrations (ng/ml) prior to sample preparation							
	8-OHdG	**$^{13}C^{15}N_5$-8-OHdG**	**MDA-DNPH**	**D_2-MDA-DNPH**	**4-HNE-MA**	**$PGF_{2\alpha}$**	**PGE_2**	**PGE_2-d_4**
LOD	0.35	950	0.95	510	10.60	0.38	0.73	780
LOQ	0.60	950	1.91	510	30.00	1.00	2.20	780
LQC	0.95	950	2.00	510	65.50	2.5	5.00	780
MQC	7.50	950	43.00	510	192.00	5.00	10.00	780
HQC	14.20	950	84.00	510	204.75	20.00	-	780
EQC	21.00	950	126.00	510	271.35	30.00	12.50	780

Table 5-21. In-vial Concentrations of QC samples after sample preparation to determine accuracy, precision, stability, recovery, and other validation parameters for DNA and lipid peroxidation markers.

QC level	In-vial concentrations (ng/ml)							
	8-OHdG	**$^{13}C^{15}N_5$-8-OHdG**	**MDA-DNPH**	**D_2-MDA-DNPH**	**4-HNE-MA**	**$PGF_{2\alpha}$**	**PGE_2**	**PGE_2-d_4**
LOD	0.69	641.25	2.50	344.25	21.21	0.75	1.45	526.50
LOQ	1.20	641.25	3.82	344.25	60.00	2.00	4.40	526.50
LQC	1.90	641.25	4.00	344.25	131.00	5.00	10.00	526.50
MQC	15.00	641.25	86.00	344.25	384.00	10.00	20.00	526.50
HQC	28.40	641.25	168.00	344.25	409.50	40.00	-	526.50
EQC	42.00	641.25	252.00	344.25	542.70	60.00	25.00	526.50

The average of the triplicate injections from day 3 was used in Equation 2-4 to calculate intraday accuracy, whereas, for inter-day accuracy, the average concentration of each day was used to calculate an average concentration over three days, this average was then used to calculate the accuracy percentage. The acceptable deviation from the mean (inaccuracy) is 20% LLOQ, and 15% for all the other concentrations, therefore, an accuracy percentage of 85% - 115% is acceptable. Table 5-22 and Table 5-23 summarise the intra- and inter-day accuracy of the DNA and lipid oxidation markers respectively.

Table 5-22. Instrument intraday inaccuracy for DNA and lipid oxidation markers.

QC level	Intraday inaccuracy (%)				
	8-OHdG	MDA-DNPH	4-HNE-MA	$PGF_{2\alpha}$	PGE_2
LOD	> 100	> 100	> 100	52.56	9.03
LOQ	> 100	99.08	99.98	> 100	23.75
LQC	19.98	> 100	99.99	> 100	0.33
MQC	22.40	20.72	99.96	> 100	9.71
HQC	27.88	32.33	99.91	> 100	47.16
EQC	2.21	31.46	99.96	> 100	61.08
Spiked urine (MQC)	> 100	51.65	99.98	7.30	76.76

Table 5-23. Instrument inter-day inaccuracy for DNA and lipid oxidation markers.

QC level	Inter-day inaccuracy (%)				
	8-OHdG	MDA-DNPH	4-HNE-MA	$PGF_{2\alpha}$	PGE_2
LOD	> 100	> 100	0.92	86.27	> 100
LOQ	> 100	> 100	0.90	94.61	80.41
LQC	93.36	> 100	0.13	> 100	81.60
MQC	84.20	65.55	0.38	> 100	62.50
HQC	86.88	56.95	0.19	> 100	34.86
EQC	84.11	53.64	0.14	> 100	25.70
Spiked urine (MQC)	61.83	26.04	0.15	33.76	71.77

From Table 5-22 and Table 5-23, the method was not accurate for the DNA and lipid oxidation metabolites, as the inaccuracy percentages were greater than 15-20%. The inaccuracy occurred throughout all concentrations, and some metabolites were affected more than others. To establish whether the inaccuracy could be ascribed to systematic or random errors, analyst accuracy (both intra- and inter-day) was determined by preparing and analysing the MQC working standard in triplicate as shown in Table 5-24.

Table 5-24. Analyst inaccuracy for DNA and lipid oxidation markers.

QC level	Intraday inaccuracy (%)					Inter-day inaccuracy (%)				
	8-OHdG	MDA-DNPH	4-HNE-MA	$PGF_{2\alpha}$	PGE_2	8-OHdG	MDA-DNPH	4-HNE-MA	$PGF_{2\alpha}$	PGE_2
MQC	3.2	21.3	99.4	> 100	61.5	15.8	34.5	99.7	37.5	19.5

The average of the triplicate injections from day 3 was used in Equation 2-4 to calculate intra-day accuracy and for inter-day accuracy, the averages for each day was used to calculate the average inaccuracy percentage over the 3 days. Intra-day accuracy for 8-OHdG was within the acceptable accuracy deviation. The percentage deviations for analyst accuracy (both inter-day and intra-day) for the other metabolites were unfortunately above the accepted 15% (Table 5-24). For $PGF_{2\alpha}$ and PGE_2 the analyst inter-day accuracy improved significantly compared to the instrument accuracy, whereas the 8-OHdG and MDA-DNPH decreased significantly. Therefore, it is believed that both random and systematic errors contributed to the inaccuracy of the method.

5.2.4 Precision

For precision analyses, the same QC samples were prepared as described in section 3.3. As with accuracy, a spiked urine sample (spiked to the same concentration as the MQC sample) was also analysed with the QC samples to establish to which extent the matrix influenced the precision. The concentrations (in ng/ml) for the QC levels are summarised in Table 5-25. Both intra- and inter-day instrument precision were determined by analysing these QC samples (6 samples) in triplicate, over three consecutive days. The precision of the method was determined by Equation 2-5, where the relative standard deviation was divided by the mean and multiplied by 100.

The method is precise if the CV percentages are below 20% (LLOQ), and 15% for the rest of the concentrations (Lynch, 2016). The intra- and inter-day precision for the QC samples and the spiked urine are displayed in Table 5-25 and Table 5-26 respectively.

Table 5-25. Instrument intra-day precision for DNA and lipid oxidation products.

QC level	Intra-day precision (%)				
	8-OHdG	**MDA-DNPH**	**4-HNE-MA**	**$PGF_{2\alpha}$**	**PGE_2**
LOD	0.43	7.64	5.97	14.38	8.97
LOQ	2.26	5.97	> 15	11.60	12.17
LQC	4.20	2.08	> 20	1.43	3.97
MQC	10.86	1.88	3.05	5.34	10.63
HQC	2.23	0.63	> 20	5.69	1.78
EQC	7.36	2.84	> 20	1.86	5.91
Spiked urine (MQC)	2.2	8.6	14.3	5.7	> 20

Table 5-26. Instrument inter-day precision for DNA and lipid oxidation markers.

QC level	Inter-day precision (%)				
	8-OHdG	**MDA-DNPH**	**4-HNE-MA**	**$PGF_{2\alpha}$**	**PGE_2**
LOD	2.87	4.80	16.80	> 20	13.82
LOQ	4.68	4.34	8.05	12.85	7.82
LQC	> 20	2.53	18.97	5.29	4.16
MQC	6.80	3.07	4.09	9.74	6.80
HQC	7.17	2.44	11.68	6.14	2.67
EQC	4.95	3.8	13.47	4.70	4.67
Spiked urine (MQC)	1.33	12.00	7.95	> 20	17.53

The average of the triplicate injections from day three was used in Equation 2-5 to calculate intraday precision (Table 5-25), whereas the average deviations for each day were used to calculate the inter-day precision (Table 5-26). In general, both intra- and inter-day precision was accepted for this method, as most analytes had an imprecision of less than 15%. The instrument intraday precision for 4-HNE-MA, however, was not acceptable as more than 50% of the concentrations deviated more than 15%. The inter-day precision for 4-HNE-MA was also not acceptable for some concentration levels (LOD and LQC). The inter-day precision for $PGF_{2\alpha}$ and the intra-day precision of PGE_2 in the urinary matrix were unacceptable as the CV% was more than 15%. During intra-day precision, a few compounds had imprecision at single concentration levels (8-OHdG; 4-HNE-MA; and $PGF_{2\alpha}$). Both intra- and inter-day analyst precision were also assessed to confirm whether the imprecision was random by preparing and analysing the MQC sample in triplicate.

Table 5-27. Intra-day analyst precision for DNA and lipid oxidation markers.

QC level	Intra-day precision (%)				
	8-OHdG	**MDA-DNPH**	**4-HNE-MA**	**$PGF_{2\alpha}$**	**PGE_2**
MQC	8.44	0.56	> 20	3.49	> 20

Table 5-28. Inter-day analyst precision for DNA and lipid oxidation markers.

QC level	Inter-day precision (%)				
	8-OHdG	**MDA-DNPH**	**4-HNE-MA**	**$PGF_{2\alpha}$**	**PGE_2**
MQC	6.80	3.07	4.09	6.80	9.74

The intra-day analyst precision was unacceptable for both 4-HNE-MA and PGE_2 (Table 5-27), whereas the inter-day analyst precision was acceptable for all metabolites (Table 5-28). This inconsistency indicated that the imprecision observed was because of random error during sample preparation. Since both accuracy and precision are important quality control parameters, the overall accuracy and precision of the methods were also investigated the average results (intra- and inter-day) for the QC samples and the spiked urine are displayed in Table 5-29.

Table 5-29. Instrument average intra-day inaccuracy and precision for DNA and lipid peroxidation markers.

QC level	Intra-day inaccuracy (%)	Intra-day precision (%)	Inter-day inaccuracy (%)	Inter-day precision (%)
LOD	> 100	9.54	> 100	10.61
LOQ	-9.54	10.32	70.84	14.15
LQC	> 100	7.94	> 100	5.94
MQC	28.24	6.35	33.65	11.40
HQC	> 100	8.19	> 100	8.19
EQC	57.26	11.01	29.71	4.15
Spiked urine (MQC)	18.51	12.19	61.30	12.19

As shown in Table 5-29, the method was inaccurate but precise for DNA and lipid oxidation markers. The spiked urine samples were significantly different compared to the working standards; this is most likely due to the matrix effect.

5.2.5 Stability

Short-term storage (24-hour) stability of the samples after sample preparation was determined to determine whether the target metabolites deteriorate when stored at different temperatures in the autosampler/fridge (4 ºC) and freezer (-20 ºC). Two sets of QC samples were prepared as described in section 4.1 and analysed freshly in duplicate. After analysis, one set was stored in the freezer for 24 hours, and the other set was left in the autosampler for 24 hours, after which the samples were re-analysed. The response of the fresh samples was compared to the response after 24 hours, the stability was then determined as a percentage of fresh samples, as seen in Table 5-30.

Table 5-30. Short-term stability of DNA and lipid peroxidation markers after sample preparation at different temperatures for 24 hours. The stability is expressed as a percentage of fresh samples. *ND: Not detected (< 10%).*

Metabolite		LOD	LOQ	LQC	MQC	HQC	EQC
8-OHdG	**Autosampler**	> 115	> 120	> 115	> 115	> 115	> 115
	Freezer	> 115	> 120	77	95	> 115	> 115
MDA-DNPH	**Autosampler**	ND	106	83	99	98	106
	Freezer	ND	98	89	> 115	> 115	> 115
4-HNE-MA	**Autosampler**	ND	ND	ND	98	99	98
	Freezer	ND	ND	> 115	ND	> 115	60
$PGF_{2\alpha}$	**Autosampler**	ND	ND	41	92	96	> 115
	Freezer	ND	ND	49	98	136	63
PGE_2	**Autosampler**	ND	ND	53	93	93	114
	Freezer	ND	ND	20	ND	12	ND

As with the other validation parameters, the acceptable deviation for all values is 15%, and the LLOQ deviation of 20% is accepted. Therefore, the accepted range for LLOQ is 80-120% and 85 – 115% for all the other QC levels. Although the lower concentrations (LOD and LOQ) could not be detected, the higher concentrations delivered irregular results. Most of the metabolites indicated good recovery during storage (> 90%) in the autosampler, but it was decided to analyse the samples as soon after sample preparation as possible, as 8-OHdG was enhanced during storage in the autosampler, which could give false elevated results.

5.2.6 Matrix effect

As mentioned in chapter 2, the matrix effect can cause compounds to respond differently in a biological matrix compared to a standard solution. The enhancement or ion suppression caused by the matrix can be calculated and expressed as a percentage by using Equation 2-6, dividing the response of the spiked urine sample by the response of the MQC sample multiplied by 100.

Urine and MQC samples were prepared as described in section 3.3 and section 4.1. The matrix effects are summarised in Table 5-31.

Table 5-31. The matrix effect of DNA and lipid peroxidation markers.

Metabolite	Matrix effect (%)	Ion suppression or enhancement
8-OHdG	25.56	Ion suppression
C^{13}, N^{15}-8-OHdG	35.54	
MDA-DNPH	19.54	
MDA- d_2-DNPH	40.22	
$PGF_{2\alpha}$	64.63	
4-HNE-MA	> 150	Ion enhancement
PGE_2	> 150	
PGE_2-d_4	117.91	

As seen in Table 5-31, some of the analytes were suppressed (8-OHdG, MDA-DNPH, $PGF_{2\alpha}$, C^{13}, N^{15}-8-OHdG, MDA-d_2-DNPH), and other enhanced (4-HNE-MA, PGE_2, and PGE_2-d_4) within the matrix. The enhanced analytes were affected much more than the suppressed analytes, with 4-HNE-MA being most enhanced, and $PGF_{2\alpha}$ most suppressed.

5.2.7 Carry-over and selectivity

As mentioned in section 5.1.7, carryover is an important parameter in method validation, as it can directly affect the accuracy of the results. A blank injection was added between the injections of each QC level (prepared as described in section 4.9.1). A carry-over is acceptable when the response of an analyte in the blank is less than 20% of the analyte concentration in the concentrated sample. Overall, the carryover of the method was acceptable, despite the response of $PGF_{2\alpha}$ in the LOD sample (Table C-5).

To determine the selectivity of the method, chromatograms of each analyte were inspected visually and compared with a standard sample, urine, and a spiked urine sample with the same analyte concentration to determine the selectivity of the method.

The standard sample represented the blank sample, in which the retention times of the analytes can be confirmed without any explainable disturbances. The blank urine sample represents a normal sample, containing matrix components that compensate for individual variation and the matrix effect. The spiked urine sample was used to ensure the detection of the target analytes as the concentration thereof is significantly elevated. No interfering peaks were observed for any of the metabolites; therefore, the method was considered selective for the DNA and lipid peroxidation markers.

5.2.8 Extraction recovery

An extraction recovery analysis was performed to determine the amount of analyte loss during the analysis since this method had a few sample preparation steps. A set of QCs was prepared as described in section 4.9.1. The samples that were not loaded onto the SPE cartridges were analysed and compared to the samples post-extraction. By analysing the same samples, any errors occurring before SPE was compensated for.

Table 5-32. Extraction recovery of DNA and lipid oxidation markers. The results are expressed as a percentage.

QC level	8-OHdG	MDA-DNPH	4-HNE-MA	$PGF_{2\alpha}$	PGE_2
LOD	> 120	29	< 10	58	< 10
LOQ	87	12	< 10	52	< 10
LQC	109	81	< 10	65	< 10
MQC	76	36	< 10	45	< 10
HQC	47	45	< 10	50	< 10
EQC	40	28	< 10	67	< 10

The recovery analysis, unfortunately, did not deliver the expected results. As seen in Table 5-32, most analytes had a significant loss during SPE. Various factors could have contributed to the loss seen, such as poor retention on the SPE columns, poor extraction from the SPE columns, loss during evaporation, and poor redissolving of analytes during resuspension.

5.3 Conclusion

Before a newly developed method can be implemented, it should be at least partially validated to ensure that the results are accurate and reliable. To partially validate the butyl ester and DNA and lipid peroxidation marker methods, linearity, accuracy, precision, carryover, stability, recovery, LLOD and LOQ were determined for each method. In general, the validation results were positive for working standards (samples with no matrix effect). The validation highlighted some strengths and limitations of the methods. Unfortunately, the instrument encountered some problems, especially during the validation of DNA and lipid peroxidation markers. Due to time constraints and the limited availability of standards, the validation could not be repeated. Furthermore, the results obtained may have been affected by multiple instrument shutdowns.

The results of the calibration curves (butyl ester and DNA and lipid peroxidation markers) showed that validation on matrix samples could not be performed. When examining the matrix effect, it also became clear that ion suppression occurred for most metabolites except tyrosine, 4-HNE-MA, PGE_2, and PGE_2-d_4. The methods were linear over a wide range for most metabolites, even in urine samples, but the physiological levels of some metabolites were below the LLOQ. The LOD varied between metabolites, with the lowest concentration in urine being 0.05 ng/ml for 8-OHdG and Tyr-BE and the highest concentration being 1.66 ng/ml for 4-HNE-MA. The LLOQ of some metabolites (3-NT-BE and $PGF_{2\alpha}$) were above the lowest physiological concentration; Should a result fall between the LOD and LLOQ for these analytes, the result was reported as <LLOQ. For the remaining metabolites, the LLOQ are below the physiological concentrations. For this specific study, unusually high results were more relevant, so it was acceptable to report <LLOQ. The ULOQ for Tyr-BE were within the expected physiological concentrations, and the ULOQ were much larger than the expected physiological concentrations for the rest of the metabolites. If a Tyr-BE result is greater than ULOQ, a dilution for that sample may be considered for accurate quantification.

Both methods were sensitive and selective for the target metabolites in the working standards. The method sensitivity was acceptable for butyl esters in the urinary matrix as well. The sensitivity was increased by using stable labelled isotopes as internal standards and by derivatizing the amino acids and MDA. Unfortunately, these efforts were not enough to increase the sensitivity of DNA and lipid oxidation markers in the working standards and urine. It is however believed that the stability of these markers could have contributed to the poor sensitivity. Overall, both methods were precise even in a spiked urine sample, but the results provided were not accurate. The accuracy of the methods could be affected by preparation errors, e.g. loss during derivatization, poor resolution when resuspending samples, etc. or by systematic errors, such as stability of stock standards, instrumental errors, decreased column efficiency, etc.

Unfortunately, the short-term stability of all the metabolites was questionable at 4 ºC and -20 ºC, and for that reason, the samples were analysed directly after sample preparation, after which it was discarded. The methods were also selective for the target metabolites, despite a contaminating peak for 3-NT that was observed in the urine sample. No carry-over effect was seen during validation, and it was assumed that the LC-MS methods were sufficient to elute all target compounds from the analytical column and that the needle wash step in the autosampler was also sufficient to prevent cross-contamination between the different injections.

To conclude, the butyl esters and the analytes (4-HNE and $PGF_{2\alpha}$) which performed poorly during validation were not absolutely quantified, and the carrier effect of the stable isotopes might have improved their performance. With the delayed delivery of most chemicals and reagents, the stability of the stock reagents was questionable. Validating the method using newly purchased standards might have also improved the overall performance of the methods during validation, especially accuracy. For the implementation of the method on the contraceptive users, 4-HNE and $PGF_{2\alpha}$ will not be included, as these compounds performed poorly for most of the validation parameters.

CHAPTER 6: IMPLEMENTATION OF THE DEVELOPED METHODS ON COMBINED ORAL CONTRACEPTIVE USERS

The secondary oxidation products reflect the turnover of oxidative damage as described in chapter 2. This study proved that the simultaneous detection of multiple oxidative stress biomarkers is a difficult analytical technique. This chapter describes how the developed methods were applied to a study group consisting of COC users and non-users to characterise their oxidative stress profiles and compare the two groups.

6.1 Sample collection and storage

Participants were recruited by placing advertisements/flyers at several pharmacies, doctor's rooms, supermarkets, and shopping centres in the Potchefstroom/Klerksdorp urban areas, as well as by placing an advertisement on the NWU Facebook page. The recruitment process started in April 2017 and was done continuously until the minimal sample size (i.e., 25 eligible volunteers of each experimental and ethnic group) was reached (Oct 2019).

Inclusion and exclusion criteria were applied to identify the eligible participants. Participants had to be healthy, be of pre-menopausal age (between 18-35 years), have a healthy weight (BMI between 18.5-29.9), the participants using COC should've been using the contraceptives for at least 3 consecutive months before participation, and non-users should not have used any type of hormonal contraceptives for four years prior to sampling. Participants were excluded if they were pregnant or breastfeeding within 6 months before participation, suffered from irregular menstruation, were excessive smokers or alcohol consumers, have been diagnosed with liver or kidney disease or peptic ulceration or hyperacidity. The eligible participants were invited to an information session, after which they had one week to give consent for participating in the study. Each participant had to contact the research assistant to arrange an appointment to sign the informed consent forms.

The participants were requested to refrain from using any nutritional supplementation for one month prior to sample collection. The participants collected their own urine samples at home in specimen bottles provided by the laboratory. A manual, indicating how and when the samples should be collected was also supplied by the North-West university. The participants were assigned unique laboratory numbers once the specimens were received. In this way, the anonymity of the participants could be ensured throughout the whole study. The collected samples were stored at -80 ºC, for possible future use.

6.2 Analytical instruments and methods

The urine samples were divided into two batches, by randomly picking samples from the sample pool, after which they were prepared and analysed separately.

The ratio of users and non-users was not controlled during the batching process, however, the first batch contained 22 control samples, and the second batch contained 26 control samples. The pooled urine sample was added to the first batch, to determine the concentrations of the metabolites as shown in chapter 3. Only one sample was discarded from the first batch before sample preparation, as the sample amount was insufficient for analyses. Therefore, the analysed cohort consisted of 74 participants, of which 48 were control participants, and 26 COC users.

Firstly, the samples were thawed after batching and two 400 µl aliquots of each sample were made. The remaining samples were stored in the -80 ºC again for seven days, after which they were discarded. Both batches were analysed using both methods as described in chapter 4 immediately after sample preparation. This was done to ensure consistency throughout sample analysis, as the metabolites were not stable in the freezer or autosampler for 24 hours. DNPH and mobile phases were prepared freshly before analyses. The same materials and instrumentation were used as detailed in chapter 3 and the samples were pre-treated, derivatised, extracted and resuspended as explained in section 4.9. The workflow of the method application is summarised in Figure 6-1.

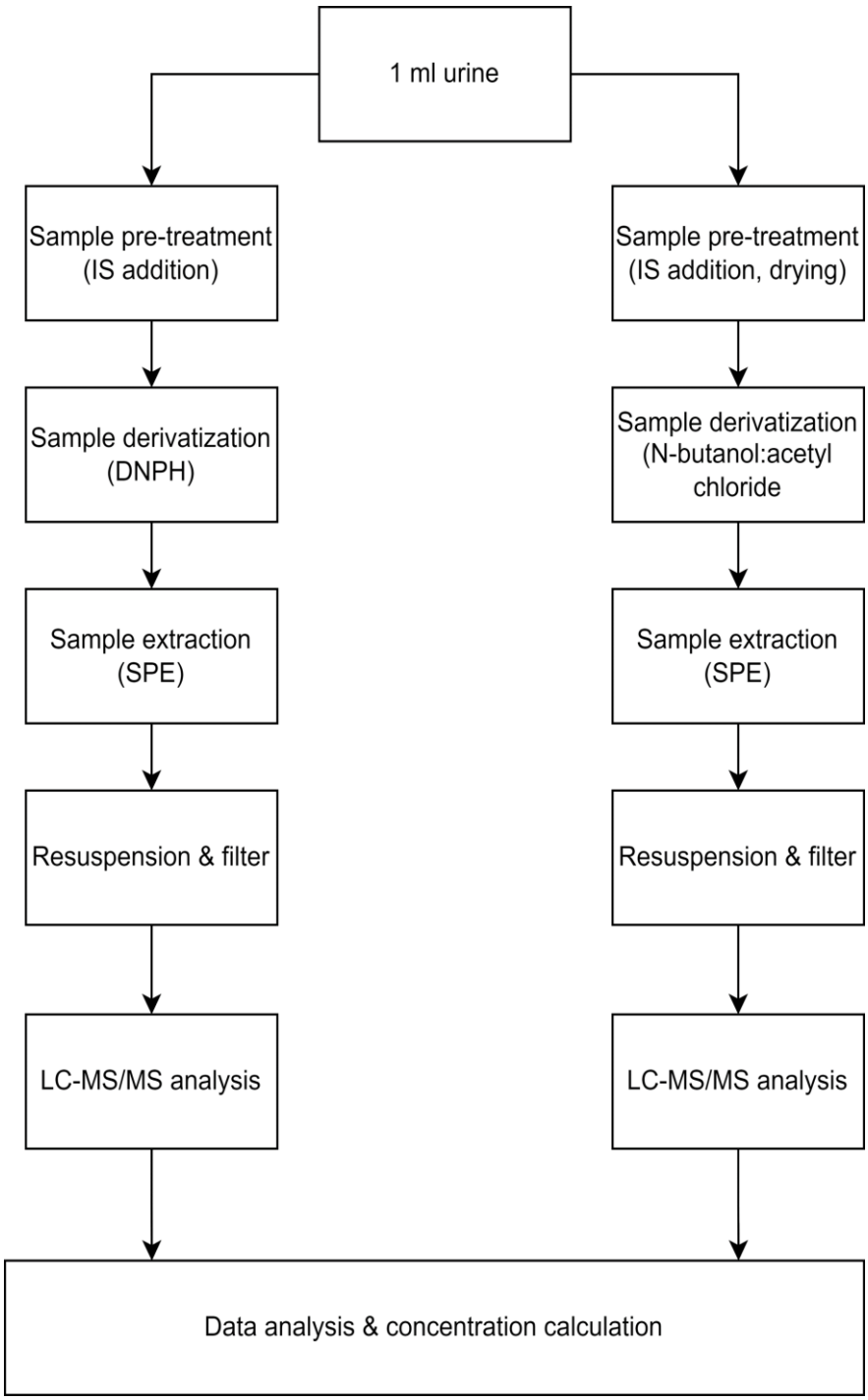

Figure 6-1. Summary of method implementation on the eBOSS samples as detailed in section 4.9.

A calibration curve, consisting of the QC samples (Table C-4) and two spiked urine samples (LQC and HQC spiked) as control samples were injected with each batch as calibrators. Each batch was quantified and analysed with the calibrators prepared and analysed with the batch. By doing this, the results could be reported much more accurately and precisely as the calibrators were exposed to the same conditions as the samples in the batch (Sonntag, 2015).

6.3 Data processing

The volumetric concentration of the metabolites was calculated by using Equation 6-1. The response factor is the ratio between concentration and response and is used to calculate the relative response factor (RRF), which is the ratio between the response factor of a metabolite and the response factor of the IS (Rozio *et al.*, 2019). The RRF is represented by the slope of the calibration curve (Chakravarthy *et al.*, 2011), which in this case was constructed for each batch separately.

Equation 6-1. Formula that was used to calculate the volumetric concentrations of the target metabolites in biological samples.

$$Volumetric\ concentration\ = Relative\ response\ \times \frac{IS\ concentration}{RR}$$

6.3.1 Creatinine analysis, creatinine correction, and concentration factor

As mentioned in chapter 4, the sample preparation resulted in concentrating the samples. The volumetric concentration had to be corrected with the concentration factor (which was 2 for this study) before further analyses could be done. The volumetric concentration was simply divided by the concentration factor to obtain the corrected concentrations.

Since the composition of urine varies between people, a normalisation process had to be followed to ensure that the measured concentrations can be compared. There are various normalisation approaches, the most frequently used in metabolomics; is the total ion count normalisation, where the response of the analyte is divided with all the ions observed in the sample (Wulff & Mitchell, 2018). Another popular and reliable way of normalising urinary components is through creatinine concentration. Creatinine is a metabolic waste product formed from creatine in muscles and excreted in urine (Price, 2013). According to Cook, there is a direct relationship between the formed creatinine and muscle mass, therefore, the creatinine excretion is assumed to be consistent as muscle mass remains unchanged from day to day (2000). For this reason, creatinine is a good indicator of urine dilution/concentration. The normalisation of urinary compounds with creatinine concentration is known as creatinine correction (Martinez-Moral & Kannan, 2019). Unfortunately, creatinine correction can be influenced by intraindividual variability, water consumption and medication (Franz et al., 2019).

This is done by dividing the volumetric concentration (ng/ml) (Equation 6-1) by the measured creatinine concentration (mmol/L). Therefore, the creatinine concentrations had to be measured before correction could take place.

The creatinine concentrations of the thawed urine samples were measured at the Potchefstroom Laboratory for inborn errors of metabolism (PLIEM, North-West University, South Africa). The results with a mmol/L concentration were used during data analysis and the final concentrations of the oxidative stress markers were reported as *ng/mg creatinine*.

6.3.2 Statistical processing

6.3.2.1 Normalisation, transformation, and scaling of dataset

After creatinine correction, it was seen that the data was not normally distributed (Figure 6-2 and Table C-5). The *normalisation by sum*, where each value in a variable was divided by the sum of the variable was applied (Di Guida *et al.*, 2016). By transforming the dataset, the same conversion was applied to each score within the dataset to correct for unequal variances, any outliers, and distribution problems (Field, 2009). As with normalisation testing, there are various types of transformation (van den Berg *et al.*, 2006; Field, 2009), *log transformation* was chosen, as there were no zero-values within the dataset. The data was also scaled using the *mean centering* function (Figure 6-2), the mean of the variable was subtracted from each value, resulting the variables to be centred around zero (Field, 2009). Normalisation, transformation, and scaling were done on the MetaboAnalyst 5.0 software.

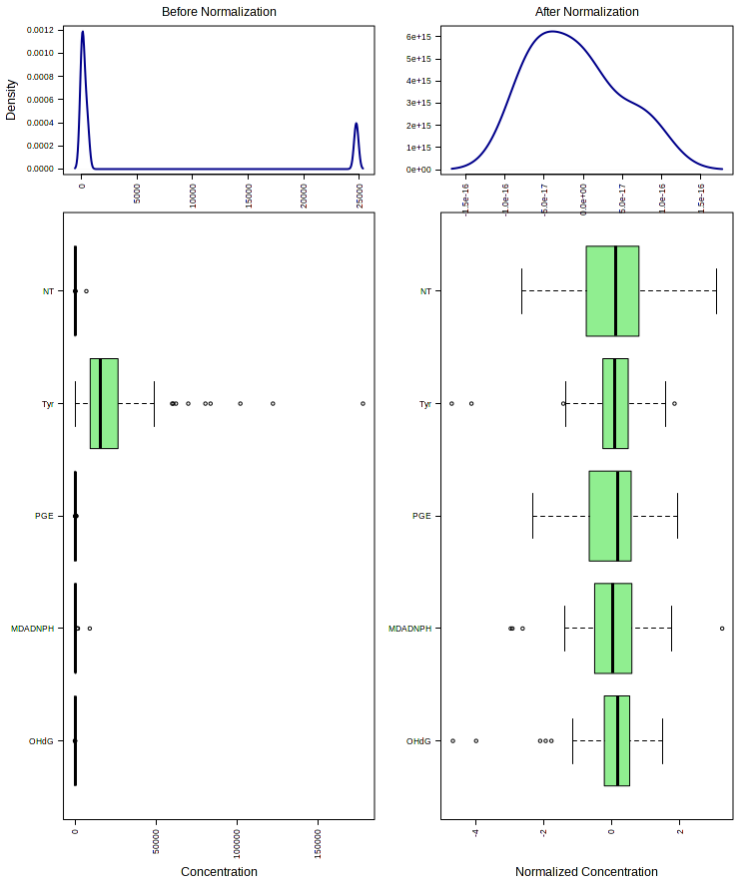

Figure 6-2. Data distribution before and after normalisation, transformation, and scaling.

Figure 6-2 illustrates the data distribution before and after transformation. Although the data still indicated a slight positive skewness, the distribution was improved significantly. The rest of the data processing and analyses were performed on the normalised dataset.

6.3.2.2 Batch effect

As described in section 6.2, the eBOSS samples were analysed in two batches, which could give rise to a possible batch effect. One way of compensating for the batch effect was to inject the calibration curve with each batch. A batch effect analysis was performed to establish if this compensation was successful (Figure 6-3). This was done with a Principal Component Analysis (PCA), which is an unsupervised multivariate statistical technique that reduces the dimensionality of the dataset without losing any data (van den Berg *et al.*, 2006). By creating new uncorrelated variables (that maximises variance), known as Principal Components (PCs), the reduction analysis can be performed (Jolliffe & Cadima, 2016).

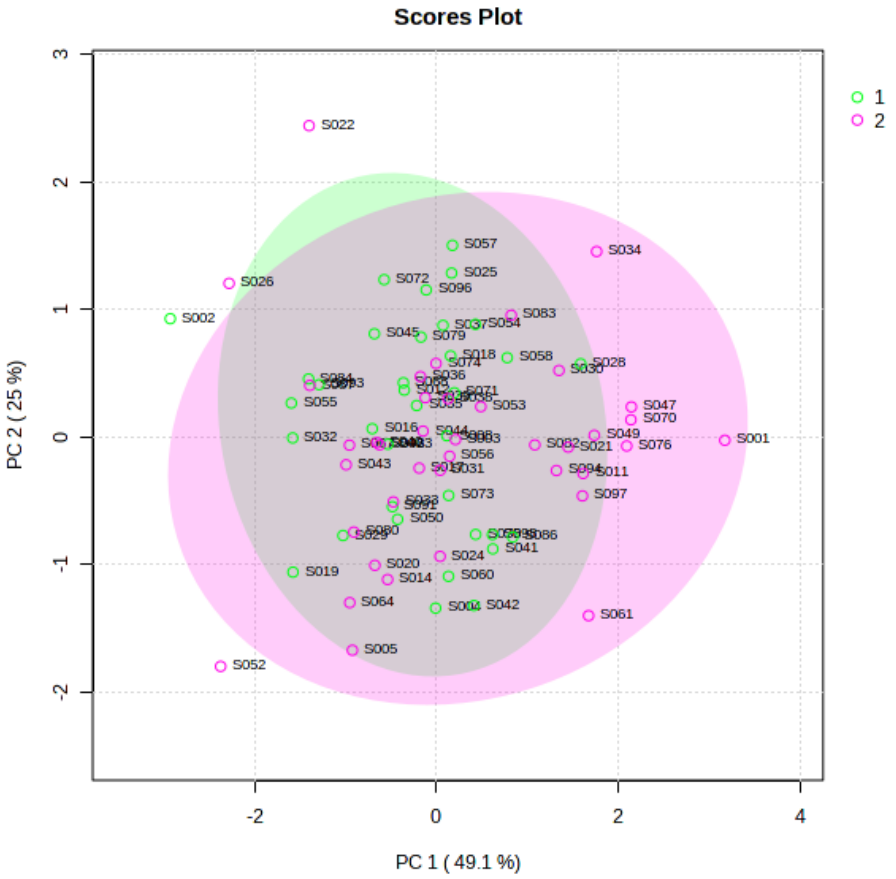

Figure 6-3. Scores plot between selected PCs after PCA to assess the batch effect. The green circle presents the first batch, and the purple circle presents the second batch.

During PCA, five principal components were identified, however, only three components were statistically significant, with PC1 being most significant and PC3 least significant.

The scores plot is one way of representing the correlation between the identified PCs, and it was decided to plot the two components with the most significance against each other. In Figure 6-3 it is shown that the samples from both batches clustered together in one big sample group. This indicated that no batch effect occurred, and that the calibration curves successfully compensated for any variances between the batches. Since no batch effect was observed, the data of both batches were combined into a single dataset comparing the non-user and user groups.

6.3.2.3 Outliers

To determine if there were any outliers in the dataset, a PCA (MetaboAnalyst) was once again used (Figure 6-4). All the samples outside the 95% confidence interval were identified as outliers (eBOSS 001, eBOSS 002, eBOSS 052, eBOSS 022, and eBOSS 0.34) and were removed from the dataset for further statistical analyses. Sample *eBOSS 034* was from the user group, whereas the other samples were from the non-user group.

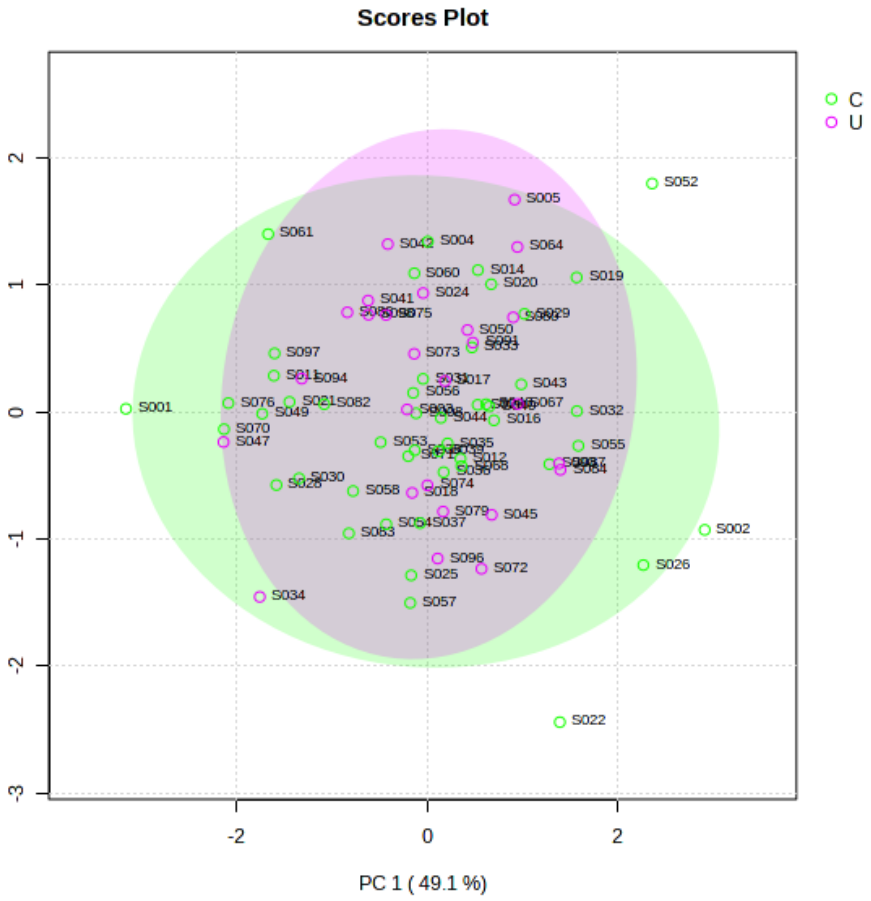

Figure 6-4. PCA score plot to determine any samples outside the 95% confidence interval. The green circle represents the non-user group, and the purple circle represents the user group.

6.3.2.4 Univariate analysis

By using the IBM SPSS software, descriptive statistics, t-tests, and box-and-whisker plots (boxplots) could be generated. The descriptive statistics included means and standard deviations, whereas the t-tests included equality of means and correlation. The boxplots were generated as a visual illustration of the univariate results.

The t-tests are dependent on the descriptive statistics (Table C-6) as the descriptives are used during the t-tests. Firstly, the homogeneity of variance was determined by using *Levene's test*, if the p-value was > 0.05, it was assumed that the variance was equally distributed between the two groups, thereafter the equality of means could be determined to establish a significant difference between the group means (p-value ≤ 0.05).

Table 6-1. Observed p-values from the applied t-tests during univariate analysis.

Metabolite	Levene's test	Equality of means
8-OHdG	0.974	0.265
MDA-DNPH	0.780	0.157
PGE_2	0.320	0.054
Tyr	0.126	**0.003**
3-NT	0.241	**0.024**

When considering Levene's test (Table 6-1), the variances for all metabolites were equal between the user and non-user groups (p-value > 0.05). The equality of means could be interpreted based on Levene's test, and both tyr and 3-NT had p-values < 0.05. Indicating that there was a significant difference between the mean concentrations of tyr and 3-NTfor the users and non-users.

The equality of means can also be used as an estimate of regression (Field, 2009). Regression is defined as a prediction of an outcome variable from another variable, by fitting a linear model (Field, 2009). From Table 6-1, both 3-NT and tyr could significantly predict the outcome variable (p-value < 0.05). Another statistical measurement of a relationship between two variables are known as correlation (Schober *et al*., 2018). Correlation is used to indicate the strength of the relationship between two variables (Field, 2009).

The *Pearson's correlation coefficient (r*) was examined to determine the correlation between metabolites in the user and non-user groups (Table 6-2 and Table 6-3 respectively).

Table 6-2. Correlation matrix containing Pearson's correlation coefficients to determine if any correlation existed between metabolites in the non-user group.

Analyte	8-OHdG	MDA-DNPH	PGE	Tyr-BE	3-NT-BE
8-OHdG	1.00	0.19	-0.15	0.00	-0.01
MDA-DNPH	0.19	1.00	0.13	0.11	0.22
PGE_2	-0.15	0.13	1.00	-0.23	-0.01
Tyr-BE	0.00	0.11	-0.23	1.00	0.24
3-NT-BE	-0.01	0.22	-0.01	0.24	1.00

If $r = 0$, no linear correlation or relationship occurred, as r draws closer to ±1 the strength of the relationship increases, $r = \pm 1$ indicates a perfect relationship between variables (Schober *et al*., 2018).

Table 6-3. Correlation matrix containing Pearson's correlation coefficients to determine if any correlation existed between metabolites in the user group.

Analyte	8-OHdG	MDA-DNPH	PGE	Tyr-BE	3-NT-BE
8-OHdG	1.00	0.14	0.09	0.03	0.11
MDA-DNPH	0.14	1.00	0.04	0.02	0.08
PGE_2	0.09	0.04	1.00	0.01	-0.07
Tyr-BE	0.03	0.02	0.01	1.00	0.26
3-NT-BE	0.11	0.08	-0.07	0.26	1.00

If $r = 0$, no linear correlation or relationship occurred, as r draws closer to ±1 the strength of the relationship increases, $r = \pm 1$ indicates a perfect relationship between variables (Schober *et al*., 2018).

Table 6-2 and Table 6-3 were used to compare how the metabolites correlate with one another, these matrixes shows that no correlation existed between the target analytes, as the correlation coefficients were all close to zero ($-0.23 < r < 0.26$). The negative correlation ($r < 0$) indicated that as the one metabolite increased, the other decreased, whereas the positive correlation ($r > 0$) indicated that as one metabolite increased, the other also increased (Schober *et al.,* 2018).

The boxplots generated for each metabolite compared the user and non-user groups with each other, as shown in Figure 6-5. From these plots, the distribution of the samples within each group could be observed, as well as a summary of the descriptive statistics (median, interquartile ranges, minimum and maximum observations). Although the boxplots indicate the median and not the mean, a difference between the user and non-user groups can still be observed.

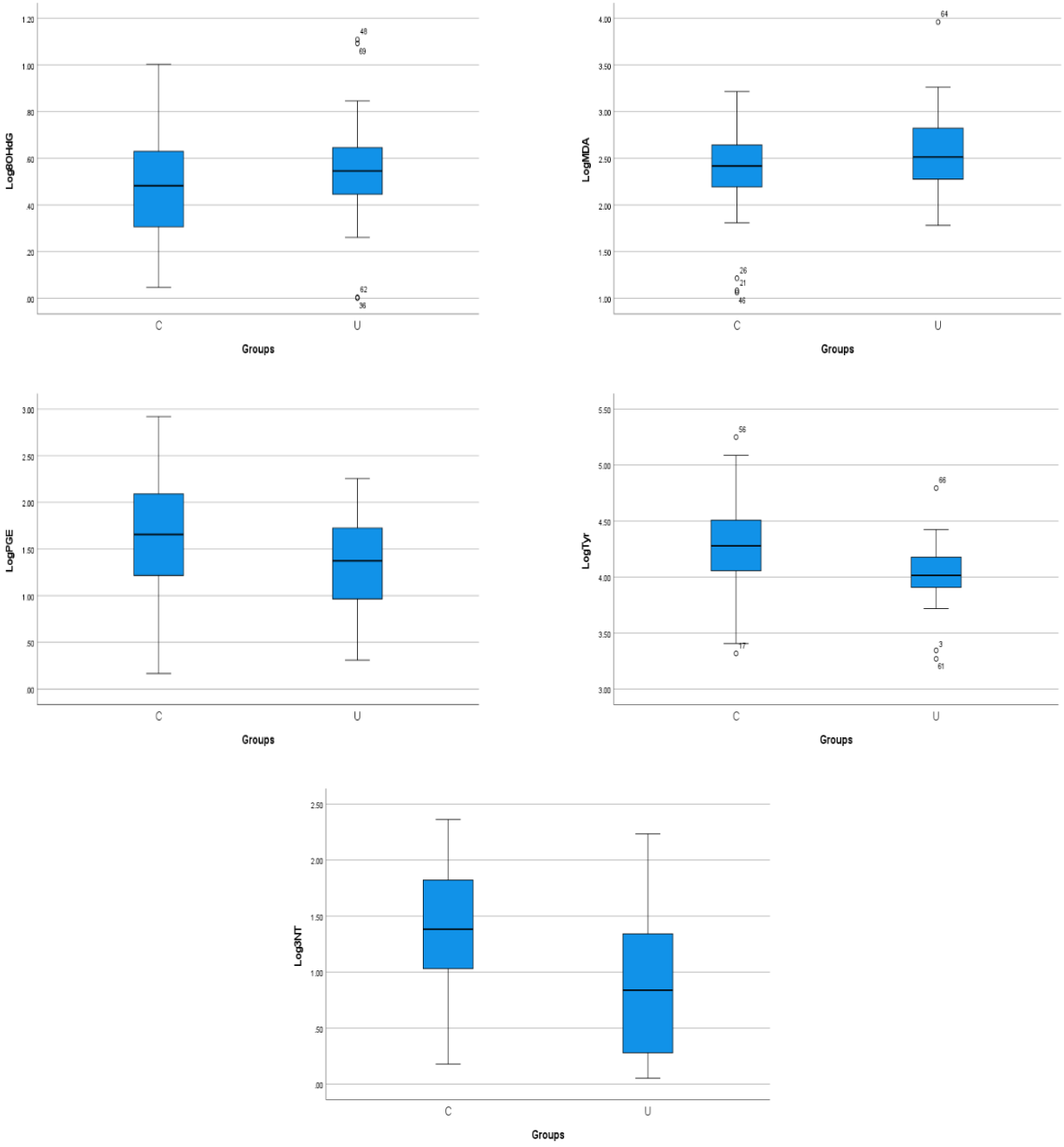

Figure 6-5. Boxplots of each metabolite comparing COC users and non-users. C: non-users, U: users.

From Figure 6-5, it can be observed that the distribution of concentrations between the users and non-users differed for most of the analytes, except MDA and 3-NT. The distribution of 8-OHdG, tyr, and PGE_2 concentrations were significantly lower in the user group compared to the non-user group. A slight increase of concentrations for users were observed for both 8-OHdG and MDA, whereas a decrease of concentrations for users were observed for PGE, Tyr, and 3-NT. The median values of the user group were significantly lower for both tyr and 3-NT (the medians from the user group were less than the lower interquartile values of the non-user group). This observation supports the findings from the equality of means t-test (Table 6-1).

6.3.2.5 Multivariate analysis

To further investigate a possible difference between the users and non-users, multivariate analysis was applied. Firstly, the differences were assessed by both PCA and Partial least square-discriminant analysis (PLS-DA) (Figure 6-6).

PLS-DA can be seen as a 'supervised' version of PCA, in the sense that it takes class labels into account during analysis (Ruiz-Perez *et al.*, 2020). The main difference between PCA and PLS-DA is that PCA preserves as much variance from the original data as possible, whereas PLS-DA preserves as much co-variance from the original data for its first principal component (Ruiz-Perez *et al.*, 2020). For this reason, both PCA and PLS-DA techniques were used during statistical processing. The multivariate analysis was done on MetaboAnalyst.

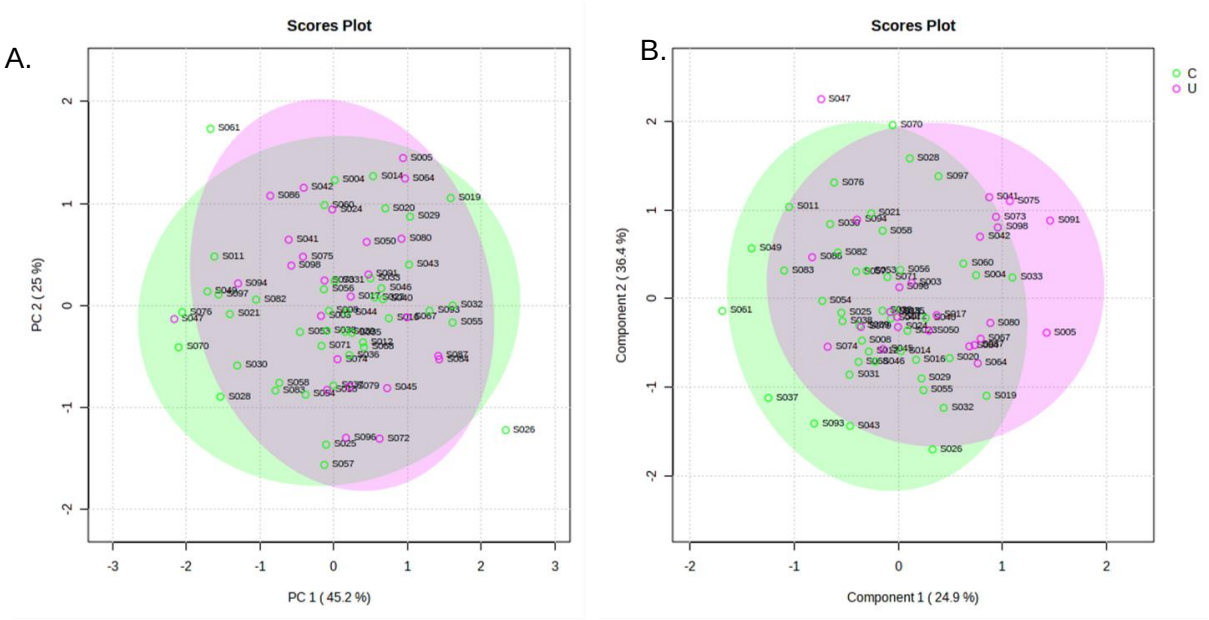

Figure 6-6. Score plots after PCA and PLS-DA to determine any difference between the users and non-users. A. PCA scores plot, where PC 1 and PC 2 was compared B. PLS-DA scores plot, where components 1 and 2 were compared. The pink circle presents the user group, and the green circle presents the non-user group.

From both the PCA and PLS-DA score plots (Figure 6-6), other outliers were observed. These outliers were ignored as they were not identified during the outlier removal analysis. The PCA score plot did not indicate any significant differences between the user and non-user groups, as the scores were clustered in the middle of the plot (Figure 6-6.A).

Despite the slight shift in the distribution of the user group, the PLS-DA score plot also did not indicate any statistical significance between the two groups (Figure 6-6.B). During PLS-DA, a VIP plot was constructed indicating which metabolites contributed most to the statistical analysis (Figure 6-7).

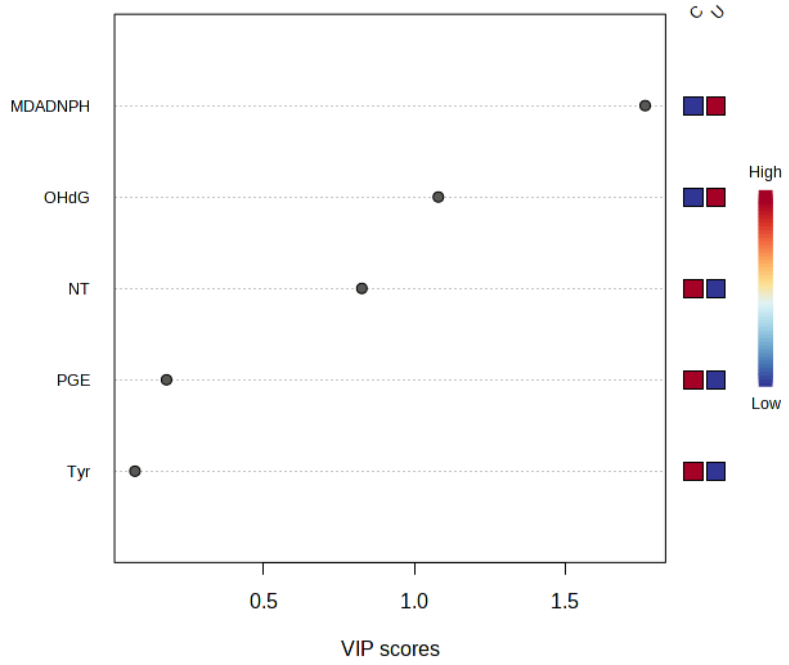

Figure 6-7. VIP scores plot obtained from PLS-DA analysis. The red indicates high contributions, and blue indicates low contributions. *C: non-user group. U: User group.*

According to Zheng and colleagues, metabolites with a VIP score greater than one was seen as significant towards the PLS-DA analysis (2023). As seen in Figure 6-7, MDA-DNPH had a VIP score of 1.76 and 8-OHdG had a VIP score: of 1.08. Both 8-OHdG and MDA-DNPH had a VIP score ≥1, indicating that they are significant towards the PLS-DA. Since the class labels (groups) are taken into consideration during PLS-DA (Ruiz-Perez *et al.*, 2020), the VIP scores plot can also indicate towards which group the analytes are significant. The VIP scores plot (Figure 6-7) indicated that 8-OHdG and MDA-DNPH are significant towards the user group.

6.4 Cross reference between butyl esters

As described in section 2.7.2, cross-referencing the 3-NT with tyr would indicate as both levels are affected by diet. Since 3-NT was the metabolite of interest it was decided to obtain the butyl ester ratios by dividing the concentration of 3-NT by the concentration of tyr (Equation 6-2).

Equation 6-2. The determination of butyl ester ratio as cross-reference.

$$Butyl\ ester\ ratio = \frac{3 - NT\ concentration}{Tyr\ concentration}$$

The butyl ester ratios were calculated for all the samples including the outliers identified in section 6.3.2.3. Since the overall responses of tyr were much greater than 3-NT, the ratios calculated were very small. This indicated that the dietary effect was negligible.

During the evaluation of these ratios, only one outlier with a highly elevated ratio (ratio >1) was identified (eBOSS 022), this sample was identified as an outlier in section 6.3.2.3.. One other outlier was identified with an elevated ratio, but not significantly (ratio < 0.5). The outliers with ratios > 0.2 were removed from the dataset to determine whether there was a significant difference in the butyl ester rations of the COC users and non-users. A simple boxplot was generated (Figure 6-8) and the equality of means were also determined.

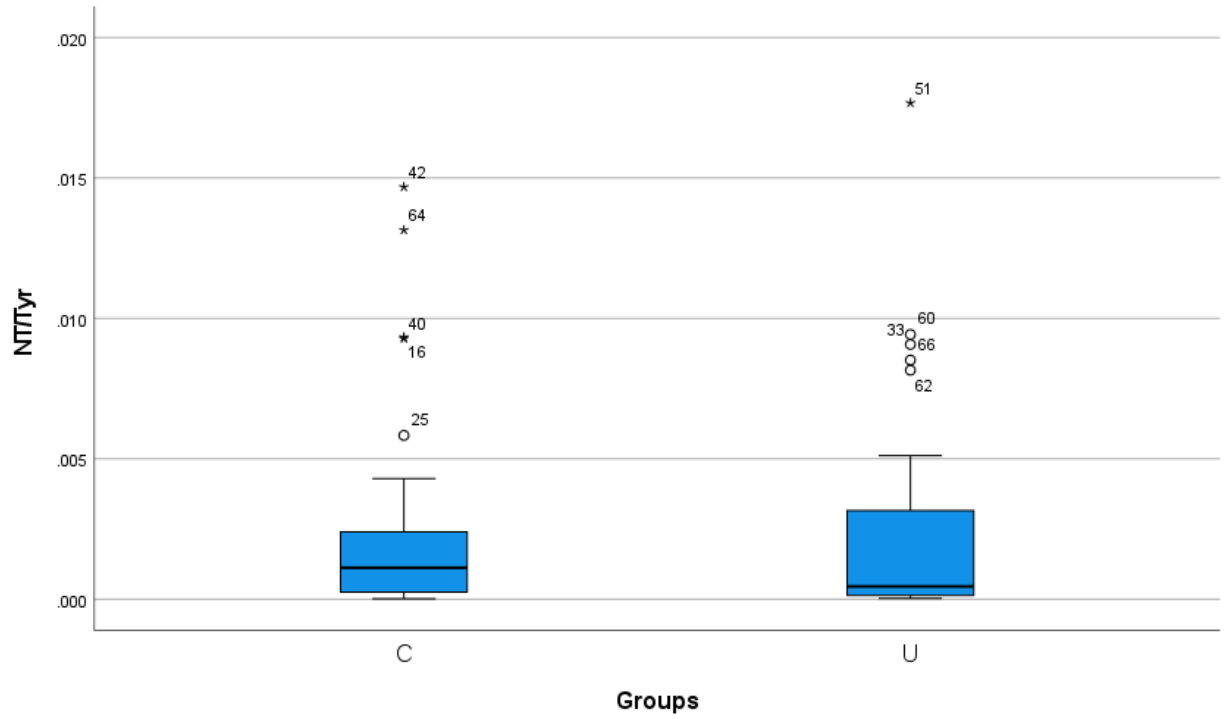

Figure 6-8. The comparison of butyl ester ratios between the user and non-user' group.

C: non-users, U: users.

After the boxplot was generated, more outliers were identified. These outliers were ignored, as their ratios were less than 0.2. There were no significant differences between the butyl ester ratios of two test groups, and the distribution across the user group was similar compared to the non-users (Figure 6-8). It was therefore concluded that the dietary effect did not lead to any false elevations in 3-NT levels.

6.5 Summary

To conclude, the use of calibration curves was successful in preventing any batch effects from occurring. For these reasons, the results obtained from the eBOSS cohort were considered acceptable. During data processing the analytical responses were converted to concentrations corrected with the creatinine and reported as *ng/mg creatinine*. This correction was made to normalise the results according to the urine concentration.

Due to the amount of variation within the non-user group, it was not possible to remove all outliers identified, therefore after some further investigation, a total of five outliers were removed from the dataset (eBOSS001, eBOSS002, eBOSS052, eBOSS022, and eBOSS034).

During univariate analysis, both tyr and 3-NT were identified as statistically different between the user and non-user groups. A slight increase in 8-OHdG and MDA concentrations, and a slight decrease in die PGE_2 concentrations was seen for the user group in the boxplots, however these observations were not statistically significant. However, during multivariate analysis, 8-OHdG and MDA were identified as statistically significant metabolites. Since both butyl esters are affected by diet, the 3-NT was cross-referenced with tyr. The possible dietary influence was excluded, as no 3-NT levels were falsely increased. Although 3-NT, 8-OHdG and MDA were not significant in both univariate and multivariate analyses, trends of these metabolites were observed in both statistical testing methods (Figure 6-5 and Figure 6-7).

From the literature review as well as previous studies (Venter et al., 2021); it is evident that COC induces oxidative stress. Considering the increased ROS exposure, one would expect an increase in oxidative stress markers. However, the amino acids (tyr & 3-NT) were slightly suppressed in the user group. This correlates with the findings of Amatayakul et al., where plasma amino acids were suppressed in women using oral contraceptives, possibly due to increased hepatic protein synthesis (1994). Lipids are very prone to oxidative damage due to their structure as described in section **Error! Reference source not found.**. A study done b y Michael et al., also indicated an increase in MDA levels during COC use (2020).

Although 8-OHdG can be used as both a carcinogenic and oxidative stress indicator, the slight increase in 8-OHdG correlates with the results obtained from previous studies (Swiegers, 2015).

Therefore, to conclude, tyr, 3-NT, 8-OHdG, and MDA were identified as statistically significant metabolites in the oxidative stress profiling of COC users. The association with COC use and these oxidative stress markers are still not fully understood, but the results from this study indicate that all three macromolecules (DNA, lipids & protein) are affected by COC usage.

CHAPTER 7: CONCLUSION

The direct analysis of free radicals is a challenging task; therefore, secondary oxidation products are measured instead. Most of these oxidation markers are usually analysed individually to investigate specific macromolecule groups such as lipids or DNA. Therefore, it could be beneficial for oxidative stress profiling, if a single method existed that could simultaneously quantify oxidative stress markers, especially in the risk assessment for oxidative stressed induced diseases such as cancer. The oxidative stress markers included in this study were representative of the oxidation of lipids (MDA, 4-HNE-MA, $PGF_{2\alpha}$, and PGE_2) and DNA (8-OHdG), as well as the oxidation and nitration of proteins (tyr, 3-NT, and dityr). The methods described by Martinez-Moral were used as a reference for this study (2018, 2022).

7.1 General conclusion

The aim of this study was first to develop a method that can simultaneously quantify oxidative stress markers, and secondly to apply this method to a cohort to compare their oxidative stress profiles. To achieve these aims, some objectives were identified.

The first objective was to optimise the detection and ionisation conditions for the target metabolites (MDA, 4-HNE-MA, $PGF_{2\alpha,}$ PGE_2, tyr, 3-NT, dityr, and 8-OHdG) from the methods described by Martinez-Moral & Kannan (2018, 2019, 2022). The optimisation included ionisation source optimisation, optimisation of precursor and product ions, as well as the ionisation parameters. This was achieved by using the MassHunter Optimiser workstation and iFunnel Source Optimiser software as described in section 4.1.

The second objective was to successfully optimise metabolite separation on the analytical column and LC-ESI-MS/MS system. As described in sections 4.1, 4.2.5, and 4.8, this included the adjustment of mobile phase gradient, column temperatures, flow rate, mobile phase composition and analytical column comparison.

The optimisation of the sample preparation as described in the literature (Martinez & Kannan, 2018; Martinez-Moral & Kannan, 2019; Martinez-Moral & Kannan, 2022; Vanova et al., 2018) was the third objective. This was achieved by optimising derivatisation with both DNPH and N-butanol: acetyl chloride (reagent concentrations, incubation temperature and incubation times), as well as optimising the solid phase extraction method (fraction analyses, washing solvents, loading volumes) as detailed in sections 4.2, 4.4, and 4.8.

The fourth objective was validating the method(s) to establish if it was reproducible and accurate. This objective is described in the whole of chapter 5 and included the investigation of linearity, sensitivity, accuracy, precision, short-term stability, the matrix effect, selectivity, and extraction recovery. Although this objective was achieved, some alterations might improve the validation of these methods.

To successfully achieve the first aim of this study, objectives one to four had to be achieved. From chapter 4, it is evident that these objectives were investigated multiple times, as both derivatisation and extraction affected the separation and detection of the metabolites. The attempt to combine all the target analytes into a single method as described by Martinez-Moral and Kannan (2018, 2022) was unsuccessful. This was mainly due to the difference in chemical characteristics of the target metabolites. However, two separate methods were successfully developed, optimised, and partially validated as described in chapters 4 and 5.

The final objective was the implementation of these optimised and validated methods to the cohort consisting of COC users and non-users. The cohort samples were analysed in two batches by using the methods described in section 4.8. This objective was successfully achieved as described in chapter 6.

The second aim of the study was achieved, as the method was successfully applied to the cohort. However, it was expected that the COC users would have a significantly different oxidative stress profile compared to the non-user group. Unfortunately, this was not the case with this specific cohort as only a slight statistical significance was observed between these two groups. A few metabolites (3-NT, Tyr, 8-OHdG, and MDA) however were identified as significant in the oxidative stress profiling of COC users. These metabolites indicate that the macromolecules (DNA, lipids & proteins) are affected by COC induced oxidative stress, the extent of the association between these oxidative stress markers and COC use are however still not fully understood.

7.2 Final remarks

During covid-19, the delay in manufacturing, supply and distribution of certain chemicals and reagents was an immense drawback of this study. During this time, the experimental approach had to be adjusted, as there was a global shortage of DNPH as described in section 4.2.

The development, optimisation, and validation of these oxidative stress markers was much more challenging than originally anticipated. Despite multiple hurdles, two methods could be partially developed, optimised and validated to quantify five oxidative stress markers using LC-ESI-MS/MS. The results obtained from this study can be used to further investigate the possibility of a single method for the characterisation of oxidative stress profiles to shed the light on oxidative stressed induced diseases, as this was the motivation for this study.

7.3 Future recommendations

1. Due to the delay in the delivery of some chemicals and reagents, the stability of the stock reagents was questionable. Repeating validation on newly purchased reagents might produce more desirable results.

2. Optimisation of the mobile phases, by adding a modifier such as ammonium formate to the mobile phase. This may improve sample load tolerance and result in improved peak shapes (sharper peaks and less peak tailing) (Boyes & Dong, 2018; Johnson *et al.*, 2013). The addition of ammonium formate could possibly increase the sensitivity of the method for the compounds that were excluded from the methods and performed sub optimally during validation (dityr, 4-HNE, $PGF_{2\alpha}$, PGE_2 and 4-HNE-MA).

3. Investigate the solubility of DNPH, the DNPH used during this study did not dissolve and the precipitate had to be filtered. By investigating the solubility of DNPH, the derivatisation efficiency and repeatability may be significantly increased if all the DNPH is dissolved.

4. Investigate the stability of N-butanol:acetyl chloride and to what extent it influences accuracy and sample stability after derivatisation.

5. Examine the storage stability of the samples throughout all phases during sample preparation (post-derivatisation, post-extraction, and post-resuspension) at room temperature (~20 ºC -25 ºC), in the fridge/autosampler (4 ºC), in the freezer (both -20 ºC, and -80 ºC).

6. Investigate the light sensitivity of the DNA and lipid peroxidation markers after derivatisation with DNPH (DNPH is light sensitive, therefore its derivatives might also be light sensitive).

7. The addition of stable isotopes for all the target metabolites, especially if this method will be used commercially. The stable isotopes allow absolute quantification instead of relative quantification, which could present more accurate results and increase the sensitivity of the method for the metabolites excluded from the study (dityr, 4-HNE, $PGF_{2\alpha}$ and 4-HNE-MA).

8. The matrix effect was much greater than originally anticipated, the sample clean-up or preparation can possibly be improved by centrifuging the samples for longer time periods, diluting the samples with an organic substance to precipitate some proteins, and further optimisation of the SPE method by using alternative cartridges (Oasis HLB). These cartridges have the advantage of increased retention times, which may improve the recovery of the analytes.

On-line SPE can also be considered, as it automates the sample clean-up process, it significantly decreases sample preparation time, and eliminates possible sample loss and analyst error (degradation, evaporation, sample spills, redissolving) (Charnot *et al.*, 2018).

9. Investigate the separation of the compounds on the Agilent Eclipse column post-extraction, as the columns were compared before extraction.

10. The addition of qualifier ions for the analytes may also increase the selectivity and sensitivity of the method especially in the urine matrix, as more than one fraction of the analyte is detected.

11. After some modifications, as mentioned in this section, the possibility of combining the methods for a single method should be re-considered.

12. Re-assessment of these methods, by applying the method to individuals with known high oxidative stress levels using freshly collected samples. As the stability of the compounds in long-term storage is unknown.

13. Investigate the effect of COC use on kidney function, or compare concentrations corrected with creatinine to concentrations normalised using total ion count approach.

14. Investigate the statistical significant analytes identified in the COC user group to determine their involvement in COC induced oxidative stress.

BIBLIOGRAPHY

Alary, J., Bravais, F., Cravedi, J.-P., Debrauwer, L., Rao, D. & Bories, G. 1995. Mercapturic Acid Conjugates as Urinary End Metabolites of the Lipid Peroxidation Product 4-Hydroxy-2-nonenal in the Rat. *Chemical Research in Toxicology*. 8(1):34–39.

Amatayakul, K., Laokuldilok, T., Koottathep, S., Dejsarai, W., Prapamontol, T., … Uttaravichai, C. 1994. The effect of oral contraceptives on protein metabolism. Journal of the Medical Association of Thailand = Chotmaihet Thangphaet. 77(10):509–516.

Anjum, I., Khalid, A., Eajaz, F. & Jaffery, S.S. 2019. Does Taking Oral Contraceptive Pills Increase your Risk for Breast Cancer? A Literature Review. *Ecronicon gynaecology*, 8(10):911–915.

APVMA. 2004. Guidelines for the validation of analytical methods for active constituent, agricultural and veterinary chemical products. http://apvma.gov.au/node/1048 Date of access: 12 Oct. 2020.

Armbruster, D.A & Pry, T. 2008. Limit of Blank, Limit of Detection and Limit of Quantitation. *The Clinical Biochemist Reviews.* 29(Suppl1):S49-S52.

Ayala, A., Muñoz, M.F. & Argüelles, S. 2014. Lipid Peroxidation: Production, Metabolism, and Signaling Mechanisms of Malondialdehyde and 4-Hydroxy-2-Nonenal. *Oxidative Medicine and Cellular Longevity*, 2014:1–31.

Banerjee, S. & Mazumdar, S. 2012. Electrospray Ionization Mass Spectrometry: A Technique to Access the Information beyond the Molecular Weight of the Analyte. *International Journal of Analytical Chemistry*, 2012:1–40.

Barbosa, M.L., de Meneses, A.-A.P.M., de Aguiar, R.P.S., de Castro e Sousa, J.M., de Carvalho Melo Cavalcante, A.A. & Maluf, S.W. 2020. Oxidative stress, antioxidant defense and depressive disorders: A systematic review of biochemical and molecular markers. *Neurology, Psychiatry and Brain Research*, 36:65–72.

Bender, D.A. 2009. Free Radicals and Antioxidant nutrients. In: 28th ed. *Harper's illustrated biochemistry*. Estados Unidos: Lange Medical Books/McGraw-Hill. p. 482–486. https://awesomechem.files.wordpress.com/2016/10/harpers-illustrated-biochemistry-28th-ed-robert-k-murray-et-al-mcgraw-hill-2009.pdf Date of access: 31 Mar 2020.

Bhandari, R.K., Deem, S.L., Holliday, D.K., Jandegian, C.M., Kassotis, C.D., … Rosenfeld, C.S. 2015. Effects of the environmental estrogenic contaminants' bisphenol A and 17α-ethinyl estradiol on sexual development and adult behaviours in aquatic wildlife species. *General and Comparative Endocrinology*, 214:195–219.

Bhattacharjee, S., Pennathur, S., Byun, J., Crowley, J., Mueller, D., … Heinecke, J.W. 2001. NADPH Oxidase of Neutrophils Elevates o,o′-Dityrosine Cross-Links in Proteins and Urine during Inflammation. *Archives of Biochemistry and Biophysics*, 395(1):69–77.

Bothma, K. 2012. The involvement of lipid and protein oxidation in hypertension: the SABPA study. Potchefstroom: NWU. (Thesis – MSc).

Bouatra, S., Aziat, F., Mandal, R., Guo, A.C., Wilson, M.R., … Wishart, D.S. 2013. The Human Urine Metabolome. *Plos one*, 8(9):e73076.

Boyes, B. & Dong, M. 2018. Modern Trends and Best Practices in Mobile-Phase Selection in Reversed-Phase Chromatography. *LCGC North America*, 36(10):752–768.

Britannica. 2019. urine | Definition, Composition, & Facts. *Encyclopaedia Britannica*. https://www.britannica.com/science/urine Date of access: 15 Oct. 2021.

Bucknall, M.P. 2006. Dityrosine as a biomarker of free radical induced oxidative damage in diseases of ageing. University of New South Wales. (Thesis -PhD). http://unsworks.unsw.edu.au/fapi/datastream/unsworks:1490/SOURCE02?view=true Date of access: 21 Feb. 2020.

Mayo Clinic, 2022. Cancer - Diagnosis and treatment - Mayo Clinic. s.a. https://www.mayoclinic.org/diseases-conditions/cancer/diagnosis-treatment/drc-20370594 Date of access: 16 Feb. 2021.

CANSA. 2022. *Cancer Statistics*. *CANSA - The Cancer Association of South Africa*. https://cansa.org.za/south-african-cancer-statistics/ Date of access: 04 Oct. 2022.

CANSA. 2022. Breast Cancer. *CANSA - The Cancer Association of South Africa*. https://cansa.org.za/breast-cancer/ Date of access: 04 Oct. 2022.

Cavalieri, E. & Rogan, E. 2014. The molecular etiology and prevention of estrogen-initiated cancers. *Molecular Aspects of Medicine*, 36:1–55.

Cavalieri, E., Chakravarti, D., Guttenplan, J., Hart, E., Ingle, J., … Sutter, T. 2006. Catechol estrogen quinones as initiators of breast and other human cancers: implications for biomarkers of susceptibility and cancer prevention. *Biochimica Et Biophysica Acta*, 1766(1):63–78.

Chakravarthy, V., Babu, G., Dasu, R., Prathyusha, P. & Kiran, G. 2011. The role of relative response factor in related substances method development by high performance liquid chromatography (HPLC). *Rasayan Journal of Chemistry*, 4(4):919–943.

Chao, M.-R., Hsu, Y.-W., Liu, H.-H., Lin, J.-H. & Hu, C.-W. 2015. Simultaneous Detection of 3-Nitrotyrosine and 3-Nitro-4-hydroxyphenylacetic Acid in Human Urine by Online SPE LC-MS/MS and Their Association with Oxidative and Methylated DNA Lesions. *Chemical Research in Toxicology*, 28(5):997–1006.

Charnot, A., Gouveia, D., Ayciriex, S., Lemoine, J., Armengaud, J., … Salvador, A. 2018. On-Line Solid Phase Extraction Liquid Chromatography-Mass Spectrometry Method for Multiplexed Proteins Quantitation in an Ecotoxicology Test Specie: Gammarus fossarum. *Journal of Applied Bioanalysis*, 4:81–101.

Chawla, G. & Chaudhary, K.K. 2019. A review of HPLC technique covering its pharmaceutical, environmental, forensic, clinical, and other applications. *International Journal of Pharmaceutical Chemistry and Analysis*, 6(2):27–39.

Chen, H.-J.C. & Chiu, W.-L. 2008. Simultaneous detection and quantification of 3-nitrotyrosine and 3-bromotyrosine in human urine by stable isotope dilution liquid chromatography tandem mass spectrometry. *Toxicology Letters*, 181(1):31–39.

Cipak Gasparovic, A., Zarkovic, N., Zarkovic, K., Semen, K., Kaminskyy, D., … Bottari, S.P. 2017. Biomarkers of oxidative and nitro-oxidative stress: conventional and novel approaches. *British Journal of Pharmacology*, 174(12):1771–1783.

Clark, J. 2013. Addition-Elimination Reactions. *Chemistry LibreTexts*. https://chem.libretexts.org/Bookshelves/Organic_Chemistry/Supplemental_Modules_(Organic_Chemistry)/Aldehydes_and_Ketones/Reactivity_of_Aldehydes_and_Ketones/Addition-Elimination_Reactions Date of access: 17 Jun. 2023.

Čolak, E. 2008. New Markers of Oxidative Damage to Macromolecules. *Journal of Medical Biochemistry*, 27(1):1–16.

Cui, X., Gong, J., Han, H., He, L., Teng, Y., … Zhang, J. (Jim). 2018. Relationship between free and total malondialdehyde, a well-established marker of oxidative stress, in various types of human biospecimens. *Journal of Thoracic Disease*, 10(5):3088–3097.

Dabrowska, N. & Wiczkowski, A. 2017. Analytics of oxidative stress markers in the early diagnosis of oxygen DNA damage. Advances in Clinical and Experimental Medicine. 26(1):155–166.

Dalle-Donne, I., Rossi, R., Giustarini, D., Milzani, A. & Colombo, R. 2003. Protein carbonyl groups as biomarkers of oxidative stress. *Clinica Chimica Acta*, 329(1):23–38.

De Groote, D., d'Hauterive, S.P., Pintiaux, A., Balteau, B., Gerday, C., … Foidart, J.-M. 2009. Effects of oral contraception with ethinylestradiol and drospirenone on oxidative stress in women 18–35 years old. Contraception. 80(2):187–193.

De Martinis, B. 2002. Methodology for urinary 8-hydroxy-2′-deoxyguanosine analysis by hplc with electrochemical detection. *Pharmacological Research*, 46(2):129–131.

Del Pup, L., Codacci-Pisanelli, G. & Peccatori, F. 2019. Breast cancer risk of hormonal contraception: Counselling considering new evidence. *Critical Reviews in Oncology/Hematology*, 137:123–130.

Delgado, B.J. & Lopez-Ojeda, W. 2021. Estrogen. In: *StatPearls*. Treasure Island (FL): StatPearls Publishing. http://www.ncbi.nlm.nih.gov/books/NBK538260/ Date of access: 17 Jul. 2021.

Deol, R. & Josephy, P.D. 2017. Acetylation of aromatic cysteine conjugates by recombinant human N-acetyltransferase 8. *Xenobiotica; the Fate of Foreign Compounds in Biological Systems*, 47(3):202–207.

Dietzen, D.J., Weindel, A.L., Carayannopoulos, M.O., Landt, M., Normansell, E.T., … Smith, C.H. 2008. Rapid comprehensive amino acid analysis by liquid chromatography/tandem mass spectrometry: comparison to cation exchange with post-column ninhydrin detection. *Rapid communications in mass spectrometry: RCM*, 22(22):3481–3488.

Di Guida, R., Engel, J., Allwood, J.W., Weber, R.J.M., Jones, M.R., … Dunn, W.B. 2016. Non-targeted UHPLC-MS metabolomic data processing methods: a comparative investigation of normalisation, missing value imputation, transformation and scaling. *Metabolomics*. 12(5):93

DiMarco, T. & Giulivi, C. 2007. Current analytical methods for the detection of dityrosine, a biomarker of oxidative stress, in biological samples. *Mass Spectrometry Reviews*, 26(1):108–120.

Dokumacioglu, E., Demiray, O., Dokumacioglu, A., Sahin, A., Sen, T.M. & Cankaya, S. 2018. Measuring urinary 8-hydroxy-2′-deoxyguanosine and malondialdehyde levels in women with overactive bladder. *Investigative and Clinical Urology*, 59(4):252–256.

Douny, C., Bayram, P., Brose, F., Degand, G. & Scippo, M.-L. 2016. Development of an LC-MS/MS analytical method for the simultaneous measurement of aldehydes from polyunsaturated fatty acids degradation in animal feed. *Drug Testing and Analysis*, 8(5–6):458–464.

El-Aneed, A., Cohen, A. & Banoub, J. 2009. Mass Spectrometry, Review of the Basics: Electrospray, MALDI, and Commonly Used Mass Analyzers. *Applied Spectroscopy Reviews*, 44(3):210–230.

Esmati, P., Najjar, N., Emamgholipour, S., Hosseinkhani, S., Arjmand, B., … Razi, F. 2021. Mass spectrometry with derivatisation method for concurrent measurement of amino acids and acylcarnitines in plasma of diabetic type 2 patients with diabetic nephropathy. *Journal of Diabetes and Metabolic Disorders*, 20(1):591–599.

Esterhuizen, K., Lindeque, J.Z., Mason, S., van der Westhuizen, F.H., Suomalainen, A., … Louw, R. 2019. A urinary biosignature for mitochondrial myopathy, encephalopathy, lactic acidosis, and stroke like episodes (MELAS). *Mitochondrion*, 45:38–45.

Fan, R., Wang, D., Ramage, R. & She, J. 2012. Fast and Simultaneous Determination of Urinary 8-Hydroxy deoxyguanosine and Ten Monohydroxylated Polycyclic Aromatic Hydrocarbons by Liquid Chromatography/Tandem Mass Spectrometry. *Chemical Research in Toxicology*, 25:491–499.

Ferrante, L. & Cameriere, R. 2009. Statistical methods to assess the reliability of measurements in procedures for forensic age estimation. *International journal of legal medicine*. 123:277–83.

Ferrante, M., Fiore, M., Conti, G.O., Fiore, V., Grasso, A., … Signorelli, S.S. 2017. Transition and heavy metals compared to oxidative parameter balance in patients with deep vein thrombosis: A case-control study. *Molecular Medicine Reports*, 15(5):3438–3444.

Field, A. 2009. *Discovering statistics using SPSS*. 3rd ed. London: SAGE publications.

Filipenko, I., Schwalm, S., Reali, L., Pfeilschifter, J., Fabbro, D., … Zangemeister-Wittke, U. 2016. Upregulation of the S1P3 receptor in metastatic breast cancer cells increases migration and invasion by induction of PGE_2 and EP2/EP4 activation. *Biochimica Et Biophysica Acta*, 1861(11):1840–1851.

Folin, O. 1905. LAWS GOVERNING THE CHEMICAL COMPOSITION OF URINE. *American Journal of Physiology-Legacy Content*, 13(1):66–115.

Fontana, J., Trnka, J., Mad'a, P., Ivák, P., Nováková, L., … Šajdíková, M. 2019. 4. Liver and Biotransformation of Xenobiotics • Functions of Cells and Human Body. In: *Functions of cells and human body*. WordPress. http://fblt.cz/en/skripta/ix-travici-soustava/5-jatra-a-biotransformace-xenobiotik/ Date of access: 08 Jun. 2020.

Forman, H.J., Zhang, H. & Rinna, A. 2009. Glutathione: Overview of its protective roles, measurement, and biosynthesis. *Molecular Aspects of Medicine*, 30(1):1–12.

Franz, S., Skopp, G., Boettcher, M. & Musshoff, F. 2019. Creatinine excretion in consecutive urine samples after controlled ingestion of water. Drug Testing and Analysis. 11(3):435–440.

Frigerio, G., Mercadante, R., Polledri, E., Missineo, P., Campo, L. & Fustinoni, S. 2019. An LC-MS/MS method to profile urinary mercapturic acids, metabolites of electrophilic intermediates of occupational and environmental toxicants. *Journal of Chromatography B*, 1117:66–76.

Fruzzetti, F., Trémollieres, F. & Bitzer, J. 2012. An overview of the development of combined oral contraceptives containing estradiol: focus on estradiol valerate/dienogest. *Gynecological Endocrinology*, 28(5):400–408.

Gào, X. & Schöttker, B. 2017. Reduction–oxidation pathways involved in cancer development: a systematic review of literature reviews. *Oncotarget*, 8(31):51888–51906.

Gârban, Z., Avacovici, A., Gârban, G., Ghibu, G.D., Velciov, B. & Pop, I. 2005. Biomarkers: theoretical aspects and applicative peculiarities note i. General characteristics of biomarkers. Agroalimentary processes and technologies, 11(1):139–146.

Gerssen, A., McElhinney, M.A., Mulder, P.P.J., Bire, R., Hess, P. & de Boer, J. 2009. Solid phase extraction for removal of matrix effects in lipophilic marine toxin analysis by liquid chromatography-tandem mass spectrometry. Analytical and Bioanalytical Chemistry. 394(4):1213–1226.

Gill, J.G., Piskounova, E. & Morrison, S.J. 2016. Cancer, Oxidative Stress, and Metastasis. *Cold Spring Harbor Symposia on Quantitative Biology*, 81:163–175.

Graafland, L., Abbott, M. & Accordino, M. 2020. Breast Cancer Risk Related to Combined Oral Contraceptive Use. *The Journal for Nurse Practitioners*, 16(2):116–120.

Griendling, K.K., Touyz, R.M., Zweier, J.L., Dikalov, S., Chilian, W., … Bhatnagar, A. 2016. Measurement of Reactive Oxygen Species, Reactive Nitrogen Species, and Redox-Dependent Signaling in the Cardiovascular System. *Circulation research*, 119(5):e39–e75.

Gropper, S.S. & Smith, J.L. 2013. *Advanced Nutrition and Human Metabolism*. 6th ed. Wadsworth: Cengage Learning.

Günther, U.L. 2015. Metabolomics Biomarkers for Breast Cancer. Pathobiology: Journal of Immunopathology, Molecular and Cellular Biology. 82(3–4):153–165.

Gupta, P.D. 2020. Natural and Synthetic Estrogens Regulate Human Health. *Journal of Chemistry and Applications*. December, 23:21–24.

Hanna, P.E. & Anders, M.W. 2019. The mercapturic acid pathway. *Critical Reviews in Toxicology*, 49(10):819–929.

Harder, U., Koletzko, B. & Peissner, W. 2011. Quantification of 22 plasma amino acids combining derivatisation and ion-pair LC–MS/MS. *Journal of Chromatography B*, 879(7):495–504.

Harvey, D. 2000. Obtaining and preparing samples for analysis. In: *Modern analytical chemistry*. Boston: McGraw-Hill. p. 285–354.

Huang, T., Cao, Y., Zeng, J., Dong, J., Sun, X., … Gao, P. 2016. Tandem mass spectrometry-based newborn screening strategy could be used to facilitate rapid and sensitive lung cancer diagnosis. *OncoTargets and Therapy*, 9:2479–2487.

Hecht, S.S. 2002. Human urinary carcinogen metabolites: biomarkers for investigating tobacco and cancer. *Carcinogenesis*, 23(6):907–922.

Hilakivi-Clarke, L., de Assis, S. & Warri, A. 2013. Exposures to Synthetic Estrogens at Different Times During the Life, and Their Effect on Breast Cancer Risk. *Journal of mammary gland biology and neoplasia*, 18(1):25–42.

Ho, E., Karimi Galougahi, K., Liu, C.-C., Bhindi, R. & Figtree, G.A. 2013. Biological markers of oxidative stress: Applications to cardiovascular research and practice. *Redox Biology*, 1(1):483–491.

Hopkins, T. 2019. The Role of Methanol and Acetonitrile as Organic Modifiers in Reversed-phase Liquid Chromatography. Chromatography Today. http://www.chromatographytoday.com/article/hplc-uhplc/31/advanced-chromatography-technologies/the-role-of-methanol-and-acetonitrile-as-organic-modifiers-in-reversed-phase-liquid-chromatography/2507 Date of access: 25 Nov. 2022.

HTA. 2016. Derivatisation in HPLC. *HTA's blog*. https://www.hta-it.com/blog/derivatisation-in-liquid-chromatography.html Date of access: 28 Jul. 2020.

Il'yasova, D., Scarbrough, P. & Spasojevic, I. 2012. Urinary Biomarkers of Oxidative Status. *Clinica chimica acta; international journal of clinical chemistry*, 413(19–20):1446–1453.

Isaguirre, A.C., Olsina, R.A., Martinez, L.D., Lapierre, A.V. & Cerutti, S. 2016. Development of solid phase extraction strategies to minimize the effect of human urine matrix effect on the response of carnitine by UPLC–MS/MS. Microchemical Journal. 129:362–367.

Islam, M.O., Bacchetti, T. & Ferretti, G. 2019. Alterations of Antioxidant Enzymes and Biomarkers of Nitro-oxidative Stress in Tissues of Bladder Cancer. *Oxidative Medicine and Cellular Longevity*, 2019: 2730896.

Ismail, R., Lee, H.Y., Mahyudin, N.A. & Abu Bakar, F. 2014. Linearity study on detection and quantification limits for the determination of avermectins using linear regression. *Journal of Food and Drug Analysis*, 22(4):407–412.

Jacobs, C.L. 2018. An analytical method to investigate the estrogen metabolism in women taking combined oral contraceptives. Potchefstroom: NWU. (Thesis- MSc).

Jardine, D., Antolovich, M., Prenzler, P.D. & Robards, K. 2002. Liquid Chromatography−Mass Spectrometry (LC-MS) Investigation of the Thiobarbituric Acid Reactive Substances (TBARS) Reaction. *Journal of Agricultural and Food Chemistry*, 50(6):1720–1724.

Ji, L.-W., Jing, C.-X., Zhuang, S.-L., Pan, W.-C. & Hu, X.-P. 2019. Effect of age at first use of oral contraceptives on breast cancer risk. *Medicine*, 98(36).

Johnson, D., Boyes, B. & Orlando, R. 2013. The Use of Ammonium Formate as a Mobile-Phase Modifier for LC-MS/MS Analysis of Tryptic Digests. *Journal of Biomolecular Techniques: JBT*, 24(4):187–197.

Jolliffe, I.T. & Cadima, J. 2016. Principal component analysis: a review and recent developments. Philosophical Transactions of the Royal Society A: Mathematical, Physical and Engineering Sciences. 374(2065):20150202.

Kishikawa, N., El-Maghrabey, M.H. & Kuroda, N. 2019. Chromatographic methods and sample pretreatment techniques for aldehydes determination in biological, food, and environmental samples. *Journal of Pharmaceutical and Biomedical Analysis*, 175:112782.

Klipping, C., Duijkers, I., Mawet, M., Maillard, C., Bastidas, A., … Foidart, J.-M. 2021. Endocrine and metabolic effects of an oral contraceptive containing estetrol and drospirenone. *Contraception*, 103(4):213–221.

Konieczka, P. 2014. Improved derivatisation of malondialdehyde with 2-thiobarbituric acid for evaluation of oxidative stress in selected tissues of chickens. *Journal of Animal and Feed Sciences*. (June,12):190–197.

Kuiper, H.C. & Stevens, J.F. 2011. LC-MS/MS Quantitation of Mercapturic Acid Conjugates of Lipid Peroxidation Products as Markers of Oxidative Stress. *Current protocols in toxicology / editorial board, Mahin D. Maines (editor-in-chief) ... [et al.]*. https://www.ncbi.nlm.nih.gov/pmc/articles/PMC3062851 Date of access: 13 Feb. 2020.

Kutomi, G., Mizuguchi, T., Satomi, F., Maeda, H., Shima, H., … Hirata, K. 2017. Current status of the prognostic molecular biomarkers in breast cancer: A systematic review. Oncology Letters. 13(3):1491–1498.

Langhorst, M.L., Hastings, M.J., Yokoyama, W.H., Hung, S., Cellar, N., … Young, S.A. 2010. Determination of F2-Isoprostanes in Urine by Online Solid Phase Extraction Coupled to Liquid Chromatography with Tandem Mass Spectrometry. *Journal of agricultural and food chemistry*, 58(11):6614–6620.

Lee, J.D., Cai, Q., Shu, X.O. & Nechuta, S.J. 2017. The Role of Biomarkers of Oxidative Stress in Breast Cancer Risk and Prognosis: A Systematic Review of the Epidemiologic Literature. *Journal of Women's Health*, 26(5):467–482.

Ligor, M., Ligor, T., Gadzała-Kopciuch, R. & Buszewski, B. 2015. The chromatographic assay of 4-hydroxynonenal as a biomarker of diseases by means of MEPS and HPLC technique. *Biomedical Chromatography*, 29(4):584–589.

Lira, L.G., Justa, R.M.D.E., Carioca, A.A.F., Verde, S.M.M.L., Sampaio, G.R., … Damasceno, N.R.T. 2019. Plasma and erythrocyte ω-3 and ω-6 fatty acids are associated with multiple inflammatory and oxidative stress biomarkers in breast cancer. *Nutrition*, 58:194–200.

Liska, D.J. 1998. The Detoxification Enzyme Systems. *Alternative Medicine Review*, 3(3):12.

Liska, D., Lyon, M. & Jones, D.M. 2006. Detoxification and Biotransformational Imbalances. *Explore*, 2(2):122–140.

Lobo, V., Patil, A., Phatak, A. & Chandra, N. 2010. Free radiantioxidants, idants and functional foods: Impact on human health. *Pharmacognosy Reviews*, 4(8):118–126.

Lone, A. & Taskén, K. 2013. Proinflammatory and Immunoregulatory Roles of Eicosanoids in T Cells. *Frontiers in immunology*, 4:130.

Lynch, K.L. 2016. CLSI C62-A: A New Standard for Clinical Mass Spectrometry. *Clinical Chemistry*, 62(1):24–29.

Maiti, S. & Nazmeen, A. 2019. Impaired redox regulation of estrogen metabolizing proteins is important determinant of human breast cancers. *Cancer Cell International*, 19(1):111.

Malencik, D.A. & Anderson, S.R. 2003. Dityrosine as a product of oxidative stress and fluorescent probe. *Amino Acids*, 25(3):233–247.

Martinez, M.P. & Kannan, K. 2018. Simultaneous Analysis of Seven Biomarkers of Oxidative Damage to Lipids, Proteins, and DNA in Urine. *Environmental Science & Technology*, 52(11):6647–6655.

Martinez-Moral, M.-P. & Kannan, K. 2019. How stable is oxidative stress level? An observational study of intra- and inter-individual variability in urinary oxidative stress biomarkers of DNA, proteins, and lipids in healthy individuals. *Environment international*, 123:382–389.

Martinez-Moral, M.-P. & Kannan, K. 2022. Analysis of 19 urinary biomarkers of oxidative stress, nitrative stress, metabolic disorders, and inflammation using liquid chromatography–tandem mass spectrometry. *Analytical and Bioanalytical Chemistry*, 414(6):2103–2116.

Marvin, L.F., Delatour, T., Tavazzi, I., Fay, L.B., Cupp, C. & Guy, P.A. 2003. Quantification of o,o‘-Dityrosine, o-Nitrotyrosine, and o-Tyrosine in Cat Urine Samples by LC/Electrospray Ionization-MS/MS Using Isotope Dilution. *Analytical Chemistry*, 75(2):261–267.

Mathias, P.I. & B’Hymer, C. 2016. Mercapturic acids: recent advances in their determination by liquid chromatography/mass spectrometry and their use in toxicant metabolism studies and in occupational and environmental exposure studies. *Biomarkers: biochemical indicators of exposure, response, and susceptibility to chemicals*, 21(4):293–315.

Mehta, S.K. & Gowder, S.J.T. 2015. Members of Antioxidant Machinery and Their Functions. In: S.J.T. Gowder, ed. *Basic Principles and Clinical Significance of Oxidative Stress*. http://www.intechopen.com/books/basic-principles-and-clinical-significance-of-oxidative-stress/members-of-antioxidant-machinery-and-their-functions Date of access: 06 Aug. 2020.

Meng, M. & Bennett, P.K. 2012. Method Development, Validation, and Sample Analysis for Regulated Quantitative Bioanalysis Using LC-MS/MS. In: Q.A. Xu & T.L. Madden, eds. *LC-MS in Drug Bioanalysis*. Boston, MA: Springer US. p. 33–66.

Milatovic, D., Montine, T.J. & Aschner, M. 2011. Prostanoid signaling: dual role for prostaglandin E2 in neurotoxicity. *Neurotoxicology*, 32(3):312–319.

Milne, G.L., Yin, H., Hardy, K.D., Davies, S.S. & Roberts, L.J. 2011. Isoprostane Generation and Function. *Chemical Reviews*, 111(10):5973–5996.

Mishra, P., Pandey, C.M., Singh, U., Gupta, A., Sahu, C. & Keshri, A. 2019. Descriptive Statistics and Normality Tests for Statistical Data. *Annals of Cardiac Anaesthesia*. 22(1):67–72.

Mongirdienė, A., Laukaitienė, J., Skipskis, V. & Kašauskas, A. 2019. The Effect of Oxidant Hypochlorous Acid on Platelet Aggregation and Dityrosine Concentration in Chronic Heart Failure Patients and Healthy Controls. *Medicina*, 55(5).

Montuschi, P., Barnes, P.J. & Roberts, L.J. 2004. Isoprostanes: markers and mediators of oxidative stress. *The FASEB Journal*, 18(15):1791–1800.

Murray, R.K., Bender, D.A., Botham, K.M., Kennelly, P.J., Rodwell, V.W. & Weil, P.A. 2009. *Harper's illustrated biochemistry*. 28th ed. McGraw Hill.

NCI. 2015. Risk Factors: Hormones - National Cancer Institute. National Cancer Institute. https://www.cancer.gov/about-cancer/causes-prevention/risk/hormones Date of access: 05 May 2021.

Nour Eldin, E.E.M., El-Readi, M.Z., Nour Eldein, M.M., Alfalki, A.A., Althubiti, M.A., … Mirza, A.A. 2019. 8-Hydroxy-2'-deoxyguanosine as a Discriminatory Biomarker for Early Detection of Breast Cancer. *Clinical Breast Cancer*, 19(2):e385–e393.

NTP. 2011. https://www.ashlandmass.com/DocumentCenter/View/442/National-Toxicology-Program-Report-on-Carcinogens-PDF Date of access: 05 May 2021.

Ohashi, N. & Yoshikawa, M. 2000. Rapid and sensitive quantification of 8-isoprostaglandin F2a in human plasma and urine by liquid chromatography–electrospray ionisation mass spectrometry. *J. Chromatogr. B*. 8. https://europepmc.org/article/med/11048736 Date of access: 21 Apr. 2020.

Oliveira, E.C. de, Muller, E.I., Abad, F., Dallarosa, J. & Adriano, C. 2010. Internal standard versus external standard calibration: an uncertainty case study of a liquid chromatography analysis. *Química Nova*, 33:984–987.

Onyango, J.P. & Plews, A.M. 1987. *A Textbook of Basic Statistics*. Nairobi: East African Publishers. https://www.google.co.za/books/edition/A_Textbook_of_Basic_Statistics/2G35r-0lNlQC?hl=en&gbpv=1&dq=percentage+error+textbook&pg=PA22&printsec=frontcover Date of access: 11 June 2023.

Orhan, H., Vermeulen, N.P.E., Tump, C., Zappey, H. & Meerman, J.H.N. 2004. Simultaneous determination of tyrosine, phenylalanine and deoxyguanosine oxidation products by liquid chromatography–tandem mass spectrometry as non-invasive biomarkers for oxidative damage. *Journal of Chromatography B*, 799(2):245–254.

Orhan, H., Coolen, S. & Meerman, J.H.N. 2005. Quantification of urinary o,o′-dityrosine, a biomarker for oxidative damage to proteins, by high performance liquid chromatography with triple quadrupole tandem mass spectrometryA comparison with ion-trap tandem mass spectrometry. *Journal of Chromatography B*, 827(1):104–108.

Ozcan, A. & Ogun, M. 2015. Biochemistry of Reactive Oxygen and Nitrogen Species. *Basic Principles and clinical significance of oxidative stress.* https://www.intechopen.com/books/basic-principles-and-clinical-significance-of-oxidative-stress/biochemistry-of-reactive-oxygen-and-nitrogen-species Date of access: 11 Nov. 2020.

Panuwet, P., Hunter, R.E., D'Souza, P.E., Chen, X., Radford, S.A., … Barr, D.B. 2016. Biological Matrix Effects in Quantitative Tandem Mass Spectrometry-Based Analytical Methods: Advancing Biomonitoring. *Critical reviews in analytical chemistry / CRC*, 46(2):93–105.

Patel, D.K. & Sen, D.D.J. 2013. Xenobiotics: An Essential Precursor for Living System. *American Journal of Advanced Drug Delivery*, 1(3):262–270.

Phaniendra, A., Jestadi, D.B. & Periyasamy, L. 2015. Free Radicals: Properties, Sources, Targets, and Their Implication in Various Diseases. *Indian Journal of Clinical Biochemistry*, 30(1):11–26.

Phenomenex. 2017. *The Complete Guide to Solid Phase Extraction (SPE) | Phenomenex UHPLC, HPLC, SPE and GC*. *Phenomenex_Documents*. https://www.phenomenex.com/ViewDocument?id=the+complete+guide+to+solid+phase+extraction+(spe)&fsr=1 Date of access: 10 Jan. 2023.

Pisoschi, A.M. & Pop, A. 2015. The role of antioxidants in the chemistry of oxidative stress: A review. *European Journal of Medicinal Chemistry*, 97:55–74.

Poole, C.F. 2013. chapter 2 - Derivatisation in Liquid Chromatography. In: S. Fanali, P.R. Haddad, C.F. Poole, P. Schoenmakers, & D. Lloyd, eds. *Liquid Chromatography*. Amsterdam: Elsevier. pp. 25–56.

Poprac, P., Jomova, K., Simunkova, M., Kollar, V., Rhodes, C.J. & Valko, M. 2017. Targeting Free Radicals in Oxidative Stress-Related Human Diseases. *Trends in Pharmacological Sciences*. 38(7):592–607.

Preedy, V.R. & Patel, V.B. 2015. *General Methods in Biomarker Research and their Applications*. London: Springer Reference. https://booksca.ca/wp-content/uploads/XPreview/Toxicology/3/general-methods-in-biomarker-research-and-their-applications-by-preedy.pdf Date of access: 04 Jul. 2020.

Price, J.W. 2013. Creatinine Normalization of Workplace Urine Drug Tests: Does It Make a Difference? *Journal of Addiction Medicine*, 7(2):129.

Prichard, L. & Barwick, V. 2003. *Preparation of Calibration Curves A Guide to Best Practice*. https://www.researchgate.net/publication/334063221_Preparation_of_Calibration_Curves_A_Guide_to_Best_Practice Date of access: 11 Nov 2022

Qi, B.-L., Liu, P., Wang, Q.-Y., Cai, W.-J., Yuan, B.-F. & Feng, Y.-Q. 2014. Derivatisation for liquid chromatography-mass spectrometry. *TrAC Trends in Analytical Chemistry*, 59:121–132.

Rahman, I. & Biswas, S.K. 2004. Non-invasive biomarkers of oxidative stress: reproducibility and methodological issues. *Redox Report*, 9(3):125–143.

Rao, T.N. 2018. *Validation of Analytical Methods*. *Calibration and Validation of Analytical Methods - A Sampling of Current Approaches* https://www.intechopen.com/chapters/57909 Date of access: 23 Feb. 2023

Rawski, R.I., Sanecki, P.T., Kijowska, K.M., Skital, P.M. & Saletnik, D.E. 2016. Regression analysis in analytical chemistry. Determination and validation of linear and quadratic regression dependencies: research article. *South African Journal of Chemistry*, 69(1):166–173.

Robinson, S., Pool, R. & Giffin, R. 2008. *Qualifying Biomarkers*. *Emerging Safety Science: Workshop Summary*. Washington: National Academies Press (US). https://www.ncbi.nlm.nih.gov/books/NBK4041/ Date of access: 06 May 2021.

Roy, D., Cai, Q., Felty, Q. & Narayan, S. 2007. Estrogen-Induced Generation of Reactive Oxygen and Nitrogen Species, Gene Damage, and Estrogen-Dependent Cancers. *Journal of Toxicology and Environmental Health, Part B*, 10(4):235–257.

Rozio, M.G., Rosato, A., Iadarola, L. & Carrara, S. 2019. Compounds relative response factor, a reliable quantification within extractale testing. *Eurofins; BioPharma Product Testing*. https://cdnmedia.eurofins.com/corporate-eurofins/media/12151515/compounds-relative-response-factor.pdf. Date of access: 17 Dec. 2021

Ruiz-Perez, D., Guan, H., Madhivanan, P., Mathee, K. & Narasimhan, G. 2020. So you think you can PLS-DA? *BMC Bioinformatics*. 21(1):2.

Saha, S.K., Lee, S.B., Won, J., Choi, H.Y., Kim, K., … Cho, S. 2017. Correlation between Oxidative Stress, Nutrition, and Cancer Initiation. *International Journal of Molecular Sciences*, 18(7):1544.

Sanchez, J.M. 2018. Estimating Detection Limits in Chromatography from Calibration Data: Ordinary Least Squares Regression vs. Weighted Least Squares. *Separations*, 5(4):49.

Sandlers, Y. 2019. Amino Acids Profiling for the Diagnosis of Metabolic Disorders. *Biochemical Testing - Clinical Correlation and Diagnosis*, https://www.intechopen.com/chapters/66048 Date of access: 08 Mar. 2020.

Sawicka, E., Piwowar, A. & Musia, T. 2017. The estrogens / chromium interaction in the nitric oxide generation. *Acta Polomiae Pharmaceutica - Drug Research*. 74(3):785–791. https://www.ptfarm.pl/pub/File/Acta_Poloniae/2017/3/785.pdf Date of access: 05 May 2021.

Scheel, B.I. & Holtedahl, K. 2015. Symptoms, signs, and tests: The general practitioner's comprehensive approach towards a cancer diagnosis. *Scandinavian Journal of Primary Health Care*, 33(3):170–177.

Schober, P., Boer, C. & Schwarte, L.A. 2018. Correlation Coefficients: Appropriate Use and Interpretation. *Anesthesia & Analgesia*. 126(5):1763

Schwedhelm, E., Benndorf, R.A. & Tsikas, R.H.B. and D. 2007. Mass Spectrometric Analysis of F2-Isoprostanes: Markers and Mediators in Human Disease. *Current Pharmaceutical Analysis*, 3(1):39–51.

Shah, D., Mahajan, N., Sah, S., Nath, S.K. & Paudyal, B. 2014. Oxidative stress and its biomarkers in systemic lupus erythematosus. *Journal of Biomedical Science*, 21(1):23.

Sharma, A.K. 2018. Emerging trends in biomarker discovery: Ease of prognosis and prediction in cancer. Seminars in Cancer Biology. 52:iii–iv.

Shrivastava, A., Aggarwal, L.M., Mishra, S.P., Khanna, H.D., Shahi, U.P. & Pradhan, S. 2019. Free radicals and antioxidants in normal versus cancerous cells — An overview. *Indian Journal of Biochemistry and Biophysics (IJBB)*, 56(1):7-19–19.

Siener, R. & Hesse, A. 2002. The Effect of Different Diets on Urine Composition and the Risk of Calcium Oxalate Crystallisation in Healthy Subjects. *European Urology*, 42(3):289–296.

Sigma Aldrich. 1998. Guide to solid phase extraction. *Supelco*. (910):12. https://www.sigmaaldrich.com/Graphics/Supelco/objects/4600/4538.pdf Date of access: 27 Jul. 2020.

Sitruk-Ware, R. & Nath, A. 2013. Characteristics and metabolic effects of estrogen and progestins contained in oral contraceptive pills. *Best Practice & Research. Clinical Endocrinology & Metabolism*, 27(1):13–24.

Siuzdak, G. 2004. An Introduction to Mass Spectrometry Ionization: An Excerpt from The Expanding Role of Mass Spectrometry in Biotechnology, 2nd ed.; MCC Press: San Diego, 2005. *JALA: Journal of the Association for Laboratory Automation*, 9(2):50–63.

Sonntag, O. 2015. Calibration. A presentation at the EuroMedLab by Bio-Rad chrome-extension://efaidnbmnnnibpcajpcglclefindmkaj/https://www.eflm.eu/files/efcc/Paris%20-%20Sonntag.pdf Date of access: 11 Mar. 2023 [powerpoint presentation].

Sonowal, H. & Ramana, K.V. 2019. 4-hydroxy-trans-2-nonenal in the regulation of anti-oxidative and pro-inflammatory signaling pathways. *Oxidative Medicine and Cellular Longevity,* 2019: 5937326.

Spickett, C.M. 2013. The lipid peroxidation product 4-hydroxy-2-nonenal: Advances in chemistry and analysis. *Redox Biology*, 1(1):145–152.

Swiegers, M. 2015. Effect of oral contraception on biotransformation, oxidative stress and oxidative damage. North-West University (South Africa), Potchefstroom Campus. (Thesis). https://repository.nwu.ac.za/handle/10394/21380 Date of access: 25 Oct. 2023.

Tafani, M., Sansone, L., Limana, F., Arcangeli, T., De Santis, E., … Russo, M.A. 2016. The Interplay of Reactive Oxygen Species, Hypoxia, Inflammation, and Sirtuins in Cancer Initiation and Progression. Oxidative Medicine and Cellular Longevity. 2016:3907147.

Tanvir, E.M., Hossen, Md.S., Hossain, Md.F., Afroz, R., Gan, S.H., … Karim, N. 2017. Antioxidant Properties of Popular Turmeric *(Curcuma longa)* Varieties from Bangladesh. *Journal of Food Quality*, 2017:1–8.

Telfer, N. 2019. *Synthetic estrogens 101*. *Clue_Hormones & your cycle*. https://helloclue.com/articles/sex/synthetic-estrogens-101 Date of access: 17 Jul. 2021.

Thammana, M. 2016. A Review on High Performance Liquid Chromatography (HPLC). *Journal of Pharmaceutical Analysis*, 5(2):7.

Trebel, N., Höltzel, A., Steinhoff, A. & Tallarek, U. 2021. Insights from molecular simulations about dead time markers in reversed-phase liquid chromatography. *Journal of Chromatography A*. 1640:461958.

Tsikas, D. 2012. Analytical methods for 3-nitrotyrosine quantification in biological samples: the unique role of tandem mass spectrometry. *Amino Acids*, 42(1):45–63.

Tsikas, D. 2017a. Assessment of lipid peroxidation by measuring malondialdehyde (MDA) and relatives in biological samples: Analytical and biological challenges. *Analytical Biochemistry*, 524:13–30.

Tsikas, D. 2017b. Pentafluorobenzyl bromide-A versatile derivatisation agent in chromatography and mass spectrometry: I. Analysis of inorganic anions and organophosphates. *Journal of Chromatography. B, Analytical Technologies in the Biomedical and Life Sciences*, 1043:187–201.

Tsikas, D., Rothmann, S., Schneider, J.Y., Suchy, M.-T., Trettin, A., … Frölich, J.C. 2016. Development, validation and biomedical applications of stable-isotope dilution GC–MS and GC–MS/MS techniques for circulating malondialdehyde (MDA) after pentafluorobenzyl bromide derivatisation: MDA as a biomarker of oxidative stress and its relati15(S 15(S)-8- iso - prostaglandin F 2α and nitric oxide (NO). *Journal of Chromatography B*, 1019:95–111.

Uchiyama, S., Inaba, Y. & Kunugita, N. 2011. Derivatisation of carbonyl compounds with 2,4-dinitrophenylhydrazine and their subsequent determination by high-performance liquid chromatography. *Journal of Chromatography B*, 879(17–18):1282–1289.

United Nations Office on Drugs and Crime. 2009. *Guidance for the Validation of Analytical Methodology and Calibration of Equipment used for Testing of Illicit Drugs in Seized Materials and Biological Specimens*. Vienna: Laboratory and Scientific Section United Nations Office on Drugs and Crime. https://www.unodc.org/documents/scientific/validation_E.pdf. Date of access: 18 Feb 2023.

Udhesister, S. 2021. The effect of impaired Cyclooxygenase 2 activity on gene regulation in the developing mouse brain and the role of PGE_2 in oxidative stress production in differentiated neuronal cells. Toronto, ontario: York university. https://yorkspace.library.yorku.ca/xmlui/bitstream/handle/10315/38246/Udhesister_Sasha_T_P_2021_Masters.pdf?sequence=2&isAllowed=y Date of access: 06 Nov. 2021.

Van de Merbel, N., Savoie, N., Yadav, M., Ohtsu, Y., White, J., … Diancin, J. 2014. Stability: Recommendation for Best Practices and Harmonization from the Global Bioanalysis Consortium Harmonization Team. *The AAPS Journal*, 16(3):392–399.

van den Berg, R.A., Hoefsloot, H.C., Westerhuis, J.A., Smilde, A.K. & van der Werf, M.J. 2006. Centering, scaling, and transformations: improving the biological information content of metabolomics data. *BMC Genomics*. 7(1):142

Vanova, N., Muckova, L., Schmidt, M., Herman, D., Dlabkova, A., … Jun, D. 2018. Simultaneous determination of malondialdehyde and 3-nitrotyrosine in cultured human hepatoma cells by liquid chromatography–mass spectrometry. *Biomedical Chromatography*, 32(12):e4349.

Venter, G., van der Berg, C.L., van der Westhuizen, F.H. & Erasmus, E. 2021. Health Status Is Affected, and Phase I/II Biotransformation Activity Altered in Young Women Using Oral Contraceptives Containing Drospirenone/Ethinyl Estradiol. *International Journal of EnvironmentalResearchandPublicHealth*.18(20):10607

Völkel, W., Alvarez-Sánchez, R., Weick, I., Mally, A., Dekant, W. & Pähler, A. 2005. Glutathione conjugates of 4-hydroxy-2(E)-nonenal as biomarkers of hepatic oxidative stress-induced lipid peroxidation in rats. *Free Radical Biology and Medicine*, 38(11):1526–1536.

Vorobiof, D.A., Sitas, F. & Vorobiof, G. 2001. Breast cancer incidence in South Africa. *Journal of Clinical Oncology: Official Journal of the American Society of Clinical Oncology*, 19(18 Suppl):125S-127S.

Wal, P., Bhandari, A., Rai, A.K. & Wal, A. 2010. Bioanalytical Method Development – Determination of Drugs in Biological Fluids. *Journal of Pharmaceutical Science and Technology*, 2(10):333–347.

Wang, Y., Liu, C., Shen, Y., Wang, Q., Pan, A., … Zeng, Q. 2019. Urinary levels of bisphenol A, F and S and markers of oxidative stress among healthy adult men: Variability and association analysis - Environ. Int. - X-MOL. *Environmental International*, 123:301–309.

Waters. 2018. *SPE Method Development: Waters*. https://www.waters.com/waters/en_ZA/SPE-Method-Development/nav.htm?cid=10083845&locale=en_ZA Date of access: 27 Jul. 2020.

Watkinson, A. 2008. Antibiotics and Antibiotic Resistant Bacteria in the Aquatic Environment: A Global Issue, an Australian Perspective. Australia: University of Queensland. (Thesis -PhD).

Wilson, K. & Walker, J. 2010. *Principals and techniques of Biochemistry and molecular biology*. 7th ed. Cambridge university press.

World Health Organization. 2018. Cancer. *World Health Organization_Health topics*. https://www.who.int/news-room/fact-sheets/detail/cancer Date of access: 10 Jun. 2020.

Wright, S.W., Hageman, D.L., Wright, A.S. & McClure, L.D. 1997. Convenient preparations of t-butyl esters and ethers from t-butanol. *Tetrahedron Letters*. 38(42):7345–7348.

Wu, C., Chen, S.-T., Peng, K.-H., Cheng, T.-J. & Wu, K.-Y. 2016. Concurrent quantification of multiple biomarkers indicative of oxidative stress status using liquid chromatography-tandem mass spectrometry. *Analytical Biochemistry*, 512:26–35.

Wulff, J.E. & Mitchell, M.W. 2018. A Comparison of Various Normalization Methods for LC/MS Metabolomics Data. Advances in Bioscience and Biotechnology. 9(8):339–351.

Xiao, S. & Zhou, L. 2017. Gastric cancer: Metabolic and metabolomics perspectives (Review). *International Journal of Oncology*, 51(1):5–17.

Yang, L., Wang, Y., Cai, H., Wang, S., Shen, Y. & Ke, C. 2020. Application of metabolomics in the diagnosis of breast cancer: a systematic review. *Journal of Cancer*, 11(9):2540–2551.

Zeb, A. & Ullah, F. 2016. A Simple Spectrophotometric Method for the Determination of Thiobarbituric Acid Reactive Substances in Fried Fast Foods. Journal of Analytical Methods in Chemistry. 2016:5.

Zhang, D., Haputhanthri, P., Ansar, S., Vangala, K., De Silva, I., … Pittman, C. 2010. Ultrasensitive detection of malondialdehyde with surface-enhanced Raman spectroscopy. *Analytical and bioanalytical chemistry*. 398:3193–201.

Zhang, X., Shi, S., Zhang, B., Ni, Q., Yu, X. & Xu, J. 2018. Circulating biomarkers for early diagnosis of pancreatic cancer: facts and hopes. *American Journal of Cancer Research*. 8(3):332–353. https://www.ncbi.nlm.nih.gov/pmc/articles/PMC5883088 Date of access: 10 Mar. 2021.

Zhao, S. & Li, L. 2020. Chemical derivatisation in LC-MS-based metabolomics study. *TrAC Trends in Analytical Chemistry*, 131:115988.

Zeng, W., Musson, D.G., Fisher, A.L. & Wang, A.Q. 2006. A new approach for evaluating carryover and its influence on quantitation in high-performance liquid chromatography and tandem mass spectrometry assay. *Rapid communications in mass spectrometry: RCM*, 20(4):635–640.

ANNEXURE A:

A.1. eBOSS study Inclusion and Exclusion criteria

A.1.1. Inclusion criteria

Participants were included if any of the following self-reported conditions were applicable:

(i) Participants had to be seemingly healthy, with no chronic disease or related use of chronic medication, because chronic disease is associated with oxidative stress.

(ii) Participants had to be of pre-menopausal age (18-35 years).

(iii) Participants had to be at a relatively healthy weight with a BMI between 18.5 and 29.9. Obesity (BMI ≥ 30.0) is also associated with oxidative stress and breast cancer.

(iv) COC users should have been using Yasmin®/ Yaz® plus/ Yaz® for at least three consecutive months prior to participating in the study.

(v) Non-COC users should not have been using COCs for at least four years prior to taking part in the study. An increased cancer risk may remain apparent for 10 to 15 years after cessation of COC use.

A.1.2. Exclusion criteria

Participants were excluded if any of the following self-reported conditions were applicable:

(i) Pregnancy or breastfeeding in the past 6 months.

(ii) HIV and AIDS. There is no consensus on the effects of sex hormones (and therefore hormone contraceptives) on HIV acquisition or disease progression Although the effect of HIV-1 infection on estrogen levels is not exactly known, several studies have found that woman with HIV and AIDS experience irregularities in their menstrual cycle.

(iii) Irregular menstrual cycle, for example due to polycystic ovary syndrome. Irregular menstrual cycles would cause shifts in the regular hormone fluctuation, making it difficult to time sampling.

(iv) The use of any food supplements, vitamin supplements or antioxidants for at least a month prior to sample collection. This could result in altered profiles not reflecting the effect accurately.

(v) Smoking 5 or more cigarettes per day or consuming more than 7 alcoholic drinks per week. This may alter the oxidative status of the participant as well as estrogen metabolism.

A.1.3. eBOSS participant recruitment

The participants were recruited for this study by placing advertisements at several pharmacies, doctor's rooms, supermarkets and shopping centers in Potchefstroom and Klerksdorp urban areas. The advertisements were also placed on social media (NWU facebook page). Recruitment started in April 2017 and was done continually until the minimal sample size (i.e., 25 eligible volunteers for each experimental and ethnic group) was reached (October 2019).

A.1.4. Participant permission and informed consent

The Eligible volunteers were invited to an information session, after which they were given 7 days to consider if they wanted to take part in the study. Thereafter, they were asked to contact the research assistant to arrange an appointment to sign the informed consent form. Informed consent was obtained from all participants in this study. The informed consent indicated that the samples will be stored for further relevant testing. Permission from the study principal investigator has been obtained to use stored samples in this study.

ANNEXURE B:

B.1. Method development & optimisation

B.1.1. Underivatised analysis

Table B-1. Gradient adjustment from Martinez & Kannan (2018).

Segments	Time (min)	Diverter Valve	Mobile phase B (%)	Flow rate (ml/min)
1.	0	MS	25	0.2
2.	4.5		50	
3.	6		55	
4.	10		60	
5.	12		75	
6.	20		Stop	

Table B-2. Adjusted gradient used for underivatised analysis.

Segments	Time (min)	Diverter valve	Mobile phase B (%)	Flow rate (ml/min)
1.	0	MS	5	0.2
2.	5		20	
3.	15		55	
4.	20		75	
5.	23		90	

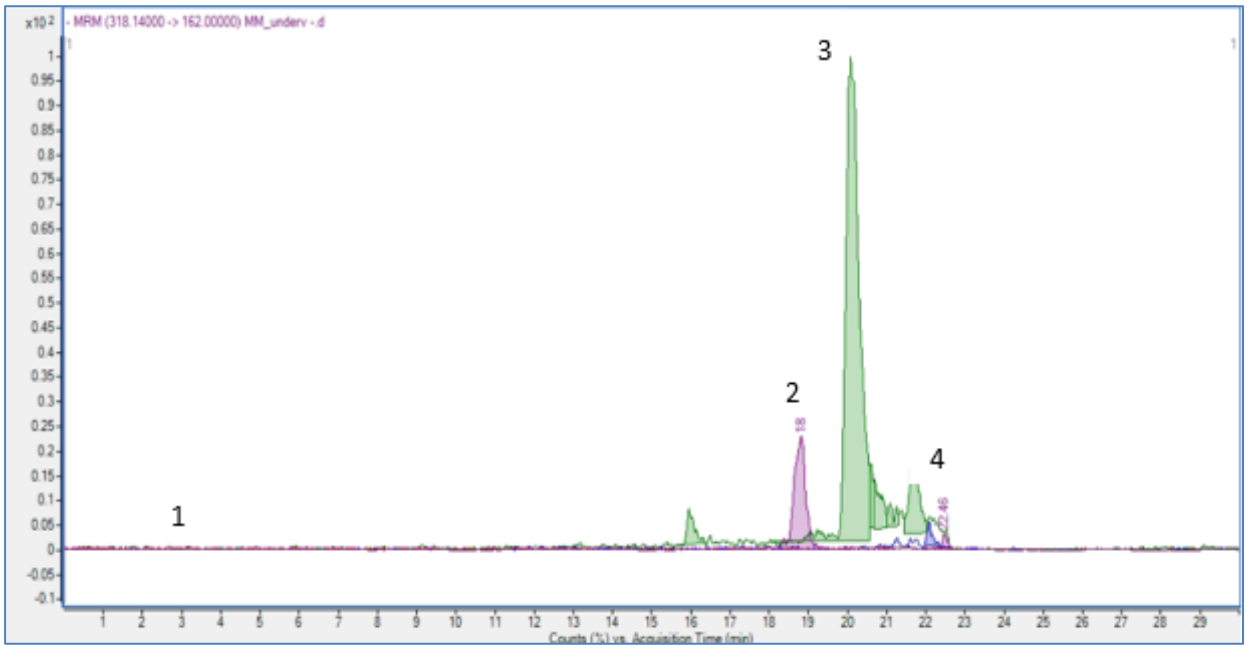

Figure B-1. Chromatogram of negative ionised analytes with adjusted gradient as seen in table B-2. *1. Malondialdehyde, 2.4-hydroxynonenal mercapturic acid, 3. Prostaglandin E_2 & Prostaglandin $F_{2\alpha}$.*

B.1.2. Derivatised analysis

Table B-3. Optimised conditions of all derivatives and isotopes analysed during this study. These parameters include the precursor and product ions used for detection, the polarity of the ions detected, the energy used to break the compounds (collision energy), energy used to carry the ions (CAV) and the energy needed in the capillary (fragmentor).

Compound	Precursor	Product	Polarity	CAV (V)	CE (V)	Fragmentor
C^{13}, N^{15}_2-8-OHdG	287.1	171	+	7	4	71
MDA-d_2	223	209	+	7	8	66
PGE_2-d_4	355	275.2	-	7	12	74
MDA-TBA	325	181	+	7	12	102
4HNE-TBA	285	143	+	7	4	76
Tyr-BE	238	136	+	7	12	97
3-NT-BE	283	195	+	7	52	170
Dityr-BE	473	269	+	7	32	134
D_5-Phe-BE	227	125	+	7	12	86
PGE_2-BE	409	335	+	7	8	76
$PGF_{2\alpha}$-BE	411	169	+	7	20	51
4HNEMA-BE	376	207	+	7	56	92
MDA-DNPH	235	189	+	7	12	135
MDA-d_2-DNPH	237	191	+	7	12	135
d_4-PGE_2-BE	359	279	+	7	12	74

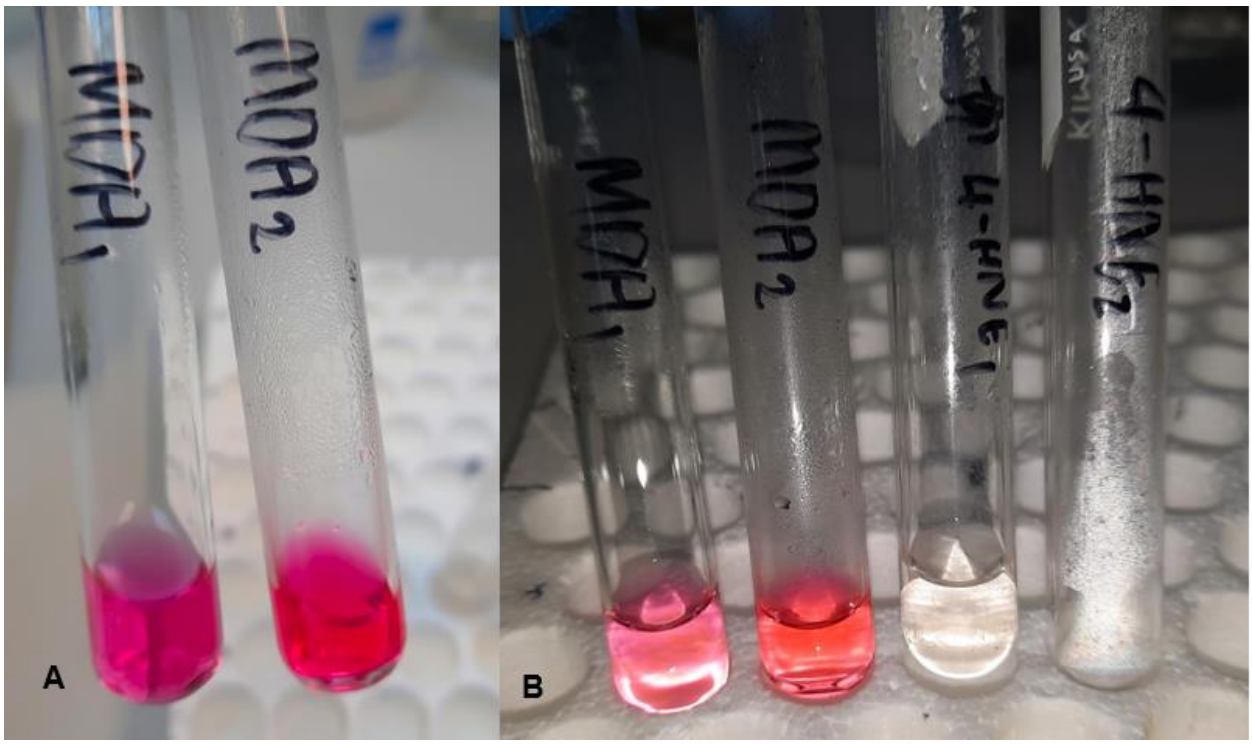

Figure B-2. Colour differences during TBARS assay. A: Colour intensity differences between two different TBARS protocols tested, B: Comparison of colours between MDA and 4-HNE samples.

Table B-4. Gradient adjustment after derivatisation.

Segments	Time (min)	Div valve	Mobile phase B (%)	Flow rate (ml/min)
1.	0	MS	25	0.2
2.	10		55	
3.	15		75	
4.	20		90	
5.	27		Stop	

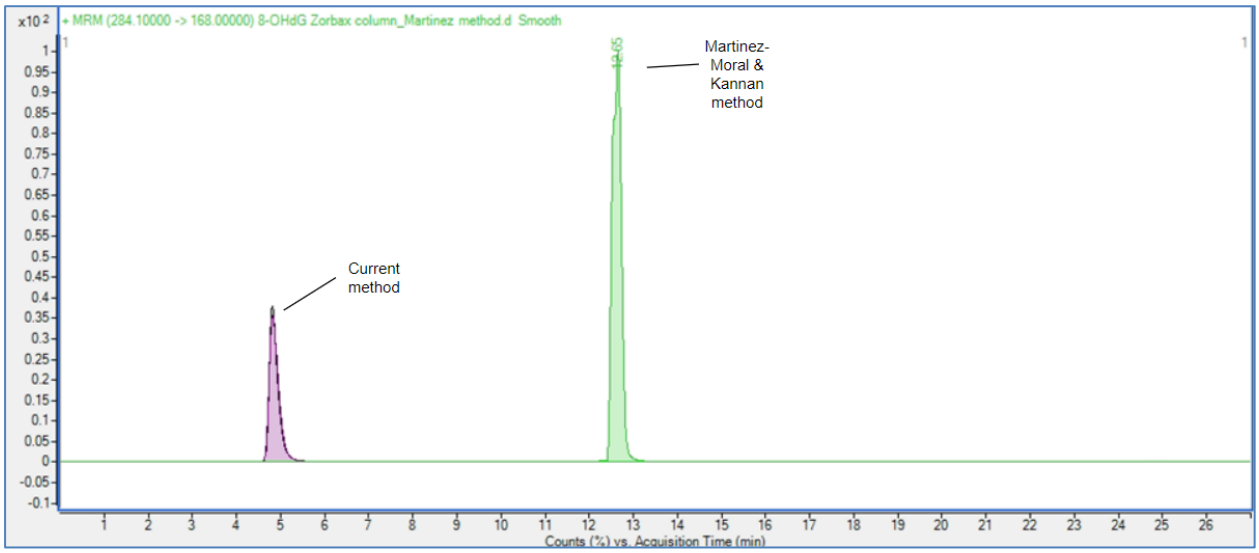

Figure B-3. Comparison of current method with method described by Martinez-Moral & Kannan on the Zorbax column. *Response indicator: 8-OHdG.*

Table B-5. Gradient adjustment as described by Martinez-Moral & Kannan (2022).

Segments	Time (min)	Div valve	Mobile phase B (%)	Flow rate (ml/min)
1.	0	MS	0	0.2
2.	5		0	
3.	11		50	
4.	20		64	
5.	21		70	
6	27		100	
7.	28		Stop	

Table B-6. Comparison of compound retention times (min) Zorbax and Eclipse columns for both methods. *ND: not detected; response was < 1000.*

Analyte	Zorbax	Eclipse
Tyr	ND	ND
3NT	8.59	9.30
Dityr	ND	ND
d_5-Phe	14.54	12.05
8OHdG	12.65	9.78
$^{13}C^{15}N_2$-8OHdG	12.65	9.78
4-HNE	ND	ND
4-HNEMA	19.50	15.94
PGE	ND	ND
PGF	21.85	20.81
MDA-DNPH	17.44	14.83

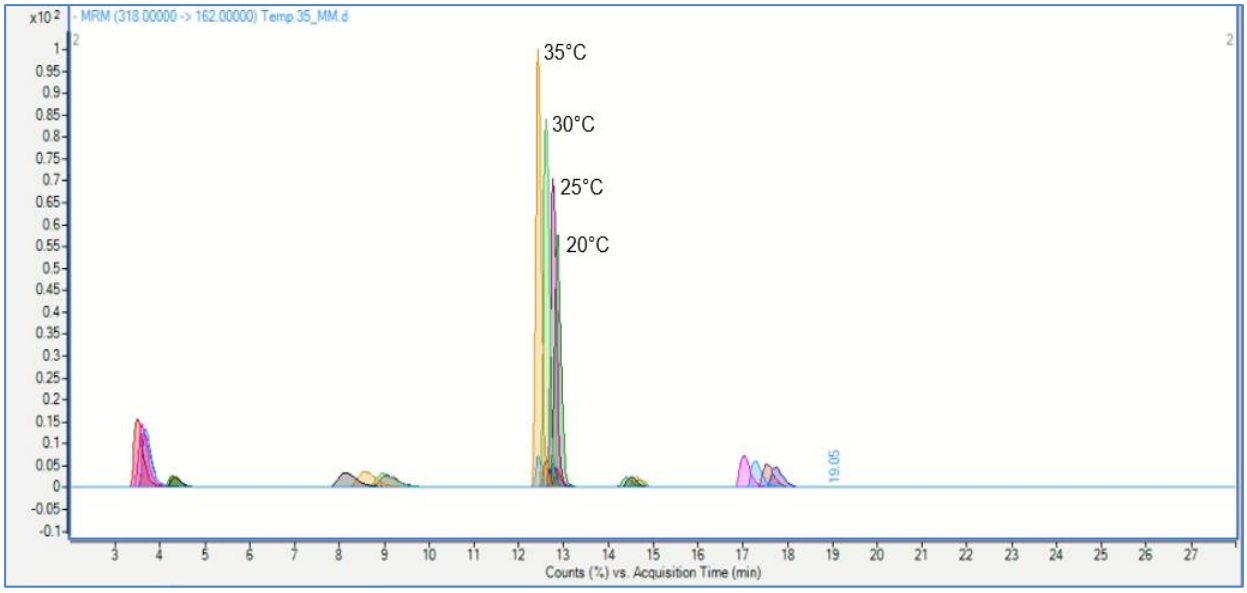

Figure B-4. Chromatogram during column optimisation after DNPH derivatisation.

Response indicator: $^{13}C^{15}N_2$-8-OHdG.

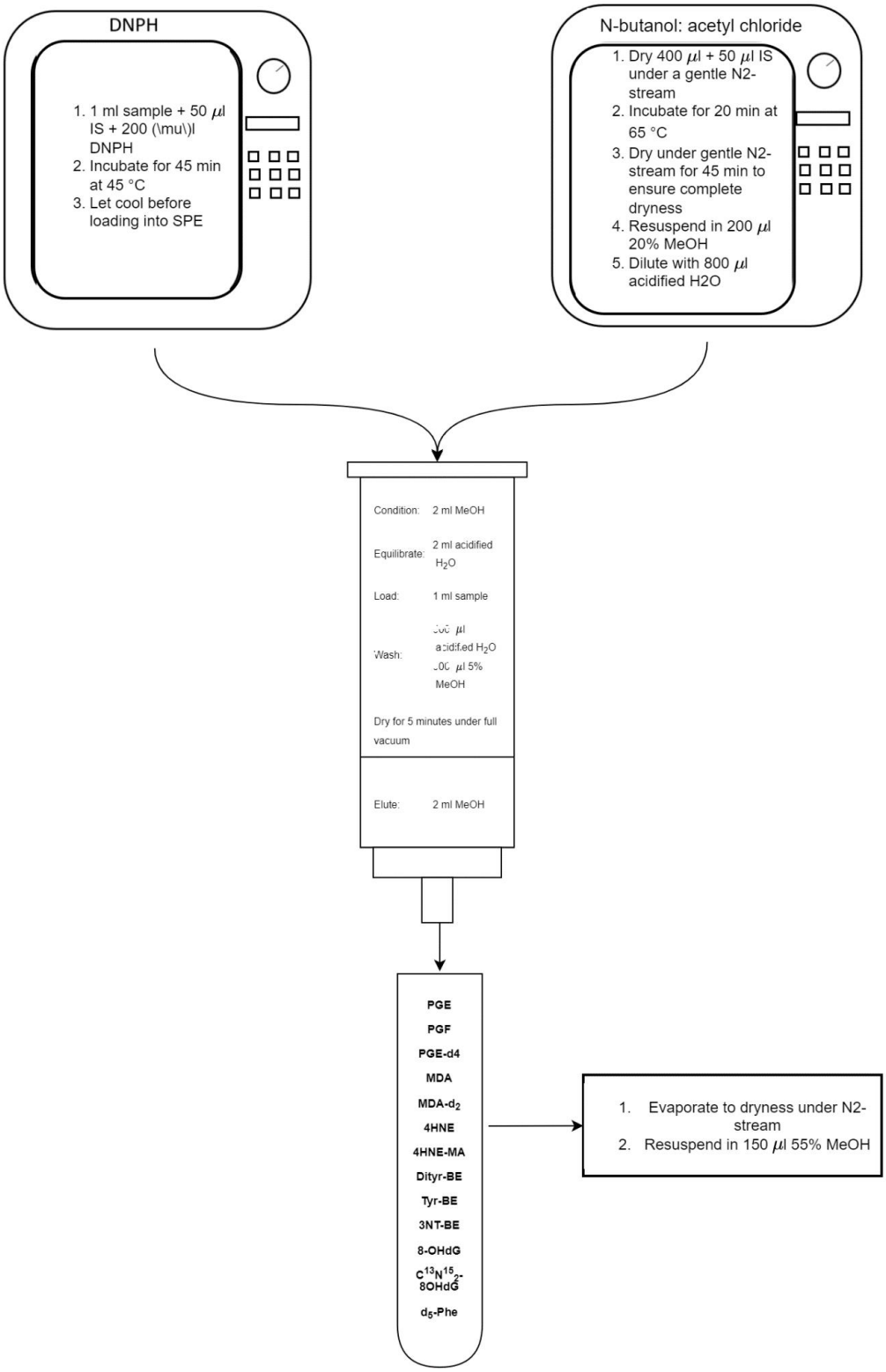

Figure B-5. Extraction with a double loading step. *DNPH: 2,4-dinitrophenylhydrazine, SPE: solid phase extraction, IS: internal standard, MeOH: methanol, BE: butyl ester,* PGE_2*: prostaglandin-*E_2*, PGF: prostaglandin-*$F\alpha_2$*, PGE-*d_4*:* d_4*- prostaglandin-*E_2*, MDA: malondialdehyde, MDA-*d_2*: malondialdehyde-*d_2*, 4-HNE: 4-hydroxynonenal, 4-HNE-MA: 4-hydroxynonenal-mercapturic acid, Dityr-BE: dityrosine butyl ester, Tyr-BE: tyrosine butyl ester, 3NT-BE: 3-nitrotyrosine butyl ester, 8-OHdG: 8-hydroxy-2-deoxyguanosine,* $^{13}C^{15}N_2$*-8OHdG: 8-oxo-2-deoxyguanosine-*^{13}C*,* $^{15}N_2$*.*

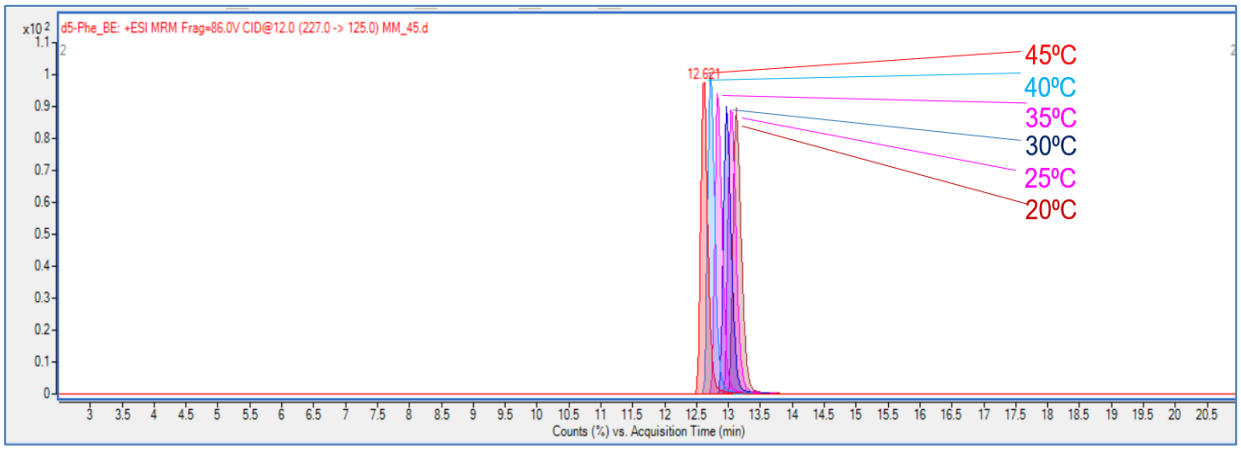

Figure B-6. Column temperature optimisation of combined SPE method. *Response indicator: d_5-Phenylalanine.*

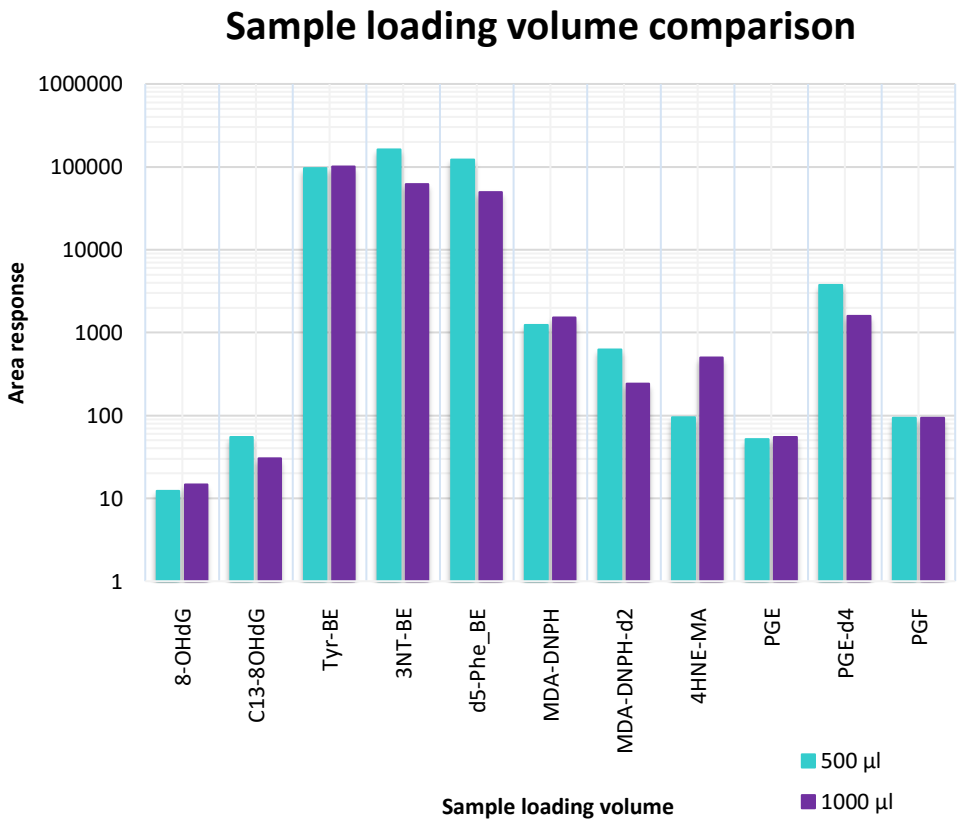

Figure B-7. Response of working standard mix with different loading volumes.

Table B-7. Serial dilution series of spiked urine based on the physiological concentrations of all the metabolites.

Sample number	Theoretical concentration (ng/ml)
1	0.12
2	0.24
3	0.49
4	0.98
5	1.95
6	3.91
7	7.81
8	15.63
9	31.25
10	62.5
11	125
12	250
13	500
14	1000

Table B-8. Comparison of analyte response in spiked urine with working standard mix of Butyl ester analysis.

Compounds	Transition	Butyl esters (Spiked urine)	Butyl esters (Working standard mix)
3NT-BE	227.0 → 125.0	3994.18	267005.96
Tyr-BE	283.2 → 181.0	2574.19	48915.39
d5-Phe_BE	238.0 →136.1	2906.10	91555.20

Table B-9. Comparison of analyte response in spiked urine and working standard mix of DNPH analysis.

Compound Method	Transition	DNPH (Spiked Urine)	DNPH (Working standard mix)
4HNE-MA	318.0 → 162.0	76.70	27.42
8-OHdG	284.1 → 168.0	1443.44	7700.78
C13-8OHdG	287.1 → 171.0	26534.78	186253.11
MDA-DNPH	235.1 → 189.0	9507.73	3228.04
MDA-DNPH-d2	237.0 → 191.0	1444.13	16874.89
PGE_2	351.0 → 271.0	336.29	ND
PGE-d4	355.2 → 275.2	8121.88	5241.58
PGF	353.0 → 309.0	286.10	151.27

ANNEXURE C:

C.1. Partial method validation of butyl esters.

Table C-1. Preliminary physiological concentrations chosen for calibration curves.

Metabolite	Physiological concentration (ng/ml)	Physiological concentration (nmol/mmol creatinine)
Tyr	5.44 – 1811.90	1 300 – 38 000
3-NT	0.36 – 28	4.5 – 31
8-OHdG	0.95 – 14.2	5.8 – 6.8
4-HNE-MA	2.85 – 128	0.2 – 2.9
$PGF_{2\alpha}$ & PGE_2	0.12 – 1.95	0.057 – 15
MDA	1.46 – 84.2	1.1 – 309

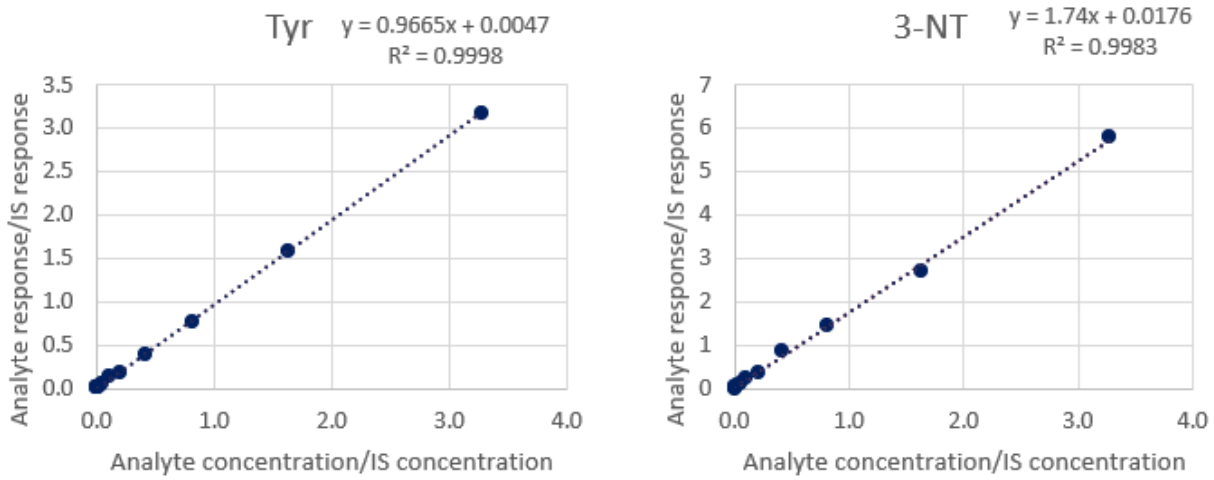

Figure C-1. Calibration curves (working standards) used to determine linearity, and detection limits of butyl esters. *r^2 is indicative of the linear range.*

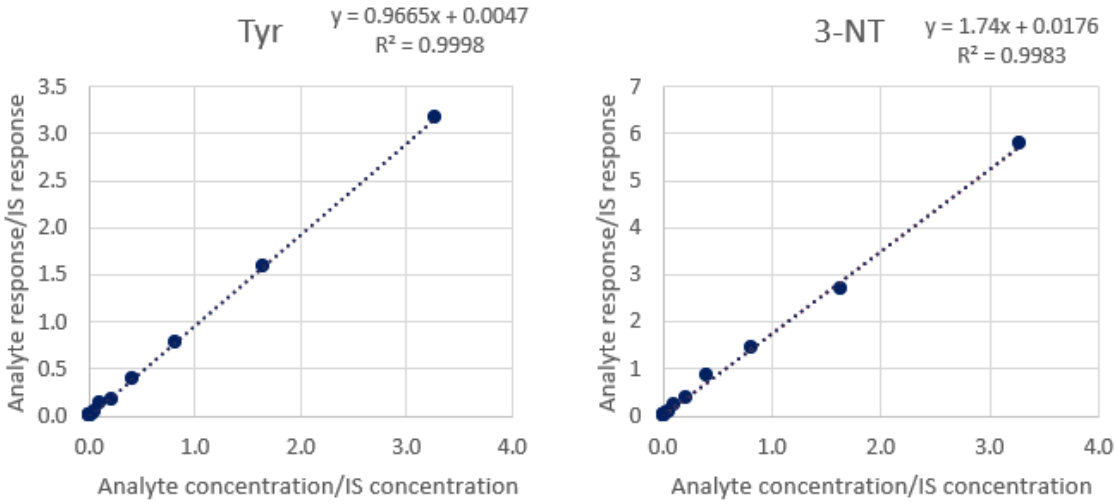

Figure C-2. Calibration curves (spiked urine) used to determine linearity, and detection limits of butyl esters. *r^2 is indicative of the linear range.*

Table -C-2. Response of the butyl esters in blanks to determine the carry over.

Metabolite	Tyr-BE	3-NT-BE	d5-Phe
Urine	7236018	87890	235384
Blank1	116	26	1392
Spiked urine	7354091	78290	1469205
Blank2	1386	422	3753
HQC	647156	429794	2659502
Blank3	399	347	1622

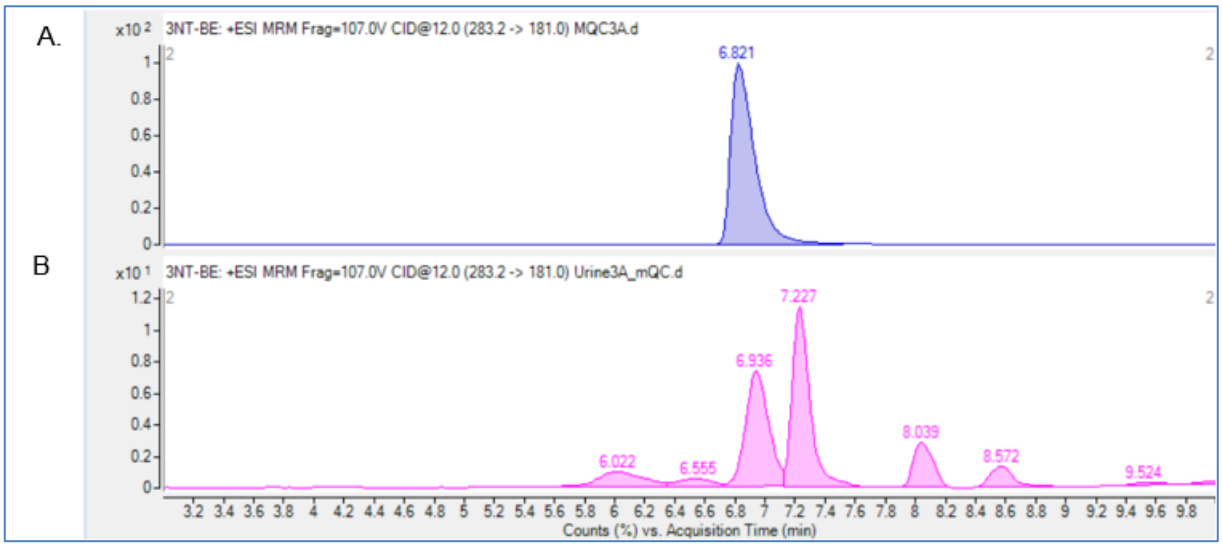

Figure C-3. Chromatograms of 3-NT. A. 3-NT in a QC sample with a concentration of 40 ng/ml, a single peak is observed. B. 3-NT in a spiked urine sample with a concentration of 40 ng/ml, two major peaks are observed.

C.2. Partial validation of DNA and lipid peroxidation markers

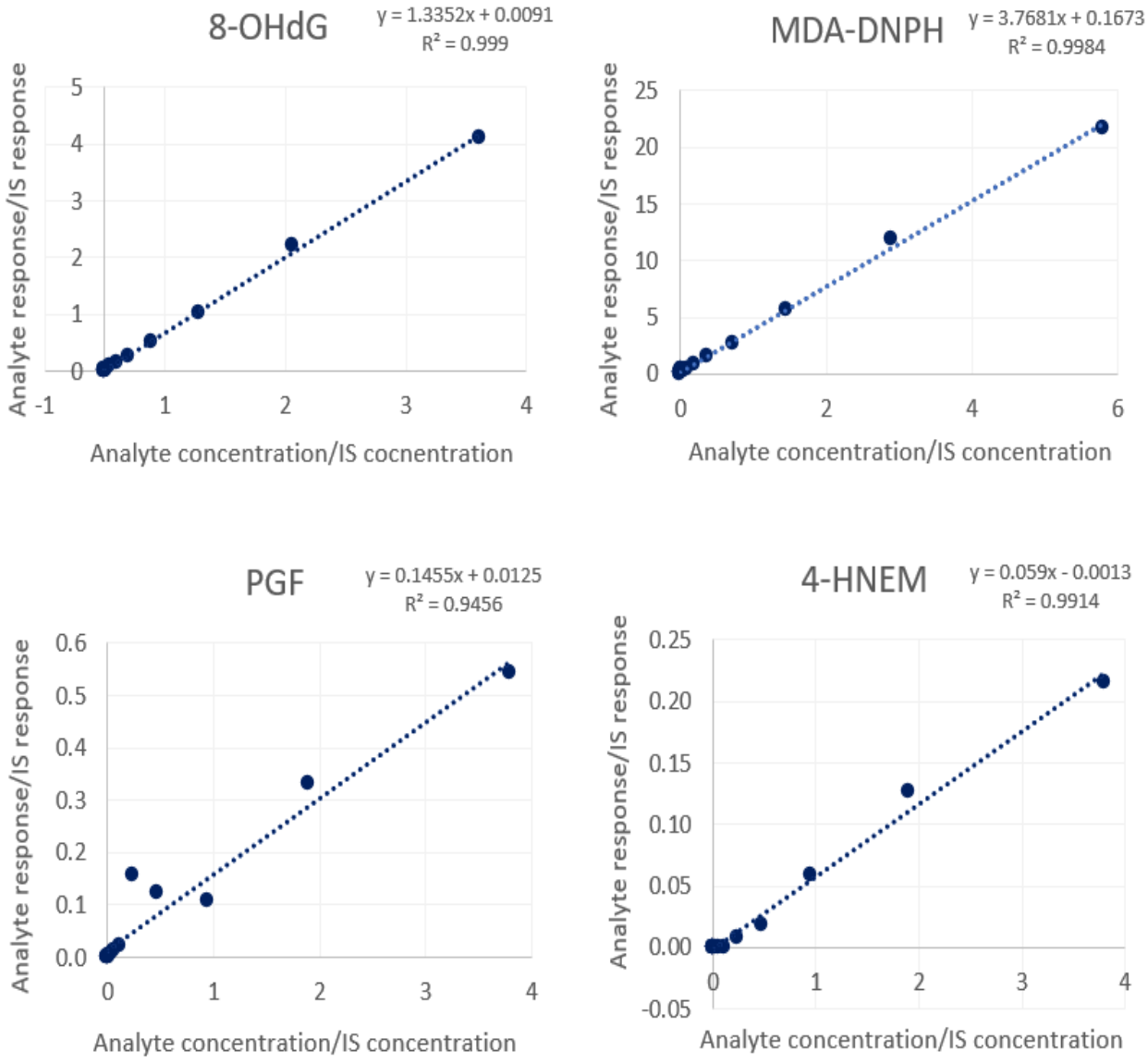

Figure C-4. Calibration curves (working standards) used to determine linearity, and detection limits of the DNPH fraction. *r^2 is indicative of the linear range.*

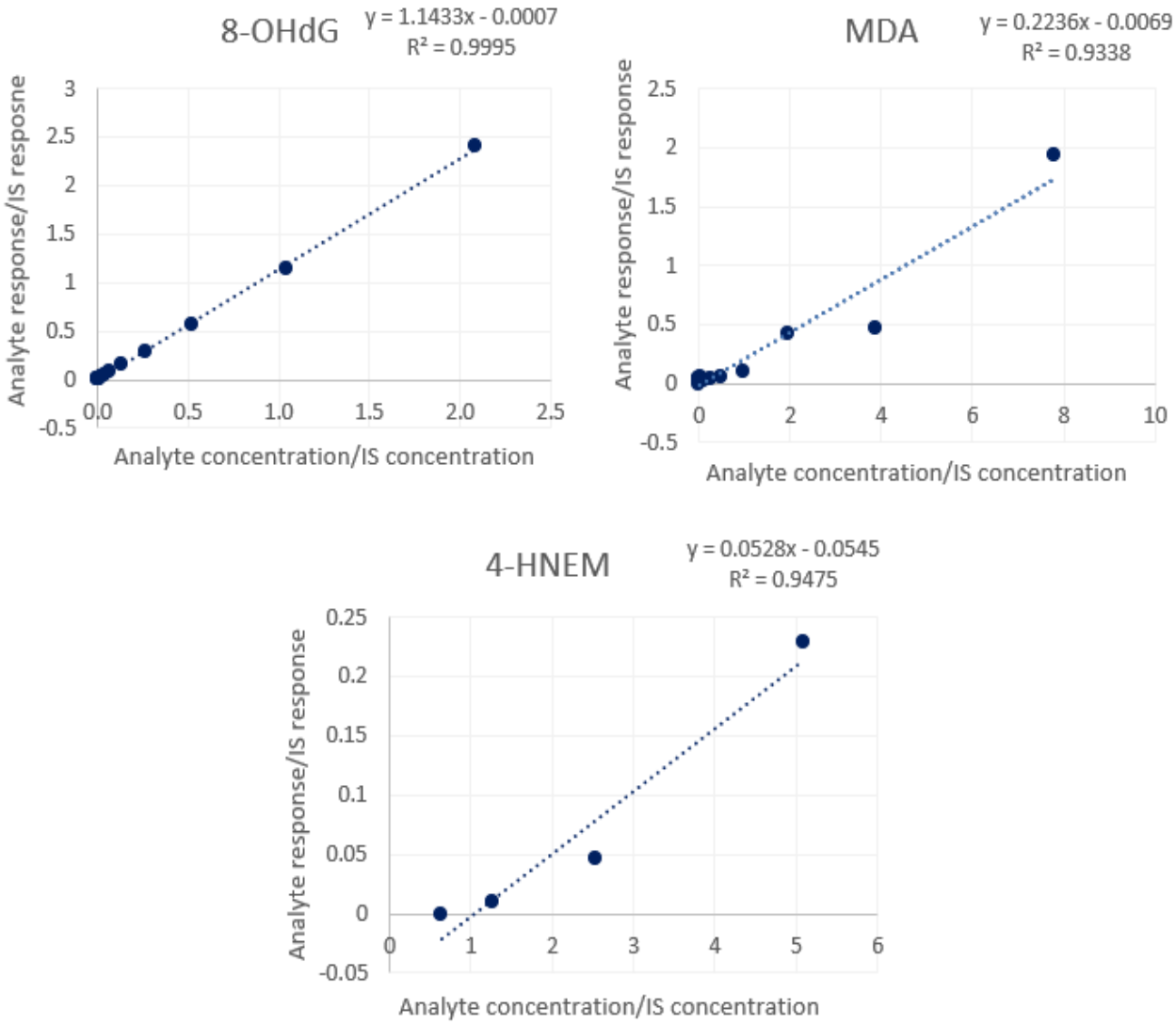

Figure C-5. Calibration curves (spiked urine) used to determine linearity, and detection limits of the DNPH fraction. *r^2 is indicative of the linear range.*

Table -C-3. Responses of DNA and lipid peroxidation markers in blank samples to determine the carry over.

Metabolite	**8-OHdG**	**C^{13}, N^{15}-8-OHdG**	**MDA-DNPH**	**MDA-DNPH-d_2**	**4-HNE-MA**	**$PGF_{2\alpha}$**	**PGE_2**	**PGE_2-d_4**
Urine	10754.50	48.20	1044.92	105.71	64.92	286.29	487.04	13743.07
Blank1	19.07	3.78	4.72	4.24	4.19	7.05	39.90	220.89
Spiked urine	21978.94	415.03	4916.32	738.37	57.33	259.07	659.65	14066.82
Blank2	158.48	7.68	8.80	18.39	3.10	4.17	7.84	143.37
HQC	152600.77	7787.80	26569.92	10878.38	32.31	742.69	71.05	1268.19
Blank3	22.04	6.58	345.18	8.98	2.43	4.25	2.28	4.45

C.3. Implementation of the methods to quantify oxidative stress markers in contraceptive users.

Table C-4. Calibration curve used during implementation of the developed methods.

Analytes	Concentration prior sample preparation (ng/ml)					
	LOD	**LOQ**	**LQC**	**MQC**	**HQC**	**EQC**
Tyr-BE	0.025	0.075	2.00	20.00	75.00	100.00
3-NT-BE	0.07	0.21	5.00	15.00	22.50	30.00
d_5-Phe-BE	111.00	111.00	111.00	111.00	111.00	111.00
8-OHdG	0.35	0.60	0.95	7.50	14.20	21.00
$^{13}C^{15}N_5$-8-OHdG	950.00	950.00	950.00	950.00	950.00	950.00
MDA-DNPH	0.95	1.91	2.00	43.00	84.00	126.00
D_2-MDA-DNPH	510.00	510.00	510.00	510.00	510.00	510.00
4-HNE-MA	10.61	30.00	65.50	192.00	204.75	271.35
$PGF_{2\alpha}$	0.73	2.20	5.00	10.00	-	12.50
PGE_2	0.38	1.00	2.50	5.00	20.00	30.00
PGE_2-d_4	780.00	780.00	780.00	780.00	780.00	780.00

Table C-5. Descriptive statistics and results from Kolmogorov-Smirnov test of the dataset to test for normality.

Metabolite	Mean	Standard deviation	Skewness	Kurtosis	p-value
8-OHdG	2.74	2.32	2.00	5.32	<0.001
MDA-DNPH	518.40	1115.85	7.03	54.30	<0.001
Tyr-BE	23831.93	28288.05	3.34	14.00	<0.001
3-NT-BE	39.75	53.68	1.88	3.34	<0.001
PGE_2	95.46	164.45	3.07	10.26	<0.001

Skewness: the measure of symmetry; kurtosis: measure of 'peakedness' of distribution. Data is normally distributed if skewness and kurtosis are between -1 and +1. Data is also normally distributed if the p-value is > 0.05.

Table C-6. Descriptive statistics of metabolites used to characterise oxidative stress profiles after normalisation, and transformation.

Metabolite	**Mean (users: ng/mg creatinine)**	**Mean (controls: ng/mg creatinine)**
8-OHdG	0.548	0.480
MDA-DNPH	2.543	2.371
PGE_2	1.336	1.652
Tyr	4.001	4.300
3-NT	0.956	1.329